STUDY REPORT

REPEATED EXPOSURE OF GINGIVAL ORGANOTYPIC CULTURES TO 3R4F CIGARETTE SMOKE AND THS2.2 AEROSOL ON PBS-COVERED (STUDY NUMBER 179800)

Table of Contents

Table of Figures

Table of Tables

1. Approval

1.1 Study Director's Statement of Compliance

Accountability for this study lies with the study director. The study director takes responsibility for the study having been executed as defined in the Study Plan (SP).
The laboratory heads take responsibility for the data generated in their labs.

Name	Date / Signature
Study Director: Filippo Zanetti	07-Mar-2017 Filippo Zanetti
Manager Cellular Lab Research: Stefan Frentzel	07-Mar-2017 S. Frentzel
Statistician: Patrice Leroy	07 MAR 2017 P.
Computational Scientist: Alain Sewer	07. MAR. 2017 A. Sewer
Test Facility Manager: Research Technologies: Nikolai Ivanov	07-MAR-2017
Director Systems Toxicology: Julia Hoeng	07-MAR-2017 Julia Hoeng

1.2 Quality Assurance Statement

Not Applicable. This study is a non-GLP study.

2. General Information

2.1 Names and Addresses

Sponsor	Manuel C. Peitsch Philip Morris Products SA Research & Development Quai Jeanrenaud 5 2000 Neuchâtel Switzerland
Test facility	Philip Morris Products SA Research & Development PMI Product Testing Quai Jeanrenaud 5 2000 Neuchâtel Switzerland
Former Study Director(s)	Filippo Zanetti
Former Study Deputy Director(s)	Anita Iskandar
Other Scientists/Technicians involved in the study	Sam Ansari, Karine Baumer, Abdelkader Benyagoub, Maica Corciulo, Remi Dulize, Stephanie Johne, Shoaib Majeed, Carole Mathis, Maude Mayer, Celine Merg, Dariusz Peric, Fabio Talamo, Laura Ortega Torres
Test site management	(b) (4), London, UK; Metabolon, Durham, NC, USA
Principal Investigators for external analysis	(b) (4) Brian Keppler and Huw Davis (Metabolon)

2.2 Study Schedule

Experiment start date:	8 February 2016
Experiment completion date:	1 July 2016

2.3 Test Guidelines

- Health Canada Intense Smoking Regimen, Official Method T-115, Determination of "Tar", Nicotine and Carbon Monoxide in Mainstream Tobacco Smoke, December 31, 1999 (adapted to meet the special conditions for the Vitrocell® system).
- International Organization for Standardization: International Standard ISO 3402, Tobacco and tobacco products – Atmosphere for conditioning and testing, 4th ed., 1999.

3. Study Plan Deviations and Amendments

The study plan (SP) can be accessed at: 1798_Organotypic_Gingival_SP.
During the execution of study S179800, deviations from the SP occurred. They are summarized below.

Study Plan Deviations and Amendments

Description of Deviation
1. The study deviates from the Study Plan S179800, pilot PBS phase I. Routinely, the medium is changed every 48 h. This does not allow measurements of accumulated adenylate kinase (AK) and multi-analyte profiling of pro-inflammatory mediators (MAP) over 72 h and 96 h time-points. Therefore, we decided to keep aliquots of the old media (up to 48-h treatments) to investigate the accumulation of AK and MAP at 72 and 96 h.
2. The study deviates from Study Plan S179800. During the first two runs of exposure with THS2.2 aerosol, the smoking machine was not working correctly.
3. The study deviates from Study Plan S179800. During the exposure to 3R4F cigarette smoke (CS) or THS2.2 aerosol as part of the dose range assessment (DRA) (only for the 24-h samples) and the main phases (MP) (all samples), the medium is changed every 24 h. This does not allow measurements of accumulated AK and cytokines over the duration of the exposures.
4. The study deviates from Study Plan S179800 because the plan does not mention that positive and negative controls for AK, MAP, and CYP of DRA and MPs I–III would be covered with PBS to align them with the treated samples.
5. The study deviates from Study Plan S179800, as the sign in the NPA calculation formula is + instead of −: $$NPA = \frac{1}{\lvert E \rvert} \sum_{e\ in\ E} (f(e_0) - \sigma(e) f(e_1))^2$$ *old version* $$NPA = \frac{1}{\lvert E \rvert} \sum_{e\ in\ E} (f(e_0) + \sigma(e) f(e_1))^2$$ *new version*
6. The study deviates from Study Plan S179800 regarding the concentration of 3R4F CS selected during the DRA. A concentration that induced less than 20% damage according to the AK assay should have been selected. However, the values of cytotoxicity determined during the DRA did not match the ones observed during the experimental repetitions because of a

mismatch in the percent of dilution and the nicotine concentration. In addition, the dose percentage and nicotine concentration do not match for the 20% (DRA) or 25% (MPs).

Table A. DRA nicotine concentrations and AK results.

% dilution	Nicotine in DRA CS (mg/L)	AK % in 3R4F CS	Nicotine in DRA Aerosol (mg/L)	AK % in THS2.2 aerosol
5%	3.11	2.9%	-	
10%	8.25	2.7%	2.18	3.0%
20%	**15.4**	**3.6%**	5.84	3.1%
35%	-		11.5	2.9%
40%	**89.1**	**15.2%**	-	
60%	201	61%	-	
75%	-	-	**79.2**	**1.9%**
100%	-	-	**147.2**	**2.2%**

Mismatched concentrations and AK values are reported in bold.

Table B. Main Phase I nicotine concentrations and AK results.

% dilution	Nicotine in MPI CS (mg/L)	AK % in 3R4F CS	Nicotine in MPI aerosol (mg/L)	AK % in THS2.2 aerosol
25%	**52.4**	**17.4%**	-	-
35%	**87.8**	**33.2%**	-	-
50%	-	-	14.8	3.3%
75%	-	-	**53.1**	**3.0%**
100%	-	-	**98.1**	**2.4%**

Mismatched concentrations and AK values are reported in bold.

7. Delivery of inserts from the supplier for MP II was originally planned for Friday, 1 April 2016. Because of problems with the shipping company, the delivery was delayed to Monday, 4 April 2016. This rendered the inserts unsuitable for the study, since cell differentiation assay could not be performed over the weekend.

Corrective Action

1. New S- numbers have been created (labeled "Aliquot Sample ID"), and metadata have been updated (https://disco.app.pmi/disco/drl/objectId/0901d4ec80563db2). Sample labels report an "OLD" for the aliquot corresponding to the old medium collected at 48 h, and a "NEW" for the samples collected at the previewed time-point (72 h or 96 h).

   AK will be measured for both the OLD and NEW samples, whereas MAP will be performed only for the NEW, and OLD samples will be kept stored in case of future assessments. AK will be measured in two different wells, and both values will be considered for analysis.

2. The leaked test was performed twice; puff volume was also measured before beginning the tissue exposure, and all Health Canada (CH) devices were replaced during the runs.

3. Aliquots were collected before beginning each exposure, starting from the second, to investigate the accumulation of AK and proinflammatory mediators. AK and MAP were measured in independent wells for each aliquot, and values were subsequently summed to yield the accumulated levels of AK or cytokines over the entire exposure period.

4. One hundred microliters of PBS were added on the apical side of each control (positive and negative) insert used for the AK, MAP, CYP testing, and metabolomics investigations.

5. The sign in the calculation is correct; the mistake in the formula appeared only in the SP, and not in the computational scientist analysis tool.

6. Since the final concentration of the medium and high THS2.2 concentration matched the low and high 3R4F concentrations, respectively, we used these paired concentrations for the comparative analysis. The actual values are reported below.

Group	**Smoke/aerosol concentration (%)**	**Nicotine (average mg/L) ± SEM**
3R4F low concentration	25	49.4 ± 1.89
3R4F high concentration	35	84.6 ± 1.43
THS2.2 low concentration	50	14.4 ± 1.17
THS2.2 medium concentration	75	54.6 ± 2.60
THS2.2 high concentration	100	100.4 ± 4.83

7. The inserts were discarded and MP-II was cancelled. MP-III became MP-II; MP-III was performed on CW22, 30 May 2016.

Assessment on Study Quality and Integrity
1. This deviation will improve the quality of the study phase, making it possible to investigate the effective accumulation of AK over the entire duration of the treatment (72 h and 96 h), or not, with PBS. 2. The deviation results in the THS2.2 aerosol exposure run completed in longer duration, so the quality of the THS2.2 aerosol during first two runs may have been affected. To ensure quality and integrity of the data, we will exclude the results of these runs from the statistics if they show inconsistencies. 3. This deviation will improve the quality of the study phase, making it possible to investigate the effective accumulation of AK over the entire duration of the exposure. 4. The deviation will improve the quality of the study by using controls that are treated in the same manner as the exposed samples. 5. The deviation does not affect the integrity of the study, as the mistake in the written formula only appeared in the SP and not in the computational scientist's tools. 6. This deviation affects the initial design of the comparative concentration analysis. We will not have a higher-than-3R4F concentration for the THS2.2 aerosol. However, by reaching 100% of the THS2.2 aerosol concentration, we will measure the non-diluted (and comparable to 3R4F) aerosol effects on gingival organotypic cultures. Quality and integrity of the results are not affected. 7. This deviation affects the timeline of the study because of the delay of MP- III. Data integrity and quality are not affected.

Amendments:

<table>
<tr><td colspan="4">Present Text Version</td></tr>
<tr><td rowspan="3">Concerning</td><td>Exposure of inserts not covered with PBS</td><td>Page 8, Paragraph 4
Page 9, Paragraph 4.1
Page 14, Table 6</td><td rowspan="3">Study Plan S179800</td></tr>
<tr><td colspan="2">After setting the experimental conditions, three main phases (MPs) will be performed. During the MPs, we will focus on the measurement of the repeated daily impact of a 28-min exposure of the selected concentrations of 3R4F CS (two concentrations) and THS2.2 aerosol (three concentrations, two matching 3R4F and one higher) (determined in Phase II) on the PBS-submersed gingival tissue cultures by analyzing different biological endpoints (AK, MAP, CYP activity, tissue histology), and the perturbation of the molecular network at a unique time-point, determined after Phase I of the study.</td></tr>
<tr><td>E-cadherin staining</td><td>Page 14, Table 6
Page 17, Paragraph 4.5
Page 14, Table 6</td></tr>
<tr><td colspan="4">New Text Version</td></tr>
<tr><td colspan="4">The study is amended to allow the exploration of human organotypic gingival epithelial tissue culture inserts covered by 100 µL of PBS on the apical side and subjected to repeated exposure to 3R4F CS and THS2.2 aerosol.

1. <u>Concerning the experimental design</u>

After setting the experimental conditions, three main phases (MPs) will be performed. During the MPs, we will focus on the measurement of the repeated daily impact of a 28-min exposure of the selected concentrations of 3R4F CS (two concentrations) and THS2.2 aerosol (three concentrations, two matching 3R4F and one higher) (determined in Phase II) on the PBS-submersed gingival tissue cultures by analyzing different biological endpoints (AK, MAP, CYP activity, tissue histology). During MP-III, the perturbation of the molecular network at two time-points, determined after Phase I of the study, will be measured. In addition, a set of samples not covered by PBS will be investigated after exposure to Sham (filtered air) and the lowest 3R4F CS and THS2.2 aerosol concentration.

We will add three Sham samples and three low-concentration samples for 3R4F (49.4 mg/L) and THS2.2 (14.4 mg/L) in MP-I and MP-II, to test the effects of the presence of PBS during exposures. Tissue histology and AK release will be measured in these samples. This will allow us to explore the eventual effect of the apical contact with PBS during exposure.
The exposure plans and metadata sheets reporting the changes are stored in the following repository:

For MP-I</td></tr>
</table>

https://disco.app.pmi/disco/drl/objectId/0901d4ec80582199
https://disco.app.pmi/disco/drl/objectId/0901d4ec8058219b

For MP-II
https://disco.app.pmi/disco/drl/objectId/0901d4ec8058b9f2
https://disco.app.pmi/disco/drl/objectId/0901d4ec8058b9f0

1. Concerning E-cadherin staining

Staining with antibodies against E-cadherin will be relevant for the investigation of the intercellular adhesion. Table 6, page 14 is modified as follows:

Experimental Phase	**Main Phases I–III**		
Experimental Week	**07-03-2016 / 04-04-2016 / 18-04-2016**		
Biological Endpoints	**Duration of Exposure (h)**	**Post-Exposure (h)**	**Tissue Inserts Per Endpoint**
Cytotoxicity (AK)* #+	According to Phase I	24	3
Gene Expression (mRNA/miRNA) #		4	3
Pro-Inflammatory Mediators (MAP)#		24	3
CYP1A1/1B1 Activity*+		24	3
Histology*		24	3
Metabolomics[$]		24	5
Immunohistochemistry		24	3
Nicotine Trapped in PBS	-	-	3
Number of Runs	Three exposures, repeated every 24 h according to Phase I		
Number of Tissue Inserts/Run	1		
Exposure Characterization			
Nicotine (PBS)	✓		
Carbonyls	Will be part of QC assessment of the smoke/aerosol generation; samples will be generated throughout the study phases		

The above table does not exclude the possibility that additional endpoints would be generated. The variations will be reported in the appropriate exposure plan. *# Common endpoints. [$] Only for one phase. Abbreviations: CYP, cytochrome; PBS, phosphate-buffered saline. + will be measured for non-PBS-exposed samples in MP-I and MP-II.

The methodology for the staining is as follows:

For immunohistochemical staining, slides were incubated at 60°C for a minimum of 30 min and then transferred to the Leica Bond-Max autostainer for immunohistochemistry using the Leica Bond™ Polymer Refine Detection Kit (#DS9800, Leica Biosystems Nussloch GmbH, Nussloch, Germany). The slides were treated with ethylenediaminetetraacetic acid (EDTA), incubated with an E-cadherin antibody (Leica Biosystems PA0387, undiluted), and counterstained with hematoxylin.
Reason for Change
The study is amended to improve the exploration of toxicity, alterations, and molecular profiles of submersed gingival tissue cultures after repeated daily exposure of 28 min to THS2.2 aerosol or 3R4F CS. Originally, the exposure session was planned without the inclusion of samples not covered by PBS. This would not have allowed us to infer possible effects of PBS during exposure on tissue histology and cytotoxicity. The immunostaining for E-cadherin will give additional information on the state of cell adhesion, an important process involved in many periodontal diseases.

Present Text Version			
Concerning	**Gene expression evolution after 24 h from exposure**	Page 8, Paragraph 4 Page 14, Table 6 Page 15-16, Paragraph 4.4.1 Page 17, Paragraph 4.4.3	Study Plan S179800
After setting the experimental conditions, three main phases (MPs) will be performed. During the MPs, we will focus on the measurement of repeated daily impact of a 28-min exposure of the selected concentrations of 3R4F CS (two concentrations) and THS2.2 aerosol (three concentrations, two matching 3R4F and one higher) (determined in Phase II) on the PBS-submersed gingival tissue cultures, by analyzing different biological endpoints (AK, MAP, CYP activity, tissue histology) and the perturbation of the molecular network at a unique time-point, determined after Phase I of the study.			

New Text Version
The study is amended to allow the exploration of gene expression evolution of human organotypic gingival epithelial tissue cultures covered by a thin layer of phosphate-buffered saline (PBS) after repeated exposures to 3R4F cigarette smoke (CS) or Tobacco Heating System 2.2 (THS2.2) aerosol. The amendment concerns only Main Phase III. 1. **<u>Concerning the experimental design</u>** After setting the experimental conditions, three main phases (MPs) will be performed. During the MPs, we will focus on the measurement of the repeated daily impact of a 28-min exposure of the selected concentrations of 3R4F CS (two concentrations) and THS2.2 aerosol (three concentrations,

two matching 3R4F and one higher) (determined in Phase II) on the PBS-submersed gingival tissue cultures, by analyzing different biological endpoints (AK, MAP, CYP activity, tissue histology). During Main Phase III, the perturbation of the molecular network at two time-points, determined after Phase I of the study, will be measured.

2. Concerning the Main Phase III list of endpoints per post-exposure time-point

To investigate the progression of gene expression, a time-point was added 24 h post-exposure. The exploration of toxicity and gene expression (GEX) of PBS-submersed gingival tissue cultures after repeated daily exposures of 28 min to THS2.2 aerosol or 3R4F CS will be performed at two time-points post-exposure (4 h and 24 h) instead of a single time-point (4 h post-exposure).
To add the 24-h collection time-point while keeping the same number of inserts and not adding subsequent changes in the statistics, some controls used for cytotoxicity (AK, histology, CYP1A1/1B1 activity, and MAP) were adapted. All tissue controls are kept, but the number of inserts is adapted to singles or duplicates. This will not impact the statistical power of the measurements, since the controls are normally loaded into the same plate, constituting a single technical replicate.

In the case of the experimental conditions for 3R4F CS and THS2.2 aerosol and their controls (air-exposed), three tissue inserts per endpoint are planned. Therefore, the statistical robustness will not be affected.

Table 1. Experimental design phase III, list of endpoints per exposure time-point and collection time-point.

Tissue	Exposure	Dose	1	2	3	4	5	6	7	Collection Time Point	Number of insert	Run	Additional remark
GI	TX100	1%	AK							AK (Friday)	2		
GI	TCDD	30 nM				CYP				Thursday	2		
GI	LuciferinCEE	-				CYP-			Histo	Thursday	1		
GI	IL1B/TNFA	10uM			MAP					Wednesday	2		
GI	PBS	-	AK-		MAP-				Histo	IncubCTRL-Wednesday	2		
GI	Sham	PBS 60% Air	AK	GEX						4h	3	A1 B1 C1	
GI	3R4F	PBS 25%	AK	GEX							3	A1 B1 C1	
GI	3R4F	PBS 35%	AK	GEX							3	A1 B1 C1	
GI	Sham	PBS 60% Air	AK	GEX						24h	3	A1 B1 C1	
GI	3R4F	PBS 25%	AK	GEX							3	A1 B1 C1	
GI	3R4F	PBS 35%	AK	GEX							3	A1 B1 C1	
GI	Sham	PBS 60% Air	AK		MAP				Histo	1 time point according to Pilot (24h PE) and concentration according to DRA	3	A1 B1 C1	
GI	3R4F	PBS 25%	AK		MAP				Histo		3	A1 B1 C1	
GI	3R4F	PBS 35%	AK		MAP				Histo		3	A1 B1 C1	
GI	Sham	PBS 60% Air	AK			Cyp1A1/1B1				1 time point according to Pilot (24h PE) and concentration according to DRA	3	A1 B1 C1	
GI	3R4F	PBS 25%	AK			Cyp1A1/1B1					3	A1 B1 C1	
GI	3R4F	PBS 35%	AK			Cyp1A1/1B1					3	A1 B1 C1	
GI	Sham	PBS 60% Air	AK	GEX						4h	3	A2 B2 C2	
GI	THS2.2	PBS 50%	AK	GEX							3	A2 B2 C2	
GI	THS2.2	PBS 70%	AK	GEX							3	A2 B2 C2	
GI	THS2.2	PBS 100%	AK	GEX							3	A2 B2 C2	
GI	Sham	PBS 60% Air	AK	GEX						24h	3	A2 B2 C2	
GI	THS2.2	PBS 50%	AK	GEX							3	A2 B2 C2	
GI	THS2.2	PBS 70%	AK	GEX							3	A2 B2 C2	
GI	THS2.2	PBS 100%	AK	GEX							3	A2 B2 C2	
GI	Sham	PBS 60% Air	AK		MAP				Histo	1 time point according to Pilot (24h PE) and concentration according to DRA	3	A2 B2 C2	
GI	THS2.2	PBS 50%	AK		MAP				Histo		3	A2 B2 C2	
GI	THS2.2	PBS 70%	AK		MAP				Histo		3	A2 B2 C2	
GI	THS2.2	PBS 100%	AK		MAP				Histo		3	A2 B2 C2	
GI	Sham	PBS 60% Air	AK			Cyp1A1/1B1				1 time point according to Pilot (24h PE) and concentration according to DRA	3	A2 B2 C2	
GI	THS2.2	PBS 50%	AK			Cyp1A1/1B1					3	A2 B2 C2	
GI	THS2.2	PBS 70%	AK			Cyp1A1/1B1					3	A2 B2 C2	
GI	THS2.2	PBS 100%	AK			Cyp1A1/1B1					3	A2 B2 C2	

3. Concerning the list of endpoints in Table 6:

Experimental Phase	Main Phases I–III		
Experimental Week	**07-03-2016 / 04-04-2016 / 18-04-2016**		
Biological Endpoints	**Duration of Exposure (h)**	**Post-Exposure (h)**	**Tissue Inserts Per Endpoint**
Cytotoxicity (AK)* #+	According to Phase I	24	3
Gene Expression (mRNA/miRNA) #		4-24^	3
Pro-Inflammatory Mediators (MAP)#		24	3
CYP1A1/1B1 Activity*+		24	3
Histology*		24	3
Metabolomics$		24	5
Immunohistochemistry		24	3
Nicotine Trapped in PBS	-	-	3
Number of Runs	Three exposures, repeated every 24 h according to Phase I		
Number of Tissue Inserts/Run	1		
Exposure Characterization			
Nicotine (PBS)	✓		
Carbonyls	Will be part of QC assessment of the smoke/aerosol generation; samples will be generated throughout the study phases		

The above table does not exclude the possibility that additional endpoints would be generated. The variations will be reported in the appropriate exposure plan. *#Common endpoints. $Only for one phase. Abbreviations: CYP, cytochrome; PBS, phosphate-buffered saline. + will be measured for non-PBS-exposed samples in MP-I and MP-II. ^ will be measured only in MP-III.

4. Concerning the exposure plan for Main Phase III

The new exposure plan is kept in: Study Documents (https://disco.app.pmi/disco/drl/objectId/0b01d4ec8055c5b1) and presented in Table 2.

Table 2. Main Phase III, exposure plan.

Run A1			A	B	C	D	E	F	
3R4F	---	8	EMPTY	EMPTY	EMPTY	EMPTY	EMPTY	EMPTY	30-31 May-1 June
	35%	7	EMPTY	EMPTY	EMPTY	EMPTY	EMPTY	EMPTY	
	35%	6	Nicotine Assessment	AK/Histo/ MAP	AK/mRNA 4h	AK/CYP	AK/mRNA 24h	Nicotine Assessment	
	25%	5	EMPTY	EMPTY	EMPTY	EMPTY	EMPTY	EMPTY	
	25%	4	Nicotine Assessment	AK/Histo/ MAP	AK/mRNA 4h	AK/CYP	AK/mRNA 24h	Nicotine Assessment	
	---	3	EMPTY	EMPTY	EMPTY	EMPTY	EMPTY	EMPTY	
A R60% Humidity	SHAM	2	EMPTY	EMPTY	EMPTY	EMPTY	EMPTY	EMPTY	
	SHAM	1	Nicotine Assessment	AK/Histo/ MAP	AK/mRNA 4h	AK/CYP	AK/mRNA 24h	Nicotine Assessment	

Run A2			A	B	C	D	E	F	
THS2.2	100%	8	EMPTY	EMPTY	EMPTY	EMPTY	EMPTY	EMPTY	30-31 May-1 June
	100%	7	Nicotine Assessment	AK/Histo/ MAP	AK/mRNA 4h	AK/CYP	AK/mRNA 24h	Nicotine Assessment	
	75%	6	EMPTY	EMPTY	EMPTY	EMPTY	EMPTY	EMPTY	
	75%	5	Nicotine Assessment	AK/Histo/ MAP	AK/mRNA 4h	AK/CYP	AK/mRNA 24h	Nicotine Assessment	
	50%	4	EMPTY	EMPTY	EMPTY	EMPTY	EMPTY	EMPTY	
	50%	3	Nicotine Assessment	AK/Histo/ MAP	AK/mRNA 4h	AK/CYP	AK/mRNA 24h	Nicotine Assessment	
AIR 60% Humidity	SHAM	2	EMPTY	EMPTY	EMPTY	EMPTY	EMPTY	EMPTY	
	SHAM	1	Nicotine Assessment	AK/Histo/ MAP	AK/mRNA 4h	AK/CYP	AK/mRNA 24h	Nicotine Assessment	

Run B1			A	B	C	D	E	F	
3R4F	---	8	EMPTY	EMPTY	EMPTY	EMPTY	EMPTY	EMPTY	30-31 May-1 June
	35%	7	EMPTY	EMPTY	EMPTY	EMPTY	EMPTY	EMPTY	
	35%	6	Nicotine Assessment	AK/Histo/ MAP	AK/mRNA 4h	AK/CYP	AK/mRNA 24h	Nicotine Assessment	
	25%	5	EMPTY	EMPTY	EMPTY	EMPTY	EMPTY	EMPTY	
	25%	4	Nicotine Assessment	AK/Histo/ MAP	AK/mRNA 4h	AK/CYP	AK/mRNA 24h	Nicotine Assessment	
	---	3	EMPTY	EMPTY	EMPTY	EMPTY	EMPTY	EMPTY	
A R60% Humidity	SHAM	2	EMPTY	EMPTY	EMPTY	EMPTY	EMPTY	EMPTY	
	SHAM	1	Nicotine Assessment	AK/Histo/ MAP	AK/mRNA 4h	AK/CYP	AK/mRNA 24h	Nicotine Assessment	

Run B2			A	B	C	D	E	F	
THS2.2	100%	8	EMPTY	EMPTY	EMPTY	EMPTY	EMPTY	EMPTY	30-31 May-1 June
	100%	7	Nicotine Assessment	AK/Histo/ MAP	AK/mRNA 4h	AK/CYP	AK/mRNA 24h	Nicotine Assessment	
	75%	6	EMPTY	EMPTY	EMPTY	EMPTY	EMPTY	EMPTY	
	75%	5	Nicotine Assessment	AK/Histo/ MAP	AK/mRNA 4h	AK/CYP	AK/mRNA 24h	Nicotine Assessment	
	50%	4	EMPTY	EMPTY	EMPTY	EMPTY	EMPTY	EMPTY	
	50%	3	Nicotine Assessment	AK/Histo/ MAP	AK/mRNA 4h	AK/CYP	AK/mRNA 24h	Nicotine Assessment	
AIR 60% Humidity	SHAM	2	EMPTY	EMPTY	EMPTY	EMPTY	EMPTY	EMPTY	
	SHAM	1	Nicotine Assessment	AK/Histo/ MAP	AK/mRNA 4h	AK/CYP	AK/mRNA 24h	Nicotine Assessment	

Run C1			A	B	C	D	E	F	
3R4F	---	8	EMPTY	EMPTY	EMPTY	EMPTY	EMPTY	EMPTY	30-31 May-1 June
	35%	7	EMPTY	EMPTY	EMPTY	EMPTY	EMPTY	EMPTY	
	35%	6	Nicotine Assessment	AK/Histo/ MAP	AK/mRNA 4h	AK/CYP	AK/mRNA 24h	Nicotine Assessment	
	25%	5	EMPTY	EMPTY	EMPTY	EMPTY	EMPTY	EMPTY	
	25%	4	Nicotine Assessment	AK/Histo/ MAP	AK/mRNA 4h	AK/CYP	AK/mRNA 24h	Nicotine Assessment	
	---	3	EMPTY	EMPTY	EMPTY	EMPTY	EMPTY	EMPTY	
A R60% Humidity	SHAM	2	EMPTY	EMPTY	EMPTY	EMPTY	EMPTY	EMPTY	
	SHAM	1	Nicotine Assessment	AK/Histo/ MAP	AK/mRNA 4h	AK/CYP	AK/mRNA 24h	Nicotine Assessment	

Run C2			A	B	C	D	E	F	
THS2.2	100%	8	EMPTY	EMPTY	EMPTY	EMPTY	EMPTY	EMPTY	30-31 May-1 June
	100%	7	Nicotine Assessment	AK/Histo/ MAP	AK/mRNA 4h	AK/CYP	AK/mRNA 24h	Nicotine Assessment	
	75%	6	EMPTY	EMPTY	EMPTY	EMPTY	EMPTY	EMPTY	
	75%	5	Nicotine Assessment	AK/Histo/ MAP	AK/mRNA 4h	AK/CYP	AK/mRNA 24h	Nicotine Assessment	
	50%	4	EMPTY	EMPTY	EMPTY	EMPTY	EMPTY	EMPTY	
	50%	3	Nicotine Assessment	AK/Histo/ MAP	AK/mRNA 4h	AK/CYP	AK/mRNA 24h	Nicotine Assessment	
AIR 60% Humidity	SHAM	2	EMPTY	EMPTY	EMPTY	EMPTY	EMPTY	EMPTY	
	SHAM	1	Nicotine Assessment	AK/Histo/ MAP	AK/mRNA 4h	AK/CYP	AK/mRNA 24h	Nicotine Assessment	

Reason for Change

The study is amended to improve the exploration of toxicity, alterations, and molecular profiles of submersed gingival tissue cultures after repeated daily exposure of 28 min to THS2.2 aerosol or 3R4F CS.

The primary objective, "To compare the impact between THS2.2 aerosol and combustible 3R4F CS repeated exposures at a comparable nicotine concentration on PBS-submersed human organotypic gingival tissue cultures by assessing tissue histology, cytotoxicity, secretion of proinflammatory mediators, and cytochrome P450 (CYP) activity, as well as transcriptomic (mRNA, miRNA) and metabolomic profiles" (Study Plan S179800, P7), could not be fully reached without the observation of gene expression evolution.

Originally, the gene expression analysis was planned for a single time-point (4 h post-exposure) with 3R4F CS or THS2.2 aerosol. This would have given insight only into a short time post-exposure, and would have not allowed the observation of gene expression evolution at a later time-point (24 h), when all the other endpoints were assessed. Therefore, a 24-h post-exposure time-point was added, to allow insights into recovery and changes in gene expression, in line with our systems toxicology paradigm.

4. Abstract/Executive Summary

Periodontal diseases are inflammatory disorders associated with the accumulation of a bacterial biofilm and characterized by the destruction of periodontal tissues. Although classified as bacterial infections, epidemiological studies have revealed that cigarette smoke (CS) is one of the major lifestyle-related risk factors for periodontal disease. CS can alter the epithelial structure of the gingival mucosa, leading to pathologies such as increased loss of attachment, development and progression of periodontal inflammation, increased gingival recession, and cancer (Genco 1996, James 1999).

The use of an organotypic culture model, which retains the three-dimensional (3D) structure of the gingival epithelium at the air-liquid interface (ALI) and resembles many of the features of the native human gum, is appropriate for *in vitro* research.

The current study aimed to investigate and compare the effects of mainstream smoke from reference cigarettes (3R4F) and aerosol from a candidate Modified Risk Tobacco Product (MRTP), the Tobacco Heating System (THS) 2.2, on human gingival organotypic epithelial cultures using well-established cell-based assays and systems toxicology approaches.

Human organotypic gingival cultures were exposed three times to 3R4F CS and THS2.2 aerosol at comparable levels of nicotine for 28 min, and analyzed at different post-exposure time-points for various endpoints. A dose range finding (DRF, also indicated as DRA) was performed to establish the maximum tolerable concentration of 3R4F CS. Histological examination, cytotoxicity, activity of cytochrome P450 (CYP) 1A1/1B1, and gene expression (mRNA and miRNA) were assessed, and data were generated at the various time-points after exposure. A systems toxicology approach leveraging the gene expression data and biological network models was used to elucidate the biological impact of the exposure.

The impact of THS2.2 aerosol at any of the concentrations tested was less than that of 3R4F CS. At the equivalent concentrations, adenylate kinase (AK) release-based cytotoxicity assays showed lower cytotoxicity after THS2.2 aerosol exposure compared with 3R4F CS, which is consistent with the tissue histology evaluation. Additionally, greater alterations in secreted proinflammatory mediators were found in the basolateral media of cultures exposed to 3R4F CS than in media of cells exposed to THS2.2 aerosol. Possible toxicity-related mechanisms associated with the exposure were investigated using a network approach of transcriptomics data. This analysis showed a lower perturbation of various biological networks in the THS2.2 aerosol-exposed cultures than in the 3R4F CS-exposed cultures.

The results of the current study showed that THS2.2 aerosol exposure had less impact on the gingival cultures than 3R4F CS exposure at equivalent concentrations. However, donor-specific factors associated with the culture model used in this study (e.g., genetic variations), that may have been undetected, yet could influence the outcome of the experiment, cannot be excluded from consideration. These factors could be addressed in future studies.

5. Introduction

This was an exploratory study to assess the impact of repeated exposures to 3R4F CS and THS2.2 aerosol on human organotypic gingival epithelial tissue cultures covered by a thin layer of phosphate buffered saline (PBS).

The impact of the aerosol was compared with the impact of smoke generated from the combustion of the reference cigarette 3R4F. The gingival organotypic culture model had been investigated before (Schlage 2014), where the effect of repeated exposure to whole CS had been assessed. The former tissue culture was the full-thickness gingival epithelium model of MatTek and was co-cultured with fibroblasts (GIN-300-FT-1, MatTek, Ashland, MA, USA).

In a recent study (S178600), we measured the response of a different gingival model, the EpiGingival™ GIN-100 (MatTek), to different concentrations of THS2.2 aerosol and 3R4F CS at the ALI. We gained information about the histology, which resembled the images provided by MatTek, with the exception of the upper cornified layers, which appeared more developed and fragile in our images (Figure 1A). Cytotoxicity was also measured (adenylate kinase [AK] assay). Moreover, we tested the induction of cytochrome P450 (CYP) 1A1/1B1 by 2,3,7,8-tetrachlorodibenzo-p-dioxin (TCDD), with positive results (Figure 1B).

In the present study, we tested the same gingival monoculture of human keratinocytes used in the last study (GIN-100, MatTek) which addressed specifically the response of a single cell type (keratinocytes) to the aerosol/smoke. In contrast with our previous studies, the apical exposure to PBS mimicked the *in vivo* situation, where saliva continuously moistens the gingival epithelium.

To robustly assess the impact of exposure to inhaled aerosols (e.g., CS and nanoparticles), the selected *in vitro* test system should display several key features, which the human gingival organotypic model fulfills.

First, the *in vitro* systems used to investigate the effects of exposure on respiratory toxicity should resemble the *in vivo* situation (Baxter 2015). Many studies have used organotypic gingival tissue cultures with comparable results to the *in vivo* paradigm (Agrawal 2013, Hai 2006, Mitchell 2012, Yang 2011). The ALI to which EpiGingival™ cultures are cultivated allows the direct exposure to CS or THS2.2 aerosol, better mimicking the *in vivo* exposure situation (Schlage 2014).

Second, the test systems should retain normal metabolic and molecular activities (Huh 2011, Nichols 2014). Interestingly, the organotypic cultured cells have been shown to retain their ability to release proinflammatory mediators (e.g., cytokines, chemokines, and growth factors) and reactive oxygen species, allowing researchers to investigate the potential mechanisms underlying the local and potentially systemic effects of the exposure (Gemmell 2001, Huh 2011, Nichols 2014, Rubini 2011, Schlage 2014). Moreover, the organotypic cultured cells express several members of the cytochrome P450 system, such as CYP1A1 and CYP1B1, whose expression and activity can be monitored following exposure to CS or other toxicants (Schlage 2014).

The MatTek gingival tissue model (EpiGingival™) contains normal human gingival keratinocytes cultured in serum-free medium to form three-dimensional (3D) differentiated tissues. Hematoxylin and eosin staining of tissue sections shows that the architecture of the tissue is very similar to that of human gingival mucosa *in vivo* (Hai 2006). The cultured tissue is 9–13 cell layers thick, and consists of a partially cornified apical surface and a non-cornified basal region (Figure 1A). The thickness and morphology of the apical stratum corneum (SC) and the basal cell layers are similar to those in the gingival tissues *in vivo*. Indeed, as happens *in vivo*, cells at the basal region of the cultured tissue

continue to divide and differentiate, and apical surface cells continue to cornify to form the SC. Furthermore, the distribution of cytokeratins (e.g., K13 and K14), as assessed by immunohistochemical staining, is similar to the *in vivo* distribution (Hai 2006, Oda 1990).

In the present study, we compared the effects of THS2.2 aerosol and CS on the gingival epithelium of the EpiGingival™ system by assessing the impact of a repeated (3-day) exposure at comparable concentrations matched by delivered nicotine dose. The endpoints of our systems toxicology approach included cytotoxicity, histopathology, secretion of inflammatory mediators, and molecular investigations using transcriptomics (mRNA and miRNA) and metabolomics, complemented by computational network biology analyses.

Overall, our findings elucidated the complex biological responses of gingival cultures to CS exposure in the EpiGingival™ model, providing evidence that the THS2.2 aerosol exerts fewer biological effects than 3R4F CS on histopathology, gene expression, inflammatory mediator secretion, and oxidative-stress related metabolism.

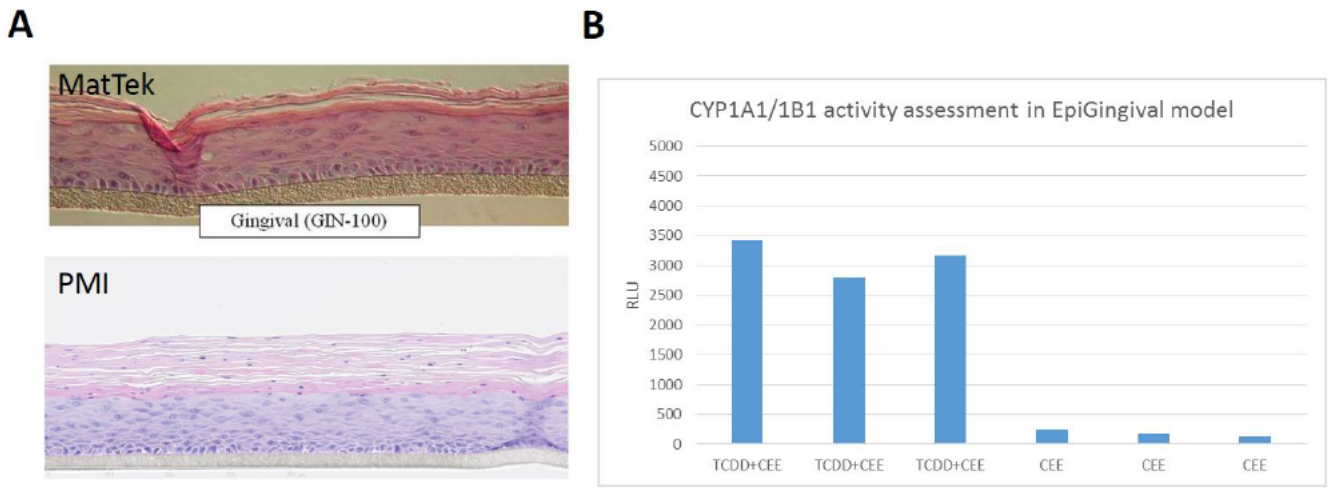

Figure 1. MatTek EpiGingival™ model.
(**A**) Comparison between a histology image of GIN-100 tissues provided by MatTek and an image generated in-house. (**B**) CYP1A1/1B1 activity in GIN-100 tissues after stimulus with TCDD (TCDD+CEE) or negative control (CEE). Abbreviations: CEE, luciferin; CYP, cytochrome P450; RLU, relative light units; TCDD, 2,3,7,8-tetrachlorodibenzo-p-dioxin.

6. Objectives

The objectives of the study were:

1. To assess if and after how long PBS apical exposure could induce alterations (cytotoxicity, osmotic stress, release of proinflammatory mediators) to the EpiGingival™ tissue model.

2. To determine the biological impact of THS2.2 aerosol exposure on a human organotypic gingival culture model, compared with that of 3R4F CS. The biological impact assessment was done by combining results obtained using well-known cellular and functional assays and those obtained using systems biology approaches (leveraging mRNA and miRNA profiles, as well as computational biology analyses).

   The biological impact of THS2.2 aerosol and 3R4F smoke exposure on the test system human organotypic gingival cultures was explored in terms of:
   - Dose-dependent responses of the test system after exposure to 3R4F CS and THS2.2 aerosol, to evaluate the toxicity or morphological changes in PBS-covered human gingival epithelium.
   - The impact of a THS2.2 aerosol and 3R4F CS repeated exposure at comparable concentrations on PBS-covered human organotypic gingival cultures, by assessing possible biological pathways/processes perturbed in the test system.

All of the above objectives were exploratory.

7. Experimental Design

7.1 Test and Reference Items

7.1.1 Identification and Description

THS2.2 and 3R4F were regarded as test and reference items, respectively (Table 3).

Table 3. Test and reference items.

Short Name	Description	Type
THS2.2	ZRH/DDA1/C3/CAST LEAF– CL/Flavor/Reynaldo	Test
3R4F	Conventional cigarettes	Reference

Information on the test item characteristics, including composition, stability, and homogeneity, was provided by the sponsor.

The 3R4F reference cigarette was purchased from the University of Kentucky (Kentucky Tobacco Research & Development Center). The specifications of the test and reference items used in this study are described in Table 4.

Table 4. Reference and test items used in experimental repetitions.

Week of Experiment	Part I: PBS Pilot	Part II: Dose Range Finding (DRF)	Part III: Main Phase (MP) I	Phase III: Metabolomics	Phase III: MP-II	Phase III: MP-III
	08 February 2016 – CW6	22 February 2016 – CW8	07 March 2016 – CW10	21 March 2016 – CW12	18 April 2016 – CW16	30 May 2016 – CW22
	Reference Item (3R4F)					
	Stick information					
Pack No.	V350Y61B5	V350Y61B5	V350Y61B5	V350Y61B5	V350Y61B5	V350Y61B5
Receiving Date	December 2014	December 2014	December 2014	December 2014	December 2014	December 2014
Expiry Date	May 2017	May 2017	May 2017	May 2017	May 2017	May 2017
	Test Item (THS2.2)					
	Stick information					
Stick Batch No.	THS2.2 Batch B-23862	THS2.2 Batch B-23862	THS2.2 Batch B-23862	THS2.2 Batch B-23862	THS2.2 Batch B-23862	THS2.2 Batch B-23862
Manufacture Date	12 October 2015	12 October 2015	12 October 2015	12 October 2015	12 October 2015	12 October 2015
Expiry Date	12 October 2016	12 October 2016	12 October 2016	12 October 2016	12 October 2016	12 October 2016
	Device Information for THS2.2					
Product Code	B-18731	B-18731	B-18731	B-18731	B-18731	B-18731
Receiving Date	27 February 2015	27 February 2015	27 February 2015	27 February 2015	27 February 2015	27 February 2015
Specific Description		Aerosol generation				
Batch Description		DC.000067.RD(1)/ZRH/FPD4.2/3.2.2/C28/FDP 4.2 Cigarette Holder/3.2.2 software upgrade/Configuration without forced-cleaning feature. Aerosol generation.				

7.1.2 Item Storage

After the items were received, they were stored in a refrigerator at 5 ± 3°C with uncontrolled humidity conditions in their original packaging.

7.1.3 Item Conditioning

All test items were conditioned between 7 and 21 days under controlled conditions at a temperature of 22 ± 1°C and a relative humidity of 60 ± 3%, according to ISO guidelines, to comply with the ISO standard 3402.

7.1.4 Carbonyl Concentrations Deposited in the Vitrocell Base Module Following Whole Smoke/Aerosol Exposure

Figure 2 shows the amount of representative carbonyls deposited in the base module of the Vitrocell® 24/48 exposure system following exposure to the reference CS and test item aerosols at the corresponding target nicotine concentrations used in this study (i.e., the concentrations applied in the four experimental repetitions, described in section Sample Generation: Experimental Repetitions)

The descriptive statistics that report the values obtained in every sampling are given in Supplementary Tables 1–8.

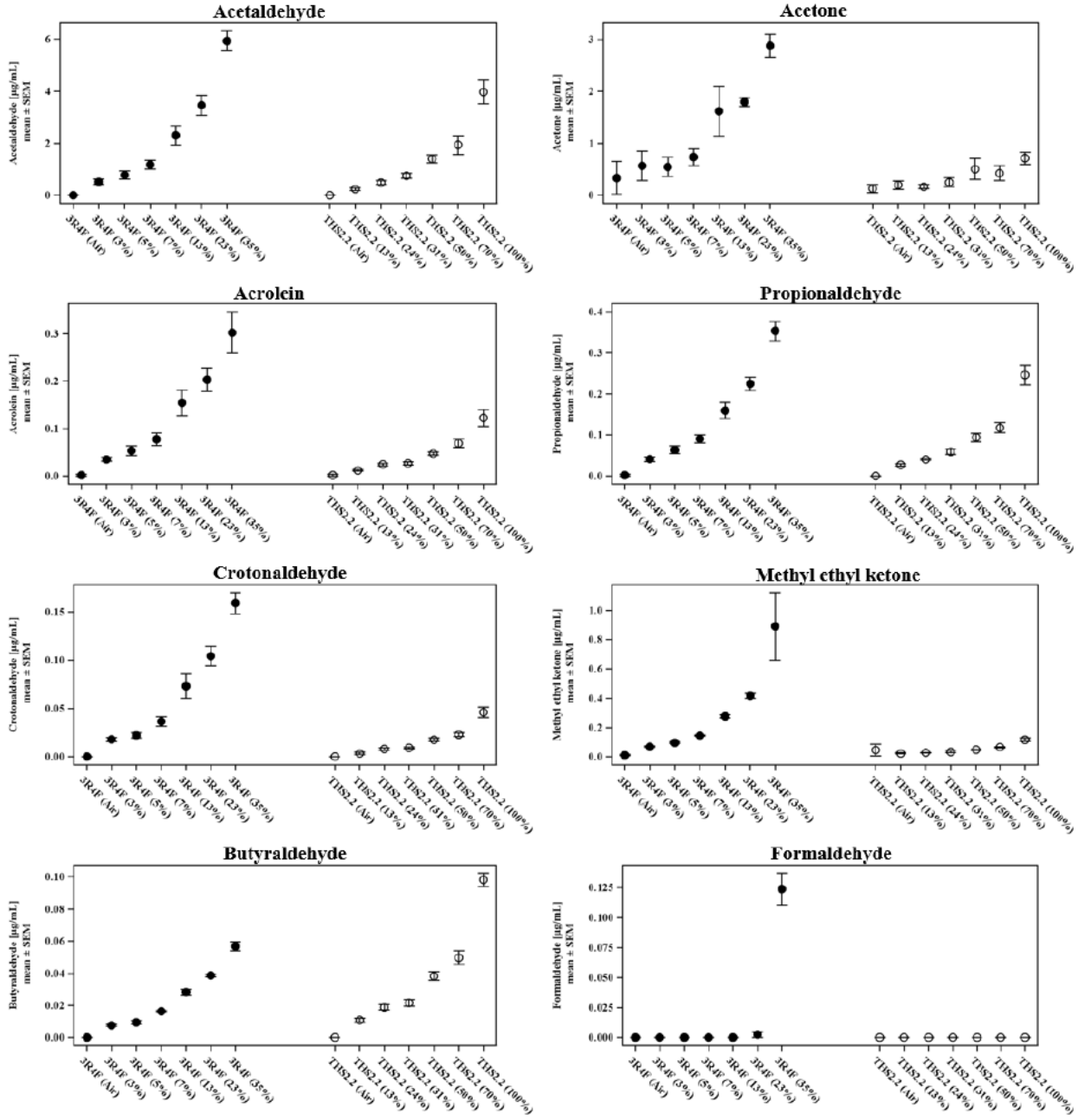

Figure 2. Concentrations of representative carbonyls deposited in the cultivation base module of Vitrocell 24/48 exposure system following exposures to 3R4F cigarette smoke (CS) and test item aerosol.

The mean of a carbonyl in phosphate-buffered saline (PBS)-filled inserts (µg/mL) ± SEM (N=2; two samplings from 2016 and one from 2015) are shown. The PBS-filled inserts were placed in the cultivation base module of the Vitrocell 24/48 exposure system and exposed to 3R4F smoke or THS2.2 aerosol according to the concentrations used in this study.

Representative carbonyls are shown. The descriptive statistics that report the values obtained in each sampling are given in Supplementary Tables 1–8. Abbreviations: N, number of samples; SEM, standard error of the mean.

7.2 Test System

7.2.1 Organotypic Culture Model

The human organotypic EpiGingival culture (product code Gin-100, MatTek Corp., Ashland, MA, USA) was used as the test item for this study. The gingival epithelial cells used throughout the study were isolated from the same donor, a healthy non-smoking male aged 46 years. Table 5 summarizes the information provided in the certificates from the supplier. The cells were covered by 100 µL PBS on the apical side, to mimic the natural moistening of the saliva *in vivo*, and cultured with 0.7 mL medium in 24-well plates with Transwell® inserts (6.5 mm diameter, 0.4 µm pore size, Greiner Bio-One, Monroe, NC, USA). Upon delivery, the oral cultures were grown for 14 days after seeding. The tissues were cultured at the ALI and maintained in-house at 37°C for 3 days before exposure experiments, to complete the differentiation with fresh medium (GIN-100-DM4a, MatTek) according to the supplier's instructions (PMI_RD_WKI_001064).
After differentiation, the organotypic cultures were incubated in maintenance medium (GIN-100-MM, MatTek). Both media used in the study (differentiation and maintenance) were produced by MatTek and their compositions have not been disclosed to the public. Three days after arrival, organotypic cultures were exposed to 3R4F CS or THS2.2 aerosol according to the experimental plan. After exposure, the tissues were placed in fresh media. For the AK assay and the collection of proinflammatory mediators, the medium was collected and frozen before the second and third exposure and at the final collection time-point. Throughout the studies, the cultures were regularly inspected microscopically, to check for potential morphological changes, as well as bacterial or fungal contamination.

Table 5. Specifications of the different batches of organotypic gingival culture used in the experimental repetitions.

	PBS Pilot	Dose Range Finding (DRF)	Main Phase (MP) I	Metabolomics	MP-II	MP- III
Week of Experiment	**08 February 2016**	**22 February 2016**	**07 March 2016**	**21 March 2016**	**18 April 2016**	**30 May 2016**
Culture Delivery Date	05 February 2016	19 February 2016	04 March 2016	18 February 2016	15 April 2016	27 May 2016
Lot No.	22971	22975	22977	22985	22998	24023
Cell Type	Gingival	Gingival	Gingival	Gingival	Gingival	Gingival
Donor's Age	46	46	46	46	46	46
Donor's Sex	Male	Male	Male	Male	Male	Male
Donor's Origin	NA	NA	NA	NA	NA	NA
Donor's Smoking Status	Non-smoker	Non-smoker	Non-smoker	Non-smoker	Non-smoker	Non-smoker
Donor's Pathology Status	None reported	None reported	None reported	None reported	None reported	None reported
Sterility	Yes	Yes	Yes	Yes	Yes	Yes
Morphology	Normal	Normal	Normal	Normal	Normal	Normal
HIV-1	Negative	Negative	Negative	Negative	Negative	Negative
Bacteria, Yeast, Fungi	Negative	Negative	Negative	Negative	Negative	Negative
Hepatitis B	Negative	Negative	Negative	Negative	Negative	Negative
Hepatitis C	Negative	Negative	Negative	Negative	Negative	Negative
Certificate of Analysis (CoA)	CoA_PBS_Pilot	CoA_DRA	CoA_Experiment 1	CoA_Metabolomics	CoA_Experiment 2	CoA_Experiment 3

On each delivery day, we monitored the quality of the organotypic gingival culture batch by analyzing hematoxylin and eosin (H&E)-stained tissue sections of incubator controls (data not shown). Abbreviations: NA, not available; PBS, phosphate-buffered saline.

7.3 Experimental Plan

The study can be divided into three sections:

1. **PBS Pilot** to assess the effects of PBS apical exposure to gingival tissue over a 96-h time frame (Figure 3A).
   Note that the results from this section are only indicative. Although the biological replicates were 5 per condition, the number of technical replicates is equal to one, being the pilot experiment performed once.
2. **Dose Range Finding (DRF, also indicated as DRA in this document)**. Organotypic gingival cultures were exposed for 3 consecutive days to a broad range of 3R4F CS or THS2.2 aerosol concentrations for 28 min. Before each exposure, the basolateral medium was collected for different assays (AK and MAP) and replaced with fresh medium; apical PBS was also replaced before each exposure. Different endpoints were analyzed at the indicated time-points. The aim was to evaluate the concentrations of 3R4F CS and THS2.2 aerosol at which toxicity or morphological changes were observed (Figure 3B).
3. **Main Phases (MPs) + Metabolomics**. Organotypic gingival cultures were exposed for 3 consecutive days to different concentrations of 3R4F CS or THS2.2 aerosol selected from the DRF. Different endpoints were analyzed at the indicated time-points to determine the biological impact of THS2.2 aerosol and combustible 3R4F CS exposure at comparable concentrations. The MP was repeated three times (Figure 3C).
   For the metabolomics phase, only the high concentrations were applied (84.6 and 100.4 mg/L for 3R4F CS and THS2.2 aerosol, respectively).

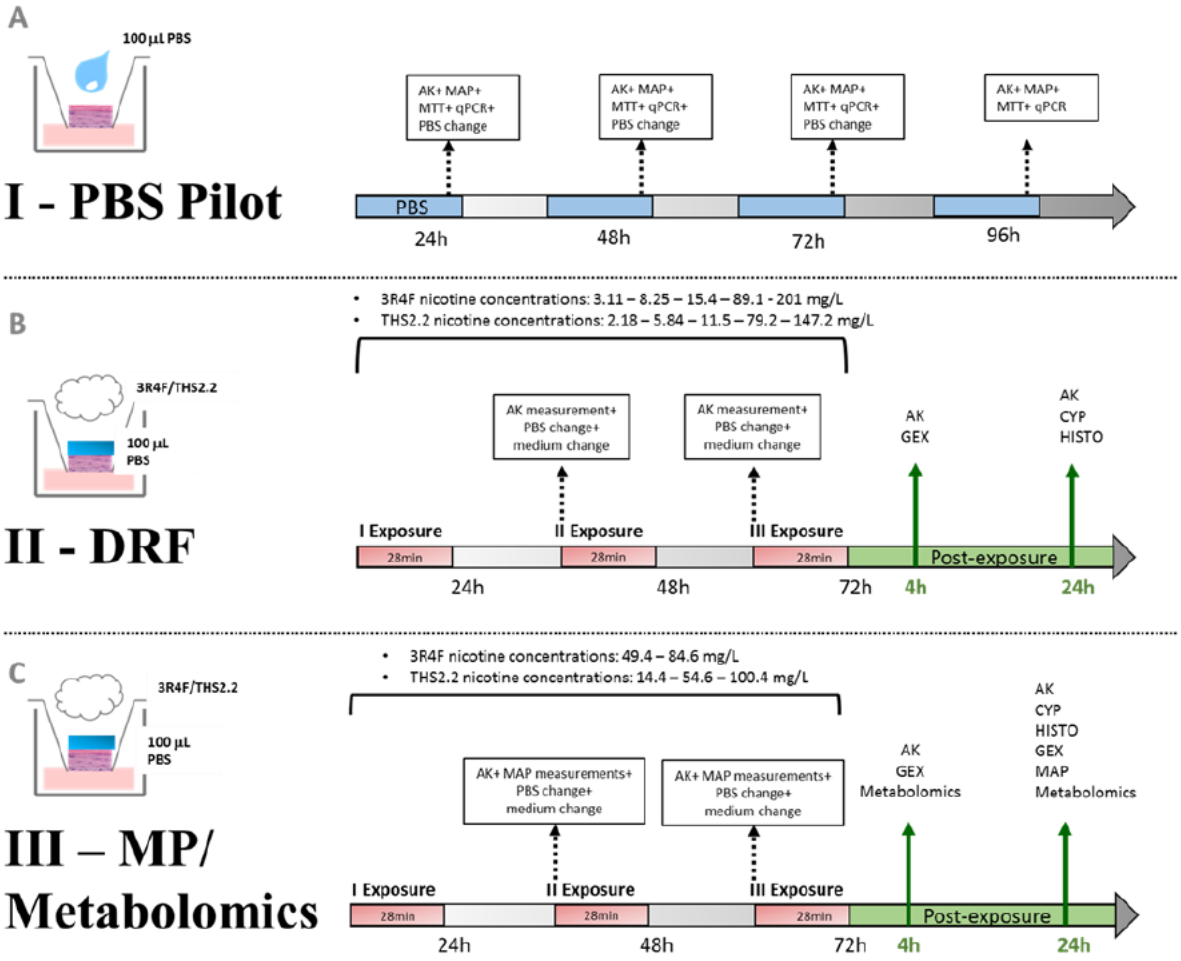

Figure 3. Study design.

(**A**) Organotypic gingival cultures were exposed for 4 days to phosphate-buffered saline (PBS) and (**B**, **C**) for 28 min on 3 consecutive days to 3R4F cigarette smoke (CS) or THS2.2 aerosol (at indicated concentrations). Before each exposure, the basolateral medium was collected for different assays (AK and MAP) and replaced with fresh medium; apical PBS was also replaced before each exposure. Different endpoints were analyzed at the indicated time-points during the three phases. Abbreviations: AK, adenylate kinase; DRF, dose range finding; GEX, gene expression for mRNA/miRNA analysis; HISTO, histological analysis; MAP, secreted inflammatory cytokine measurement; MP, main phase (repeated three times). For the metabolomic phase, only the highest CS and aerosol concentrations were applied.

7.3.1 Experimental Repetitions: The Impact Assessment of THS2.2 Aerosol Compared with 3R4F Smoke Exposure

The study to assess the biological impact of THS2.2 aerosol compared with 3R4F CS exposure on a human organotypic gingival culture model comprised three main phases and an exploratory metabolomic phase. During each of the three main phases, the cultures were exposed to the reference item 3R4F CS or test item THS2.2 aerosol. We used nicotine as the internal compound to normalize and compare the effects of 3R4F CS and THS2.2 aerosol on the cultures (Table 6).
We extrapolated the values of nicotine from the DRF phase, where broader concentrations of 3R4F CS and THS2.2 aerosol were tested (Table 7). We selected two 3R4F CS and THS2.2 aerosol concentrations, each pair-matched for the delivered nicotine doses, for the comparative analysis. By diluting 3R4F CS with air to 25% we obtained an average concentration of 49.4 mg nicotine/L in the 0.1 mL PBS volume. This lower concentration of 3R4F CS was selected to achieve moderate damage, allowing the assessment of effects relevant to toxicity-related mechanisms associated with exposure. To match, the THS2.2 aerosol was diluted with air to 75%, resulting in a delivered dose of 54.6 mg nicotine/L (low matching concentration) (Table 6). The highest concentration was selected to reflect morphological alterations associated with severely damaged tissue. For this high matching concentration, 3R4F CS was diluted to 35% yielding a deposited dose of 84.6 mg nicotine/L, and THS2.2 aerosol was applied undiluted (100%), corresponding to 100.4 mg nicotine/L.

Important note: The lowest THS2.2 concentration (14.4 mg/L) did not match any of the 3R4F CS concentrations because of a problem ascribable to the DRF phase (for details, see Section 3).

Table 6. Target nicotine concentrations in the smoke/aerosol (mg nicotine/L) applied in the study.

	Experiment Week				
	Main Phase (MP) I	Metabolomics	MP- II	MP- III	
	07 March 2016	21 March 2016	18 April 2016	30 May 2016	
Group name of 3R4F-exposed cultures	**mg nicotine/L smoke**	**mg nicotine/L smoke**	**mg nicotine/L smoke**	**mg nicotine/L smoke**	**Smoking Machine**
Air Control (3R4F)	0.0125	0.154	0.0125	0.944	SM-2000
3R4F (49.4)	56.216	NA	48.602	43.539	
3R4F (84.6)	87.227	82.727	88.313	78.162	
Exposure Run Number	3	6	3	3	
Group name of THS2.2-exposed cultures	**mg nicotine/L smoke**	**mg nicotine/L smoke**	**mg nicotine/L smoke**	**mg nicotine/L smoke**	**Smoking Machine**
Air Control (THS2.2)	0.0125	0.112	0.0125	0.662	SM-2000 THS2.2
THS2.2 (14.4)	13.842	NA	15.807	13.650	
THS2.2 (54.6)	55.010	NA	51.151	57.649	
THS2.2 (100.4)	107.818	101.175	88.338	105.023	
Exposure Run Number	3	5	3	3	

Abbreviation: NA, not available.

Table 7. Dilutions of aerosol (%) applied and endpoints tested in the DRF.

Group concentration (mg/L)	DRF Experiment Week: 10 August 2015	Endpoint Measured 24 h Post-Exposure		Smoking Machine
	Aerosol Concentration (%)	Cytotoxicity (N)	Tissue Histology (N)	
3R4F (Air)	**0**	(3)	(3)	SM-2000
3R4F (3.11)	**5**	(3)	(3)	
3R4F (8.25)	**10**	(3)	(3)	
3R4F (15.4)	**20**	(3)	(3)	
3R4F (89.1)	**40**	(3)	(3)	
3R4F (201)	**50**	(3)	(3)	
THS2.2 (Air)	**0**	(3)	(3)	SM-2000 THS2.2
THS2.2 (2.18)	**10**	(3)	(3)	
THS2.2 (5.84)	**20**	(3)	(3)	
THS2.2 (11.5)	**35**	(3)	(3)	
THS2.2 (79.2)	**75**	(3)	(3)	
THS2.2 (147.2)	**100**	(3)	(3)	

Numbers in brackets indicate the total number of paired samples collected for the indicated endpoints. Abbreviation: N, number of replicates.

7.4 Sample Generation

Smoke from the reference item (3R4F) was generated using a 30-port carousel smoking machine (SM-2000, Philip Morris International, Neuchâtel, Switzerland). Aerosol from the test item (THS2.2) was generated using a modified 30-port carousel smoking machine (SM-2000 THS2.2, Philip Morris International). Each of the smoking machines was connected to a Vitrocell® 24/48 exposure system (Vitrocell Systems GmbH, Waldkirch, Germany), where the culture inserts were exposed.
The Vitrocell exposure system is equipped with a dilution system. To achieve the desired concentrations of nicotine, the smoke and aerosol were diluted with fresh air. Figure 4 illustrates the setup of the exposure run for 3R4F and THS2.2, applying the concentrations described in Table 6.

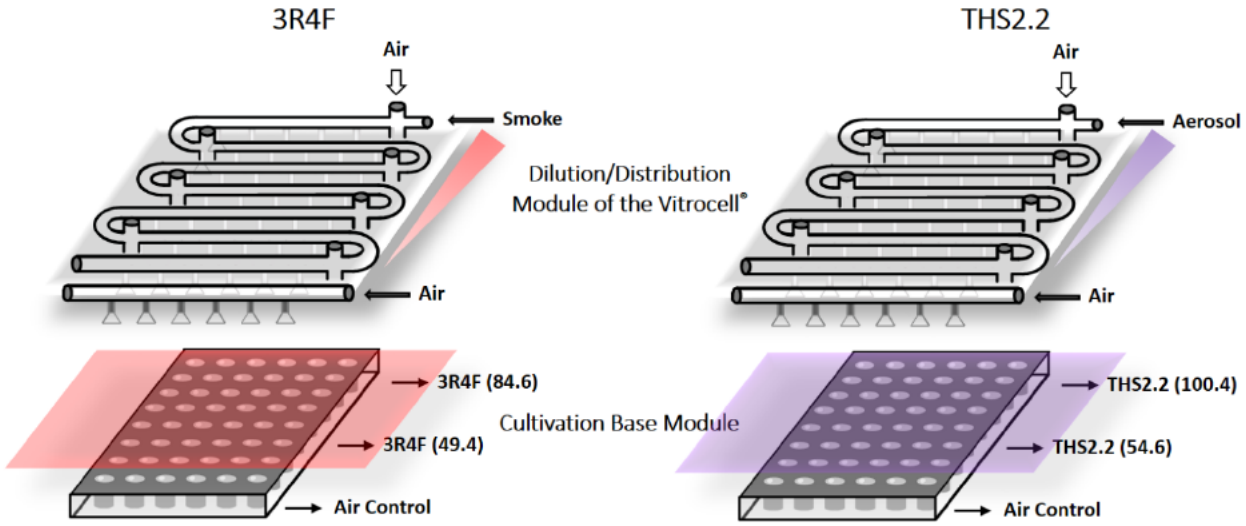

Figure 4. Scheme of an exposure run for 3R4F and THS2.2.
A dilution/distribution module of the Vitrocell 24/48 exposure system located on top of a cultivation base module is illustrated. Each Vitrocell 24/48 exposure system was connected to a smoking machine (SM) ("SM-2000" for 3R4F smoke exposure and "SM-2000 THS2.2" for THS2.2 aerosol exposure). In the base module, up to 48 wells (culture inserts) can be simultaneously exposed in a single run. Diluted whole smoke and aerosols were delivered through individual trumpets to each well. An exposure run consisted of the applied target concentration (mg/L) paired with its air control.

In each of the four experimental repetitions (three main phases + Metabolomics), various endpoints were measured 4 h and 24 h post-exposure, for each applied concentration and air control (Table 8). The results reported in this document were calculated from the aggregated data obtained from main phases I–III.

Table 8. Post-exposure endpoints.

Experimental Week		Cytotoxicity**		Gene Expression/ Microarray		Secreted Pro-Inflammatory Mediators**		CYP1A1/1B1 Activity		Histology		Metabolomics	
		Post-exposure (h)		Post-exposure (h)		Post-exposure (h)		Post-exposure (h)		Post-exposure (h)		Post-exposure (h)	
		4	24	4	24	4	24	4	24	4	24	4	24
Exp 1	**07 March 2016**	(3)	(3)	(3)	NA	NA	(3)	NA	(3)	NA	(3)	NA	NA
Exp 2	**18 April 2016**	(3)	(3)	(3)	NA	NA	(3)	NA	(3)	NA	(3)	NA	NA
Exp 3	**30 May 2016**	(3)	(3)	(3)	(3)	NA	(3)	NA	(3)	NA	(3)	NA	NA
Metabolomics	**21 March 2016**	NA	NA	NA	NA	NA	NA	NA	NA	NA	NA	(5)*	(5)*

Numbers in parentheses indicate the total number of paired samples collected for the indicated endpoints per post-exposure time-point at any given experimental repetition. One exposure run consisted of the applied target concentration(s) paired with air controls (N=1 paired sample per run, for any given endpoint and post-exposure time-point). * Only high comparable concentrations. ** Intermediate time-points were collected for cytotoxicity and secreted proinflammatory mediators 24 h after each exposure (see section 7.3). Abbreviations: CYP, cytochrome P450; Exp, experiment; h, hours; NA, not available (i.e., endpoints were not generated/collected at the indicated experimental repetition).

7.5 Testing Procedure

7.5.1 Apical Exposure of EpiGingival™ Tissues to PBS

EpiGingival™ cultures were covered with 100 µL PBS (D8662 with calcium and magnesium, Sigma-Aldrich, St. Louis, MO, USA). PBS was replaced every 24 h until 96 h for the pilot section and until the selected time-point for the main phases and metabolomic sections. During DRF and the main phases, PBS was kept on the apical surface of the gingival culture after exposure and changed before the following exposure, after 24 h.

7.5.2 Aerosol/Smoke Generation and *In Vitro* Exposure Regimens

Reference smoke were generated from 3R4F reference cigarettes (University of Kentucky, www.ca.uky.edu/refcig) using a 30-port carousel smoking machine type SM2000 (Philip Morris International) with a programmable dual syringe pump (PDSP) connected to the Vitrocell® 24/48 (Vitrocell® Systems GmbH). Another 30-port carousel smoking machine with a PDSP was used to generate the test aerosol from the candidate MRTP (THS2.2). The reference smoke and the test aerosol were generated according to PMI_RD_WKI_001145 and PMI_RD_WKI_001155, respectively.

The reference smoke and test aerosol were generated according to the Health Canada Intense protocol with a puff volume of 55 mL, puff duration of 2 sec, and a puff frequency of 2 puffs per min. Supplementary, the ventilation holes of the reference cigarette were blocked by installing special Health Canada (HC) mouthpieces into the carousel of the SM2000. As a special requirement for the Vitrocell® 24/48, the exhaust time from the PDSP was set to 8 sec.

For the exposure experiments, each 3R4F cigarette was smoked to a mean butt length of 35 ± 1 mm, and each THS2.2 stick was aerosolized with a pre-defined puff count of 12 puffs per stick. Before starting the 28-min exposure experiment, a pre-smoke/aerosol phase was implemented to get a steady state for both smoking machines. During the exposure experiment itself, approximately 10 3R4F cigarettes were smoked and approximately 10 THS2.2 sticks were aerosolized using the dedicated smoking machine.

7.5.3 Nicotine Determination in PBS Exposed to Whole Smoke/Aerosol

Nicotine deposition was measured in PBS-exposed samples. Briefly, 100 µL of PBS were placed into steel inserts and exposed to 3R4F CS or THS2.2 aerosol using the Vitrocell system. The nicotine concentrations were measured using an LC-HRAM-MS (Q Exactive™, Thermo Fisher Scientific, Waltham, MA, USA). An LC-HRAM-MS is a multi-analyte method in full-scan positive electrospray ionization mode, using two sequential analytical columns (strong anion exchange/polymer backbone reversed phase). Quantification was performed by calibration curves of the analytes with stable isotope-labeled internal standards for each analyte or analyte group. d3-Nicotine was used as the internal standard for the determination of nicotine (PMI_RD_WKI_001066, PMI_RD_WKI_000409).

7.5.4 Carbonyl Concentrations Deposited in the Vitrocell Base Module Following Whole Smoke/Aerosol Exposure

The deposition of representative carbonyls was measured in PBS following a 28-min exposure to whole smoke or test aerosol (10–12 sticks per item, each smoked/aerosolized by applying a modified Health Canada Intense puffing protocol of a 55-mL puff over 2 sec, twice per min, with an 8-sec pump exhaust time) (PMI_RD_WKI_001094). Briefly, before exposure, each row in the cultivation base module of the Vitrocell 24/48 system was filled with 18.5 mL PBS. Following exposure, an aliquot of 1.2 mL PBS-exposed sample (per row) was collected and mixed with 1.8 mL 2,4-dinitrophenylhydrazine solution (15 mM). Subsequently, 150 µL pyridine were added to quench the chemical derivatization. From this mixture, a 500-µL aliquot was placed into a liquid chromatography-mass spectrometry (LC-MS) amber glass vial. After 30 min, 485 µL acetonitrile and 15 µL internal standard mixture (24 µg/mL acetone-d6 and 21 µg/mL methyl ethyl ketone-d5) were added. Finally, 5 µL of the mixture were injected into a high-performance liquid chromatography (HPLC) instrument coupled with a tandem MS (HPLC-MS/MS) to determine the quantity of the analytes using an isotope dilution technique.

7.5.5 Maintenance of EpiGingival™ 3D-Organotypic Cultures (Air-Liquid Interface Cultures)

Upon arrival, human organotypic gingival cultures (EpiGingival™, MatTek Corporation) were handled under sterile conditions under the hood (PMI_RD_WKI_001064). The tissues were cultured at the ALI in a pre-warmed 37°C EpiGingival™ differentiation medium (GIN-100-DM4a, 5.5 mL/well in sterile modified two-hole tops and 12-well plates) according to the supplier's instructions. After 3 days, the cultures were fully differentiated and 5.5 mL/well fresh supplemented maintenance medium (GIN-100-MM, provided by MatTek Corp) was used to maintain the culture according to the supplier's guidelines. After the exposure to smoke or aerosol, the inserts were placed in 24-well plates with 0.5 mL/well of GIN-100-MM. After each exposure, the tissues were placed in fresh media.

7.5.6 Adenylate Kinase (AK) Cytotoxicity Assay

AK release was used as a marker for cytotoxicity. AK was sampled 24 h after the first and second exposures and 4 h or 24 h after the third, according to the Experimental Plan. The ToxiLight™ bioassay kit (Lonza, Basel, Switzerland) was used to determine cytotoxicity upon aerosol exposure of 3D-organotypic cultures (PMI_RD_WKI_001048). For this, 20 µL of basolateral medium were transferred to the well of a luminescence-compatible 96-well microtiter plate and mixed with 100 µL AK detection reagent. After 5 min of incubation, luminescence was measured using a FluoStar Omega reader (BMG Labtech GmbH, Ortenberg, Germany). The three aliquots collected at the different time-points were measured independently, and the AK values were then summed to indicate cumulative cytotoxicity over the entire experimental session. The AK values were calculated by normalizing the mean of the positive control (cultures treated with 1% Triton X-100 for 24 h at the basolateral side) and negative control (untreated cultures). AK values from samples treated with 1% Triton X-100 were considered to be 100% cytotoxicity (complete lysis of the cells).

7.5.7 Methyl Thiazolyl Tetrazolium (MTT) Metabolic Assay

Seven hundred microliters of 3-(4,5-dimethylthiazole-2-yl)-2,5-diphenyl tetrazolium bromide (MTT) solution (1 mg/mL) were added to each well. Tissues were incubated in MTT at 37°C for 3 h. After the MTT reaction, the tissue inserts were blotted on dry absorbent paper, cleared of excess liquid, and

then transferred to a second 24-well plate containing 1 mL of isopropyl alcohol (0.5 mL on the apical side and 0.5 mL in the basal-side medium) to stop the reaction and extract the formazan. The 24-well plate was sealed in a plastic bag, and the extraction was allowed to proceed for 2 h at room temperature in the dark. Afterwards, 200 µL of the formazan extract were quantified by measuring optical density (OD) at 570 nm using a FluoStar Omega reader (BMG Labtech GmbH).

7.5.8 Cytochrome P450 (CYP) 1A1/1B1 Activity Assay

The activity of CYP1A1/CYP1B1 (combined) was determined using the non-lytic P450-Glo™ assay (Promega, Madison, WI, USA), according to the manufacturer's instructions (PMI_RD_WKI_001049; PMI_RD_FOR_000846). Briefly, the luminogenic CYP-Glo substrate luciferin-6′ chloroethyl ether (luciferin-CEE), which is a substrate for both CYP1A1 and CYP1B1, was added to the basolateral medium 24 h prior to sample collection. For this reason, it was not possible to measure the CYP1A1/1B1 activity at the 4-h post-exposure time-point. The luciferin product of the CYP reaction was detected by mixing 50 µL of the collected medium with 50 µL of Luciferin Detection Reagent. After 20 min of incubation at room temperature, luminescence was measured in a FluoStar Omega reader (BMG Labtech GmbH). For each of the three experimental repetitions, three organotypic culture inserts were treated with 30 nM 2,3,7,8-tetrachlorodibenzo-p-dioxin (TCDD) as a positive control, which was added to the basolateral medium 48 h before sample collection and replenished after 24 h. Three other inserts per experimental repetition were treated with PBS in the basolateral medium, as negative controls (0% activity).

7.5.9 Measurements of Secreted Inflammatory Mediators

The measurement of secreted proinflammatory mediators was performed 24 h after the first two exposures and 24 h after the third exposure (Experimental Plan), by collecting 200-µL aliquots of the basolateral medium from EpiGingival™ cultures (PMI_RD_SOP_000361; PMI_RD_WKI_001032; PMI_RD_WKI_001273, PMI_RD_WKI_001450, PMI_RD_WKI_001274; PMI_RD_FOR_000803). Luminex® xMAP® technology was used for the analysis (Luminex, Austin, TX, USA), along with commercially available assay panels (Milliplex®, EMD Millipore Corp., Schwalbach, Germany), as outlined in Table 9, according to the manufacturer's instructions. Briefly, 25 µL of diluted or non-diluted sample were used for each detection, and the analysis was run on a Luminex® xMAP® instrument (Luminex). Data are represented as median fluorescent intensity (MFI) units using a five-parameter logistic or spline curve-fitting method for calculating the analyte concentrations in the basal medium sample. As a positive control, EpiGingival™ inserts were treated for 24 h with tumor necrosis factor alpha (TNFα) and interleukin 1 beta (IL1β) (PMI_RD_FOR_000849), each added to the basolateral medium at a final concentration of 10 ng/mL, to induce secretion of (majority) mediators targeted by the MAP analysis. As a negative control, a second set of triplicate samples was treated for 24 h with PBS in the basolateral medium. Whenever measured concentrations fell below the limit of quantitation, a constant value was used (i.e., half of the lower limit of detection).

Table 9. Summary of Milliplex kits used in the experimental repetitions.

	PBS Pilot	Main Phase I	Main Phase II	Main Phase III
Experiment Week	**08 February 2016**	**07 March 2016**	**18 April 2016**	**30 May 2016**
GRO/CXCL1	A	A	A	A
CFS3/G-CSF	A	A	A	A
CSF2/GM-CSF	A	A	A	A
IL1α	A	A	A	A
IL1β	A	A	A	A
IL6	A	A	A	A
CXCL8/IL8	A	A	A	A
CXCL10/IP-10	A	A	A	A
CCL2/MCP-1	A	A	A	A
CCL5/RANTES	A	A	A	A
VEGF	A	A	A	A
TNFα	A	A	A	A
MMP-1	B	B	B	B
MMP-9	B	B	B	B

Milliplex kits were purchased from EMD Millipore Corp. **A**, custom panel HCYTOMAG-60K-12; **B**, custom panel HMMP2MAG-55K-02. Abbreviations: CCL, chemokine (C-C motif) ligand; CSF, colony-stimulating factor; CXCL, chemokine (C-X-C motif) ligand; G-CSF, granulocyte colony-stimulating factor; GM-CSF, granulocyte-macrophage colony-stimulating factor; GRO, melanoma growth-stimulating activity alpha; IL, interleukin; IP-10, interferon gamma-induced protein 10; MCP-1, monocyte chemoattractant protein-1; MMP, matrix metalloproteinase; RANTES, regulated on activation, normal T-cell expressed and secreted; TNFα, tumor necrosis factor alpha; VEGF, vascular endothelial growth factor.

7.5.10 Tissue Processing, Embedding, Sectioning, and Staining

Histological assessment was performed 24 h after the last exposure to 3R4F CS or THS2.2 aerosol. Tissue inserts were washed three times with PBS and fixed for 2 h in freshly prepared 4% paraformaldehyde (PMI_RD_WKI_001242). Upon completion of the fixation, the fixative was aspirated and the fixed gingival cultures were washed three times with PBS both apically and basally at room temperature. Following this process, the fixed tissues were separated from the inserts by detaching the membrane from the plastic using forceps, and bisected at the midpoint prior to processing using a Leica ASP300 S tissue processor (Leica Biosystems) (PMI_RD_WKI_001243). Subsequently, the two sections (per tissue sample) were placed in a cassette for embedding in paraffin (PMI_RD_WKI_001260). Microscopy sections of the paraffin block (5-µm thickness) were obtained using a microtome (PMI_RD_WKI_001262) and mounted on glass slides that were then transferred to a Leica ST5020 automated slide stainer (Leica Biosystems) for staining with hematoxylin (Merck Millipore) and eosin (Sigma-Aldrich) (PMI_RD_WKI_001266, PMI_RD_WKI_001309). The stained slides were covered with a glass coverslip using a Leica CV5030 fully automated coverslipper (Leica Biosystems).

For immunohistochemical staining, slides were incubated at 60°C for a minimum of 30 min. They were then transferred to the Leica Bond-Max autostainer for immunohistochemistry using Leica Bond™ Polymer Refine Detection Kit (DS9800). The slides were treated with EDTA, incubated with an E-cadherin antibody (Leica Biosystems PA0387, undiluted) and counterstained with hematoxylin.

Three slides per condition/experimental replicate were stained. A Hamamatsu NanoZoomer slide scanner (Hamamatsu Photonics, K.K., Hamamatsu City, Japan) was used to generate digital images of each slide. Images were acquired at 10×, 63×, and 100× magnification (PMI_RD_WKI_001314).

7.5.11 Morphological Assessment of H&E-stained Tissue Sections

The digital images of the H&E-stained sections were independently assessed in a blinded manner by (b) (4) (London, UK). Briefly, the two bisected pieces per tissue sample (per slide) were examined simultaneously, and one unique description was reported for one sample. The microscopic findings were recorded during the evaluation and entered manually into Excel spreadsheets (Microsoft, Redmond, WA, USA). Various histological features were selected for the systematic histological assessment of each section (Table 10). The evaluation of the findings was described with patterns (0–5), resembling specific features as described in Table 11. The results were reported in a Report.

Table 10. Outline for the systematic assessment of histological features in gingival epithelial tissue sections.

Finding	Explanation	Representative Image of the Finding (Gingival)
Assessment of layers	Measurement of cornified layer as a percent of the whole. SC: Stratum corneum SG: Stratum granulosum (granular layer) SS: Stratum spinosum SB: Stratum basale M: membrane Layers are discrete.	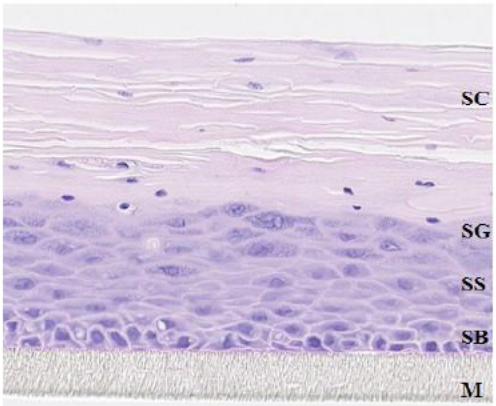
Apoptosis	Single-cell degeneration.	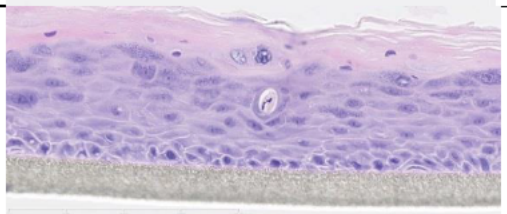
Artefact at tissue border	Alterations found to be systematically present and deemed to be unlikely associated with the exposure. Uniformly present.	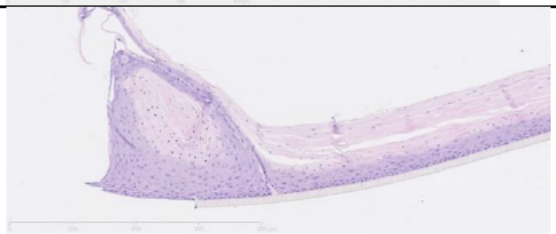

Table continues

Atrophy	Thinning of non-keratinized portion of epithelium (lower layers) or whole epithelium.	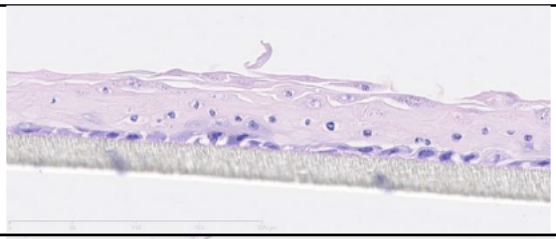
Atypia	Nuclear irregularity, abnormal chromatin, and increased nuclear-to-cytoplasmic ratio.	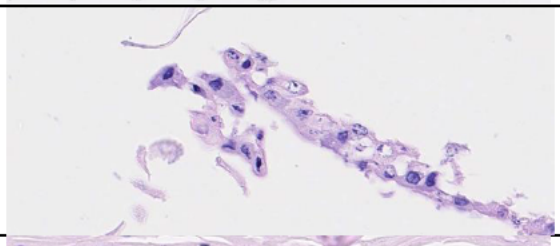
Cell degeneration, including apoptosis/karyorrhexis	Degeneration of cells, often seen with fragmentation and vacuolation of cytoplasm and breakup of nuclei.	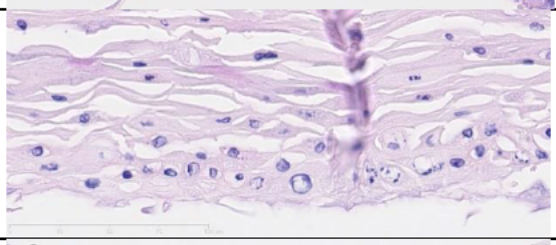
Corrugations	Parallel ridges or grooves in the culture perpendicular to the long axis. (Tissue was lifted from slide and scanned in a different plane to adherent epithelium). A very common artefact. Occasionally, the scan focused on the smaller corrugations so much of the culture was blurred.	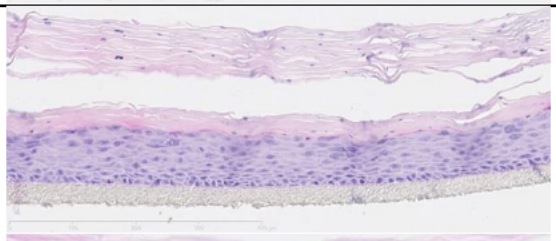 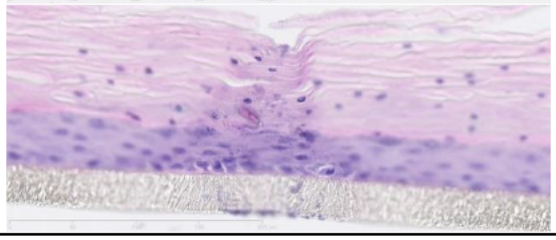
Dyskeratosis	Abnormal single-cell keratinization.	Not seen in this study.
Epithelial detachment from membrane	Seen as an artefact (upper image) or as an abnormal finding due to reduced culture integrity in damaged epithelium (lower image).	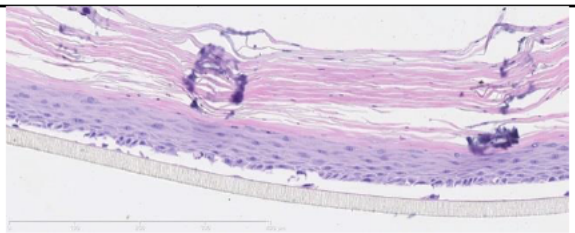 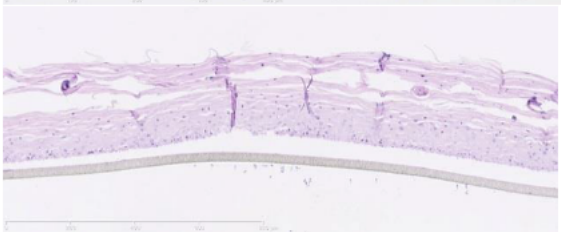

Table continues

Epithelial disintegration and splits within epithelium (not within normal stratum corneum)	Loss of cell cohesion and fragmentation within damaged epithelium.	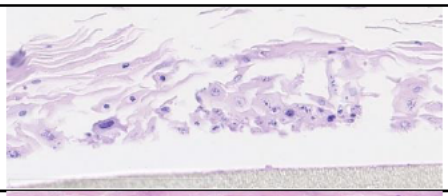
Hypergranulosis	Increased keratohyaline granules, included span within tissue and mainly increased coarseness.	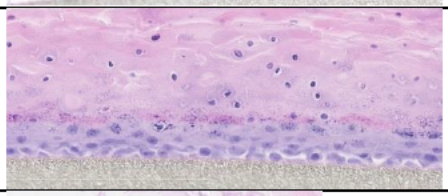
Keratin pearls	Abnormal rounded keratinized structure with concentric layers of keratinization.	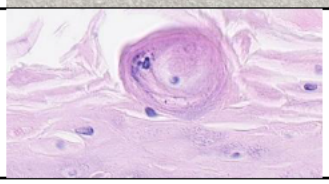
Mineralization	Typical abnormal (dystrophic) calcification – mentioned in guidelines on oral mucosa assessment.	Not seen in this study.
Mitosis	Present within basal layer in control epithelium and above basal layer in damaged/regenerating epithelium.	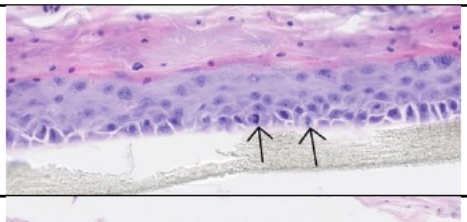
Parakeratosis	Excess persistence of nuclei within keratinized epithelium.	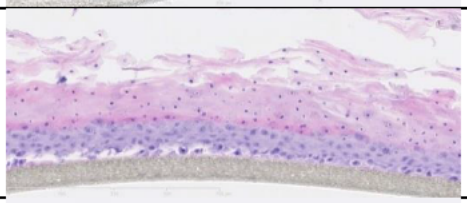
Split within stratum corneum (intracorneal split)	Separation of keratin layers, as one or more splits, more common when keratin is less compact – uniformly present.	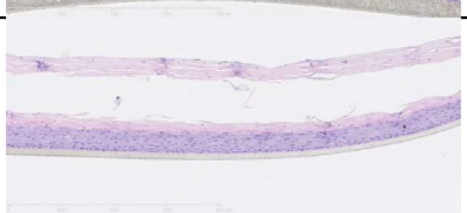
Vacuolation	Nuclear clearing. Seen as an artefact at the edge (top image), and also as a finding within degenerative epithelium (bottom image).	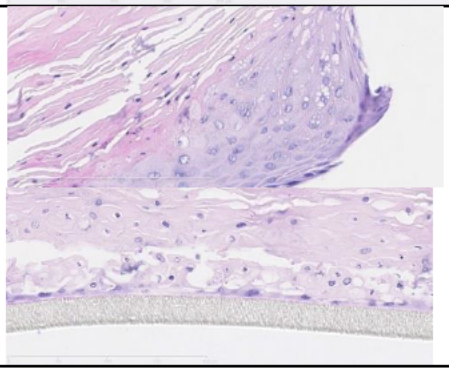

End of the Table

Table 11. Morphological assessment pattern of evaluation.

Finding	Explanation	Representative Image of the Pattern
Pattern 0 Normal (control)	Well-delineated layers, occasional mitosis and apoptosis noted.	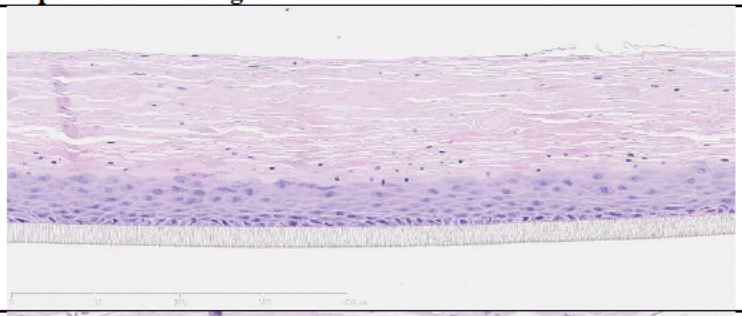
Pattern 1	Mild alteration leading to blurring of the distinction between the stratum granulosum and the stratum corneum. This resulted in increased keratinization of the stratum granulosum and pyknosis of nuclei, so the sharp cutoff was diminished.	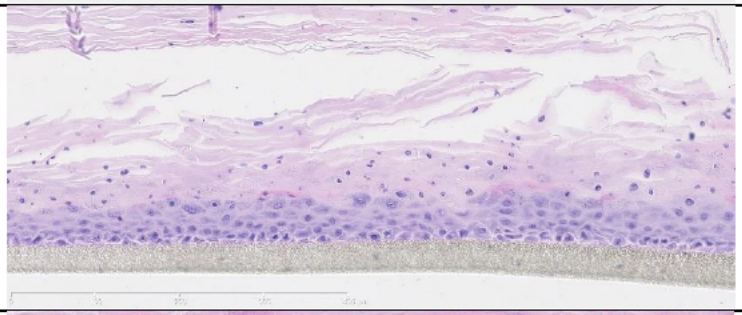
Pattern 2	More-pronounced blurring of and loss of distinction between the stratum granulosum and the stratum corneum, with or without hypergranulosis and with keratohyaline granules straddling both the stratum granulosum and the stratum corneum. The stratum spinosum (prickle layer) may be slightly thinned (atrophy), but shows no overt apoptosis.	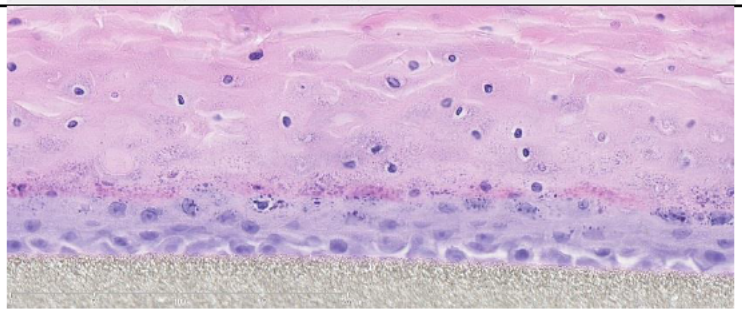
Pattern 3	Pronounced blurring of and loss of distinction between the stratum granulosum and the stratum corneum, typically with hypergranulosis and with keratohyaline granules straddling both the stratum granulosum and the stratum corneum. The stratum spinosum (prickle layer) typically shows atrophy, but no overt apoptosis.	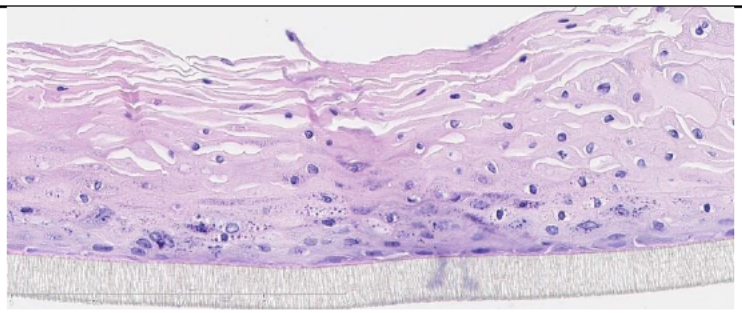

Table continues

Pattern 4	Almost complete loss of the stratum spinosum (atrophy), with keratinization beginning soon after the stratum basale, and only 2–4 basal cell thickness before keratinization. Apoptosis/karyorrhexis/pyknosis is increased up to 15–20 cells per mm length, but is difficult to quantitate. There is typically coarse hypergranulosis.	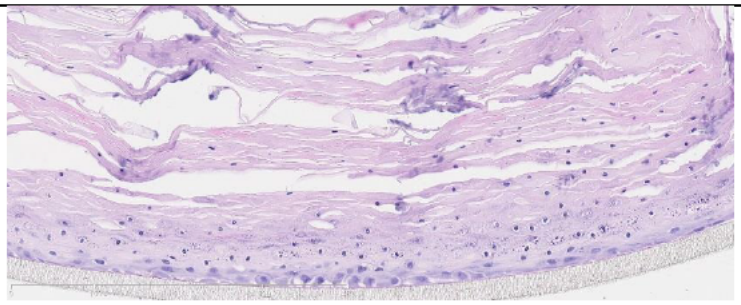
Pattern 5	Complete loss of the stratum spinosum and basal layer (atrophy) with keratinization/maturation extending down to the membrane. Apoptosis/karyorrhexis/pyknosis is increased up to 20+ cells per mm length. There may or may not be hypergranulosis, and keratohyaline granules may be absent.	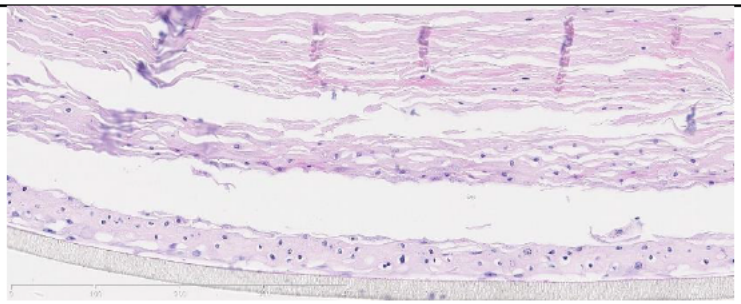

End of the Table

7.5.12 Metabolomic Assessment

Metabolomics analysis was performed in collaboration with Metabolon (Durham, NC, USA). Briefly, organotypic gingival cultures were exposed to fresh air, 3R4F CS (84.6 mg/L), and THS2.2 aerosol (100.4 mg/L). For each sample, five cultures were pooled to obtain sufficient cellular material for the assay (approximately 25 mg). The assay was performed in five replicates (i.e., five separate exposure repetitions for each sample type), and metabolic alterations were measured 4 h after the last exposure by Metabolon's global untargeted biochemical profiling platform. Samples were prepared using an automated MicroLab STAR® system from Hamilton Company (Reno, NV, USA). For extraction, the samples were normalized to the same tissue weight. Several recovery standards were added prior to the first step in the extraction process for QC purposes. To remove protein and dissociate small molecules bound to protein or trapped in the precipitated protein matrix, and to recover chemically diverse metabolites, proteins were precipitated with methanol under vigorous shaking for 2 min (Glen Mills GenoGrinder 2000, Glen Mills, Clifton, NJ, USA), followed by centrifugation. The resulting extract was divided into five fractions: Two for analysis by two separate reverse-phase (RP)/ultra-performance liquid chromatography (UPLC)-MS/MS methods with positive ion mode electrospray ionization (ESI), one for analysis by RP/UPLC-MS/MS with negative ion mode ESI, one for analysis by HILIC/UPLC-MS/MS with negative ion mode ESI, and one reserved for backup. Samples were placed briefly on a TurboVap® (Zymark, Hopkinton, MA, USA) to remove the organic solvent. The sample extracts were stored overnight under nitrogen before preparation for analysis.

Several quality control (QC) measures were utilized to ensure data quality: The experimental samples were aliquots from the same lot of human plasma; extracted water samples served as process blanks

to assess compounds introduced as a result of processing and storage; a cocktail of QC standards (isotopically labeled compounds), which were carefully selected not to interfere with the measurement of endogenous compounds, were spiked into every analyzed sample. These QC standards were used to assess instrument performance and aided chromatographic alignment. Experimental samples were randomized across the platform run, with QC samples spaced evenly among the injections.

All methods utilized a Waters ACQUITY UPLC system (Waters, Milford, MA, USA), which was plumbed such that experimental samples were injected on one of two separate LC columns. While one column was running the gradient into the mass spectrometer for analysis, the alternate column was simultaneously washed and equilibrated. All methods utilized a Thermo Fisher Scientific Q-Exactive high resolution/accurate mass spectrometer interfaced with a heated electrospray ionization (HESI-II) source and Orbitrap mass analyzer operated at 35,000 mass resolution in full scan mode and 17,500 mass resolution in MSn mode. Detailed source conditions and MS method settings can be found in Table 12. The sample extracts were dried and then reconstituted in solvents compatible to each of the four methods. Each reconstitution solvent contained a series of standards (isotopically labeled compounds) at fixed concentrations to ensure injection and chromatographic consistency. One aliquot was analyzed using acidic positive ion conditions with d7-glucose, d5-glutamine, d2-threonine, d5-hippuric acid, d3-methionine, d3-leucine, and Br-phenylalanine as internal standards, and fluorophenylglycine and Cl-phenylalanine as recovery standards. In this method, the extracts were eluted from a C18 column (Waters UPLC BEH C18-2.1×100 mm, 1.7 µm) using 0.05% perfluoropentanoic acid (PFPA) and 0.1% formic acid (FA) in water as solvent A and 0.05% PFPA and 0.1% FA in methanol (MeOH) as solvent B in 5% to 80% B in 3.35 min, then rapidly returning to starting conditions (3.5 min total MS acquisition time) at a flow rate of 0.35 mL/min. Another aliquot was also analyzed using acidic positive ion conditions; however, it was chromatographically optimized for more hydrophobic compounds and used Br-phenylalanine, d5-androstene, d9-progesterone, and d4-dioctyphthalate as internal standards and d6-cholesterol and Cl-phenylalanine as recovery standards. In this method, the extract was eluted from the same aforementioned C18 column using 0.05% PFPA and 0.1% FA in water as solvent A and 0.05% PFPA and 0.01% FA in 1:1 MeOH:acetonitrile (ACN) as solvent B in 40% to 99.5% B in 1 min, hold 99.5% B for 2.4 min, then rapidly returning to starting conditions (3.5 min total MS acquisition time) at a flow rate of 0.6 mL/min. A third aliquot was analyzed using basic negative ion optimized conditions with a separate dedicated LC/MS system and a C18 column (same column type as described above). The internal standards used were d7-glucose, d3-methionine, d3-leucine, d8-phenylalanine, d5-tryptophan, Br-phenylalanine, d15-octanoic acid, d19-decanoic acid, d27-tetradecanoic acid, d35-octadecanoic acid, and d2-eicosanoic acid. Recovery standards were tridecanoic acid and Cl-phenylalanine. These extracts were gradient-eluted using 6.5 mM ammonium bicarbonate in water at pH 8 as solvent A and 6.5 mM ammonium bicarbonate at pH 8 in 95% MeOH and 5% water as solvent B in the following gradient: 0.5% to 70% B in 4 min, 70% to 98% B in 0.5 min, hold at 98% B for 0.9 min, then rapidly returning to starting conditions (6.5 min total MS acquisition time) at a flow rate of 0.35 mL/min. The fourth aliquot was analyzed via negative ionization, and used d35-octadecanoic acid, d5-indole acetate, Br-phenylalanine, d5-tryptophan, d4-tyrosine, d3-serine, d3-aspartic acid, d7-ornithine, and d4-lysine as internal standards. Recovery standards were fluorophenylglycine and Cl-phenylalanine. Extracts were eluted from a HILIC column (Waters UPLC BEH Amide 2.1×150 mm, 1.7 µm) using 80% ACN, 15% water, and 5% MeOH with 10 mM ammonium formate, pH 10.8 as solvent A and 50% ACN and 50% water with 10 mM ammonium formate as solvent B in the following gradient:

5% to 50% B in 3.5 min, 50% to 95% B in 2 min, hold at 95% B for 1 min, then rapidly return to starting conditions (6.7 min total MS acquisition time). All the methods alternated between full-scan MS and data-dependent MSn scans using dynamic exclusion. The scan range varied slightly between methods but generally covered 70–1,000 m/z. Raw data files were archived and data extracted as described below (Table 12).

Table 12. MS source conditions and settings.

Instrument	**Q-Exactive**			
Method	RP Pos Polar	RP Pos Lipid	RP Neg	HILIC Neg
Sheath Gas (au)	70	45	70	70
Auxiliary Gas (au)	15	30	25	20
Spray Voltage (kV)	4	4.2	3.2	3.2
Source Heater Temp. (°C)	300	400	300	300
Ion Transfer Tube Temp. (°C)	250	350	300	300
Normalized Collision Energy (au)	65	65	65	60
Stepped Normalized Collision Energy (%)	20	20	20	20
S-Lens RF Level	40	40	40	40
Mass Range (m/z)	70–1,000	110–1,000	80–1,000	80–1,000
MS AGC target (au)	1E+06			
MS Max Fill Time (ms)	60			
MS^n Ion Target (au)	2E+05			
MS^n Max Time (ms)	120			
MS^n Isolation Window (m/z)	3			
MS^n Dynamic Exclusion Time (s)	3			
MSn Isolation Window (m/z)	3			
MSn Dynamic Exclusion Time (s)	3			

The informatics system consisted of four major components: The Laboratory Information Management System (LIMS), the data extraction and peak-identification software, data processing tools for QC and compound identification, and a collection of information interpretation and visualization tools for use by data analysts. The hardware and software foundations for these informatics components were the LAN backbone, and a database server running Oracle 10.2.0.1 Enterprise Edition (Oracle Corporation, Redwood City, CA).

Data Extraction, Compound Identification and Quantification: Raw data was extracted, peak-identified, and QC-processed using Metabolon's hardware and software. Compounds were identified by comparison to a library of entries of purified standards or recurrent unknown entities. Metabolon maintains this library based on authenticated standards that contain the retention time/index (RI), mass-to-charge ratio (m/z), and chromatographic data (including MS/MS spectral data) on all molecules present in the library per method. Biochemical identifications are therefore based on three criteria: Retention index within a narrow retention window of the proposed identification, accurate mass match to the library +/− 10 ppm, and the MS/MS forward and reverse scores for the experimental data and authentic standards. The MS/MS scores are based on a comparison of the ions

present in the experimental spectrum to the ions present in the library spectrum. While there may be similarities between these molecules based on one of these factors, the use of all three data points can be leveraged to distinguish and differentiate biochemicals. More than 3,300 commercially available purified standard compounds have been acquired and registered in the LIMS for analysis on all platforms to determine analytical characteristics. Additional mass spectral entries have been created for structurally unnamed biochemicals, which have been identified by virtue of their recurrent nature (both chromatographic and mass spectral). These compounds may be identified by future acquisition of a matching purified standard or by classical structural analysis. Peaks were quantified using the area under the curve of primary MS ions.

A variety of curation procedures were carried out to ensure that a high-quality dataset was made available for statistical analysis and data interpretation. The QC and curation processes were designed to ensure accurate and consistent identification of true chemical entities, and to remove those representing system artefacts, mis-assignments, and background noise. Metabolon data analysts use proprietary visualization and interpretation software to confirm the consistency of peak identification among the various samples. Library matches for each compound were checked for each sample and corrected if necessary.

A global variance-stabilizing normalization (VSN) of the raw abundance data was performed with the corresponding Bioconductor package in R (Huber 2002, Hultin-Rosenberg 2013). Missing values were imputed as the minimum value separately for each metabolite. A linear model was fitted for each exposure condition and the corresponding air-exposed groups, and *p*-values from a moderated *t*-statistic were calculated with the empirical Bayes approach (Gentleman 2004). The Benjamini–Hochberg false discovery rate (FDR) method was used to correct for multiple testing effects. Metabolites with an adjusted *p*-value <0.05 were considered differentially abundant.

7.5.13 RNA/MicroRNA Purification

Total RNA, including microRNA (miRNA), was isolated after washing the organotypic gingival culture inserts twice with cold (4°C) PBS at both the basal and apical sides. The cells were then disrupted in 700 µL QIAzol™ lysis buffer (Qiagen, Hilden, Germany), followed by RNA extraction using a Qiagen miRNeasy Mini Kit and a QIAcube robot (Qiagen). The final elution was done in 30 µL RNAse-free water (PMI_RD_WKI_001117). The concentration and purity of the RNA were determined using a UV spectrophotometer (NanoDrop ND1000; Thermo Fisher Scientific) by measuring the absorbance at 230, 260, and 280 nm. The integrity of the RNA was further checked with the Agilent 2100 Bioanalyzer (Agilent, Santa Clara, CA, USA) (PMI_RD_WKI_000978), considering only RNA integrity number (RIN) values of 6 and above.
All related work instructions are found in PMI_RD_SOP_000354: SOP RNA Extractions.

7.5.14 mRNA Profiling Analysis Using GeneChip

The target preparation workflow was performed using a liquid handling system, Biomek FXP Target Prep Express (Beckman Coulter, Pasadena, CA, USA). One hundred nanograms of total RNA were reverse-transcribed to cDNA using an Affymetrix® HT 3′ IVT PLUS kit (Affymetrix, Santa Clara, CA, USA) (PMI_RD_WKI_001109). The cDNA was labeled and amplified to cRNA (complementary RNA, also referred to as amplified RNA), and the cRNA was purified using

magnetic beads to remove unincorporated nucleotide triphosphates, salts, enzymes, and inorganic phosphates (PMI_RD_WKI_001109). Purified cRNA (≥12 µg) was quantified, normalized, and quality-checked using a Fragment Analyzer™ (Advanced Analytical Technologies, Ames, IA, USA) (PMI_RD_WKI_001125) and chemically fragmented (PMI_RD_WKI_001109). The completion of fragmentation was checked on an Agilent 2100 Bioanalyzer (Agilent Technologies). Next, 29.4 µL of fragmented and labeled cRNA were added to 190.6 µL of hybridization cocktail. After denaturation for 5 min at 95°C and 5 min at 45°C, followed by centrifugation at V_{max} (16,000× *g*) for 1 min, 200 µL of the cRNA cocktail were hybridized to a GeneChip® Human Genome U133 Plus 2.0 Array (Agilent Technologies) (PMI_RD_WKI_001126). The arrays were incubated in a GeneChip® Hybridization Oven 645 (Affymetrix) for 16 h at 45°C with a rotation speed of 60 rpm. Arrays were washed and stained on a GeneChip® Fluidics Station FS450 DX (Affymetrix) using the Affymetrix® GeneChip® Command Console® Software (AGCC software version 3.2) with protocol FS450_0001. Finally, the arrays were scanned using a GeneChip® Scanner 3000 7G (Affymetrix). Raw images from the scanner were saved as DAT files. The AGCC software automatically gridded the DAT file image and extracted probe cell intensities into a CEL file.
The work instructions related to gene expression are found in PMI_RD_SOP_000347: Gene Expression Profiling.

7.5.15 qPCR Array for Candidate Genes

The expression of genes involved in the osmotic stress response was measured using the RT² Profiler™ PCR Arrays (Qiagen). The Human Osmotic Stress RT² Profiler PCR Array profiles the expression of 84 key genes involved in the cellular response to changes in osmolarity. Housekeeping genes are included in this panel (ACTB, B2M, GAPDH, HPRT1, RPLP0), along with a control to check genomic DNA contamination (HGDC) and a positive PCR control, which is a predispensed artificial DNA sequence detected at the qPCR level.
Reverse transcription (normalized at 400 ng) reactions were performed by using the RT² First Strand Kit (Qiagen), and the qPCR was carried out on a ViiA 7 instrument (Thermo Fisher Scientific) using a Human Osmotic Stress PCR Array (PAHS-151Z).

For this specific panel, the following WKIs will be used:
PMI_RD_WKI_001334: qRTPCR SA Bioscience.
PMI_RD_FOR_000999: Form qRT-PCR Qiagen / SA Bioscience.
After selecting a single threshold for all the genes in 'Analysis settings', the Ct values were calculated. qPCR was analyzed by calculating the fold changes using the ΔΔCT method.

7.5.16 miRNA Profiling

A FlashTag™ Biotin HSR kit (Affymetrix) was used to label the miRNA (PMI_RD_WKI_001123). Briefly, 200 ng of total RNA (PMI_RD_WKI_001358) containing low-molecular-weight RNA were subjected to a brief tailing reaction, followed by ligation of the biotinylated signal molecule to the target RNA sample. After denaturation for 5 min at 99°C and 5 min at 45°C, followed by centrifugation at V_{max} (16,000× *g*) for 1 min, 21.5 µL of the biotin-labeled sample were mixed with 110.5 µL hybridization cocktail. Hybridization was performed on an Affymetrix GeneChip® miRNA V4.0 Array. The arrays (miRNA version 4.0) were incubated in a GeneChip Hybridization Oven 645

(Affymetrix) for 16 h at 48°C with a rotation speed of 60 rpm. Arrays were washed and stained on a GeneChip Fluidics Station FS 450 DX (Affymetrix) using the Affymetrix GeneChip Command Console Software (AGCC software version 3.2) with protocol FS450_0002 (PMI_RD_WKI_001123). Finally, the arrays were scanned using a GeneChip Scanner 3000 7G (Affymetrix). Raw images from the scanner were saved as DAT files. The AGCC software automatically gridded the DAT file image and extracted probe cell intensities into a CEL file.

PMI_RD_WKI_001358: Normalization Macro prior to Nugen WB, IVT or FlashTag protocol
PMI_RD_FOR_001072: Nugen, IVT, FlashTag calculation and tracking sheet

8. Statistical and Computational Methods

8.1 Statistical Methods

The analysis and graphical display of the data were performed using SAS version 9.2 (SAS Institute, Cary, NC, USA).

8.1.1 Experimental Unit

For the exposure experiments using organotypic gingival culture models and the Vitrocell 24/48 cultivation and exposure system, the experimental unit was the smoke exposure run. If a particular endpoint was measured several times in the same culture insert or in different inserts exposed to the same experimental condition (e.g., a specific dose of smoke/aerosol concentration at a specific post-exposure time) during the same smoke exposure run, then all the mean values of a given endpoint were calculated.
For the controls, endpoints were measured from tissue inserts that were not exposed to smoke/aerosol in the Vitrocell 24/48 cultivation and exposure system but treated by reagents/chemicals. In this case, the experimental unit was the study phase, i.e., a single experimental repetition, and the mean values of a given endpoint were calculated from the measurements performed on culture inserts that were treated identically with the specific corresponding reagent/chemical.

8.1.2 Derived Variables

8.1.2.1 Normalized Cytotoxicity Levels

Cytotoxicity of the cultures was derived from AK values. All values of the AK assay readout were normalized using the mean of the positive control (Triton X-100-treated culture inserts) and negative control (PBS-treated or untreated culture inserts [unexposed, incubator control]), and the percentage of cytotoxicity was calculated as follows:

$$Cytotoxicity\ (\%) = \frac{AK_{tissue} - AK_{Neg\ CTRL}}{AK_{Pos\ CTRL} - AK_{Neg\ CTRL}}\ x\ 100\ \text{, where}$$

$$AK_{Neg\ CTRL} = \sum_{i=1}^{nbPhase} \frac{\sum_{j=1}^{nbCTRL^i} \frac{AK_{i,j}}{nbCTRL^i}}{nbPhase}$$

$$AK_{Pos\ CTRL} = \sum_{i=1}^{nbPhase} \frac{AK_{TX-100}}{nbPhase}$$

$$AK_{Tissue} = relative\ luminescence\ unit\ of\ a\ given\ sample$$
$$nbPhase = number\ of\ experimental\ phase$$
$$Neg = negative$$
$$Pos = positive$$
$$CTRL = control$$

8.1.2.2 Normalized CYP Activity (%)

All measured activity of CYP1A1/CYP1B1 was normalized using the mean of the positive control (TCDD-treated culture inserts) and negative control (luciferin substrate-treated, non-exposed culture inserts) as follows:

$$Normalized\ CYP\ activity\ (\%) = \frac{CYP_{tissue} - CYP_{Neg\ CTRL}}{CYP_{Pos\ CTRL} - CYP_{Neg\ CTRL}}\ x\ 100\ ,\ \text{where}$$

$$CYP_{Neg\ CTRL} = \sum_{i=1}^{nbPhase} \frac{\sum_{j=1}^{nbCTRL^i} \frac{CYP_{i,j}}{nbCTRL^i}}{nbPhase}$$

$$CYP_{Pos\ CTRL} = \sum_{i=1}^{nbPhase} \frac{CYP_{TCDD}}{nbPhase}$$

$$CYP_{Tissue} = relative\ luminescence\ unit\ of\ a\ given\ tissue\ culture\ sample$$
$$nbPhase = number\ of\ experimental\ phase$$
$$Neg = negative$$
$$Pos = positive$$
$$CTRL = control$$

8.1.3 Data Transformation

All numerical values from the MAP analysis were transformed using the natural log transformation.

8.1.4 MTT Metabolic Assay

Raw OD_{565} absorbance values were measured, and the following calculations made. Generally, calculations were performed using an Excel spreadsheet.
The mean OD_{565} value of the extraction solvent (blank) wells was calculated.
The corrected mean OD_{565} value of the negative control(s) was determined by subtracting the mean OD_{565} value of the blank wells from their mean OD_{565} values.
The corrected OD_{565} values of the individual test article exposures and the positive control exposures were determined by subtracting from each the mean OD_{565} value of the blank.

Corrected test article exposure OD_{565} = Test article exposure OD_{565} – Blank mean OD_{565}

The following % of Control calculations were made:

$$\% \text{ of Control} = \frac{\text{Final corrected } OD_{565} \text{ of each Test Article or Positive Control exposure}}{\text{Corrected mean } OD_{565} \text{ of Negative Control exposure}} \times 100$$

The individual % of Control values (relative viability) were then averaged to calculate the mean % of Control per exposure. Test article and positive control viability calculations were performed by comparing the corrected OD_{565} values of each test article or positive control exposure time to the appropriate negative control.

8.1.5 Statistical Comparison

8.1.5.1 For Continuous Variables

- The comparison of an exposed sample and the corresponding air control (i.e., the paired samples from the same exposure run at a given experimental repetition) was done using a paired *t*-test.
- The comparison of 3R4F-exposed and THS2.2-exposed samples was done after subtracting the values of the corresponding air controls (i.e., the paired samples). The comparison was then done using a *t*-test corrected for non-equal variance (Satterthwaite correction).
- *p*-values were not adjusted for multiple testing.

8.1.5.2 For Categorical Variables

- The comparisons of an exposed sample and its air control (i.e., the paired samples from the same exposure run at a given experimental repetition) were done using a Cochran-Mantel-Haenszel test, on the row mean scores differences, with the MODRIDIT score type. The test was stratified by the exposure run.
- The comparisons of the effects between the reference-item-exposed samples and test-item-exposed samples were done after subtracting the values of the corresponding air controls (i.e., the paired samples). Next, the comparisons were done using an unstratified Cochran-Mantel-Haenszel test, on the row mean scores differences, with the MODRIDIT score type.

8.1.5.3 For Binary Variables

- The comparisons of an exposed sample and its air control (i.e., the paired samples from the same exposure run at a given experimental repetition) were done using an exact McNemar's test. The test was stratified by the exposure run.
- The comparisons of the effects between the reference-item-exposed samples and test-item-exposed samples were done after subtracting the values of the corresponding air controls (i.e., the paired samples). Next, the comparisons were done using a Fisher's exact test.

8.2 Computational Methods: Affymetrix Gene Expression Analysis

8.2.1 Sample Randomization

Randomization was performed for RNA extraction and defined prior to the experimental exposures. Array hybridization was performed as a complete block randomization, where the blocking factor was defined by both the exposure run ID and the post-exposure time. A single randomization for RNA extraction and hybridization was performed. When placing sample aliquots in 96-well plates during the analysis, samples within a block were always analyzed together. Finally, samples within a given block were hybridized using the same chip lot and same target preparation batch.

8.2.2 Nicotine Analysis

PBS-exposed samples were quantified with a "10" calibration level of nicotine. Quantitation was performed using isotopic dilution with d3-nicotine as the labeled internal standard. Unknown samples were quantified while their concentration fit within the calibration curve. If their concentrations were out of the curve, a dilution step was performed prior to analysis of the batch. Samples were prepared by direct addition of internal standard solution to the sample aliquots.
The sample measurement involved a calibration curve at the beginning and the end of the analytical sequence, including QC measures to control system performance. These last ones were distributed along the sequence, to ensure that all samples were accurately measured following defined parameters from the validated method. The complete analytical sequence was run by LC-HRAM-MS using positive ionization and data were collected in full-scan mode, monitored by Xcalibur® software (version SP1.48) (PMI_RD_WKI_001498, PMI_RD_WKI_001458).
Once the analytical sequence was terminated, raw data were processed with TraceFinder® software (version 3.1.416.13) using a quantitative method based on the ratio between nicotine and d3-nicotine. The value was then reported on the calibration curve to determine the corresponding concentration. The nicotine amount per sample was also reported.

8.2.3 Processing and Quality Control (QC) of Raw CEL Files

The Affymetrix GeneChip Human Genome U133 Plus 2.0 Array was used for hybridization, as it can simultaneously probe the expression of thousands of genes. In accordance with PMI_RD_WKI_001228 and PMI_RD_SOP_000346, raw CEL files were background-corrected, normalized, and summarized using frozen robust multiarray analysis (fRMA). Background correction and quantile normalization were used to generate microarray expression values from all arrays passing QC checks, which were performed using the custom CDF environment HGU133Plus2_Hs_ENTREZG v16.0. A log-intensities plot, normalized unscaled standard error (NUSE) plot, relative log expression (RLE) plot, median absolute value RLE (MARLE), and pseudo-images, as well as raw images, were generated for quality checks using the R package (AffyPLM; Bioconductor, Seattle, WA, USA) .

CEL files that fulfilled at least one of the quality metric rules described below were dropped from further analysis:

a) Pseudo-image displaying a spatial pattern covering approximately 10% of the pseudo-image.
b) Median NUSE > 1.05
c) |Median RLE| > 0.1

d) |(MARLE−median(MARLE))| / (1.4826 × mad(MARLE)) > 1/√0.01 (where mad is the median absolute deviation)

Subsequently, the RLE- and NUSE-based metrics were recomputed, until no more CEL files were removed.

8.2.4 Gene-Level Analysis

For each experimental factor combination item, dose and post-exposure, a model for estimating the treatment effect was fitted using *limma* software by including the covariate "smoking run" as a blocking variable to account for insert pairing during an exposure experiment (an exposure run comprises samples exposed to a reference or test item and air-exposed controls; see Figure 4). The *p*-values for each computed effect were adjusted across genes using the Benjamini–Hochberg FDR method. The results were displayed as volcano plots (x-axis representing the estimated effect and y-axis representing the $-\log_{10}$(FDR) for each gene). Differentially expressed genes (DEGs) were defined as the set of genes whose FDR was below 0.05.
Reproducibility was estimated by correlating the fold-changes (exposed samples vs. controls) across experimental repetitions.

8.2.5 qPCR Analysis

The Ct data contained in the *.xlsx* file generated after completion of the "qPCR array for candidate genes" procedure were imported into the R environment for statistical computing. The data were converted into objects of the Bioconductor *ReadqPCR* package. The optimal ("most stable") selection of reference/housekeeping genes was performed using the *geNorm* method implemented in the Bioconductor *NormqPCR* package. This reference/housekeeping genes subset was used to generate the ΔCt values by normalizing the Ct values. This step was performed using the function *deltaCq* of the *NormqPCR* package, which essentially consists of subtracting from the Ct values of each sample the arithmetic mean of the corresponding Ct values of the subset of most stable reference/housekeeping genes. The differential expression ΔΔCt values and their significance (*p*-values) were calculated based on the −ΔCt values by using the standard two-sided *t*-test implemented in R. The cases of non-detected signal (Ct ≥ 40) were treated in an appropriate way. No multiple testing corrections were performed on the obtained *p*-values.

8.2.6 Statistical Analysis: Network-Level Analysis

8.2.6.1 Network Perturbation Amplitude

The collection of causal biological networks used in the study was the human network suite CBN version 1.3. These networks contain from a few dozen to 200 nodes. The relevant network models considered in this study are summarized in Table 13. The network models can be organized into four major families, representing global biological processes: Cell stress (CST), cell proliferation (CPR), inflammatory process network (IPN), and cell fate and angiogenesis (CFA).

Table 13. Network and network models used in the analysis.

No.	Abbreviated Network Family Name	Network
1	CFA	Apoptosis
2	CFA	Autophagy
3	CFA	Necroptosis
4	CFA	Response to DNA Damage
5	CFA	Senescence
6	CPR	Calcium
7	CPR	Cell Cycle
8	CPR	Cell Interaction
9	CPR	Clock
10	CPR	Epigenetics
11	CPR	Growth Factor
12	CPR	Hedgehog
13	CPR	Hox
14	CPR	Jak-STAT
15	CPR	MAPK
16	CPR	mTor
17	CPR	Notch
18	CPR	Nuclear Receptors
19	CPR	PGE2
20	CPR	Wnt
21	CST	Endoplasmic Reticulum Stress
22	CST	Hypoxic Stress
23	CST	NFE2L2 Signaling
24	CST	Osmotic Stress
25	CST	Oxidative Stress
26	CST	Xenobiotic Metabolism Response
27	IPN	Epithelial Innate Immune Activation
28	IPN	Tissue Damage

Abbreviations: CFA, cell fate and angiogenesis; CPR, cell proliferation; CST, cell stress; Hox, homeobox; IPN, inflammatory process network; Jak-STAT, Janus kinase/signal transducers and activators of transcription; MAPK, mitogen-activated protein kinases; mTor, mechanistic target of rapamycin; NFE2L2, nuclear factor, erythroid 2-like 2; PGE2, prostaglandin E2; Wnt, wingless-type.

Network scoring exploits the network backbone nodes that are connected to downstream mRNA-abundance nodes based on their known relationship reported in the literature. These signed relationships can be the backbone node, increasing or decreasing the abundance of certain mRNAs, and are used to infer the activation of a backbone node using transcriptomics data. Because not all backbone nodes have downstream mRNA nodes, the network models should be prepared for scoring to improve the specificity and relevancy of the overall network perturbation amplitude (NPA) score. Only backbone nodes that are on a directed path that starts and ends with a node that has downstream mRNA nodes are considered. After removing the nodes that do not satisfy the criteria above, the

largest connected component is kept. Finally, the edges "causesNoChange" are disregarded for the scoring.

The NPA methodology aims to contextualize the high-dimensional transcriptomics data by combining gene expression (log_2) fold-changes, β, into fewer differential node values (one value for each node of the network), f. The differential node values are determined by a fitting procedure that infers the values that best satisfy the directionality of the causal relationships (positive or negative) contained in the network model, while being constrained by the experimental data (the gene log_2-fold-changes, which are described as downstream effects of the network itself):

$$f = L_3^{-1} L_2^T \beta$$

where L is the signed weighted Laplacian of the network and the extra edges and nodes describing the downstream effects (to gene expression nodes); L3 is the sub-matrix of L for the nodes in the network, and L2 is the sub-matrix corresponding to the edges connecting the network nodes to the downstream gene expression nodes. The differential node values are in turn summarized as a single positive number, referred to as the amplitude of perturbation (NPA scores):

$$NPA = \frac{1}{|E|} \sum_{e\ in\ E} (f(e_0) + \sigma(e) f(e_1))^2$$

where E is the set of edges in the network; |E| is its size, and e_0 and e_1 denote the start and the end, respectively, of an edge e. The sum computing the NPA score can be expressed as fTQf, where Q is the signed Laplacian of the network when all of the edge signs have been reversed. All details of the methodology have been described in a previous publication (Martin 2014).

For the NPA scores, a confidence interval accounting for experimental variation and associated *p*-values is computed. Additionally, companion statistics, derived to inform on the specificity of the NPA score with respect to the biology described in the network model, are shown as *O and K* if their *p*-values are below the significance level (0.05). A network is considered to be significantly affected if three values (the confidence interval, *O, and K* statistics) are below 0.05.

8.2.6.2 Biological Impact Factor (BIF)

The BIF methodology provides a unified and coherent framework for investigating mechanistic effects at each level of granularity of the biological processes represented in the network models. The method enables the derivation of a relative BIF, which is a measure of the overall biological impact across all network models. The BIF methodology allows an assessment of the exposures in an objective, systematic, and quantifiable manner, by computing a systems-wide and pan-mechanistic biological impact measure for a given substance, mixture, or test item.
An aggregation of the NPA should satisfy the following criteria:

a) *Credibility*: The BIF should be an intuitive and logical aggregation scheme.
b) *Fairness*: All network families are equally important.
c) *Understandable*: Each decision or step should have a defined rationale.

To fulfill the first criterion, network scores are aggregated via a weighted sum (because every scoring in NPA is additive). In addition, only networks that have *p*-values of the three statistics below 0.05 (*O, *, K*) are considered (denoted by N_i*). The BIF is defined as:

$$BIF = \sum_{N_i^*} \omega_i \, NPA(N_i) = \sum_{N_i^*} \omega_i \sum_{e \epsilon E(N_i)} (f(e_0) + \sigma(e) f(e_1))^2$$

where f is the function of the network nodes that describe the differential node values; E(N_i*) represents the network edges, and e_0 and e_1 are the start and end, respectively, of an edge e.

For the second criterion, a *fair* BIF would represent the equality of the biological processes (networks) in a given system (e.g., 2D cultures of normal human oral epithelial cells, 3D organotypic cultures, or lung tissue samples from *in vivo* studies). If all the network models were fitted perfectly by the gene expression data, the contribution of each network to the BIF is assumed to be equal. Therefore, the BIF methodology considers that all specific processes represented in the network models are equally involved and important for a given network family. A perfect fit of the network will maximize the NPA value and be smooth over the network. Using the notation defined above, a "perfect" network response (differential node values) would both maximize $f^T Qf$ with $\|f\|_2 = 1$ and minimize $f^T L_3 f$ (the NPA criteria). Additionally, there is a constraint that $L_3 f$ vanishes for network nodes that do not have direct downstream gene expression nodes, because they are expected to be in the image of L^T_2.

Such nodes are denoted as NH. Therefore, the following optimization problem can be solved as:

$$argmax_{f \; s.t.(L_3 f)|_{NH}=0} \frac{f^T Q f}{f^T L_3 f}$$

To rebalance the network families, the mean over the networks will be considered.

For each edge $e = (e_0, \sigma(e), e_1)$, the number of occurrences of edge e in the set of networks used in the BIF calculation is denoted by $o(e)$. Therefore, the maximum occurrence-corrected amplitude of a network N_i can be defined as:

$$NPA_{max}(N_i) \doteq \sum_{e \epsilon E(N_i)} \frac{1}{o(e)} (f_{max}(e_0) + \sigma(e) f_{max}(e_1))^2$$

Finally, to normalize the NPAs, a correction factor of $|E(N_i)|/NPA_{max}(N_i)$ is applied. Considering all of these factors, the BIF is defined as the weighted sum (F denotes the network families), as follows:

$$\sum_F \frac{1}{|F|} \sum_{N_i^* \in F} \frac{1}{NPA_{max}(N_i)} \sum_{e \epsilon E(N_i)} \frac{1}{o(e)} (f(e_0) + \sigma(e) f(e_1))^2$$

Therefore, the contribution of each network F is:

$$\frac{\frac{1}{|F|}\sum_{N_i^* \in F}\frac{1}{NPA_{max}(N_i)}\sum_{e \in E\,(N_i)}\frac{1}{o\,(e)}(f(e_0) + \sigma\,(e)f(e_1))^2}{BIF_{SDP}}$$

8.2.7 Gene-Set Analysis (GSA)

This standard approach for interpreting gene differential expressions was performed using the *piano* Bioconductor package (Väremo 2013). Pathway maps were obtained from the KEGG knowledgebase (Kanehisa 2014) and exported into the R environment using the *graphite* package (Sales 2012). Gene-set enrichment was assessed using over-representation analysis ("Q1") as well as sample permutation ("Q2") (Ackermann 2009). In both cases, the fold-changes β_{mRNA} were used as the gene-level statistic, while the mean was used as the gene-set-level statistic. The resulting *p*-values were adjusted using the Benjamini-Hochberg procedure (Benjamini 1995)

8.3 Computational Methods: Affymetrix miRNA Expression Analysis

8.3.1 Processing and QC of Raw CEL Files

The raw array data in the CEL files were pre-processed through a standard pipeline based on the generic documents PMI_RD_WKI_001228 and PMI_RD_SOP_000346. CEL files were read using the *read.celfiles* function of the Oligo package in the Bioconductor suite of microarray analysis tools for the R statistical software environment. The quality of the array data was controlled using the *arrayQualityMetrics* package in Bioconductor, and examined according to the following four metrics:

a) Distances between arrays at the raw-data level
b) Distances between arrays at the normalized-data level
c) NUSE
d) Array intensity distributions.

Arrays that were found to be outliers by at least two of these metrics were discarded. The quality was iteratively re-examined for the remaining arrays until all were accepted. For the experimental repetitions, the QC procedure for the miRNA expression analysis was applied separately to each miRNA processing batch (each processing batch was composed of samples obtained from two consecutive experimental repetitions). This approach was used to avoid batch effects on the QC. Subsequently, normalized probe-level data were obtained by applying robust multiarray (RMA) normalization, and summarized using the median polish method at the probe-set level.

8.3.2 miRNA Differential Expression Calculation

The raw data contained in the CEL files were pre-processed using the Bioconductor *oligo* package (Carvalho 2010). Their quality was controlled using the *arrayQualityMetrics* package (Kauffmann 2009) by examining four metrics: Euclidean distances between arrays in the raw data matrix, Euclidean distances between arrays in the normalized data matrix, NUSE, and raw intensity distributions. The normalized probe-level data were calculated by applying RMA normalization and summarized at the probe set-level using the median polish method (Bolstad 2003, Irizarry 2003). Using the annotation provided by Affymetrix, all non-human probe sets were filtered out of the expression matrix. Additionally, a detection call-based filtering procedure was applied to retain only

the miRNA probe sets displaying intensities that were significantly higher than their matched background probes (miRNA QCTool, Affymetrix). The miRNA expression matrix finally contained 564 human miRNA probe sets. The miRNA differential expressions and their corresponding (raw) *p*-values were obtained using the *limma* package (Smyth 2004), with Benjamini–Hochberg false discovery rate (FDR) multiple test corrections (Benjamini 1995).

8.3.3 Integrated Analysis of microRNA and Target mRNA Expression Profiles

To assess the mRNA-miRNA interactions, we analyzed the target genes of differentially expressed miRNAs using Qiagen's Ingenuity® Pathway Analysis (IPA®, Qiagen) tools (version March 2016). In detail, we set the cutoff for the upregulated miRNA as ≥1.2 fold change, or ≤0.83 for downregulated miRNAs. No significant number of differentially expressed miRNAs was found for most of the 3R4F CS and THS2.2 aerosol concentrations. Thus, we decided to use only the highest doses of nicotine in 3R4F smoke (84.6 mg/L) and THS2.2 aerosol (100.4 mg/L). We generated high-confidence miRNA target predictions, as well as experimentally observed miRNA-mRNA interactions, using the IPA tool "MicroRNA Target Filter", which integrates multiple target prediction algorithms such as TargetScan, TarBase, miRecords, and the Ingenuity Knowledge Base. Opposite expression pairing between miRNA and mRNA levels was implemented to further refine the analysis. Further filtering options, such as specific tissue/cell line related to epidermis, were applied, including the confidence parameter. The resulting miRNA-mRNA interaction pairs were mapped with the previously identified differentially expressed mRNAs, and a threshold was set at FDR ≤ 0.05, which was calculated by Fisher's exact test. The resulting interaction networks of differentially expressed miRNAs and mRNAs were visualized by IPA. To identify the most relevant canonical pathways affected in our biological system, we excluded some pathways not related to gingival biology: Cancer, cardiovascular signaling, pathogen-influenced signaling, and neurotransmitters and other nervous system signaling. By using the "Build-Path Explorer" option in IPA, we identified all the relationships among genes and miRNAs in the cluster. We selected the option "Interactions = only direct"; all other options were left as defaults. Subsequently, using the "Path Designer" tool in IPA and the "Overlay-Canonical Pathways" option, we added all the canonical pathways involved in oxidative, xenobiotic, and inflammation stress.

8.3.4 Network-Based Integrated miRNA-mRNA Assessment

This assessment consisted of applying the NPA approach described above to the three candidate miRNA-mRNA networks, to comparatively assess their perturbations upon exposure to 3R4F CS or THS2.2 aerosol (see paragraph Statistical Analysis: Network-Level Analysis). Taking into account the repressive effect of miRNAs on their target genes, the adapted NPA formula $(1/N_{edges}) \cdot \sum_{(miRNA,mRNA)\ edges} (\beta_{miRNA} - \beta_{mRNA})^2$ was evaluated using the miRNA and mRNA differential expressions β_{miRNA} and β_{mRNA}. The resulting "miRNPA" scores carry a confidence interval accounting for the experimental variation of the differential expressions, which was computed using an explicit analytical formula. The two other companion specificity statistics, "O" and "K", were not applicable in the integrated miRNA-mRNA context.

9. Results

9.1 PBS Pilot

9.1.1 Cell Viability Assessment Using AK and MTT Assays

To be closer to the physiological situation and mimic the presence of saliva in the oral cavity, we exposed the gingival organotypic cultures to PBS on the apical side over the duration of the experiments. We selected PBS because it shares a similar composition but does not contain the additives normally present in artificial saliva (Moharamzadeh 2009). Moreover, many different types of artificial saliva are available and their composition vary largely, not meeting the biophysical properties of real saliva; some may even induce an inflammatory condition in various cell types (Kho 2014, Malpass 2013, Preetha 2005).

To investigate alterations possibly due to the presence of PBS, we exposed gingival cultures to PBS for up to 96 h and analyzed mitochondrial functionality using the MTT assay, an indicator of cell viability. We observed that cell viability was reduced in both groups in a time-dependent manner (Figure 5A). This reflects natural tissue aging over time. The metabolic activity of the PBS-exposed cultures was minimally perturbed.

Cytotoxicity was also assessed, measuring the cumulative AK release in the basolateral media over the entire exposure period compared with untreated (control) cultures. We noted that exposure to PBS did not cause any relevant cytotoxicity across the 96 h of incubation (Figure 5B), following the trend observed in control cultures, except for a putative initial adaptive increase at 24 h that shifted the AK release from 1% in cultures without PBS to 3% for PBS-covered cultures.

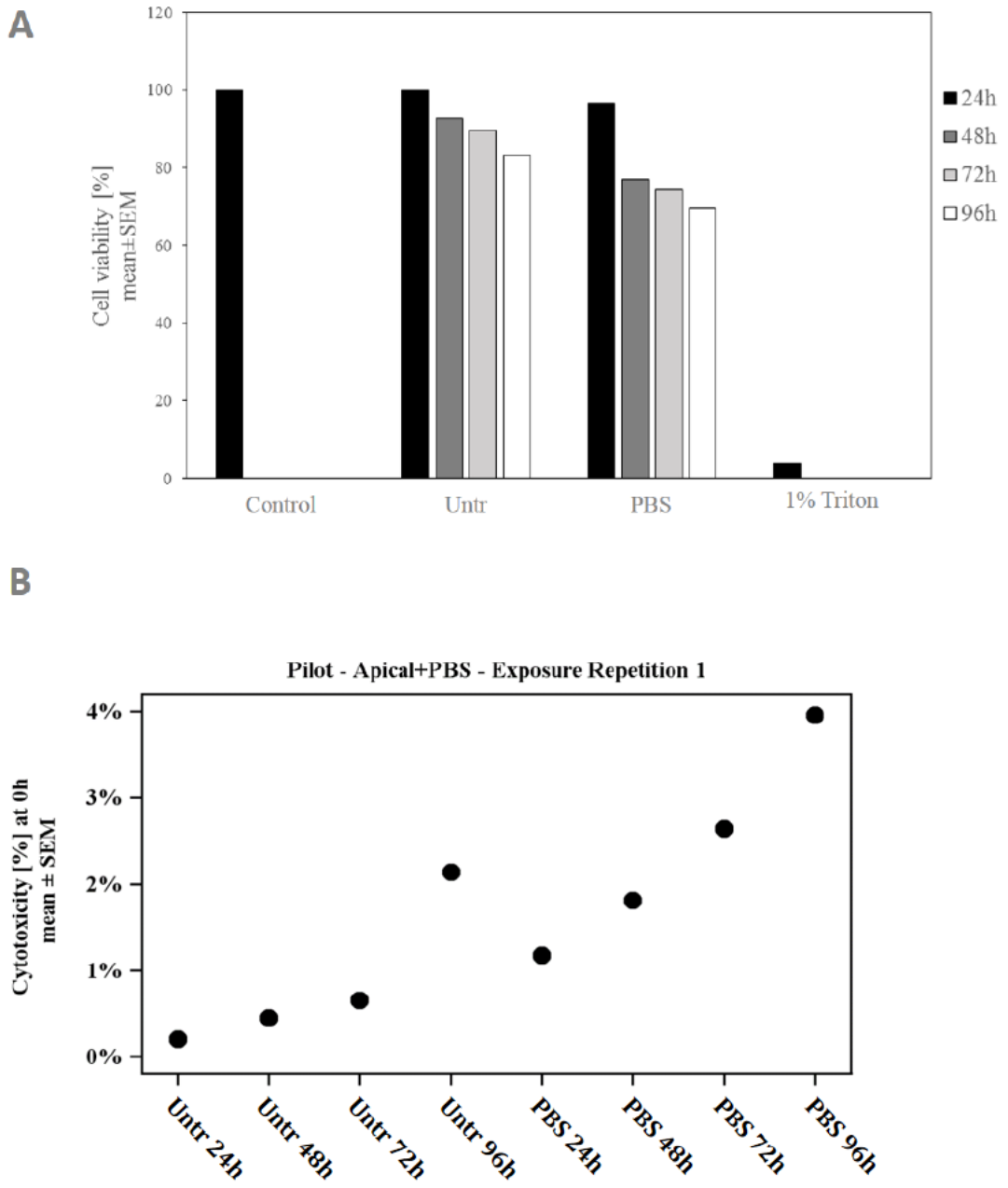

Figure 5. Cytotoxicity in organotypic cultures following phosphate-buffered saline (PBS) exposure.

(**A**) Cell viability was assessed by measuring the mitochondrial activity using the MTT test. Results are expressed as a percentage of the untreated control group viability at 24 h (100% viability). (**B**) Cytotoxicity-based adenylate kinase (AK) activity was assessed in gingival culture following PBS apical exposure. The AK levels were normalized to those in the positive (Triton-X-treated cultures considered to represent 100% cytotoxicity) and negative (untreated) control. N=1.

Descriptive statistics for these results are reported in Supplementary Table 9.

9.1.2 Secretion of Proinflammatory Mediators

The proinflammatory mediators released by gingival organotypic cultures following PBS exposure were assessed by measuring the analytes secreted into the basolateral media 24, 48, 72, and 96 h post-exposure. Most cytokine levels did not change or even decrease after PBS exposure (Figure 6). After 72 h of incubation, the basolateral medium was replaced; for this reason, we observed a decrease in proinflammatory mediator release.

Figure 6

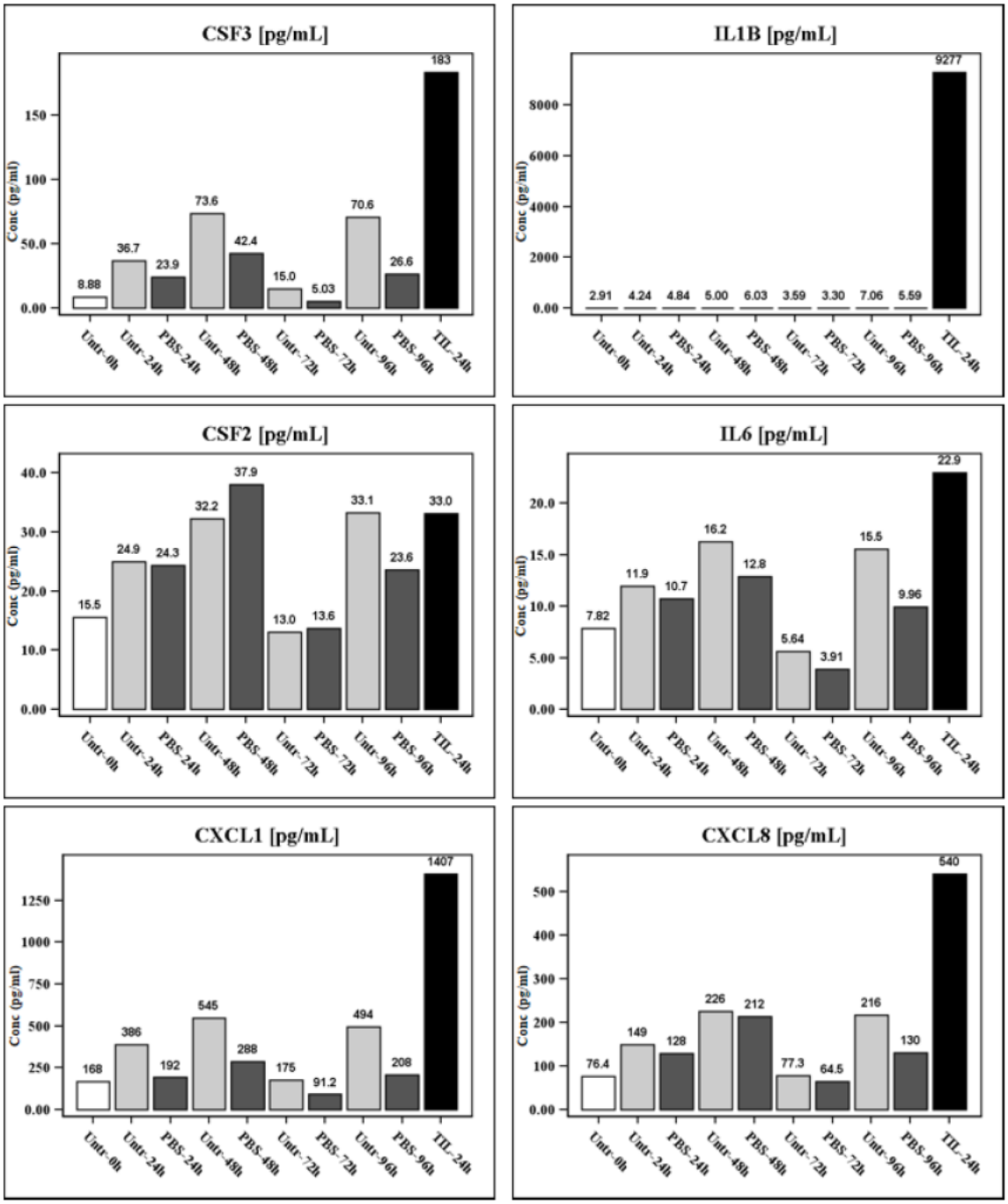

Figure continues

Figure 6. Secretion levels of proinflammatory mediators into the basolateral medium of the organotypic gingival cultures following exposure.

Proinflammatory mediators (listed in the title of each graph) were measured in the basolateral media of gingival cultures after 24, 48, 72, and 96 h of apical phosphate-buffered saline (PBS) exposure. Concentration is reported in pg/mL. N=1. Abbreviations: Conc, concentration; NegCtrl, negative control; PosCtrl, positive control; Unt, untreated.

9.1.3 Alterations in Expression Levels of Genes Regulating Osmolarity

Alterations in the expression levels of genes known to regulate osmotic stress are displayed in Figure 7. Gene expression results highlighted an overall adaptive response to the presence of PBS, with an altered expression of different aquaporins (*AQP1–5*), ion channels (*CFTR, KCNJ1*, *TRPV4*), and other transporters (*SLC5A3, SLC6A12, SLC14A2,* and *SLC9A2* among the most represented).

24 h PBS vs. no PBS (fold change)				48 h PBS vs. no PBS (fold change)					
Upregulated		Downregulated		Upregulated				Downregulated	
TAT	16.903	CFTR	−15.9258	ADM	8.9434	NFKBIA	2.8379	CFTR	−8.9286
ADM	7.8479	SLC14A2	−10.4164	SLC5A3	8.1942	DUSP1	2.823	NOS3	−5.3392
ABCB1	3.9612	PCK2	−5.8285	SLC6A12	7.8839	SLC2A1	2.8036	AQP3	−4.7948
GUCA2A	3.955	NPR1	−5.443	GADD45B	7.3889	HMOX1	2.7781	SLC14A2	−4.7373
TRPV4	3.6908	PLAT	−4.4644	AQP1	7.1665	GADD45A	2.7473	ODC1	−3.2877
KCNJ1	3.6143	TP53	−3.3991	SLC6A6	5.4751	GUCA2A	2.6113	TP53	−3.2679
NFKBIA	2.9371	OXT	−3.3567	VEGFA	4.6704	TRPV4	2.4543		
SLC6A6	2.5853	ODC1	−2.8685	MAPK8	3.9837	NFAT5	2.271		
VEGFA	2.4146	DDIT3	−2.6697	HSPA5	3.3604	TPM4	2.2306		
AQP4	2.1683	AQP3	−2.6094	SLC38A2	3.1502	AQP2	2.1273		
INS	2.0577	PDIA4	−2.5346	SNAI1	2.9628	CTGF	2.1147		
TNF	2.0207	CALR	−2.2712	AQP4	2.8903	CRYAB	2.0445		
		ATF4	−2.0618	AKR1B1	2.8476	KCNJ1	2.0263		
				OXT	2.8429				

72 h PBS vs. no PBS (fold change)				96 h PBS vs. no PBS (fold change)			
Upregulated		Downregulated		Upregulated		Downregulated	
SLC14A2	9.6901	SLC9A2	−30.7657	GUCA2A	11.329	ODC1	−5.5007
EDN1	2.6269	CFTR	−11.2537	AQP1	11.3183	PLAT	−4.7395
AQP9	2.4422	OXT	−5.0323	SLC14A2	4.8738	CFTR	−4.1065
PCK2	2.3782	NPR1	−3.8809	SLC6A12	3.8352	SLC9A2	−3.6729
EGR3	2.2846	ODC1	−3.8607	KCNJ1	3.0215	ABCB1	−3.6269
AQP2	2.1032	AGT	−2.7779	VEGFA	2.9124	NPR1	−3.0377
ADM	2.0929	LCN2	−2.3513	AQP9	2.7592	LCN2	−2.8089
SLC6A6	2.0056	NOS3	−2.1282	EGR3	2.5505	OXT	−2.2058
SLC14A2	9.6901			EGR1	2.4068		
				EDN1	2.3988		
				TRPV4	2.2079		
				TPM4	2.1363		
				AGT	2.1054		

Figure 7. Altered expression levels of genes regulating osmotic stress after phosphate-buffered saline (PBS) apical treatment.

Gene expression levels were measured using the Human Osmotic Stress PCR Array (PAHS-151Z). The table shows changes in gene expression expressed as fold changes at different time-points (24, 48, 72, and 96 h). Upregulated and downregulated gene expression levels compared with the corresponding air controls are marked in red or blue, respectively. N=1.

9.2 Dose Range Finding (DRF)

Nicotine was used as an internal compound to normalize and compare the effects of 3R4F CS and THS2.2 aerosol on organotypic gingival cultures. We extrapolated the values of PBS-deposited nicotine (see 7.5.3) from a DRF experiment in which different concentrations of 3R4F CS and THS2.2 aerosol were tested.

9.2.1 Cell Viability Assessment Using the AK Assay.

Cytotoxicity following exposure to 3R4F CS or THS2.2 aerosol was assessed by measuring the activity of AK released from the cells into the basolateral media. The data were collected before the second and third exposures and 24 h post-exposure. Figure 8 shows that 3R4F CS-exposed cultures exhibited increased cytotoxicity compared with air controls. The cytotoxicity levels of the THS2.2 aerosol-exposed cultures were not different from those of the air controls, independently of dose or collection time, except a slight increase for the 2.18 mg/L concentration after the second day of exposure (approximately 1%).
Descriptive statistics for these results are reported in Supplementary Table 11.

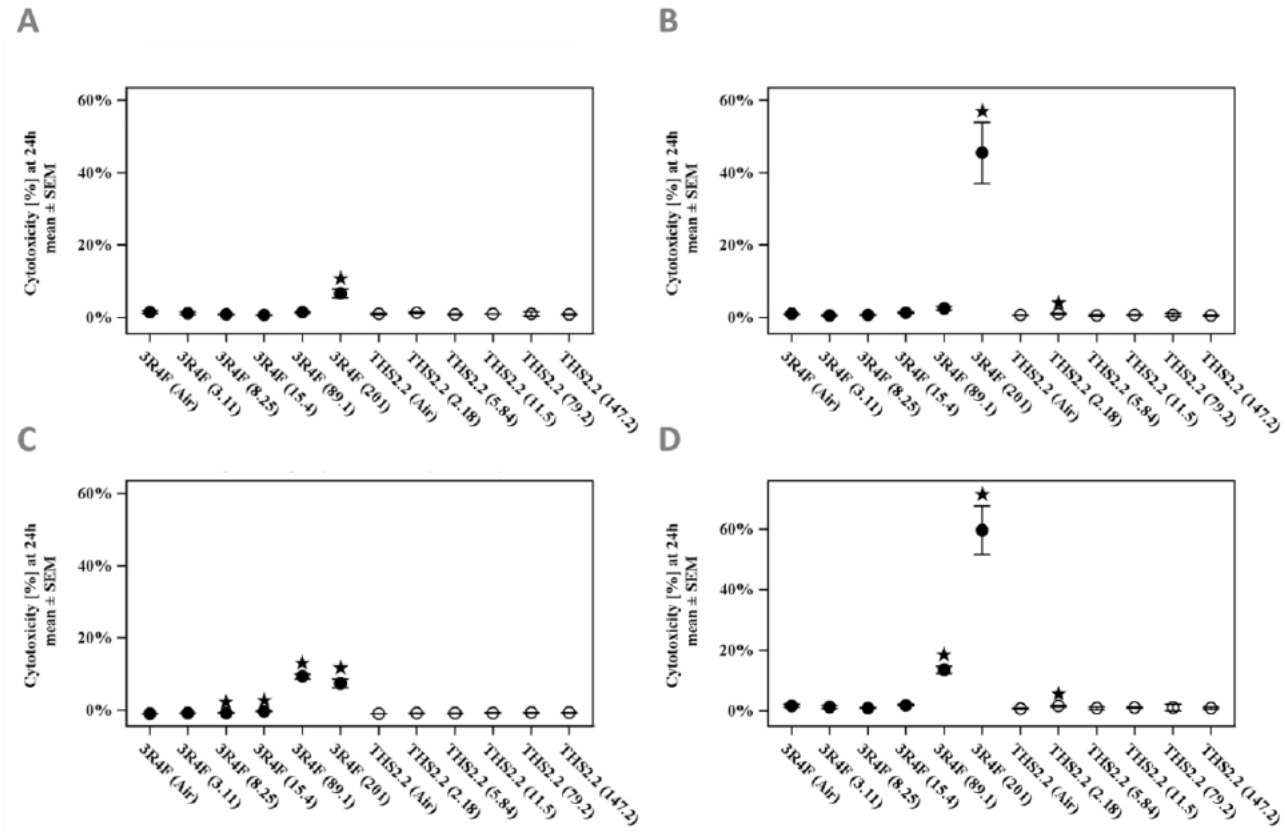

Figure 8. Cytotoxicity in organotypic gingival cultures following 3R4F cigarette smoke (CS) and THS2.2 aerosol exposure.
The release of adenylate kinase (AK) into the basolateral media of cultures was measured on day 2 (**A**), day 3 (**B**), and 24 h after all three exposures to 3R4F CS or THS2.2 aerosol at the indicated concentrations (mg/L) (**C**). The average of these values collected along the experiment is indicated in **D**. Data are presented as the mean of the normalized

cytotoxicity relative to the positive control (Triton X-100-treated culture was taken as 100% cytotoxicity) ± SEM (N=3, from one experimental repetition with three exposure runs/repetition). ★ indicates a significant difference compared with the corresponding air controls (p<0.05).

9.2.2 Cytochrome P450 (CYP) 1A1/1B1 Activity

The combined activity of CYP1A1 and CYP1B1 enzymes was measured in organotypic gingival cultures 24 h post-exposure.

Figure 9 shows that 24 h post-exposure, there was a significant increase in the CYP activity at 3R4F CS low-nicotine concentrations (3.11 and 8.25 mg/L); the activity decreased with increasing concentrations. In contrast, a milder dose-dependent increase in the activity was observed in cultures exposed to THS2.2 aerosol. Descriptive statistics of these results are reported in Supplementary Table 11.

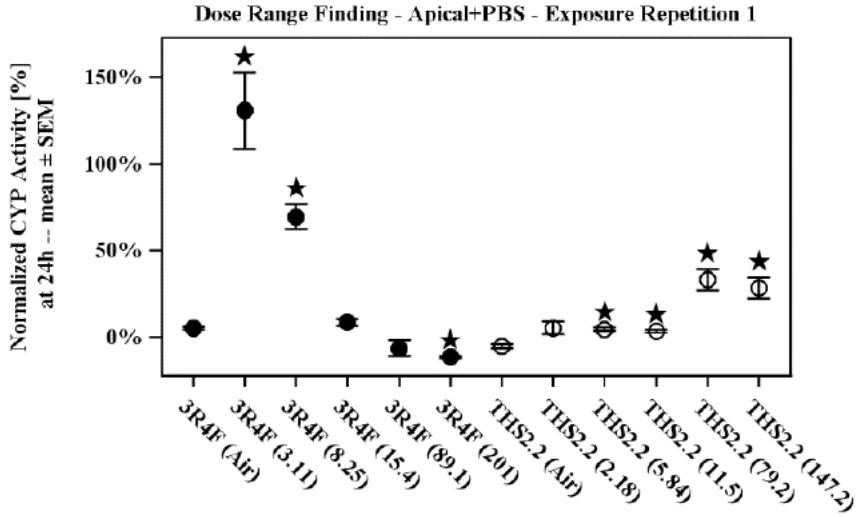

Figure 9. CYP1A1/CYP1B1 activity in organotypic gingival cultures following exposure.
The combined CYP1A1 and CYP1B1 activity was measured 24 h after cultures were exposed to three repetitions of 3R4F cigarette smoke (CS) or THS2.2 aerosol for 28 min at the indicated concentrations (mg/L). Data are presented as the mean of the normalized activity relative to the positive control (2,3,7,8-tetrachlorodibenzo-p-dioxin-treated culture was considered to be 100% induction) ± SEM (N=3, from one experimental repetition with three exposure runs/repetition). ★ indicates a significant difference compared with the corresponding air controls (p<0.05).

9.2.3 Histological Evaluation

We assessed the effects of a wider range of 3R4F CS and THS2.2 aerosol concentrations on tissue morphology 24 h post-exposure. Representative H&E sections are shown in Figure 10.

Control sections exposed to air (Sham) for both 3R4F and THS2.2 groups maintained the physiological structure of the stratified-cornified squamous epithelium, composed of the stratum basale (SB), stratum spinosum (SS), stratum granulosum (SG), and stratum corneum (SC). Twenty-four hours after the last exposure to 3R4F CS, the presence of keratohyaline granules was observed, starting at the low CS concentration (8.25 mg/L).

At the highest CS concentrations (89.1–201 mg/L), the distinction between the SG and the SC was lost. The gingival tissue appeared severely damaged, showing complete loss of the SS (atrophy), and keratinization extending into the SB or even the membrane. Moreover, apoptosis/karyorrhexis/pyknosis was present.

In contrast, THS2.2 aerosol-exposed samples showed minor changes. Only at the highest concentration (147.2 mg/L) did we observe a sporadic atrophy and loss of clear distinction between the SG and SC. In general, the morphological alterations were clearly less pronounced with respect to the corresponding 3R4F CS-exposed counterparts.

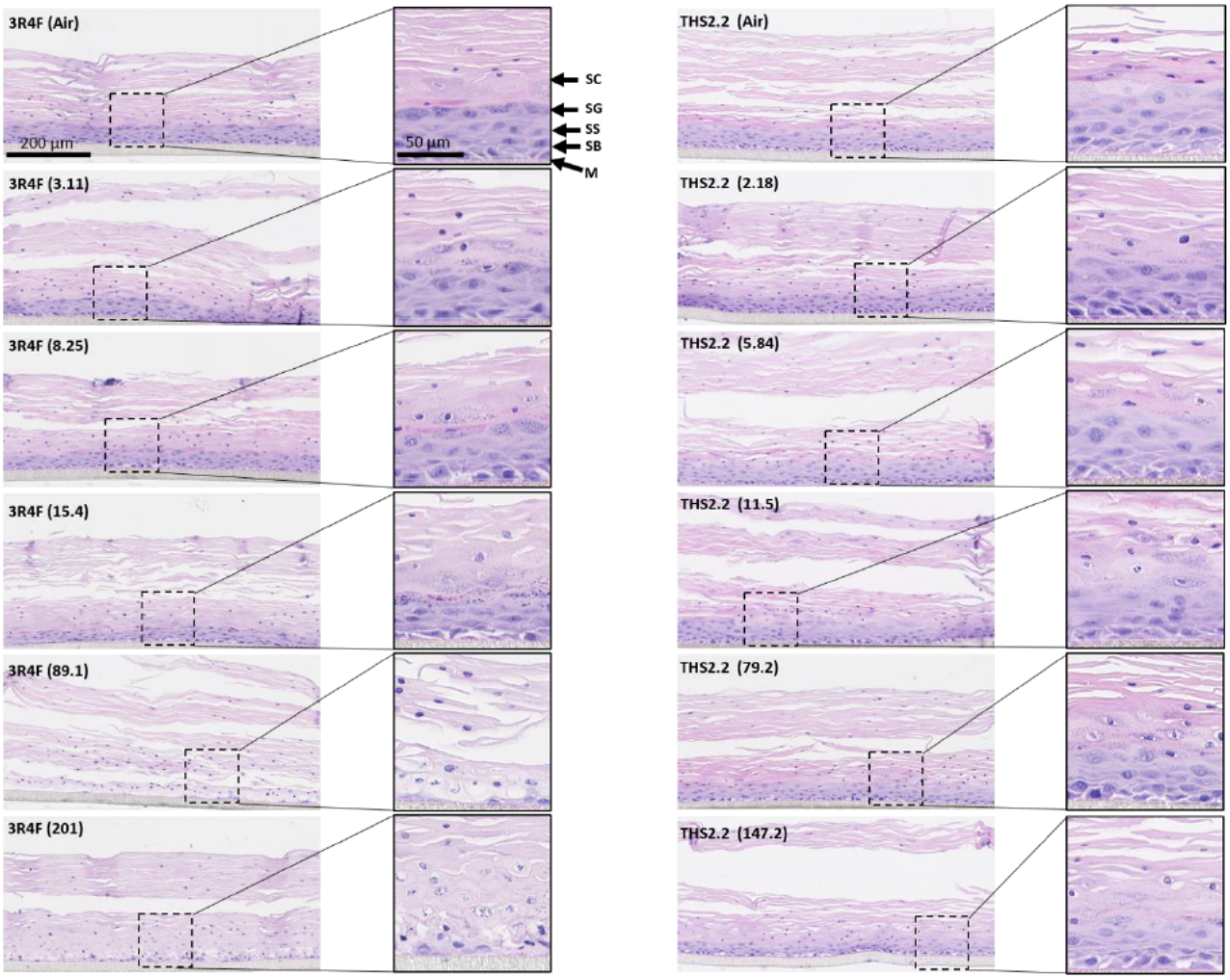

Figure 10. Histology following exposure of organotypic gingival cultures to smoke/aerosol.

Representative images of hematoxylin and eosin (H&E)-stained gingival cultures after 24 h from the last exposure to 3R4F cigarette smoke (CS) (left) or THS2.2 aerosol (right). Abbreviations indicate the different layers of the gingival cultures: M, membrane; SB, stratum basale, SS, stratum spinosum; SG, stratum granulosum; SC, stratum corneum. Nicotine concentrations are indicated in brackets (in mg/L). H&E images show a 10× magnification (63× for the image insets). N=3.

9.2.4 Alterations in Expression Levels of Genes Regulating Cellular Stress and Inflammation

The investigation of possible toxicity-specific mechanisms associated with 3R4F CS and THS2.2 aerosol exposure was conducted in gingival cultures using a wide range of concentrations. Gene expression was evaluated using the transcriptomic data from all 3R4F CS and THS2.2 aerosol concentrations.

The overall systems impact (the aggregation of the network perturbation) is referred to as the biological impact factor (BIF).

Figure 11 shows the overall biological impact, in the context of the biology covered in the network models (Table 13) for each exposure condition compared with the respective air controls. Four hours post-exposure, 3R4F CS exposure (89.1 mg/L nicotine concentration) produced the highest impact on the cultures. For all THS2.2 aerosol concentrations, lower BIF values were observed at the different concentrations compared with the corresponding 3R4F CS exposure groups. The networks affected most by 3R4F CS exposure were cell fate and angiogenesis (CFA), cell proliferation (CPR), cell stress (CST), and inflammatory processes (IPN). The same networks were less affected by the THS2.2 aerosol concentrations analyzed, independent of the concentrations.

Each network family comprises a set of network models, and the BIF can be decomposed down to network level.

Figure 11 (NPA panel) shows the perturbation of each network across the comparisons.

The highest BIF, seen in the 3R4F CS (89.1 mg/L) cultures 4 h post-exposure, is reflected in the heatmap as the highest perturbation scores in the majority of networks (network perturbation amplitude, NPA), compared with the other contrasts, mirroring the trend of the BIF pattern. Notably, the networks describing the biology of response to mTOR, autophagy, epigenetics, and Hedgehog, along with the xenobiotic metabolism response, were most affected by CS.

In contrast, at comparable nicotine concentrations, THS2.2 aerosol exposure did not result in substantial perturbations of these networks. THS2.2 aerosol-exposed cultures were affected only at the higher concentrations (79.2 and 147.2 mg/L), as indicated by the NPA scores for xenobiotic metabolism and NFE2L2 signaling. Nevertheless, the degree of impact (i.e., their NPA scores) was lower, compared with the impact of 3R4F CS at the matching concentration (79.2 mg/L for THS2.2 aerosol vs. 89.1 mg/L for 3R4F CS).

The highest concentration for 3R4F CS was not included in this analysis because of the low quantity of the mRNA extracted, possibly resulting from the extensive tissue damage observed.

We completed our network-based systems toxicology assessment by performing a more “standard” gene-set analysis (see section 8.2.7) (Figure 11, GSA panel). gene-set analysis (GSA) involves gene-sets covering biological processes that are not necessarily included in the networks used in the NPA/BIF calculations, and is therefore also suitable for exploratory investigations. We first extracted 22 “confirmatory” KEGG pathways overlapping with key molecules belonging to our network list. Next, five broad pathway categories were defined by grouping the 209 KEGG pathways by gene content and biological processes (Zanetti 2016). We applied two standard GSA statistical tests, the competitive Q1 and the self-contained Q2 (Nam 2008). The heatmap shows that the gene expression data from the cultures exposed to 3R4F CS had higher enrichment scores for the various biological annotations, compared with the data from the cultures exposed to all three concentrations of THS2.2

aerosol. However, the sample groups contain only three samples, and do not provide reliable Q2 (sample reshuffling) statistics.

The differentially expressed (DE) genes panel shown in the bottom of Figure 11 indicates that the impact of 3R4F CS on gene expression was higher than that of THS2.2 aerosol at all concentrations tested. Moreover, the impact on gene expression was concentration-dependent.

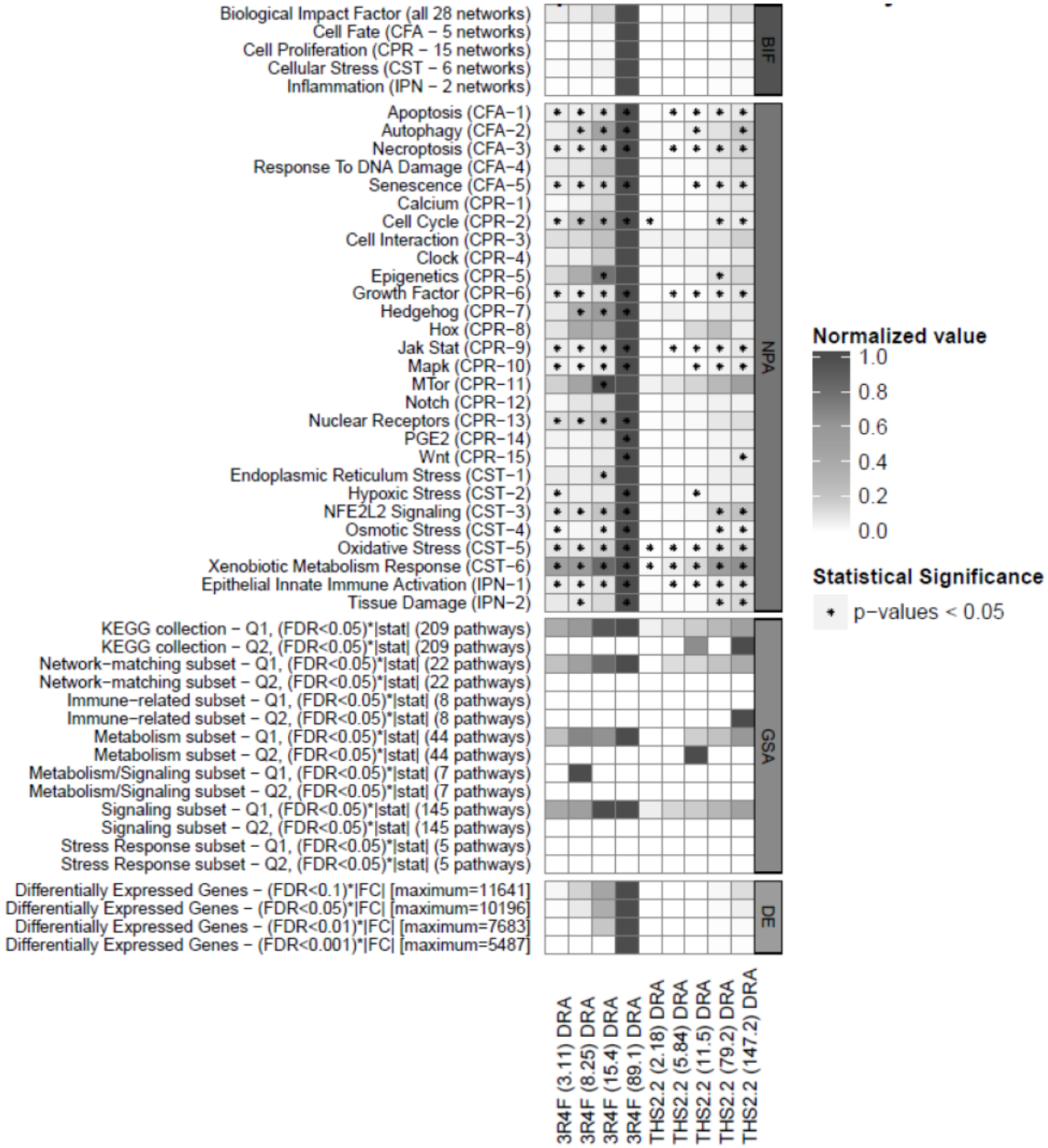

Figure 11. Heatmap of the impact of 3R4F cigarette smoke (CS) or THS2.2 aerosol exposures on differential expression of genes.

The values are normalized to the interval [0, 1] in a row-wise manner, and the details of their calculations and meanings are given in section 8.2. The uppermost panel displays the biological impact factor (BIF), which quantifies the overall impact of the exposures using the full suite of networks. It also includes the contribution of the four network families to the overall BIF (cell fate and angiogenesis–CFA, cell proliferation–CPR, cellular stress–CST, and pulmonary inflammation–IPN). The network names are listed on the left side of the heatmap, with the corresponding network family on the right. All networks that were significantly affected in at least one comparison are listed. The shading gradient of the NPA score was normalized to the maximum NPA score per network. * indicates the statistical significance of network perturbations, as explained in the Statistical and Computational Methods section. Overall results of gene-set analyses (GSA) are displayed in the next panel as the counts of statistically significant gene-sets for the KEGG collection and the standard statistical tests (Q1 and Q2). Finally, the lowermost panel shows the number of differentially expressed (DE) genes for four distinct statistical significance thresholds, to identify possible threshold effects. For completeness, the Q2 GSA results are shown for the nine dose range assessment (DRA) contrasts, although the small size of the sample groups (three elements at most) does not allow their reliable use to confirm the NPA results. Abbreviations: CFA, cell fate and angiogenesis; CPR, cell proliferation; CST, cell stress; IPN, inflammatory process network.

9.3 Main Phases (I–III)

From the DRF experiment, we selected two concentrations for the Main Phases (see Table 6): The lower concentration of 3R4F CS (49.4 mg/L of nicotine), to obtain moderate damage, allowing the assessment of effects relevant to toxicity-related mechanisms associated with exposure (Davis 2013), and the highest concentration (84.6 mg/L), to reflect morphological alterations associated with severely damaged tissue. One lower and two matching concentrations of THS2.2 aerosol were selected for the comparative analysis (14.4, 54.6, and 100.4 mg/L).

Note: the cytotoxicity values determined during the DRF do not match the ones observed during the experimental repetitions due to a mismatch of the percent of dilution and the nicotine concentration. This explains the lower THS2.2 aerosol concentration not matching the low 3R4F CS (for details, please check Section 3, deviation #6).

The main phase was repeated three times. The results are shown as a mean of the three repetitions or, in some cases, as individual results for the main phase.

9.3.1 Cell Viability Assessment (AK Assay)

Cytotoxicity of the tissue model following 3R4F CS or THS2.2 aerosol exposure was assessed over the entire period of exposure and 4 or 24 h post-exposure. Figure 12 shows the levels of AK activity on day 2 and day 3 of exposure and 4 h post-exposure. We observed minimal cytotoxicity after 3R4F CS exposure (maximum 1.47% for the 84.6 mg/L), and none after THS2.2 aerosol exposure up to 4 h after the last exposure.

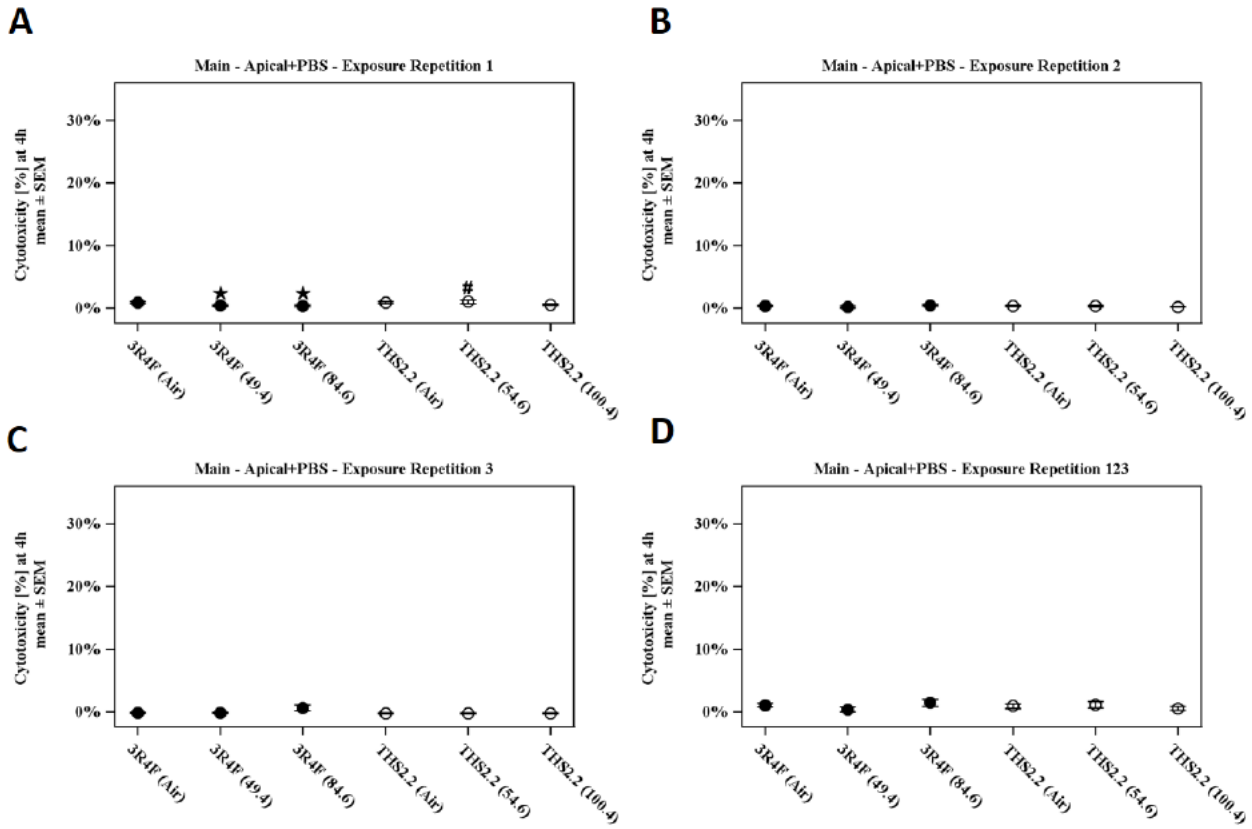

Figure 12. Cytotoxicity in organotypic gingival cultures exposed to 3R4F cigarette smoke (CS) and THS2.2 aerosol (4 h post-exposure).

Mean cytotoxicity levels were determined using the AK assay 24 h after the first exposure (**A**), 24 h after the second exposure (**B**), and 4 h post-exposure (**C**). Panel **D** indicates accumulation of adenylate kinase (AK) activity over the entire time frame. AK levels were normalized relative to those in the positive control (Triton-X-treated cultures considered to represent 100% cytotoxicity). Error bars indicate SEM (N=9, from three experimental repetitions with three exposure runs/repetition). Nicotine concentrations in 3R4F CS or THS2.2 aerosol are indicated for each group (mg/L, x-axis). ★ $p<0.05$, compared with the corresponding air control. # indicates a significant difference compared with 3R4F at the comparable concentration ($p<0.05$).

Figure 13 illustrates cytotoxicity levels 24 h after the first (panel A), second (panel B), and third (panel C) exposure to 3R4F CS or THS2.2 aerosol, along with the aggregated results (panel D). We observed a significant increase in AK 24 h after the last exposure, suggesting considerable tissue damage; this cytotoxicity was proportional to the 3R4F CS concentration applied (nearly 9% for 49.4 mg/L and around 30% for 84.6 mg/L). Minimal cytotoxicity was observed for THS2.2 aerosol-exposed samples.

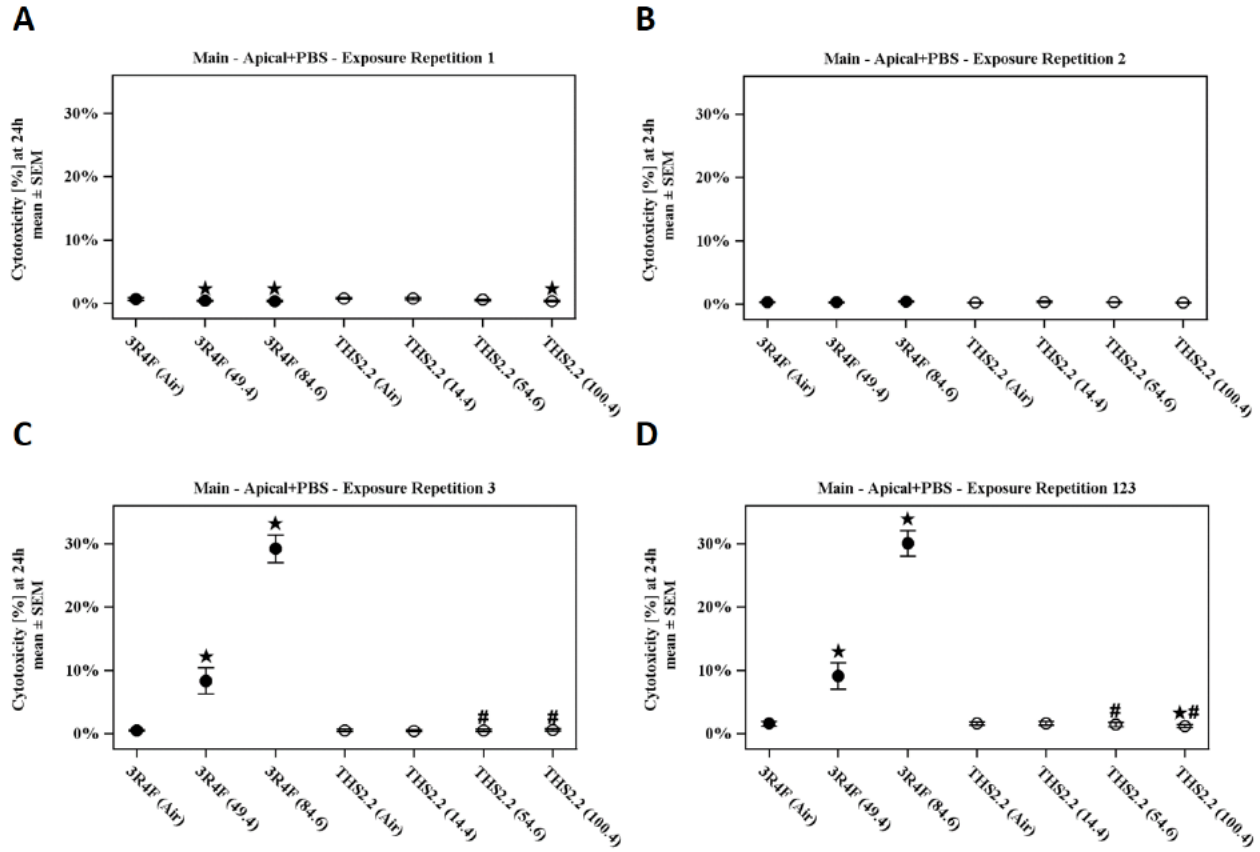

Figure 13. Cytotoxicity in organotypic gingival cultures exposed to 3R4F cigarette smoke (CS) and THS2.2 aerosol (24 h post-exposure).

Cytotoxicity-based adenylate kinase (AK) activity was assessed in the gingival culture on day 2 (**A**) and day 3 (**B**) of treatments, and 24 h post-exposure (**C**). Panel **D** indicates mean cumulative cytotoxicity levels over the entire time frame. AK levels were normalized relative to those in the positive control. Error bars indicate SEM (N=9, from three experimental repetitions with three exposure runs/repetition). Nicotine concentrations in 3R4F CS or THS2.2 aerosol are indicated for each group (mg/L, x-axis). ★ $p<0.05$, compared with the corresponding air control; # $p<0.05$, compared with the corresponding smoke matching concentrations.

Descriptive statistics for these results are reported in Supplementary Table 12.

Overall, CS-induced cytotoxicity increased with post-exposure duration, whereas THS2.2 aerosol exerted only a minimal, if any, effect on cell viability.

9.3.2 Histological Evaluation

The impact of exposure on tissue morphology was evaluated by histological assessment 24 h after the repeated exposures (Figure 14).

Gingival tissue models exposed to air (Sham) for both the 3R4F and THS2.2 groups maintained the physiological structure of the cornified squamous epithelium, with the distinct cell layers observable. Twenty-four hours after the last exposure to 3R4F CS, clear histological modifications were observed: At the low CS concentration (49.4 mg/L), the distinction between the SG and SC became blurry, or was completely lost with the presence of keratohyaline granules in both layers; moreover, atrophy of the SS was observed. At the high CS concentration (84.6 mg/L), the tissue models appeared severely damaged, showing complete loss of the SS (atrophy), and keratinization extending into the SB or even the membrane. Overt apoptosis/karyorrhexis/pyknosis was present.

THS2.2 aerosol-exposed samples showed minor changes, with only sporadic atrophy observed and loss of clear distinction between the SG and SC proportional to the THS2.2 aerosol concentrations; the morphological alterations observed were clearly less pronounced with respect to the corresponding 3R4F CS-exposed counterparts.

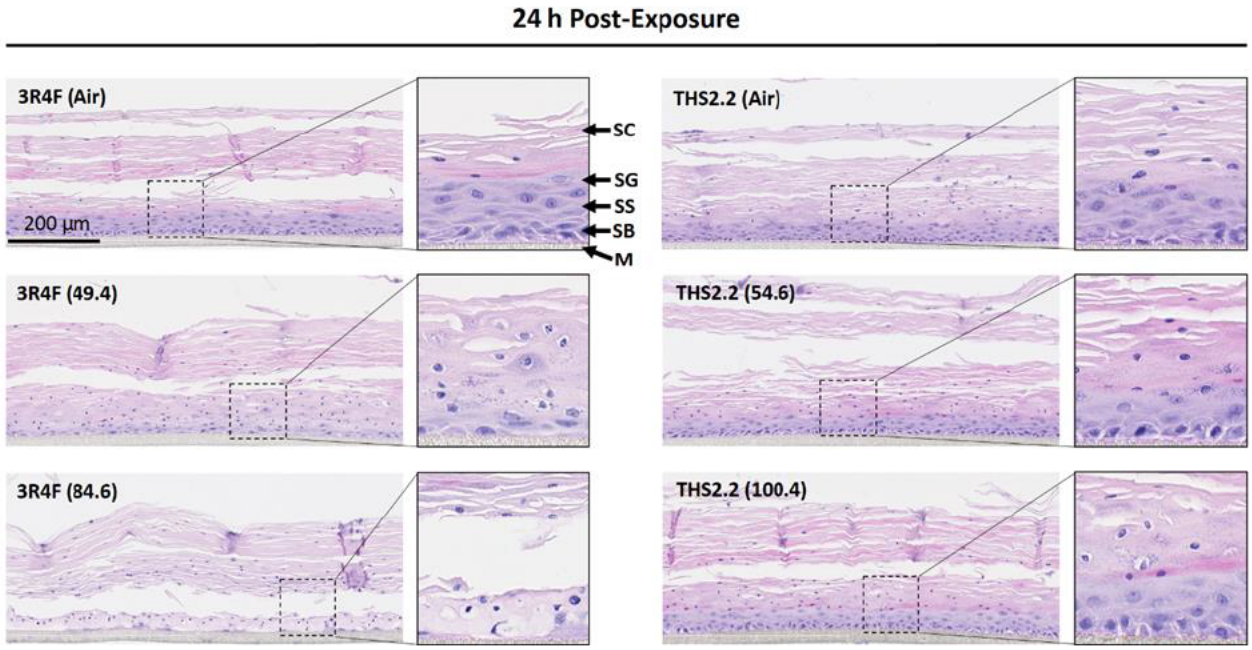

Figure 14. Histological assessment following exposure of organotypic gingival cultures to 3R4F cigarette smoke (CS) or THS2.2 aerosol.

Representative images of hematoxylin and eosin (H&E)-stained gingival cultures after 24 h from the last exposure to 3R4F CS (left) or THS2.2 aerosol (right). Abbreviations indicate the different layers of the gingival cultures: M, membrane; SB, stratum basale, SS, stratum spinosum; SG, stratum granulosum; SC, stratum corneum. Concentrations are indicated in brackets (nicotine, mg/L). H&E images show a 10× magnification (63× for the image insets). N=9.

9.3.3 Transcriptome of Organotypic Gingival Cultures Exposed to 3R4F CS or THS2.2 Aerosol

Measurement of cytotoxicity by the AK assay indicated that 4 h after the third exposure to 3R4F CS the tissue damage was very limited, whereas at 24 h we observed extensive morphological alteration and cytotoxicity (Figure 12, Figure 13, Figure 14). The absence of overt cell death allows the investigation of toxicity-specific mechanisms associated with exposure, instead of effects reflecting morphological alterations associated only with severely damaged tissue. Therefore, we mainly focused on the 4-h post-exposure time-point to measure gene expression and mechanistic gene network alterations induced by 3R4F CS and THS2.2 aerosol exposure. To note, we complemented this analysis with an assessment of the transcriptional changes 24 h after the last exposure; this more-exploratory analysis was done in only three replicates (rather than nine), and no data were obtained for the destructive high 3R4F CS concentration.

In the BIF panel illustrated in Figure 15, we describe the biological impact of 3R4F CS and THS2.2 aerosol as defined by the four network families (CFA, CPR, CST, IPN; see also section 9.2.4). The heatmap shows that, for both the 28 networks and the four network families, the impact of the 3R4F CS was higher than that of THS2.2 aerosol, and proportional to the CS concentration.

The NPA panel (Figure 15) illustrates the effects of 3R4F CS and THS2.2 aerosol for each of the 28 networks. The major changes were induced by 3R4F CS exposure and affected all networks, in a concentration-dependent manner. The most significant alterations were recorded for networks belonging to the CFA-, CST-, and IPN-related families; in particular, the xenobiotic metabolism network responded equally to 3R4F CS low and high concentrations, while the reductions following exposure to THS2.2 aerosol were less pronounced than in other networks. Some of the networks were exclusively impacted by 3R4F CS, such as Calcium, Hedgehog, PGE2, Endoplasmic Reticulum Stress, and Hypoxic Stress.
Overall, the response to THS2.2 aerosol was always much lower than to 3R4F CS at the comparable concentration.

The GSA panel (Figure 15) shows that the Q2 results follow the same pattern as the network-based systems toxicology results: strong concentration-dependent enrichments for the gingival cultures exposed to 3R4F CS, while exposure to THS2.2 aerosol did not return comparable values. These results support the suitability of the GSA Q2 tests as a confirmatory quantification of the biological impact of exposure. The findings reflect the fact that Q2 specifically tests the association between one gene-set and the treatment effects, whereas Q1 compares gene-sets to other gene-sets. A detailed illustration of the 22 network-matching pathways of the KEGG collection can be found in Supplementary Figure 1. Heatmap of the gene-set analysis (GSA) results for the network-related gene-set collection.
The DE panel of Figure 15 indicates that the impact of 3R4F CS on gene expression was higher than that of THS2.2 aerosol at all concentrations tested. Moreover, the impact on gene expression was concentration-dependent.

Twenty-four hours after the last exposure, the lower concentration of 3R4F CS (49.4 mg/L) and both THS2.2 aerosol concentrations were analyzed over a reduced number of replicates, as described above (Supplementary Figure 2). However, to make fair comparisons between the three replicates at the 24-h time-point and the nine replicates at the 4-h post-exposure time-point, we split the 4-h

samples into three groups of three samples matching the batches of the experiment execution. For the low 3R4F CS concentration, results showed an increase in values of the BIF, the network-family BIFs, and most of the 28 network NPAs with respect to the 4-h post-exposure time-point. One notable exception was the Xenobiotic Metabolism Response network, where a decrease in NPA was observed. For THS2.2 aerosol-exposed samples, all BIF/NPA values were lower. Globally, the lower impact of exposure to THS2.2 aerosol compared with 3R4F CS was confirmed. Interestingly, the differentially expressed gene panel (Figure 15 and Supplementary Figure 2, DE panel) shows decreased values following the 4-h-to-24-h recovery period for both 3R4F and THS2.2 treatments.
In summary, including the 24-h data suggested that while the CS-exposed cultures showed an exacerbation of the response at the 24-h time-point, cultures exposed to THS2.2 aerosol yielded a slightly less-impacted BIF panel, indicating a recovery trend over time.

miRNA analysis focused on all the networks highlighted 66 differentially expressed miRNAs, 41 regulated only by 3R4F CS, one regulated only by THS2.2 aerosol, and 21 commonly regulated by both treatments (Table 14). The number of significantly regulated miRNAs was higher for 3R4F than for THS2.2 (Figure 15 miRDE, bottom panel), without any differential expression for the low concentration 24 h post-exposure (Supplementary Figure 2). In the next paragraphs, we will focus our analysis on selected networks relevant for smoking- and periodontal disease-induced alterations.

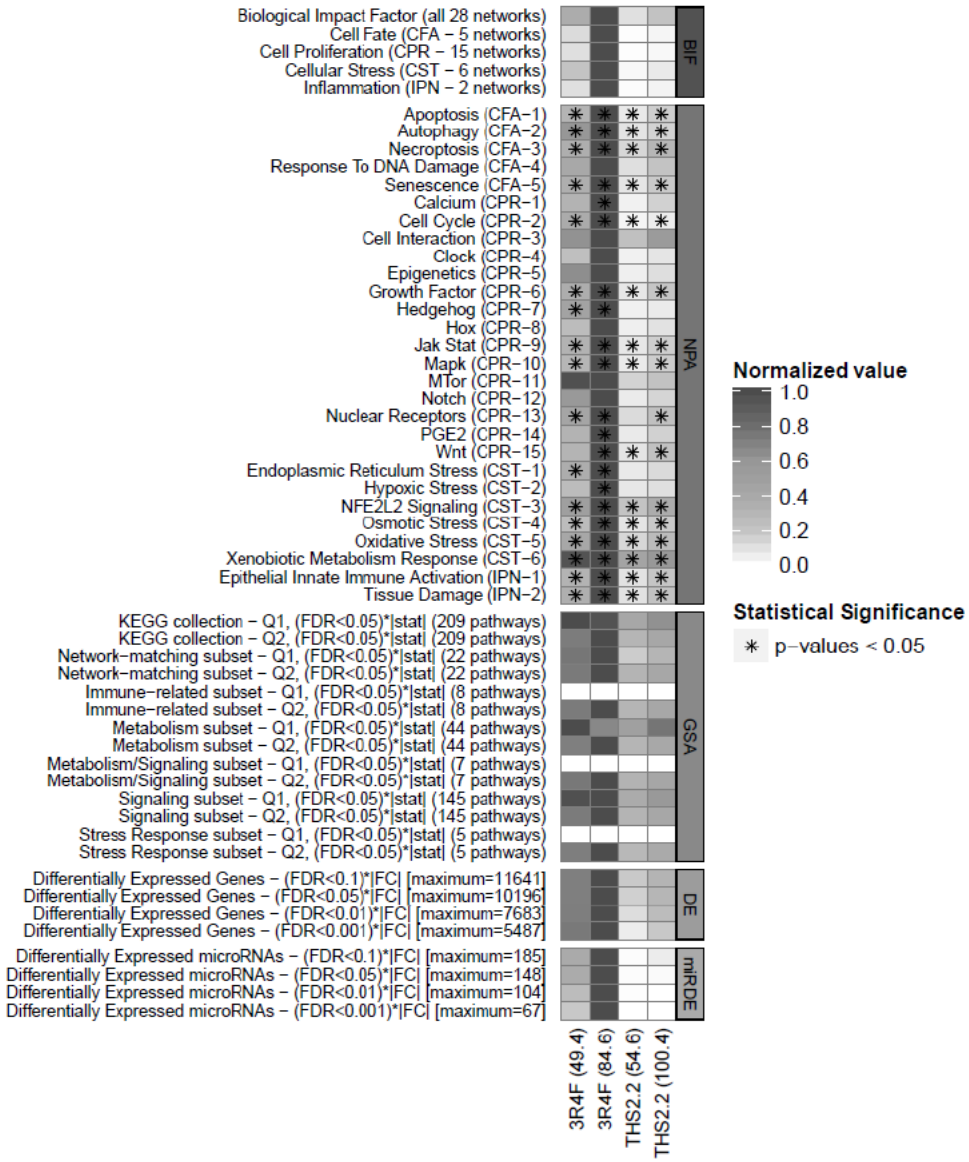

Figure 15. Overview of the impact of 3R4F cigarette smoke (CS) or THS2.2 aerosol exposures on differential expression of genes.

Values are normalized to the interval [0, 1] in a row-wise manner. Details of their calculations and meanings are given in the Statistical and Computational Methods section. The uppermost panel displays the biological impact factor (BIF), which quantifies the overall impact of the exposures using the full suite of networks. It also includes the contribution of the four network families to the overall BIF (cell fate and angiogenesis–CFA, cell proliferation–CPR, cellular stress–CST, and pulmonary inflammation–IPN). The contributions of network families result from aggregation of network perturbation amplitudes (NPA) for each single network; these are shown for each relevant network in the middle panel. * indicates statistically significant network perturbations, as explained in the Statistical and Computational Methods section. Overall results of gene-set analyses (GSA) are displayed in the next panel for the KEGG collection and the two standard statistical tests (Q1 and Q2). Also shown are specific subsets of the KEGG collection: First, the 22 pathways matching the mechanistic networks, and second, the five broad categories of the 228 pathways contained in the KEGG collection. To enhance the differences between the columns, displayed values were defined as sums of absolute values of gene-set-level statistics (i.e., fold-change mean) for the statistically significant gene-sets in each category. The two lower panels show the number of differentially expressed genes (DEGs) and differentially expressed miRNAs (miRDE) for four distinct statistical significance thresholds, to identify possible threshold effects. Sums of absolute values of fold-changes of statistically significant genes or miRNAs are displayed, to enhance differences between columns. N=6–9.

Table 14. List of miRNAs affected by 3R4F CS and THS2.2 aerosol exposure.

3R4F		Symbol	Log2 Ratio 3R4F (High)	
	miRNA upregulated	miR-149-3p (and other miRNAs with seed GGGAGGG)	1.069	
		miR-4454 (miRNAs with seed GAUCCGA)	0.971	
		miR-762 (and other miRNAs with seed GGGCUGG)	0.776	
		miR-1343-5p (and other miRNAs with seed GGGGAGC)	0.741	
		miR-150-3p (miRNAs with seed UGGUACA)	0.740	
		miR-92b-5p (miRNAs with seed GGGACGG)	0.721	
		miR-572 (miRNAs with seed UCCGCUC)	0.618	
		miR-292b-5p (and other miRNAs with seed CUCAAAA)	0.600	
		miR-4734 (miRNAs with seed CUGCGGG)	0.591	
		miR-4707-5p (miRNAs with seed CCCCGGC)	0.574	
		miR-4467 (miRNAs with seed GGCGGCG)	0.568	
		miR-1908-5p (and other miRNAs with seed GGCGGGG)	0.552	
		miR-1275 (and other miRNAs with seed UGGGGGA)	0.544	
		miR-4634 (miRNAs with seed GGCGCGA)	0.491	
		miR-4651 (and other miRNAs with seed GGGGUGG)	0.485	
		miR-1207-5p (and other miRNAs with seed GGCAGGG)	0.473	
		miR-3473b (and other miRNAs with seed GGCUGGA)	0.448	
		miR-3937 (miRNAs with seed CAGGCGG)	0.448	
		miR-29b-1-5p (miRNAs with seed CUGGUUU)	0.423	
		miR-4676-5p (and other miRNAs with seed AGCCAGU)	0.410	
		miR-3648 (miRNAs with seed GCCGCGG)	0.385	
		miR-320b (and other miRNAs with seed AAAGCUG)	0.384	
		miR-4690-5p (miRNAs with seed AGCAGGC)	0.381	
		miR-665 (and other miRNAs with seed CCAGGAG)	0.357	
		miR-2861 (and other miRNAs with seed GGGCCUG)	0.323	

Table continues

		miR-375-3p (and other miRNAs with seed UUGUUCG)	0.309	
		miR-3187-3p (miRNAs with seed UGGCCAU)	0.308	
		miR-194-5p (miRNAs with seed GUAACAG)	0.307	
		miR-4508 (and other miRNAs with seed CGGGGCU)	0.305	
		miR-3621 (miRNAs with seed GCGGGUC)	0.296	
		miR-675-5p (and other miRNAs with seed GGUGCGG)	0.286	
		miR-658 (miRNAs with seed GCGGAGG)	0.278	
		miR-224-5p (miRNAs with seed AAGUCAC)	0.274	
		miR-324-5p (miRNAs with seed GCAUCCC)	0.269	
		miR-24-1-5p (and other miRNAs with seed GCCUACU)	0.265	
	miRNA down-regulated	miR-30c-5p (and other miRNAs with seed GUAAACA)	-0.269	
		miR-342-3p (miRNAs with seed CUCACAC)	-0.432	
		miR-423-3p (miRNAs with seed GCUCGGU)	-0.466	
		miR-4710 (miRNAs with seed GGUGAGG)	-0.471	
		miR-125b-5p (and other miRNAs with seed CCCUGAG)	-0.497	
		miR-3935 (miRNAs with seed GUAGAUA)	-0.542	
THS2.2		**Symbol**	**Log2 Ratio THS2.2 (High)**	
	miRNA upregulated	-	-	
	miRNA downregulated	miR-23a-5p (and other miRNAs with seed GGGUUCC)	−0.299	
3R4F+THS2.2		**Symbol**	**Log2 Ratio 3R4F (High)**	**Log2 Ratio THS2.2 (High)**
	miRNA upregulated	miR-4530 (miRNAs with seed CCAGCAG)	1.75	0.306
		miR-4443 (miRNAs with seed UGGAGGC)	1.117	0.466
		miR-494-3p (miRNAs with seed GAAACAU)	0.564	0.37
		miR-642a-3p (and other miRNAs with seed GACACAU)	0.461	0.275
	miRNA down-regulated	miR-296-3p (miRNAs with seed AGGGUUG)	−1.835	−0.696

Table continues

		miR-4669 (miRNAs with seed GUGUCCG)	−1.505	−0.625
		miR-3141 (miRNAs with seed AGGGCGG)	−1.415	−0.602
		miR-188-5p (and other miRNAs with seed AUCCCUU)	−1.27	−0.551
		miR-3682-3p (miRNAs with seed GAUGAUA)	−1.242	−0.555
		miR-3911 (and other miRNAs with seed GUGUGGA)	−1.236	−0.576
		miR-4462 (miRNAs with seed GACACGG)	−1.113	−0.428
		miR-4459 (miRNAs with seed CAGGAGG)	−0.994	−0.521
		miR-1268a (and other miRNAs with seed GGGCGUG)	−0.952	−0.387
		miR-1302 (and other miRNAs with seed UGGGACA)	−0.888	−0.315
		miR-617 (miRNAs with seed GACUUCC)	−0.862	−0.277
		miR-1306-3p (miRNAs with seed CGUUGGC)	−0.824	−0.276
		miR-193a-5p (miRNAs with seed GGGUCUU)	−0.812	−0.273
		miR-4521 (miRNAs with seed CUAAGGA)	−0.77	−0.368
		miR-1224-5p (and other miRNAs with seed UGAGGAC)	−0.728	−0.406
		miR-3613-5p (miRNAs with seed GUUGUAC)	−0.448	−0.281
		miR-4750-5p (miRNAs with seed UCGGGCG)	−0.324	−0.263

End of Table

9.3.4 Oxidative Stress Response Following 3R4F CS and THS2.2 Aerosol Exposure

To assess the induction of an oxidative stress response, we first evaluated differential gene expression for the reactive oxygen species pathway 4 h after the third 3R4F CS or THS2.2 exposure (Figure 16A). 3R4F CS broadly affected this pathway, with an especially strong upregulation of the oxidative stress response genes glutamate-cysteine ligase modifier subunit (*GCLM*), thioredoxin reductase 1 (*TXNRD1*), NAD(P)H quinone dehydrogenase 1 (*NQO1*), sulfiredoxin 1 (*SRXN1*), glutaredoxin (*GLRX*), and ATP binding cassette subfamily C member 1 (*ABCC1*). Generally, the response to THS2.2 aerosol exposure was reduced, e.g., by 48% (GCLM), 20% (TXNRD1), 22% (NQO1), 21% (SRXN1), 41% (GLRX), and 34% (ABCC1) in the low-concentration comparisons.

To better quantify the oxidative stress response, we leveraged a previously described oxidative stress causal network model, and scored its perturbation based on downstream affected gene expression: All exposure conditions resulted in significant perturbation of this network, but the perturbation amplitudes were lower for THS2.2 aerosol than for 3R4F CS exposure (with an approximate 70% reduction in the NPA values for THS2.2 vs. 3R4F for both matched concentrations) (Figure 16B). Gene expression data for the 24-h time-point after exposure were also investigated in an exploratory manner, with a limited number of replicates (n=3 instead of 9; see above) (Supplementary Figure 3B and C). We observed that 24 h after the last exposure, the general gene expression response decreased, with few significant gene alterations in the THS2.2 aerosol-exposed cultures at the matching concentration and a much reduced NPA score.

For the miRNA analysis, we focused our attention on commonly regulated miRNAs, and selected the corresponding mRNA targets as described in the Testing Procedure section. Since miRNAs are known to effect relatively small changes in target mRNA expression, we analyzed only the most significant regulated target genes with FDR $\leq$ 0.05. To further understand their functional involvement, the group of differentially expressed target genes was used for IPA Canonical Pathways analysis. Selected cellular functions significantly enriched in the DEGs are listed in Supplementary Table 27. IPA analysis revealed that 13 commonly regulated miRNAs could also play a role in the regulation of different target genes involved in the oxidative stress response (miRNA target panel and Supplementary Figure 3A), such as glutathione peroxidase 4 (*GPX4*), nitric oxide synthase 1 (*NOS1*), γ-glutamyl hydrolase (*GGH*), and autophagy-related protein 13 (*ATG13*).

We complemented these mRNA and miRNA expression analyses with metabolic profiling, for which we focused on the high 3R4F CS and THS2.2 aerosol concentrations 4 h after the third exposure (Figure 16D–F, Supplementary Figure 3D–E). The 4-h time-point was selected to capture the direct effects of CS and THS2.2 aerosol on the metabolome, and to allow for comparison with the robust gene expression statistics. 3R4F (high) CS exposure significantly affected several metabolites that directly reflect the oxidative challenge induced by CS (Figure 16D): Methionine is prone to oxidation, and increased levels of both methionine sulfoxide and N-acetyl-methionine-sulfoxide were observed following 3R4F CS exposure; 3R4F CS shifted the balance from reduced cysteine to oxidized cysteine (cystine); 2-hydroxy fatty acids have been used previously as oxidative stress markers (D'Alessandro 2015, Tucci 2013), and both 2-hydroxypalmitate and 2-hydroxystearate significantly increased following 3R4F CS exposure. The data also indicated an effect of 3R4F CS exposure on antioxidants: Levels of vitamin E (gamma-/beta-tocopherol) and threonate (a vitamin C metabolite) in the 3R4F CS group increased, and the antioxidant urate decreased (Ames 1981, Battino 2002). In contrast to 3R4F CS, THS2.2 aerosol exposure displayed only limited effects on levels of these metabolites, such as a non-significant increase in threonate.

Reduced glutathione (GSH) is a central player in the cellular response to oxidative stress, as well as in periodontal diseases (Bains and Bains, 2015). Four hours after 3R4F CS exposure, GSH levels were significantly reduced (Figure 16E and F; for gene expression, see Supplementary Figure 3F). Several metabolites interlinked with glutathione were altered by 3R4F CS exposure; we observed depletion of cysteine and glycine, increases in γ-glutamyl amino acids, 5-oxoproline, S-adenosyl homocysteine (SAH), and 2-hydroxybutyrate, and, finally, a decrease in S-adenosyl methionine (SAM) and serine.

Cells exposed to THS2.2 aerosol exhibited a significant increase only in levels of cysteinylglycine and γ-glutamyl threonine and a decrease in guanidinoacetate, but in contrast with cells exposed to 3R4F CS, could still maintain high GSH levels and, for example, showed less depletion of cysteine and glycine (see Figure 16F).

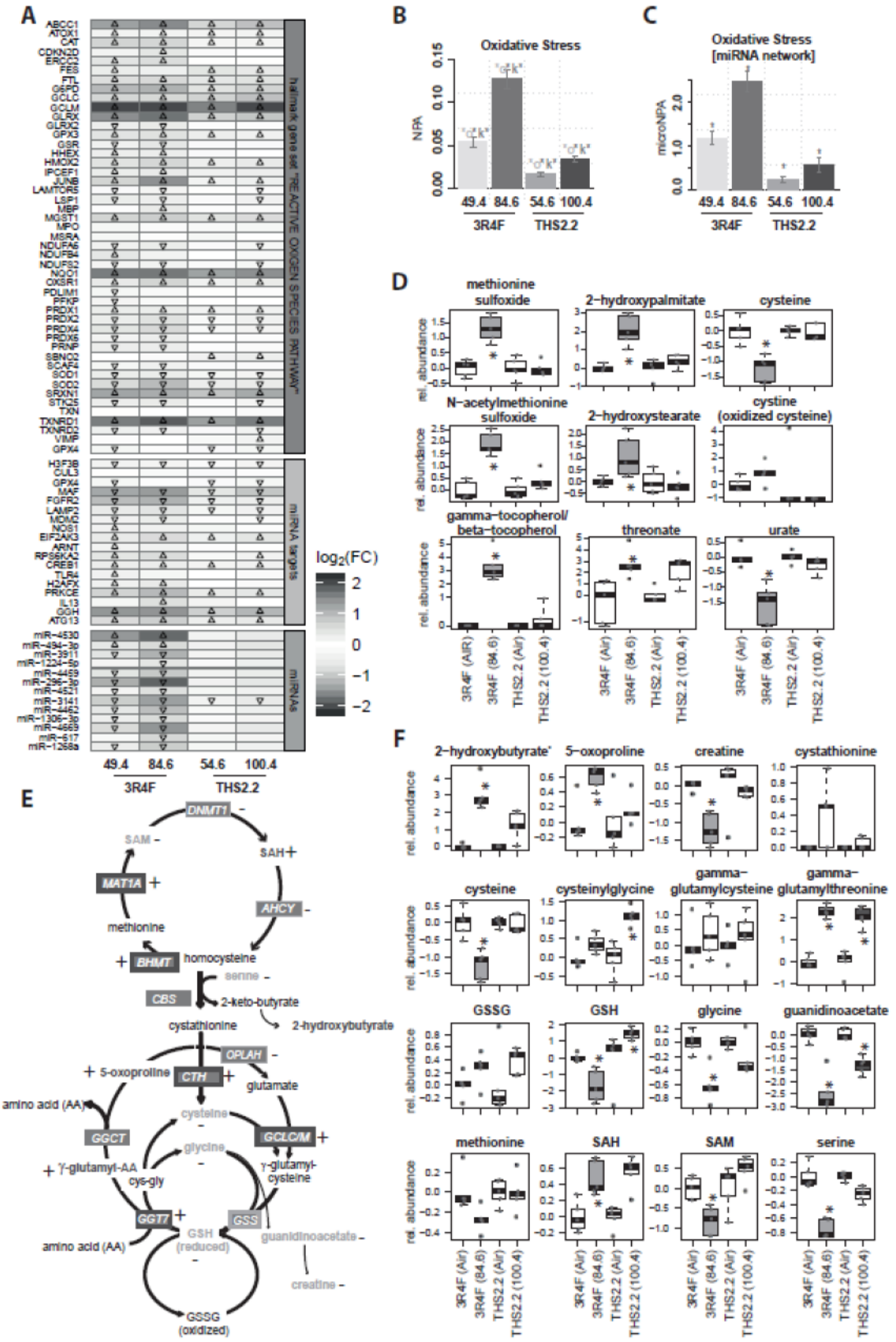
A
B
Oxidative Stress
NPA
C
Oxidative Stress
[miRNA network]
microNPA
49.4 84.6 54.6 100.4
3R4F THS2.2
D
methionine sulfoxide
2−hydroxypalmitate
cysteine
N−acetylmethionine sulfoxide
2−hydroxystearate
cystine (oxidized cysteine)
gamma−tocopherol/ beta−tocopherol
threonate
urate
rel. abundance
3R4F (AIR)
3R4F (84.6)
THS2.2 (Air)
THS2.2 (100.4)
E
DNMT1
SAM
SAH
MAT1A
AHCY
methionine
BHMT
homocysteine
serine
CBS
2-keto-butyrate
cystathionine
2-hydroxybutyrate
OPLAH
5-oxoproline
CTH
glutamate
amino acid (AA)
cysteine
GGCT
glycine
GCLC/M
γ-glutamyl-AA
cys-gly
γ-glutamyl-cysteine
GGT7
GSS
GSH (reduced)
guanidinoacetate
amino acid (AA)
creatine
GSSG (oxidized)
F
2−hydroxybutyrate
5−oxoproline
creatine
cystathionine
cysteine
cysteinylglycine
gamma−glutamylcysteine
gamma−glutamylthreonine
GSSG
GSH
glycine
guanidinoacetate
methionine
SAH
SAM
serine
rel. abundance
3R4F (Air)
3R4F (84.6)
THS2.2 (Air)
THS2.2 (100.4)
log2(FC)
2
1
0
−1
−2
hallmark gene set "REACTIVE OXYGEN SPECIES PATHWAY"
miRNA targets
miRNAs
ABCC1
ATOX1
CAT
CDKN2D
ERCC3
FES
FTL
G6PD
GCLC
GCLM
GLRX
GLRX2
GPX3
GSR
HHEX
HMOX2
IPCEF1
JUNB
LAMTOR5
LSP1
MBP
MGST1
MPO
MSRA
NDUFA6
NDUFB4
NDUFS2
NQO1
OXSR1
PDLIM1
PFKP
PRDX1
PRDX2
PRDX4
PRDX5
PRNP
SBNO2
SCAF4
SOD1
SOD2
SRXN1
STK25
TXN
TXNRD1
TXNRD2
VIMP
GPX4
H3F3B
CUL3
GPX4
MAF
FGFR2
LAMP2
MDM2
NOS1
EIF2AK3
ARNT
RPS6KA2
CREB1
TLR4
H2AFX
PRKCE
IL13
GGH
ATG13
miR-4530
miR-484-3p
miR-3911
miR-1224-5p
miR-4459
miR-296-3p
miR-4521
miR-3141
miR-4462
miR-1305-3p
miR-4669
miR-617
miR-1268a

Figure 16. Differential induction of oxidative stress by 3R4F cigarette smoke (CS) and THS2.2 aerosol.

Induction of oxidative stress response program: Differential expression heatmap for genes of the reactive oxygen species pathway (HALLMARK_REACTIVE_OXIGEN_SPECIES_PATHWAY, M5938) (Liberzon 2015), as well as for genes and miRNAs belonging to the "oxidative stress" candidate miRNA-mRNA network. The fold-change for each comparison is gray shade-coded (see grey-shade key) and its statistical significance is noted (arrow up indicates FDR<0.05 for upregulated genes/miRNA, arrow down indicates FDR<0.05 for downregulated genes/miRNA). N=6–9. (**B**) Assessment of exposure effects on the "oxidative stress" network. The bars show the overall network perturbation amplitudes ("NPA scores") based on the transcriptomics data, while the error bars delimit their 95% confidence intervals. Three statistics are shown: The red star indicates statistical significance with respect to the biological replication (i.e., the 95% confidence intervals do not contain the 0 value), while the green and red stars indicate significant specificity statistics with respect to the network structure ("O" and "K" statistics, see the Statistical and Computational Methods section). (**C**) Assessment of exposure effects on the candidate integrated miRNA-mRNA network for oxidative stress based on the miRNomics and transcriptomics data ("miRNPA scores"), the error bars delimit the 95% confidence intervals (see Statistical and Computational Methods). (**D**) Metabolomics profiling was conducted 4h after exposure of the tissue to the high 3R4F CS and THS2.2 aerosol concentrations. Boxplots summarize the response of metabolites sensitive to oxidative stress (blue dots indicate the individual samples, N=5). Significant differences between the exposed groups and their respective Sham groups are indicated by filled, colored boxes and a star (* indicates FDR<0.05). (**E**) Summary of the exposure effects on glutathione and related metabolic reactions. Relevant metabolic reactions of the glutathione pathway, including the γ-glutamyl cycle, and cysteine and methionine metabolism, and glycine, serine, and threonine metabolism (Kanehisa 2014). Significantly upregulated or downregulated metabolites and genes are marked by + and -, respectively. (**F**) Boxplots for metabolites from E. Note that 2-hydroxybutyrate is isobar with 2-hydroxyisobutyrate.

9.3.5 Impact of 3R4F CS and THS2.2 Aerosol on Xenobiotic Metabolism

Among the networks presented in this study, the xenobiotic metabolism network exhibited a very strong perturbation after 3R4F CS exposure and a relatively higher impact of THS2.2 aerosol with respect to other networks (Figure 15, NPA panel). We investigated in detail the genes which affected this network. The findings reported in the heatmap (Figure 17) indicate a strong upregulation by all 3R4F CS and THS2.2 aerosol concentrations of *CYP1A1*/*CYP1B1*, aldo-keto reductases (*AKR*) *1C1/1C2/1C3*, TCDD-inducible poly(ADP-ribose) polymerase (*TIPARP*), and aryl-hydrocarbon receptor repressor (*AHRR*) genes.

Biological function analysis of target genes of miRNAs from the IPA database showed that xenobiotic metabolism was one of the main regulated pathways. The filtering used in IPA allowed us to connect two upregulated and six downregulated miRNAs (Figure 17A miRNAs panel, and Supplementary Figure 4A) with target genes involved in xenobiotic signaling, such as aryl hydrocarbon receptor nuclear translocator (*ARNT*), nuclear factor IB (*NFIB*), protein kinase C epsilon (*PRKCE*), the transcription factor *MAF*, and fibroblast growth factor receptor 2 (*FGFR2*). Interestingly, miRNAs were less affected in THS2.2 aerosol-exposed cultures.

The gene expression response 24 h after the last exposure showed an increased impact in 3R4F CS-exposed cultures compared with the 4-h time-point, while a general decreased response was recorded for THS2.2 aerosol-exposed cultures at the low comparable concentration (Supplementary Figure 4B). Although the latter results were obtained with a lower number of replicates (n=3), they indicate that gingival cultures could recover from THS2.2 aerosol exposure, while 3R4F CS exposure displayed persisting perturbations.

These differences between the exposure conditions were also confirmed for the xenobiotic metabolism-related miRNA/mRNA network, as illustrated by the bar graphs showing the NPA scores for the different networks (Figure 17B and C, and Supplementary Figure 4C).

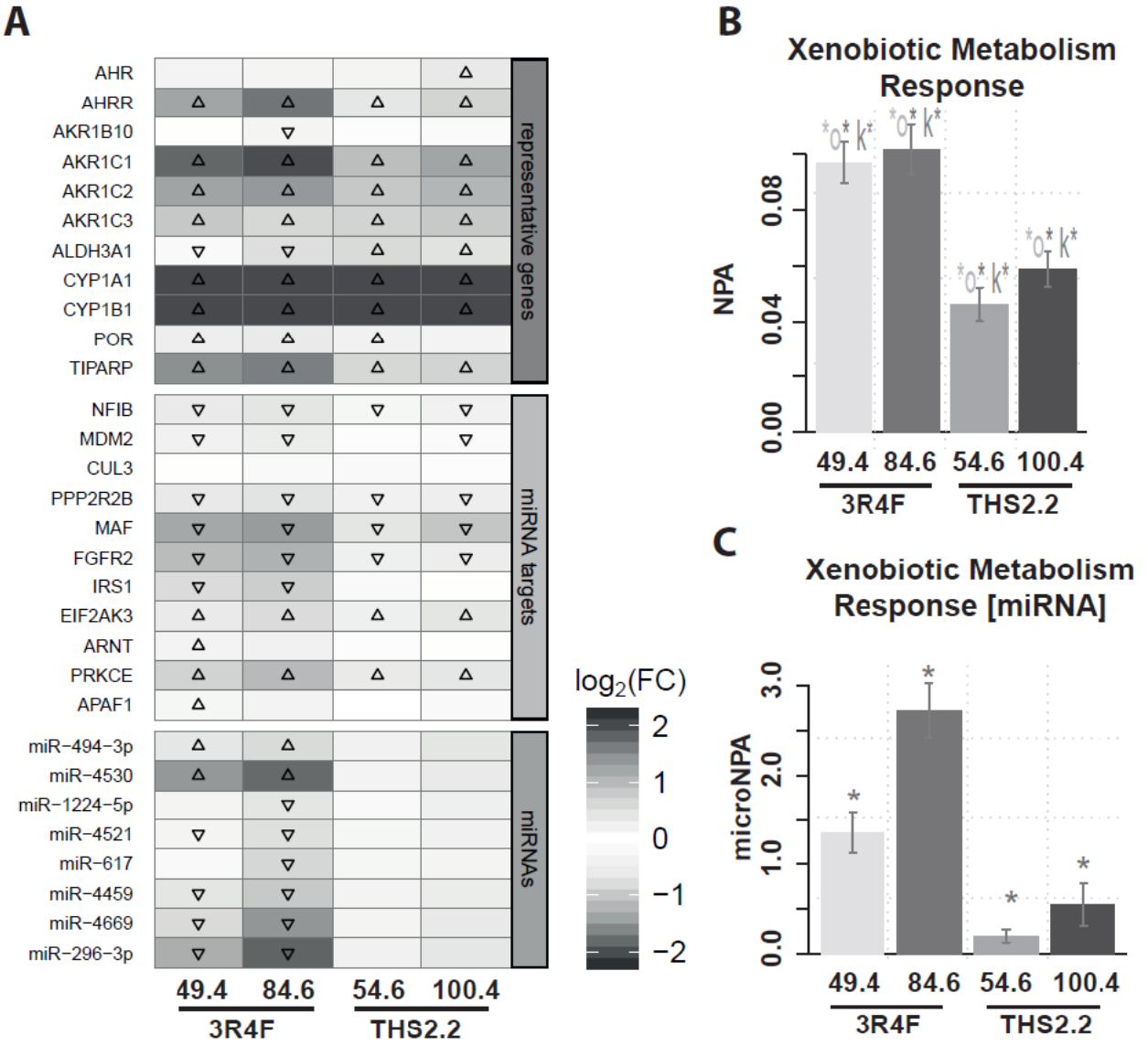

Figure 17. Xenobiotic metabolism is altered in 3R4F cigarette smoke (CS)- and THS2.2-exposed organotypic gingival cultures.

(**A**) Heatmap shows the differential expression of genes representative of the xenobiotic metabolism pathway, as well as of genes and miRNAs belonging to the "xenobiotic metabolism" candidate miRNA-mRNA network. The fold-change for each comparison is gray shade-coded (see grey-shade key) and its statistical significance is noted (arrow up indicates FDR<0.05 for upregulated genes/miRNA, arrow down indicates FDR<0.05 for downregulated genes/miRNA). (**B**) Assessment of exposure effects on the "xenobiotic metabolism response" network. The bars show the overall network perturbation amplitudes ("NPA scores"), while the error bars delimit their 95% confidence intervals. Statistical significance with respect to three different criteria is indicated by colored stars (see Figure 16B legend for details). (**C**) Assessment of exposure effects on the candidate integrated miRNA-mRNA network for "xenobiotic metabolism", based on the miRNomics and transcriptomics data ("miRNPA scores"); the error bars delimit the 95% confidence intervals (see

the Statistical and Computational Methods section). Error bars indicate SEM (N=6–9). Nicotine concentrations in the smoke or aerosol are indicated for each group (mg/L). * $p<0.05$, compared with corresponding air control.

We analyzed the combined activity of CYP1A1/1B1 (Figure 18), enzymes involved in phase I metabolism of xenobiotics and whose mRNA was shown to be highly upregulated by both 3R4F CS and THS2.2 aerosol. These CYPs are of particular importance since they metabolize several toxicants present in CS, such as polycyclic aromatic hydrocarbons (PAHs), nitrosamines, acrylamines, and nicotine, and can also be induced in the buccal epithelium *in vivo* and *in vitro* (Schlage 2014, Vondracek 2001). Figure 18 shows that 24 h post-exposure, there were no substantial changes in the CYP activity between the 3R4F CS-exposed inserts and their air controls. Surprisingly, high activity (approximately 40% of the positive control), although not statistically different from activity in 3R4F CS-exposed cultures, was observed after repeated exposures to THS2.2 aerosol.
Descriptive statistics of these results are reported in Supplementary Table 12.

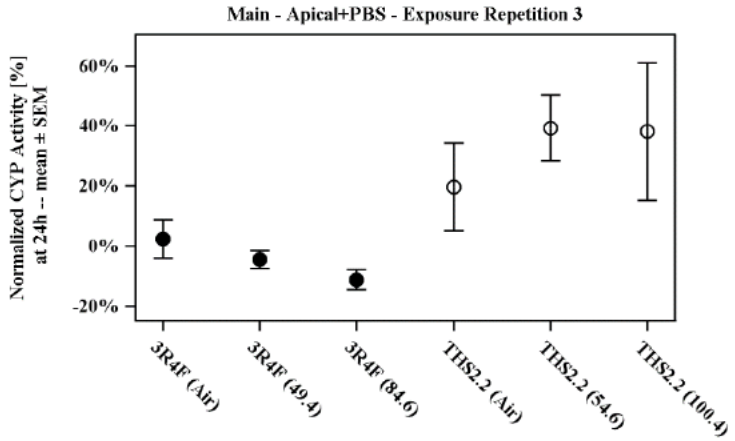

Figure 18. CYP1A1/CYP1B1 activity in the organotypic gingival cultures following exposure.
Combined activity of CYP1A1/CYP1B1 was measured 24 h after cultures were exposed to 3R4F cigarette smoke (CS) or THS2.2 aerosol at the indicated concentrations (mg/L). Data are presented as the mean of the normalized activity relative to the positive control (TCDD-treated cultures were considered as having 100% activity). Error bars indicate SEM (N=9, from three experimental repetitions with three exposure runs/repetition). * $p<0.05$, compared with corresponding air control.

9.3.6 Proinflammatory Mediator Secretion and Expression

CS has been linked to impairment of the inflammatory response, which is a major feature of periodontal diseases (Giannopoulou 2003a, Guentsch 2008).
Inflammatory mediator release by the organotypic gingival cultures was assessed by measuring the analytes secreted into the basolateral medium before the second and third exposures and 24 h post-exposure.

In general, major changes were observed 24 h after the last exposure to 3R4F CS; secretion of TNFα, MMP-1, CXCL1, IL8/CXCL8, IL1A, CSF2, and CSF3 increased slightly compared with the air

control after the second CS exposure, but became markedly higher after the third exposure, with values reaching up to 16-fold increases over the control (IL1A).

VEGFA, CCL5, MMP-9, and IL6 were downregulated after 3R4F CS exposure (Figure 19A). In contrast with the increased secretion of proinflammatory mediators, mostly observable after the third exposure, the inhibition of secretion of these markers did not follow a trend, leading to mixed responses over the exposure period.

There was not always a clear dose-dependency in the amplitude of the release; this may have been due to the strong damage observed at the high 3R4F CS concentration (84.6 mg/L), which could indicate an impairment in the cells' ability to secrete proinflammatory mediators.

The response of the gingival cultures exposed to THS2.2 aerosol was milder if any, with the same secretion trend observable for a few proinflammatory mediators (CSF2, CSF3, CCL5, MMP-1), although to a much lower degree than was observed in the 3R4F CS-exposed counterparts.

A statistical analysis showing the ratio between mediators secreted following 3R4F CS and THS2.2 aerosol exposures showed that TNFα, MMP-1, CXCL8, IL1A, CXCL1, CSF2, and CSF3 levels were significantly higher in the medium of 3R4F CS-exposed cultures than in that of the THS2.2 aerosol-exposed counterparts, while MMP-9 and CCL-5 levels were significantly lower (Figure 19B).

Descriptive statistics of these findings are reported in Supplementary Tables 13–26; individual representations of the mediators are reported in Supplementary Figure 5.

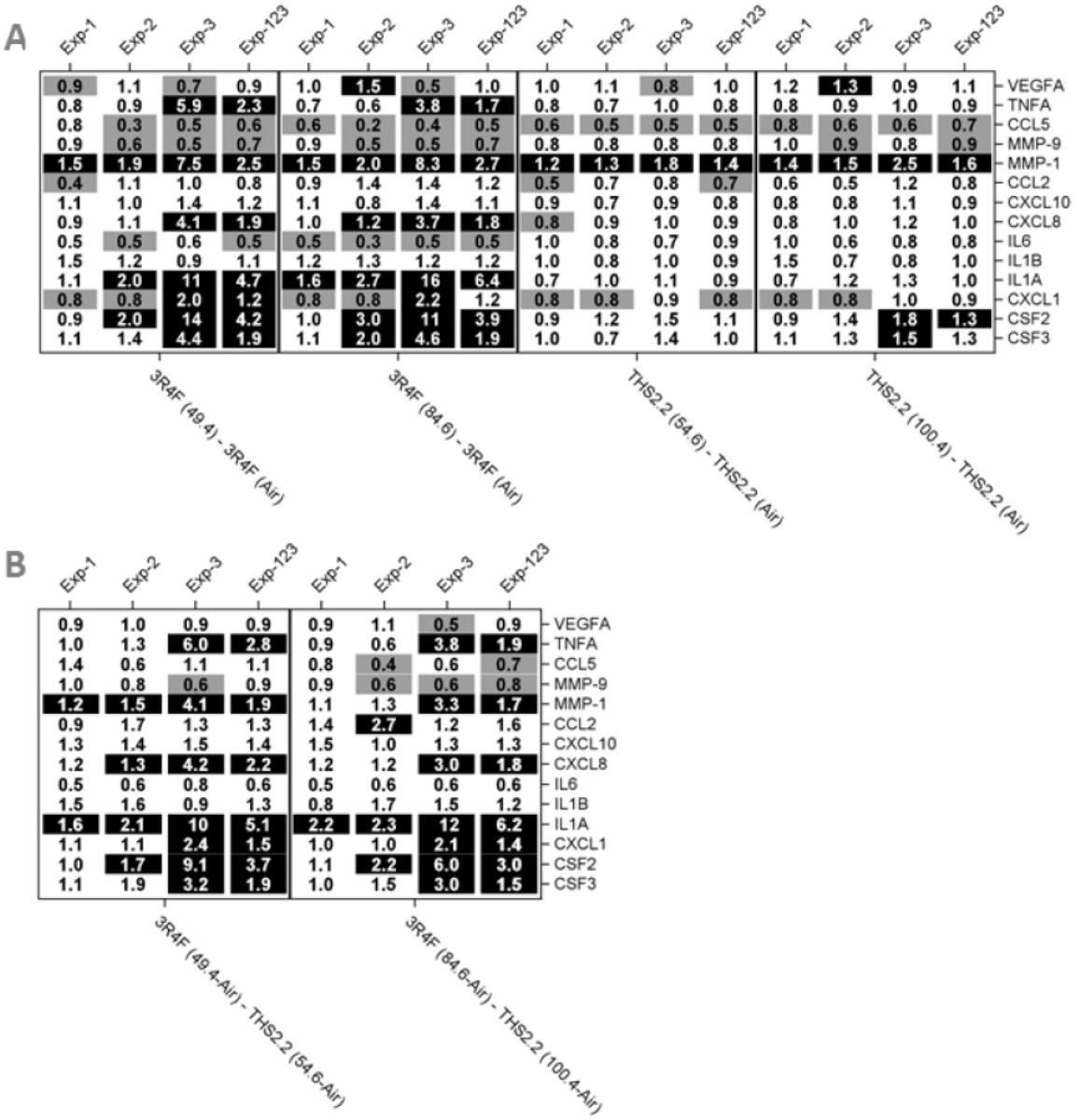

Figure 19. Assessment of the secretion levels of proinflammatory mediators in organotypic gingival cultures after exposure.

Fold-changes of the concentrations of mediators (listed on the y-axis, right) were measured in the basolateral media of gingival cultures 24 h after the first exposure (Exp-1), and 24 h after the second exposure (Exp-2) to 3R4F cigarette smoke (CS) or THS2.2 aerosol at the indicated concentrations (mg/L) for 28 min, and 24 h post-treatment (Exp-3). The last column (Exp-123) shows the sum of the cumulative values of all exposures. Fold-changes are expressed relative to the air control (N=9, from three experimental repetitions with three exposure runs/repetition). (**A**) Values indicate the fold changes compared with the air-exposed controls. (**B**) At comparable concentrations, differences between 3R4F CS- and THS2.2 aerosol-induced mediator levels are reported as the ratio of the fold-changes. Dark and light grey shading indicates significant increases and decreases, respectively, between the comparisons (p<0.05).

The heatmap in Figure 20 illustrates the gene expression changes measured 4 h after the third exposure. Among the genes shown in the heatmap, *IL1A*, *IL1B*, *CSF2*, *MMP1*, *MMP3*, *MMP10*, *IL24*, connective tissue growth factor (*CTGF*), early growth response 1 (*EGR*), and prostaglandin-endoperoxide synthase 2 (*PTGS2*) showed a considerably high upregulation following 3R4F CS

exposure, whereas only *CXCL14* was markedly downregulated by 3R4F CS. In general, we observed the same regulation patterns in THS2.2 aerosol-exposed gingival cultures, although to a much lesser extent.
Twenty-four hours after the third exposure, we observed a reduction in gene expression alterations in THS2.2 aerosol-exposed cultures, whereas in the 3R4F CS-exposed counterparts, the changes were still higher and, in some cases, exacerbated when compared to the 4-h post-exposure period (Supplementary Figure 6B).

NPA scores for the Epithelial Innate Immune Activation and Tissue Damage networks (Figure 20B and C, and Supplementary Figure 6C and D), as well as miRNPA scores for a candidate integrated miRNA-mRNA network (Figure 20D) all indicated a concentration-dependent effect in both 3R4F CS- and THS2.2 aerosol-exposed cultures, although THS2.2 aerosol-exposed cultures displayed reduced effects.
Furthermore, we found that 11 of the 3R4F CS- and THS2.2 aerosol-regulated miRNAs may also have an impact on the inflammatory response (Figure 20A miRNA panel). In fact, our IPA analysis (Supplementary Figure 6A) showed that some of these miRNA-mRNA target genes are associated with the cytokine-mediated inflammatory responses: *NFκB*, *IL1*, *IL6*, *IL8*, *GMCSF* (*CSF2*), *VEGF*, *CXCR4*, and *TNFα*. Among these genes, we found interleukin 6 signal transducer (*IL-6ST*) (Scheller 2011), toll-like receptor 4 (*TLR4*), and CD 40 ligand (*CD40LG*) (Figure 20A, miRNA targets panel).

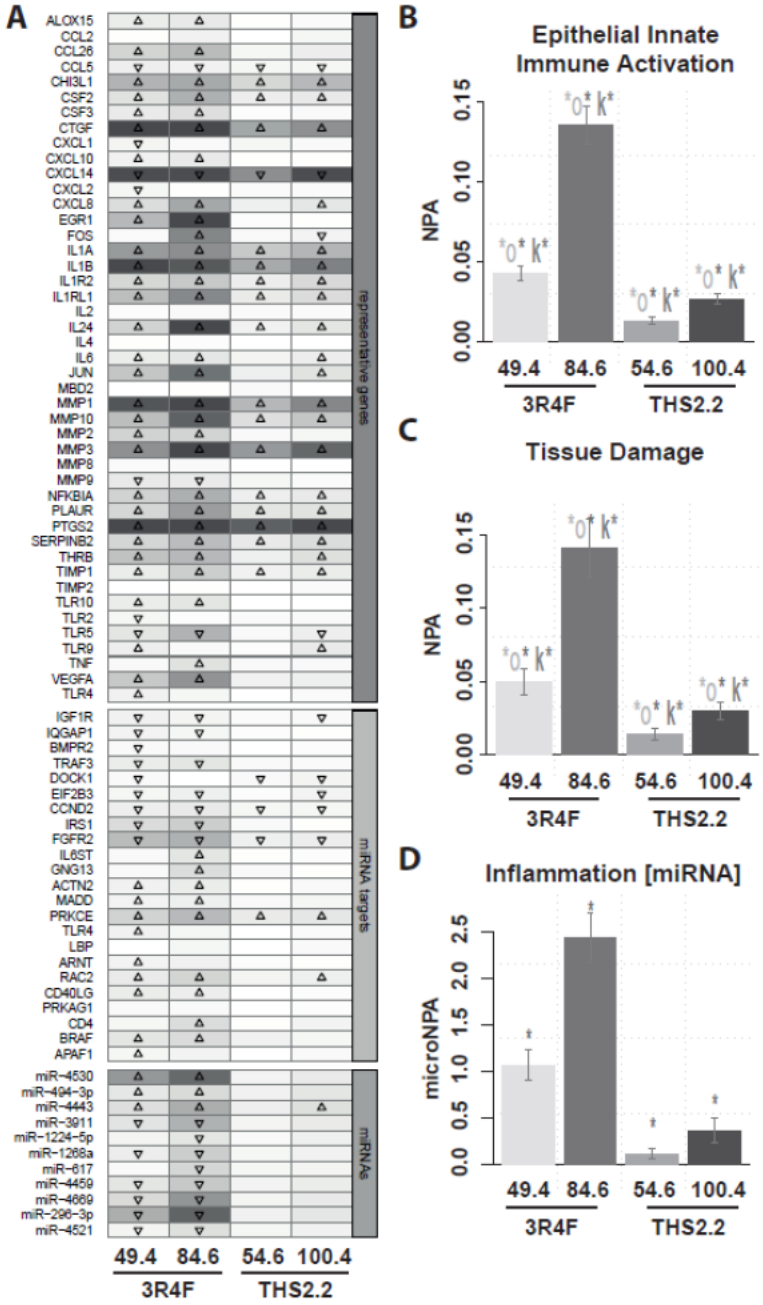

Figure 20. Profile of inflammation in 3R4F cigarette smoke (CS)- and THS2.2 aerosol-exposed organotypic gingival cultures.

(**A**) The heatmap shows the differential expression of genes representative of inflammation, as well as of genes and miRNAs belonging to the "Inflammation" candidate miRNA-mRNA network. The fold-change for each comparison is gray shade-coded (see grey-shade key) and its statistical significance is noted (arrow up indicates FDR<0.05 for upregulated genes/miRNA, arrow down indicates FDR<0.05 for downregulated genes/miRNA). (**B**–**C**) Assessment of exposure effects on the inflammation networks "Epithelial Innate Immune Activation" and "Tissue Damage". The bars show the overall network perturbation amplitudes ("NPA scores"), while the error bars delimit their 95% confidence intervals. Statistical significance with respect to three different criteria is indicated by colored stars (see Figure 4B for details). (**D**) Assessment of exposure effects on the candidate integrated miRNA-mRNA network for "Inflammation" (Supplementary Figure 5A), based on the miRNomics and transcriptomics data ("miRNPA scores"); the error bars delimit the 95% confidence intervals (see section 8.3.4). N=9.

Metabolomics analysis performed on the high 3R4F CS and THS2.2 aerosol concentrations 4 h after the last exposure found a significant increase in the regulation of 15-hydroxyeicosatetraenoic acid (15-HETE) by 3R4F CS but not by THS2.2 aerosol (Figure 21). 15-HETE is generated by oxidation of arachidonic acid by LOX-15 enzymes and has been associated with immuno-regulatory effects and atherosclerotic processes.

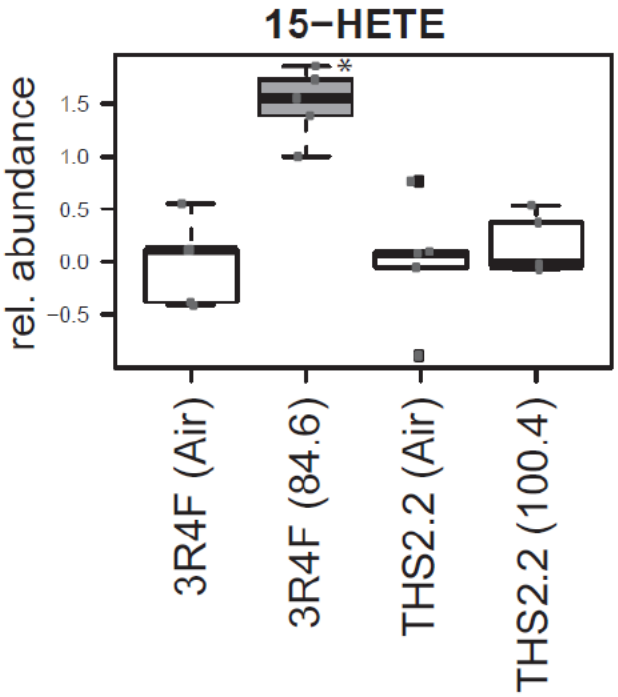

Figure 21. 15-Hydroxyeicosatetraenoic acid (15-HETE) abundance after exposure to the high 3R4F cigarette smoke (CS) and THS2.2 aerosol concentrations.

The boxplot summarizes the response of 15-HETE to 3R4F CS or THS2.2 aerosol exposure (blue dots indicate the individual samples, N=5). Significant differences between the exposed groups and their respective Sham groups are indicated by filled, colored boxes and a star (*) (FDR adjusted *p*-value <0.05).

9.3.7 Keratinization and Cell Adhesion Profile

Overt keratinization of the organotypic gingival epithelium was observed after exposure to 3R4F CS, in particular after exposure to the highest (84.6 mg/L) concentration. Hyperkeratinization of the oral epithelia can occur in response to chemical inducers such as CS, and the presence of keratohyalin granules is often an indication of keratinizing epithelia. As shown in Figure 22, 24 h after three repeated exposures to 3R4F CS at the low concentration, hypergranulosis with coarse keratohyalin granules was present in both the SG and SC (arrows). The high 3R4F CS concentration showed complete keratinization of the epithelium, extending into the membrane, along with overt parakeratosis (arrows). THS2.2 aerosol-exposed cultures also showed the presence of keratohyalin granules at both high and low concentrations (arrows), although hyperkeratinization of the epithelial cells was not detected.

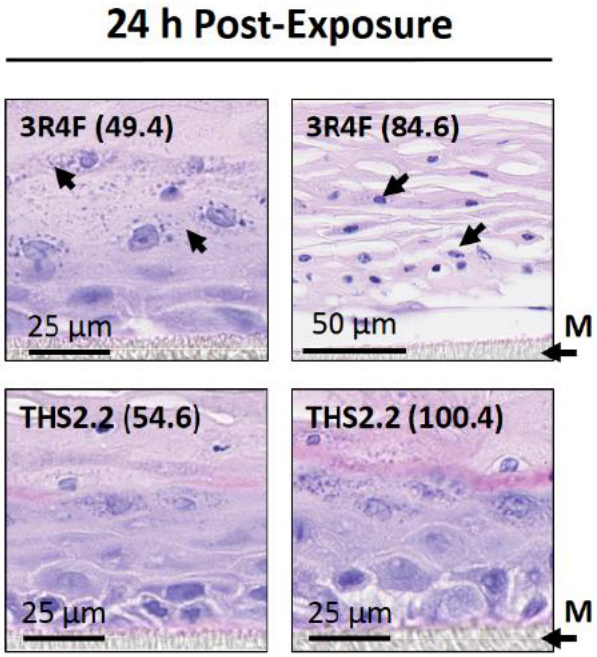

Figure 22. Staining of 3R4F cigarette smoke (CS)- and THS2.2 aerosol-exposed samples.
Representative images of hematoxylin and eosin (H&E)-stained organotypic gingival culture sections observed 24 h after the last exposure. Staining was performed as described in Section 7.5.10. The applied concentration (mg/L) for each condition is shown in brackets; 63× and 100× magnification. N=9.

We also measured a set of genes related to normal buccal epithelial differentiation or previously described in non-neoplastic lesions and in reconstituted *in vitro* tissues (Figure 23, cell type panel). The majority of the keratin (*KRT*) genes represented were downregulated by exposure to 3R4F CS, with almost no difference between the low and high concentrations (*KRT1*, *KRT5*, *KRT10*, *KRT13, KRT14*, *KRT15*, *KRT19*). Among the KRT genes analyzed, only *KRT2*, *KRT17*, and *KRT76* were upregulated. The RNAs of the keratinization-related genes involucrin (*IVL*) and filaggrin (*FLG*) were upregulated differentially by the low and high 3R4F CS concentrations. In contrast, *MKI67*, a marker of cell cycle activation, and proliferating cell nuclear antigen (*PCNA*) were significantly downregulated in both 3R4F CS- and THS2.2 aerosol-exposed samples. *MAPK14* and *DEFB1* were upregulated in both 3R4F CS- and THS2.2 aerosol-exposed samples. The overall impact of THS2.2 aerosol was reduced compared to that of 3R4F CS.

We also investigated the expression of some representative genes involved in cell adhesion and formation 4 h after the last exposure (Figure 23, cell adhesion panel). We observed that *CDH1*, the gene encoding for E-cadherin, a well-studied adhesion molecule in epithelial tissues with important functions in cell-cell adhesion and cell signaling, was significantly downregulated by 3R4F CS. The expression of other cadherins was, however, not univocal: Only *CDH3* was downregulated, while *CDH2*, *CDH4*, and *CDH5* were all upregulated. Overall, the cell adhesion genes were mostly downregulated by 3R4F CS with sporadic exceptions (*PVRL2* and *NOTCH4*). The heatmap representing tight junction-related genes showed a general upregulation, with only *CLDN1* and *F11R* exhibiting reduced expression after 3R4F CS exposure. THS2.2 aerosol-induced alterations, where present, were reduced with respect to their corresponding 3R4F CS counterparts.

Gene expression changes 24 h after the last exposure (Figure 23) were assessed in an exploratory manner, as described in section 9.3.4. The heatmap shows that there was no relevant alteration in gene expression, except for sporadic cases in 3R4F CS-exposed samples (*PCNA*, *COL1A1*, *PHLDA*, *MAPK8*, *DSC1*, *DSC3*, *NOTCH3*, *CLDN4*) and only three genes in the case of the high THS2.2 aerosol exposures (*KRT13*, *PHLDA1, DCS1*).

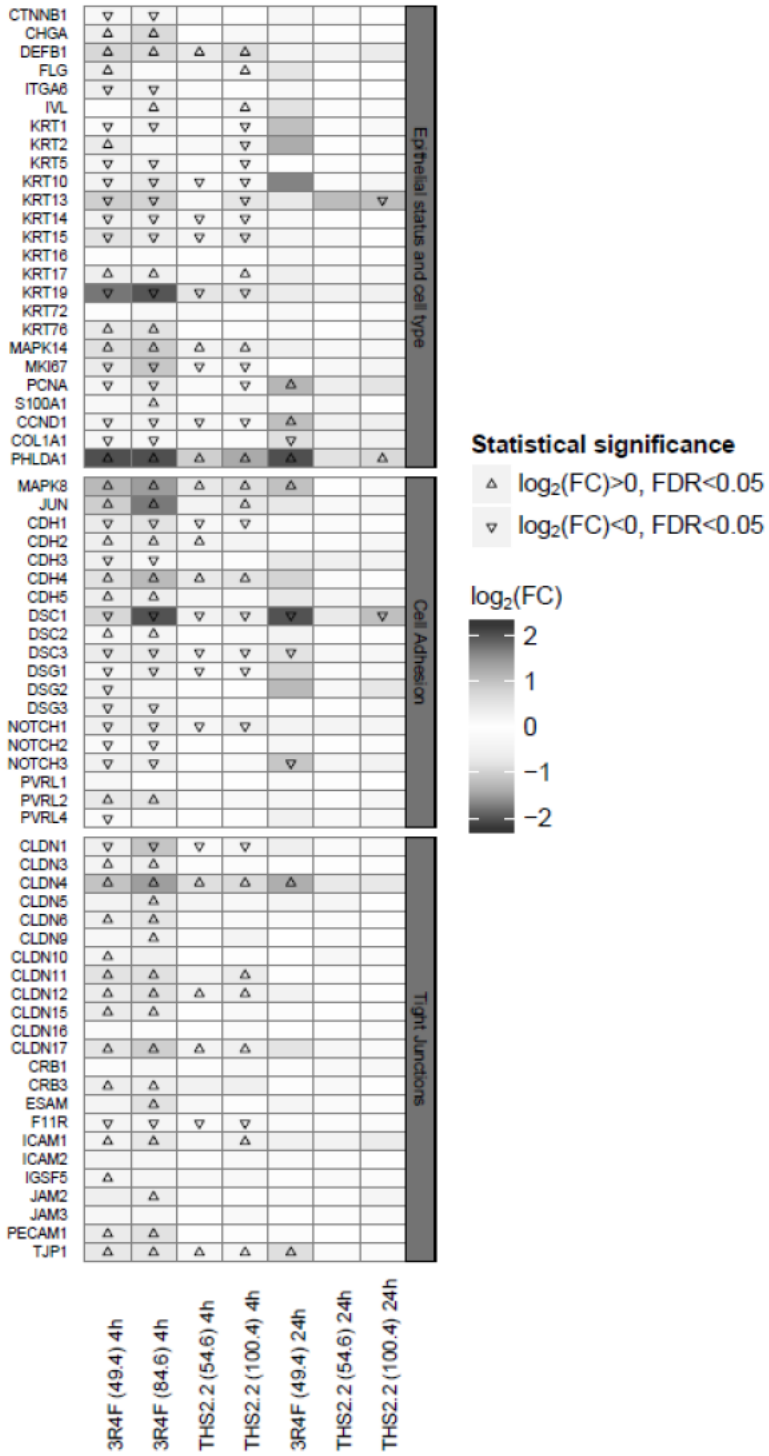

Figure 23. Expression of genes involved in epithelial differentiation, cell adhesion, and barrier formation after 3R4F cigarette smoke (CS) or THS2.2 aerosol exposure.

The heatmap shows genes that were significantly altered 4 h after three exposures to 3R4F CS or THS2.2 aerosol. The fold-change for each comparison is gray shade-coded (see grey-shade key) and its statistical significance is noted (arrow up indicates FDR<0.05 for upregulated genes/miRNA, arrow down indicates FDR<0.05 for downregulated genes/miRNA). Gene symbols are listed on the left of the heatmap. N=6–9.

Since we found downregulation in E-cadherin gene expression, we performed a staining 24 h after the last exposure session, using a specific antibody. The images in Figure 24 show that E-cadherin abundance decreased markedly following 3R4F CS exposure, proportionally to the CS concentration applied. THS2.2 aerosol was reduced E-cadherin expression slightly only at the high concentration (100.4 mg/L).

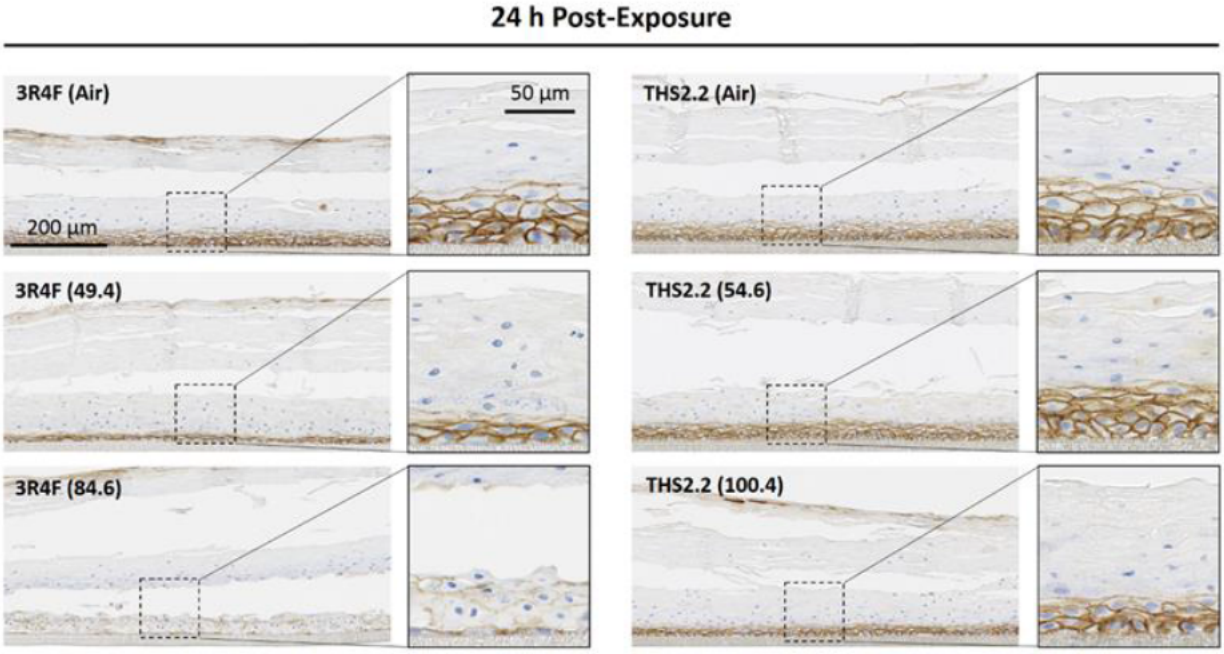

Figure 24. E-cadherin staining in 3R4F cigarette smoke (CS)- and THS2.2 aerosol-exposed samples.

Representative images of E-cadherin-stained organotypic gingival culture sections observed 24 h after the last exposure. Staining was performed as described in Section 7.5.10. The applied concentration (mg/L) for each condition is shown in brackets. Magnification is set at 20× (63× for the insets). N=9.

9.3.8 Findings in Samples Not Covered by PBS on the Apical Side

To assess the effects of apical PBS on the samples exposed to CS or THS2.2 aerosol, we included in main phases I and II some inserts not moistened with PBS. We assessed cytotoxicity 24 h post-exposure, along with culture morphology. The results shown in Figure 25 indicate that cultures did not display major differences in cytotoxicity with respect to the PBS-covered control samples (1.63% vs. 1.05% for 3R4F CS, and 1.62% vs. 0.94% for the THS2.2 aerosol), whereas a higher cytotoxicity was observed for 3R4F CS (49.4 mg/L)-exposed samples (9.1% vs. 3.6%), but no major differences for THS2.2 aerosol (14.4 mg/L)-exposed ones (0.62% *vs.* 1.66%) (compare Figure 25A with Figure 13). Descriptive statistics for these results are reported in Supplementary Table 11.

The morphology of the air controls and exposed samples did not show major differences, except a slight increase in the keratinized layers of the treated cultures and an increased general thickness (Figure 25B).

A

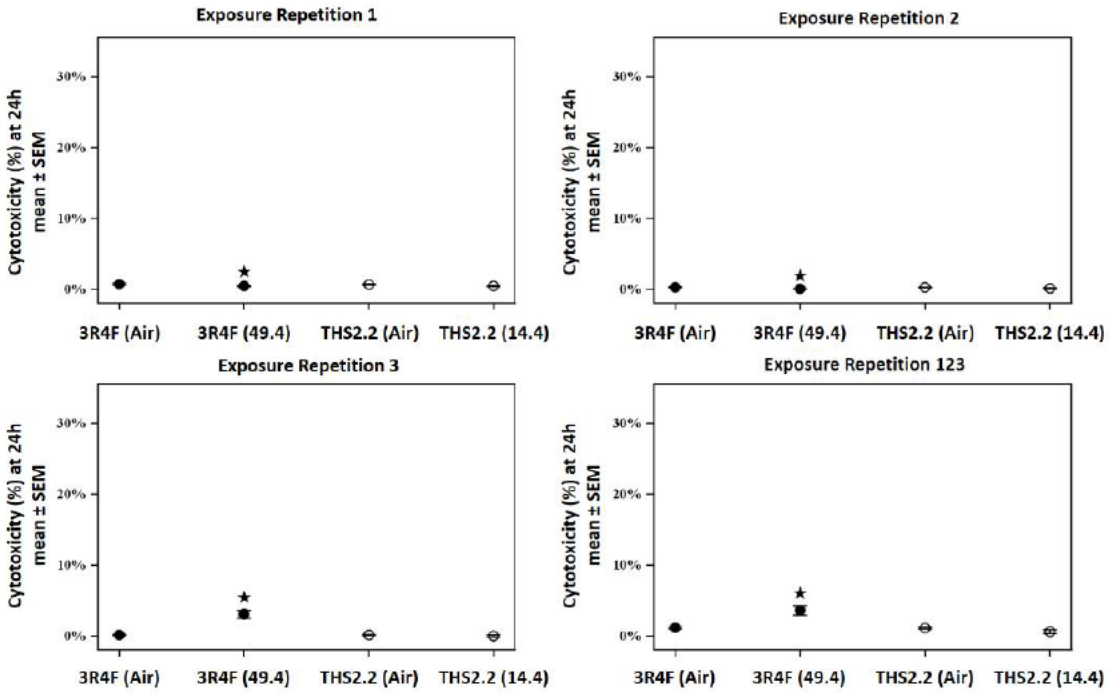
Exposure Repetition 1
Exposure Repetition 2
Exposure Repetition 3
Exposure Repetition 123
Cytotoxicity (%) at 24h mean ± SEM
30%
20%
10%
0%
3R4F (Air)
3R4F (49.4)
THS2.2 (Air)
THS2.2 (14.4)

B

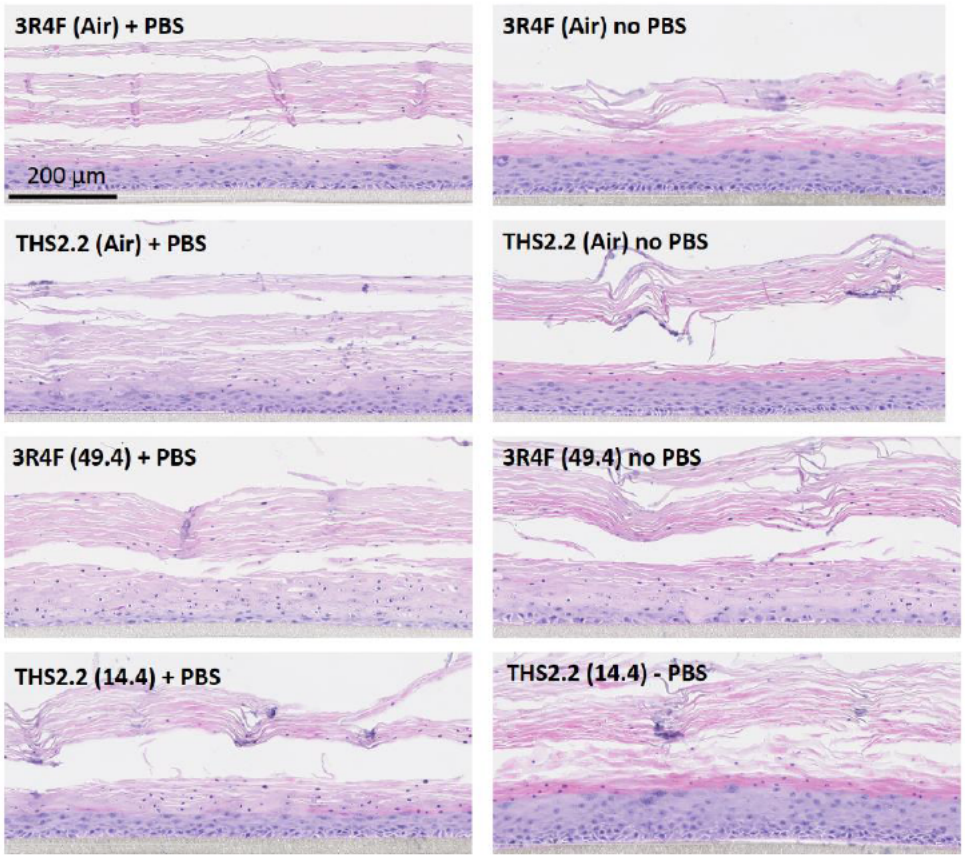
3R4F (Air) + PBS
200 µm
3R4F (Air) no PBS
THS2.2 (Air) + PBS
THS2.2 (Air) no PBS
3R4F (49.4) + PBS
3R4F (49.4) no PBS
THS2.2 (14.4) + PBS
THS2.2 (14.4) - PBS

Figure 25. Cytotoxicity and culture morphology in samples not covered by apical phosphate-buffered saline (PBS).

(**A**) Cytotoxicity-based adenylate kinase (AK) activity was assessed in the organotypic gingival culture 24 h after the first exposure (upper left), 24 h after the second (upper right), and 24 h after the third (lower left). The lower right panel indicates mean cumulative cytotoxicity levels over the entire time frame. AK levels were normalized relative to those in the positive control. Error bars indicate SEM (N=6, from two experimental repetitions with three exposure runs/repetition). Nicotine concentrations in 3R4F cigarette smoke (CS) or THS2.2 aerosols are indicated for each group (mg/L, x-axis). ★ $p<0.05$, compared with the corresponding air control. (**B**) Representative images of hematoxylin and eosin (H&E)-stained gingival culture sections observed 24 h after the last exposure to fresh (60%) air (Sham) and covered (left), or not (right), by 100 µL PBS. Nicotine concentrations are indicated in brackets (in mg/L). 20× magnification. N=6.

10. Discussion and Conclusion

The experimental plan comprised three sections: The PBS pilot, where we tested the effect of PBS apical moistening on gingival tissue; the DRF, where a wide range of 3R4F smoke and THS2.2 aerosol concentrations were tested, and three main phases and metabolomic assessment, where we compared the impact of two selected comparable concentrations for 3R4F CS and THS2.2 aerosol on the biological system. Moreover, to obtain robust data, three experimental repetitions were conducted for each main phase. Within each of the experimental repetitions, three independent exposure runs were carried out.

Pilot PBS exposure. To mimic an *in vivo* situation, we moistened the apical side of the gingival tissue model with PBS. Analysis of tissue morphology and molecular profiling indicated that the presence of PBS caused an adaptive response of the tissue without showing signs of toxicity in the basal conditions, while slightly reducing the basal inflammatory status.

Dose range finding. A DRF of 3R4F CS and THS2.2 aerosol was conducted to select the concentrations to apply to the main phases and to evaluate the toxicity related to a broader range of concentrations. For this purpose, we analyzed different endpoints (AK, CYP activity, 3D culture histology, and gene expression).
Cytotoxicity and tissue destruction were observed in 3R4F CS-exposed tissues at the highest concentrations: 89.1 and 201 mg/L. Neither cytotoxic effects nor major histopathological effects were observed at the tested THS2.2 aerosol concentrations.
The combined activity of CYP1A1 and 1B1 was enhanced by low 3R4F CS concentrations. THS2.2 aerosol caused a milder concentration-dependent increase in the activity of CYP1A1/1B1 24 h post-exposure.
Gene expression analysis revealed that the overall biological impact of each THS2.2 aerosol concentration was always lower than that of the corresponding 3R4F CS concentration.

Main phases. From the DRF phase, we selected two matching concentrations, a high and a low, of 3R4F CS and THS2.2 aerosol, and applied them to the samples throughout the study.
During the main phases, we analyzed different biological endpoints (AK, MAP, CYP activity, tissue histology), the perturbation of the molecular network, and the metabolomic profile.
At the equivalent concentrations, AK release was lower 24 h post-exposure to THS2.2 aerosol than to 3R4F CS.
As reported for native gingival epithelium in response to mechanical or chemical stress, our organotypic model underwent extensive hyperkeratinization in response to CS, which extended into deeper layers, such as the SS (Shetty 2012, Shirani 2014, Villar 2003). This morphological alteration was evidenced by the accumulation of nuclei in the SC (parakeratinization), which indicates a lack of balance between keratinization and proliferation and is associated with inflammatory infiltrates (Andreescu 2013). We also observed significant signs of apoptosis/karyorrhexis/pyknosis after exposure to the high concentration 3R4F CS. In contrast, THS2.2 aerosol-exposed gingival cultures showed milder alterations in cell morphology (sporadic atrophy was observed, and loss of clear distinction between the SG and SC). The presence of PBS enhanced slightly the cytotoxicity levels in 3R4F CS-exposed samples compared with the ALI counterparts, with some adaptation observed in the morphology. This was expected, since after each exposure, the PBS trapping the toxic

components of CS remained on the apical side of the cultures for 24 h, continuing to exert its harmful effects, as may happen with saliva in smokers.

The exposure-related mechanisms associated with 3R4F CS and THS2.2 aerosol were assessed by evaluating the expression of global mRNA and miRNA in the cultures. The impact of the exposure was higher and sustained over time for 3R4F CS-exposed cultures, whereas the response following THS2.2 exposure was lower, and markedly decreased at a longer post-exposure time-point (24 h).
Our multi-omics approach (mRNA, miRNA, and metabolite analysis) showed perturbation of three biological processes that are commonly perturbed by CS exposure and periodontal diseases (Babu 2013, Conard 1975, Giannopoulou 2003a, Guentsch 2008): Oxidative stress, xenobiotic metabolism, and inflammation. These three response programs were also highly affected in previous studies, in which both our group and others found that CS exposure led to several changes in these core processes in buccal and gingival organotypic cultures (Goldkorn 2014, Iskandar 2013, Kirkham 2013, Schlage 2014, Zanetti 2016). Moreover, we focused our analysis on genes involved in keratinization and adhesion, to obtain additional information to support the histology results.

Oxidative stress
Both 3R4F CS and THS2.2 aerosol affected the expression of genes involved in the reactive oxygen species pathway, with only a slightly reduced effect for THS2.2 aerosol at the 4-h post-exposure time-point. However, the quantified impact at the level of the causal oxidative stress network, which represents a prediction of the activity state of this process, was notably reduced in THS2.2 aerosol-exposed cultures. This difference in the (predicted) activation state of the oxidative stress response was supported by the metabolomics data, which clearly showed a reduced perturbation of metabolites related to oxidative damage in THS2.2 aerosol-exposed cells compared with CS-exposed cells, especially for the glutathione pathway. The increase in the glutathione regeneration pathway (increases in γ-glutamyl amino acids and the pathway intermediate 5-oxoproline) (Inoue 2016) and the SAM cycle and transsulfuration (Beatty 1980, Mosharov 2000) (e.g., increase in SAH and 2-hydroxybutyrate; decrease in SAM and serine) may indicate an attempt to restore the levels of cysteine and glycine.
In contrast with 3R4F CS exposure, cells exposed to THS2.2 aerosol maintained high GSH levels; this effect is likely ascribable to the reduced oxidative challenge of THS2.2 aerosol compared with 3R4F CS.
This differential engagement of the oxidative stress response program by CS and THS2.2 aerosol was further supported by the gene expression measurements at the 24-h time-point, which showed that the response to THS2.2 aerosol diminished with post-exposure duration, indicating that the cells would more easily cope with the reduced oxidative challenge of THS2.2 aerosol than with that of CS.
Moreover, IPA analysis suggested that 14 commonly regulated miRNAs may also play a role in the regulation of important pathways related to oxidative stress in the context of gingival pathologies. Notably, the majority of the miRNAs were less affected by THS2.2 aerosol.

Xenobiotic metabolism
The network clearly most affected by CS according to NPA analysis and the IPA investigation was xenobiotic metabolism. The overall gene expression 4 h after repeated exposures showed relevant differences between 3R4F CS- and THS2.2 aerosol-exposed cultures. The NPA score for both miRNA and mRNA subsets of data was much lower for THS2.2 aerosol-exposed cultures. A closer investigation of miRNA expression by the IPA analysis supported a lower impact on xenobiotic

metabolism by THS2.2 aerosol than by CS, indicating lower alteration levels for common miRNA and gene targets. Among the predicted genes modulated by miRNAs, we found the aryl hydrocarbon receptor nuclear translocator (*ARNT*), required for the proper function of the aryl hydrocarbon receptor and a mediator of xenobiotic toxicity (Monnouchi 2016), and nuclear factor IB (*NFIB*), which binds to the ARNT complex (Ingenuity Database).

The exploratory analysis 24 h post-exposure revealed that THS2.2 aerosol-exposed cultures showed a recovery trend.

We found that THS2.2 aerosol-exposed cultures exhibited a higher CYP1A1/1B1 activity than 3R4F CS-exposed cultures. The differential induction of these CYPs has been observed in our previous study, and an extensive discussion has been provided on this finding (Zanetti 2016). One possibility is that metal-induced heme oxygenase potently inhibited CYP1A1 enzyme activity, as has been reported for TCDD-induced CYP1A1 in human and rat hepatocytes (Amara 2010, Anwar-Mohamed 2012, Korashy 2012). Interestingly, in our results, the heme oxygenase 1 gene (*HMOX1*) was upregulated by CS (1.39- and 1.86-fold for low and high 3R4F CS, respectively; data not shown), and decreased by THS2.2 aerosol (0.51- and 0.77-fold for low and high THS2.2 aerosol, respectively; data not shown) 4 h post-exposure.

Inflammation

We analyzed gene and miRNA expression levels, as well as proinflammatory mediator secretion, in gingival cultures exposed to 3R4F CS or THS2.2 aerosol. Significant alterations in the secretion of proinflammatory mediators in CS-exposed cultures were observed. Interestingly, the highest alteration in inflammatory marker secretion was recorded 24 h after the last exposure session, indicating, to some extent, the ability of the gingival cultures to handle multiple CS exposures, as was evidenced also by the low cytotoxicity levels. Among these alterations, there was a significant upregulation of IL-8 secretion by CS. We also observed upregulated gene levels of *MMP-1*, *MMP-2*, *MMP-3*, and *MMP-10*, with concomitant increases in the expression of the MMP inhibitor *TIMP1*, but not *TIMP2*, to a smaller fold change. Luminex-based analysis revealed a strong upregulation by 3R4F CS of MMP-1 and downregulation of MMP-9. We also observed a strong increase in secretion of CSF2 (also named GM-CSF), TNFα, and IL1A. THS2.2 aerosol at both concentrations exerted a notably reduced effect on the inflammatory status of gingival epithelial cells compared with 3R4F CS, with only a weak response observed for MMP-1, CSF2, and CSF3 and an attenuated gene expression profile modulation.

Notably, all these mediators have been widely described in the literature in association with CS and/or periodontal disease (Bostrom 1998, Bostrom 1999, De Nardin 2001, Giannopoulou 2003b, Kim 2006, Mahanonda 2009, Ojima 2010, Ozcaka 2011, Popat 2014, Romanelli 1999, Sapna 2014, Sugiyama 2002).

In accordance with these findings, the IPA analysis also suggested that some of the miRNA target genes were associated, predominantly upon CS exposure, with cytokine-mediated inflammatory response: *NF-κB*, *IL-1*, *IL-6*, *IL-8*, *GM-CSF* (*CSF2*), *VEGF*, *CXCR4*, and *TNFα*.

Lastly, metabolomics analysis showed that the lipid mediator 15-HETE was upregulated by 3R4F CS but not THS2.2 aerosol. 15-HETE is generated by oxidation of arachidonic acid by the ALOX-15 enzyme and associated with immuno-regulatory effects and atherosclerotic processes (Henriksson 1985, Kundumani-Sridharan 2013, Powell 2015, Serhan 2003). The overexpressed activity of ALOX-15 has been associated with bone loss and inflammation in a rabbit model of periodontitis (Serhan 2003). Interestingly, the mRNA expression of *ALOX-15* was upregulated in our experimental model following CS exposure but not THS2.2 aerosol exposure.

Effects on cell keratinization/adhesion

Finally, we analyzed genes involved in keratinization, cell adhesion, and epithelial barrier formation. Increased expression of crosslinking proteins, such as *FLG* and *IVL*, which are expressed in keratohyaline granules in keratinizing tissues (Candi 2005, Henry 2012, Koster 2007, Shetty 2012, Toulza 2007), provides further evidence for CS-mediated keratinization.

In contrast, other genes involved in keratinization, such as several keratin family members (*KRT13*, *KRT19*), were downregulated. As terminal cellular differentiation can further decouple mRNA and protein levels, protein expression and localization analysis of these markers in future studies may help to elucidate the cellular and molecular basis of these changes. Supporting the translatability potential of our model, the observed downregulation of certain keratin genes is consistent with previous studies on gene and protein expression in smokers (Alharbi 2016, Donetti 2010).

A clear loss of cellular adhesion in gingival cultures exposed to CS was measured. This effect could be ascribed to the general downregulation of the expression of many genes involved in cell adhesion (*DCS1*, *DCS3*, *DSG1*, *DSG2*, *DSG3*). Notably, both the *CDH1* gene and its coded protein E-cadherin were downregulated by CS exposure, as previously reported (Coppe 2008, Hasegawa 2002).

In our analysis, we observed that expression of N-cadherin (*CDH2*) was upregulated, which indicates an epithelial mesenchymal transition-like switch (*CDH1* downregulated, *CDH2* upregulated) upon CS exposure (Huang 2013).

Tight junction-related genes were, on the contrary, mostly upregulated following CS exposure, except *CLDN1*, whose depletion has been linked to hyperkeratosis in mice (Furuse 2002, Morita 2011, Zhou 2013), and which was found to be downregulated in human biopsies from patients with periodontitis (Ye 2000). We could interpret these findings as a rapidly initiated adaptive response to rescue or increase tight junctional barrier function in response to CS. We observed a similar scenario in our previous study, focused on buccal organotypic cultures exposed to CS and THS2.2 aerosol (Zanetti 2016); these findings indicate a common response of oral tissues, despite the diversity of the epithelial structures and the difference in exposure design in the two studies (acute exposure vs. repeated exposures).

Limitations of the study

Although in this study donor-specific factors cannot be excluded and could be associated with the exposure response of the cultures that we used (e.g., undetected genetic variations influencing the outcome of the experiments), the overall findings show a substantially reduced impact of THS2.2 aerosol exposure on gingival cultures compared with 3R4F CS exposure at comparable concentrations. Future studies using a larger number of donors could confirm the observations reported here. Moreover, the employed organotypic culture was composed of only keratinocytes. Other cell types relevant to the pathogenesis of periodontal diseases (Di Benedetto 2013), notably fibroblasts in the periodontal soft connective tissue and immune cells, were not included in our model. Thus, our model is focused on the initial mechanisms centered on the epithelium.

In conclusion, this study indicates that exposure to THS2.2 aerosol exerts no obvious acute toxicity and a lower impact on the pathophysiology of human gingival organotypic cultures. The effects of CS on gingival cultures mirrored several pathophysiological conditions and molecular changes observed in the native gingival mucosa of smokers, making this model a potential tool for pre-clinical predictive *in vitro* research.

11. Archiving

After completion of the study, the following will be archived: Study Plan with any amendment, test/reference item retention samples, all raw data, report with any amendment, and all study-related records needed to reconstruct the study. These will be retained for at least 10 years according to the applicable archiving procedures. Paper records will be stored in the archive at Philip Morris Products S.A., Research & Development, PMI Product Testing, Neuchâtel, Switzerland; electronic records will be managed by the PMI Product Testing e-archivist on the central archiving server at Philip Morris S.A., Lausanne, Switzerland.

12. Abbreviations

Abbreviation	Term
3D	Three-dimensional
3R4F	Reference cigarettes
ACN	Acetonitrile
AK	Adenylate kinase
ALI	Air-liquid interface
BIF	Biological impact factor
cDNA	Complementary DNA
CFA	Cell fate and angiogenesis
CoA	Certificate of Analysis
Cor	Correlation
CPR	Cell proliferation
cRNA	Complementary RNA
CS	Cigarette smoke
CSF	Colony-stimulating factor
CST	Cellular stress
CXCL	Chemokine (C-X-C motif) ligand
CYP	Cytochrome P450
DEG	Differentially expressed gene
DNA	Deoxyribonucleic acid
DRA	Dose range assessment, also reported as DRF
DRF	Dose range finding, see DRA
EDMS	Electronic Document Management System
EDTA	Ethylenediaminetetraacetic acid
FC	Fold-change

FDR	False discovery rate
fRMA	Frozen robust multiarray analysis
GC-FID	Gas chromatography-flame ionization detection
G-CSF	Granulocyte colony-stimulating factor
GIN-100	EpiGingival epithelial tissues
GIN-100-DM4a	EpiGingival differentiation medium
GIN-100-MM	EpiGingival maintenance medium
GM-CSF	Granulocyte-macrophage colony-stimulating factor
GRO	Melanoma growth stimulating activity, alpha
GSA	Gene-set analysis
H_2SO_4	Sulfuric acid
H&E	Hematoxylin and eosin
HESI	Heated electrospray ionization
HCN	Hydrogen cyanide
HPLC	High-performance liquid chromatography
HRAM	High-resolution, accurate-mass
IL	Interleukin
IP-10	Interferon gamma-induced protein 10
IPN	Inflammatory process network
ISO	International Organization for Standardization
KEGG	Kyoto Encyclopedia of Genes and Genomes
LCLM	Lower confidence limit of the mean
LC-MS/MS	Liquid chromatography-tandem mass spectrometry
LIMS	Laboratory information management system
Limma	Linear Models for Microarray Data
M	Membrane

MAD	Median absolute deviation
MAP	Multi-analyte profiling
MAPK	Mitogen-activated protein kinase
MARLE	Median absolute value relative log expression
mHCI	Modified Health Canada Intense
miRNA	Micro RNA
MMP	Matrix metalloproteinase
MP	Main phase
mRNA	Messenger RNA
MRTP	Modified-risk tobacco product
MS	Mass spectrometry
MTD	Maximum tolerable dose
mTOR	Mechanistic target of rapamycin
MTT	3-(4,5-Dimethylthiazole-2-yl)-2,5-diphenyl tetrazolium bromide
NA	Not available
NFE2L2	Nuclear factor (erythroid-derived 2)-like 2
NHOC	Normal human oral cells
NPA	Network perturbation amplitude
Nrf2	See NFE2L2
NUSE	Normalized unscaled standard error
ORA	Over-representation analysis
P2	Platform 2
PAH	Polycyclic aromatic hydrocarbon
PAHS	Human Osmotic Stress PCR Array
PBS	Phosphate-buffered saline
PE	Post-exposure
PFPA	Perfluoropentanoic acid

PGE2	Prostaglandin E2
PMI	Philip Morris International
QC	Quality control
QQ	Quantile–quantile
RBIF	Relative BIF
REF	Reference
RI	Retention time/index
RIN	RNA integrity number
RLE	Relative log expression
RMA	Robust multiarray
RNA	Ribonucleic acid
RP	Reverse phase
RRP	Reduced-risk product
SB	Stratum basale
SC	Stratum corneum
SE	Standard error
SEM	Standard error of the mean
SG	Stratum granulosum
SM	Smoking machine
SOP	Standard operating procedure
SP	Study Plan
SS	Stratum spinosum
STAT	Signal transducer and activator of transcription
TAK	Total adenylate kinase
TCDD	2,3,7,8-Tetrachlorodibenzodioxin
TGFA	Transforming growth factor alpha
THS	Tobacco Heating System (also referred to as ZRH)

TNFα	Tumor necrosis factor alpha
UCLM	Upper confidence limit of the mean
Untr	Untreated
UPLC	Ultra performance liquid chromatography
VEGFA	Vascular endothelial growth factor alpha
VSN	Variance-stabilizing normalization
v/v	Volume/volume
WKI	Work instruction
Wnt	Proto-oncogene protein
w/v	Weight/volume
ZRH	See THS

13. TABLES AND SUPPLEMENTARY FIGURES

13.1 Supplementary Tables

13.1.1 Descriptive Statistics: Levels of Various Carbonyls

13.1.1.1 **Supplementary Table 1**. Acetaldehyde levels deposited in the cultivation base module of the Vitrocell 24/48 exposure system.

Descriptive Statistics: Acetaldehyde (deposited µg/mL)				
Year and calendar week	**2016.20**		**2016.28**	
	M	**SEM**	**M**	**SEM**
3R4F (Air)	0.00	0.00	0.00	0.00
3R4F (3%)	0.35	0.04	0.69	0.08
3R4F (5%)	0.52	0.08	1.04	0.03
3R4F (7%)	0.89	0.05	1.46	0.02
3R4F (13%)	1.70	0.10	2.92	0.22
3R4F (23%)	2.81	0.13	4.11	0.01
3R4F (35%)	5.32	0.20	6.55	0.27
THS2.2 (Air)	0.00	0.00	0.00	0.00
THS2.2 (13%)	0.20	0.01	0.28	0.10
THS2.2 (24%)	0.43	0.02	0.56	0.15
THS2.2 (31%)	0.59	0.02	0.92	0.04
THS2.2 (50%)	1.14	0.05	1.66	0.07
THS2.2 (70%)	1.41	0.11	2.46	0.45
THS2.2 (100%)	3.20	0.20	4.74	0.09

The method to measure various carbonyls in phosphate-buffered saline (PBS)-exposed samples has not been validated. For the indicated nicotine doses (in percentage of dilution) of the reference smoke and test aerosols, as well as the corresponding air controls, carbonyls were measured in PBS following a 28-min exposure (see Testing Procedure). Abbreviations: M, mean; SEM, standard error of the mean. N = 6.

13.1.1.2 **Supplementary Table 2**. Acetone levels deposited in the cultivation base module of the Vitrocell 24/48 exposure system.

Descriptive Statistics: Acetone (deposited µg/mL)				
Year and calendar week	**2016.20**		**2016.28**	
	M	**SEM**	**M**	**SEM**
3R4F (Air)	0.00	0.00	0.67	0.61
3R4F (3%)	0.23	0.00	0.91	0.49
3R4F (5%)	0.31	0.02	0.79	0.28
3R4F (7%)	0.51	0.03	0.96	0.22
3R4F (13%)	1.04	0.01	2.20	0.85
3R4F (23%)	1.66	0.04	1.93	0.05
3R4F (35%)	2.67	0.13	3.08	0.44
THS2.2 (Air)	0.00	0.00	0.26	0.04
THS2.2 (13%)	0.06	0.00	0.33	0.04
THS2.2 (24%)	0.10	0.00	0.23	0.01
THS2.2 (31%)	0.13	0.00	0.38	0.13
THS2.2 (50%)	0.21	0.00	0.81	0.24
THS2.2 (70%)	0.26	0.01	0.60	0.26
THS2.2 (100%)	0.56	0.02	0.86	0.18

The method to measure various carbonyls in phosphate-buffered saline (PBS)-exposed samples has not been validated. For the indicated nicotine doses (in percentage of dilution) of the reference smoke and test aerosols, as well as the corresponding air controls, carbonyls were measured in PBS following a 28-min exposure (see Testing Procedure). Abbreviations: M, mean; SEM, standard error of the mean. N = 6.

13.1.1.3 **Supplementary Table 3**. Acrolein levels deposited in the cultivation base module of the Vitrocell 24/48 exposure system.

Descriptive Statistics: Acrolein (deposited µg/mL)				
Year and calendar week	**2016.20**		**2016.28**	
	M	**SEM**	**M**	**SEM**
3R4F (Air)	0.00	0.00	0.00	0.00
3R4F (3%)	0.03	0.00	0.04	0.00
3R4F (5%)	0.04	0.00	0.07	0.00
3R4F (7%)	0.06	0.00	0.10	0.00
3R4F (13%)	0.11	0.01	0.20	0.00
3R4F (23%)	0.16	0.00	0.25	0.01
3R4F (35%)	0.23	0.00	0.38	0.01
THS2.2 (Air)	0.00	0.00	0.00	0.00
THS2.2 (13%)	0.01	0.00	0.01	0.00
THS2.2 (24%)	0.02	0.00	0.03	0.00
THS2.2 (31%)	0.02	0.00	0.03	0.00
THS2.2 (50%)	0.04	0.00	0.05	0.00
THS2.2 (70%)	0.06	0.00	0.08	0.00
THS2.2 (100%)	0.09	0.00	0.15	0.01

The method to measure various carbonyls in phosphate-buffered saline (PBS)-exposed samples has not been validated. For the indicated nicotine doses (in percentage of dilution) of the reference smoke and test aerosols, as well as the corresponding air controls, carbonyls were measured in PBS following a 28-min exposure (see Testing Procedure). Abbreviations: M, mean; SEM, standard error of the mean. N = 6.

13.1.1.4 **Supplementary Table 4**. Propionaldehyde levels deposited in the cultivation base module of the Vitrocell 24/48 exposure system.

Descriptive Statistics: Propionaldehyde (deposited µg/mL)				
Year and calendar week	**2016.20**		**2016.28**	
	M	**SEM**	**M**	**SEM**
3R4F (Air)	0.00	0.00	0.00	0.00
3R4F (3%)	0.03	0.00	0.05	0.01
3R4F (5%)	0.05	0.01	0.08	0.00
3R4F (7%)	0.07	0.01	0.11	0.00
3R4F (13%)	0.13	0.01	0.19	0.01
3R4F (23%)	0.20	0.01	0.25	0.01
3R4F (35%)	0.31	0.00	0.39	0.01
THS2.2 (Air)	0.00	0.00	0.00	0.00
THS2.2 (13%)	0.02	0.00	0.03	0.00
THS2.2 (24%)	0.04	0.00	0.04	0.00
THS2.2 (31%)	0.05	0.00	0.07	0.00
THS2.2 (50%)	0.08	0.01	0.11	0.00
THS2.2 (70%)	0.10	0.00	0.14	0.02
THS2.2 (100%)	0.21	0.00	0.28	0.02

The method to measure various carbonyls in phosphate-buffered saline (PBS)-exposed samples has not been validated. For the indicated nicotine doses (in percentage of dilution) of the reference smoke and test aerosols, as well as the corresponding air controls, carbonyls were measured in PBS following a 28-min exposure (see Testing Procedure). Abbreviations: M, mean; SEM, standard error of the mean. N = 6.

13.1.1.5 **Supplementary Table 5**. Crotonaldehyde levels deposited in the cultivation base module of the Vitrocell 24/48 exposure system.

Descriptive Statistics: Crotonaldehyde (deposited µg/mL)				
Year and calendar week	**2016.20**		**2016.28**	
	M	**SEM**	**M**	**SEM**
3R4F (Air)	0.00	0.00	0.00	0.00
3R4F (3%)	0.01	0.00	0.02	0.00
3R4F (5%)	0.02	0.00	0.03	0.00
3R4F (7%)	0.03	0.00	0.04	0.00
3R4F (13%)	0.05	0.00	0.09	0.02
3R4F (23%)	0.09	0.01	0.12	0.01
3R4F (35%)	0.14	0.00	0.18	0.01
THS2.2 (Air)	0.00	0.00	0.00	0.00
THS2.2 (13%)	0.00	0.00	0.00	0.00
THS2.2 (24%)	0.01	0.00	0.01	0.00
THS2.2 (31%)	0.01	0.00	0.01	0.00
THS2.2 (50%)	0.01	0.00	0.02	0.00
THS2.2 (70%)	0.02	0.00	0.03	0.00
THS2.2 (100%)	0.04	0.00	0.05	0.00

The method to measure various carbonyls in phosphate-buffered saline (PBS)-exposed samples has not been validated. For the indicated nicotine doses (in percentage of dilution) of the reference smoke and test aerosols, as well as the corresponding air controls, carbonyls were measured in PBS following a 28-min exposure (see Testing Procedure). Abbreviations: M, mean; SEM, standard error of the mean. N = 6.

13.1.1.6 **Supplementary Table 6**. Methyl ethyl ketone levels deposited in the cultivation base module of the Vitrocell 24/48 exposure system.

Descriptive Statistics: Methyl ethyl ketone (deposited µg/mL)				
Year and calendar week	2016.20		2016.28	
	M	SEM	M	SEM
3R4F (Air)	0.01	0.01	0.02	0.00
3R4F (3%)	0.06	0.00	0.08	0.00
3R4F (5%)	0.09	0.01	0.10	0.00
3R4F (7%)	0.14	0.00	0.15	0.00
3R4F (13%)	0.28	0.00	0.27	0.02
3R4F (23%)	0.44	0.01	0.39	0.02
3R4F (35%)	0.72	0.04	1.06	0.51
THS2.2 (Air)	0.00	0.00	0.09	0.08
THS2.2 (13%)	0.02	0.00	0.03	0.01
THS2.2 (24%)	0.03	0.00	0.03	0.00
THS2.2 (31%)	0.03	0.00	0.04	0.01
THS2.2 (50%)	0.04	0.01	0.05	0.00
THS2.2 (70%)	0.06	0.00	0.07	0.01
THS2.2 (100%)	0.11	0.01	0.13	0.02

The method to measure various carbonyls in phosphate-buffered saline (PBS)-exposed samples has not been validated. For the indicated nicotine doses (in percentage of dilution) of the reference smoke and test aerosols, as well as the corresponding air controls, carbonyls were measured in PBS following a 28-min exposure (see Testing Procedure). Abbreviations: M, mean; SEM, standard error of the mean. N = 6.

13.1.1.7 **Supplementary Table 7**. Butyraldehyde levels deposited in the cultivation base module of the Vitrocell 24/48 exposure system.

Descriptive Statistics: Butyraldehyde (deposited µg/mL)				
Year and calendar week	**2016.20**		**2016.28**	
	M	**SEM**	**M**	**SEM**
3R4F (Air)	0.00	0.00	0.00	0.00
3R4F (3%)	0.01	0.00	0.01	0.00
3R4F (5%)	0.01	0.00	0.01	0.00
3R4F (7%)	0.02	0.00	0.02	0.00
3R4F (13%)	0.03	0.00	0.03	0.00
3R4F (23%)	0.04	0.00	0.04	0.00
3R4F (35%)	0.06	0.00	0.05	0.00
THS2.2 (Air)	0.00	0.00	0.00	0.00
THS2.2 (13%)	0.01	0.00	0.01	0.00
THS2.2 (24%)	0.02	0.00	0.02	0.00
THS2.2 (31%)	0.02	0.00	0.02	0.00
THS2.2 (50%)	0.04	0.00	0.03	0.00
THS2.2 (70%)	0.06	0.00	0.04	0.01
THS2.2 (100%)	0.10	0.00	0.09	0.00

The method to measure various carbonyls in phosphate-buffered saline (PBS)-exposed samples has not been validated. For the indicated nicotine doses (in percentage of dilution) of the reference smoke and test aerosols, as well as the corresponding air controls, carbonyls were measured in PBS following a 28-min exposure (see Testing Procedure). Abbreviations: M, mean; SEM, standard error of the mean. N = 6.

13.1.1.8 **Supplementary Table 8**. Formaldehyde levels deposited in the cultivation base module of the Vitrocell 24/48 exposure system.

Descriptive Statistics: Formaldehyde (deposited µg/mL)				
Year and calendar week	2016.20		2016.28	
	M	SEM	M	SEM
3R4F (Air)	0.00	0.00	0.00	0.00
3R4F (3%)	0.00	0.00	0.00	0.00
3R4F (5%)	0.00	0.00	0.00	0.00
3R4F (7%)	0.00	0.00	0.00	0.00
3R4F (13%)	0.00	0.00	0.00	0.00
3R4F (23%)	0.00	0.00	0.01	0.01
3R4F (35%)	0.11	0.02	0.14	0.01
THS2.2 (Air)	0.00	0.00	0.00	0.00
THS2.2 (13%)	0.00	0.00	0.00	0.00
THS2.2 (24%)	0.00	0.00	0.00	0.00
THS2.2 (31%)	0.00	0.00	0.00	0.00
THS2.2 (50%)	0.00	0.00	0.00	0.00
THS2.2 (70%)	0.00	0.00	0.00	0.00
THS2.2 (100%)	0.00	0.00	0.00	0.00

The method to measure various carbonyls in phosphate-buffered saline (PBS)-exposed samples has not been validated. For the indicated nicotine doses (in percentage of dilution) of the reference smoke and test aerosols, as well as the corresponding air controls, carbonyls were measured in PBS following a 28-min exposure (see Testing Procedure). Abbreviations: M, mean; SEM, standard error of the mean. N = 6.

13.1.2 **Supplementary Table 9.** Descriptive Statistics: Cytotoxicity (%, no phosphate-buffered saline).

	Exposure		Descriptive Statistics								
PE [h]	**Rep**	**Dose**	**N**	**M**	**SEM**	**Q1**	**Median**	**Q3**	**LCLM**	**UCLM**	**Skew**
24:00	1	3R4F (Air)	6	0.75%	0.13%	0.47%	0.78%	1.01%	0.41%	1.10%	−0.10
		3R4F (49.4)	6	0.47%	0.14%	0.09%	0.60%	0.71%	0.11%	0.83%	−0.78
		THS2.2 (Air)	6	0.69%	0.11%	0.43%	0.68%	0.87%	0.40%	0.98%	0.34
		THS2.2 (14.4)	6	0.48%	0.12%	0.27%	0.38%	0.64%	0.17%	0.79%	1.18
	2	3R4F (Air)	6	0.29%	0.06%	0.16%	0.25%	0.37%	0.13%	0.46%	1.20
		3R4F (49.4)	6	0.06%	0.05%	0.05%	0.05%	0.14%	−0.07%	0.19%	−0.71
		THS2.2 (Air)	6	0.25%	0.06%	0.11%	0.22%	0.42%	0.10%	0.41%	0.39
		THS2.2 (14.4)	6	0.12%	0.10%	−0.03 %	0.05%	0.12%	−0.13%	0.37%	2.10
	3	3R4F (Air)	6	0.14%	0.06%	0.04%	0.13%	0.23%	−0.02%	0.31%	0.35
		3R4F (49.4)	6	3.07%	0.56%	2.15%	3.56%	4.04%	1.64%	4.50%	−1.15
		THS2.2 (Air)	6	0.16%	0.08%	0.05%	0.24%	0.27%	−0.05%	0.37%	−1.31
		THS2.2 (14.4)	6	0.02%	0.11%	−0.08 %	−0.07%	−0.04 %	−0.27%	0.32%	2.23
	123	3R4F (Air)	6	1.19%	0.19%	0.88%	1.20%	1.62%	0.71%	1.67%	−0.26
		3R4F (49.4)	6	3.60%	0.63%	1.98%	4.10%	4.69%	1.97%	5.23%	−0.64
		THS2.2 (Air)	6	1.10%	0.13%	0.82%	1.10%	1.21%	0.78%	1.43%	0.81
		THS2.2 (14.4)	6	0.62%	0.26%	0.21%	0.29%	0.94%	−0.06%	1.30%	1.64

Abbreviations: 123, cumulative data from three repetitions; h, hour; LCLM, lower confidence limit of the mean; M, mean; N, number of replicates; PE, post-exposure; Q1, first quartile; Q3, third quartile; Rep, repetition number; SEM, standard error of the mean; UCLM, upper confidence limit of the mean.

13.1.3 **Supplementary Table 10.** Descriptive Statistics: Cytotoxicity (%, dose range assessment).

	Exposure		Descriptive Statistics							
PE [h]	**Rep**	**Dose**	**N**	**M**	**SEM**	**Q1**	**Median**	**Q3**	**LCLM**	**UCLM**
DRA 24:00	1	3R4F (Air)	3	1.57%	0.36%	1.19%	1.23%	2.29%	0.02%	3.12%
		3R4F (3.11)	3	1.29%	0.36%	0.84%	1.02%	2.01%	−0.27%	2.85%
		3R4F (8.25)	3	0.94%	0.19%	0.68%	0.82%	1.32%	0.10%	1.78%
		3R4F (15.4)	3	0.73%	0.06%	0.62%	0.77%	0.81%	0.48%	0.99%
		3R4F (89.1)	3	1.52%	0.13%	1.27%	1.57%	1.73%	0.95%	2.10%
		3R4F (201)	3	6.68%	1.17%	4.41%	7.38%	8.27%	1.66%	11.70%
		THS2.2 (Air)	3	1.01%	0.19%	0.78%	0.86%	1.39%	0.19%	1.83%
		THS2.2 (2.18)	3	1.43%	0.25%	0.92%	1.62%	1.73%	0.34%	2.52%
		THS2.2 (5.84)	3	0.95%	0.19%	0.72%	0.78%	1.33%	0.11%	1.78%
		THS2.2 (11.5)	3	1.07%	0.06%	0.99%	1.03%	1.20%	0.81%	1.34%
		THS2.2 (79.2)	3	1.05%	0.56%	0.44%	0.55%	2.17%	−1.35%	3.45%
		THS2.2 (147.2)	3	0.91%	0.18%	0.68%	0.79%	1.27%	0.14%	1.69%
	2	3R4F (Air)	3	1.00%	0.09%	0.82%	1.06%	1.12%	0.60%	1.40%
		3R4F (3.11)	3	0.69%	0.22%	0.45%	0.49%	1.13%	−0.26%	1.64%
		3R4F (8.25)	3	0.76%	0.16%	0.55%	0.65%	1.07%	0.08%	1.43%
		3R4F (15.4)	3	1.42%	0.25%	0.95%	1.54%	1.78%	0.36%	2.49%
		3R4F (89.1)	3	2.60%	0.43%	1.89%	2.55%	3.37%	0.76%	4.45%
		3R4F (201)	3	45.51%	8.46%	28.82%	51.43%	56.28%	9.11%	81.91%
		THS2.2 (Air)	3	0.73%	0.10%	0.61%	0.65%	0.93%	0.29%	1.16%
		THS2.2 (2.18)	3	1.01%	0.15%	0.77%	0.96%	1.30%	0.35%	1.67%
		THS2.2 (5.84)	3	0.69%	0.20%	0.37%	0.64%	1.05%	−0.17%	1.54%
		THS2.2 (11.5)	3	0.78%	0.17%	0.60%	0.63%	1.13%	0.04%	1.53%
		THS2.2 (79.2)	3	0.73%	0.42%	0.19%	0.46%	1.55%	−1.07%	2.53%
		THS2.2 (147.2)	3	0.63%	0.21%	0.29%	0.61%	1.00%	−0.26%	1.52%
	3	3R4F (Air)	3	−0.87%	0.03%	−0.92%	−0.86%	−0.82%	−0.99%	−0.75%
		3R4F (3.11)	3	−0.75%	0.03%	−0.79%	−0.77%	−0.69%	−0.90%	−0.61%
		3R4F (8.25)	3	−0.69%	0.03%	−0.75%	−0.67%	−0.65%	−0.83%	−0.55%
		3R4F (15.4)	3	−0.27%	0.06%	−0.36%	−0.27%	−0.17%	−0.51%	−0.02%
		3R4F (89.1)	3	9.40%	0.68%	8.67%	8.77%	10.75%	6.48%	12.31%
		3R4F (201)	3	7.48%	1.21%	6.00%	6.57%	9.87%	2.29%	12.68%
		THS2.2 (Air)	3	−0.93%	0.02%	−0.96%	−0.93%	−0.88%	−1.02%	−0.83%
		THS2.2 (2.18)	3	−0.82%	0.07%	−0.94%	−0.79%	−0.72%	−1.10%	−0.54%

Table Continues

		THS2.2 (5.84)	3	−0.80%	0.10%	−0.91%	−0.89%	−0.59%	−1.25%	−0.35%
		THS2.2 (11.5)	3	−0.74%	0.07%	−0.83%	−0.78%	−0.59%	−1.06%	−0.41%
		THS2.2 (79.2)	3	−0.67%	0.10%	−0.87%	−0.58%	−0.56%	−1.10%	−0.24%
		THS2.2 (147.2)	3	−0.67%	0.08%	−0.81%	−0.64%	−0.56%	−1.00%	−0.35%
	123	3R4F (Air)	3	0.06%	0.07%	−0.03%	0.00%	0.21%	−0.26%	0.38%
		3R4F (3.11)	3	−0.07%	0.25%	−0.40%	−0.22%	0.41%	−1.13%	0.98%
		3R4F (8.25)	3	−0.13%	0.08%	−0.21%	−0.20%	0.03%	−0.47%	0.21%
		3R4F (15.4)	3	0.28%	0.07%	0.19%	0.24%	0.41%	−0.01%	0.56%
		3R4F (89.1)	3	5.83%	0.34%	5.29%	5.74%	6.44%	4.38%	7.27%
		3R4F (201)	3	13.65%	2.72%	8.38%	15.08%	17.49%	1.93%	25.37%
		THS2.2 (Air)	3	−0.14%	0.19%	−0.50%	−0.03%	0.11%	−0.94%	0.66%
		THS2.2 (2.18)	3	−0.00%	0.03%	−0.05%	−0.02%	0.05%	−0.13%	0.13%
		THS2.2 (5.84)	3	−0.27%	0.01%	−0.28%	−0.28%	−0.24%	−0.33%	−0.21%
		THS2.2 (11.5)	3	−0.04%	0.10%	−0.20%	−0.04%	0.13%	−0.45%	0.38%
		THS2.2 (79.2)	3	−0.11%	0.22%	−0.39%	−0.25%	0.31%	−1.04%	0.82%
		THS2.2 (147.2)	3	−0.07%	0.18%	−0.44%	0.10%	0.13%	−0.86%	0.72%

End of Table

Abbreviations: 123, cumulative data from three repetitions; h, hour; LCLM, lower confidence limit of the mean; M, mean; N, number of replicates; PE, post-exposure; Q1, first quartile; Q3, third quartile; Rep, repetition number; SEM, standard error of the mean; UCLM, upper confidence limit of the mean.

13.1.4 **Supplementary Table 11.** Descriptive Statistics: CYP1A1/1B1 Activity (%).

	Exposure		Descriptive Statistics (Dose Range Assessment)							
PE [h]	**Rep**	**Dose**	**N**	**M**	**SEM**	**Q1**	**Median**	**Q3**	**LCLM**	**UCLM**
DRA 24:00	1	3R4F (Air)	3	5.19%	1.02%	3.32%	5.40%	6.85%	0.78%	9.60%
		3R4F (3.11)	3	130.7%	22.18%	90.16%	135.3%	166.6%	35.24%	226.1%
		3R4F (8.25)	3	69.40%	7.27%	55.16%	73.94%	79.08%	38.12%	100.7%
		3R4F (15.4)	3	8.51%	1.86%	5.40%	8.29%	11.82%	0.52%	16.50%
		3R4F (89.1)	3	−6.42%	4.67%	−13.86%	−7.60%	2.19%	−26.52%	13.68%
		3R4F (201)	3	−11.61%	0.82%	−13.22%	−11.13%	−10.49%	−15.15%	-8.07%
		THS2.2 (Air)	3	−5.30%	1.12%	−7.12%	−5.51%	−3.26%	−10.10%	−0.49%
		THS2.2 (2.18)	3	5.19%	3.73%	−1.98%	7.01%	10.54%	−10.85%	21.23%
		THS2.2 (5.84)	3	4.33%	1.07%	2.51%	4.28%	6.21%	−0.25%	8.92%
		THS2.2 (11.5)	3	3.37%	0.75%	1.87%	3.96%	4.28%	0.12%	6.62%
		THS2.2 (79.2)	3	33.12%	6.21%	23.22%	31.57%	44.57%	6.39%	59.84%
		THS2.2 (147.2)	3	28.46%	6.10%	20.33%	24.67%	40.40%	2.24%	54.69%
	Exposure		**Descriptive Statistics (Main Phase)**							
PE [h]	**Rep**	**Dose**	**N**	**M**	**SEM**	**Q1**	**Median**	**Q3**	**LCLM**	**UCLM**
MP 24:00	3	3R4F (Air)	9	2.40%	6.42%	−1.84%	−1.06%	10.56%	−12.39%	17.20%
		3R4F (49.4)	9	−4.34%	3.02%	−7.39%	−2.64%	−1.91%	−11.31%	2.63%
		3R4F (84.6)	9	−11.16%	3.32%	−17.87%	−8.98%	−2.91%	−18.81%	−3.51%
		THS2.2 (Air)	9	19.74%	14.64%	−1.56%	−1.06%	8.21%	−14.02%	53.51%
		THS2.2 (14.4)	9	44.13%	14.26%	5.46%	34.30%	51.23%	11.24%	77.01%
		THS2.2 (54.6)	9	39.34%	10.98%	6.95%	43.84%	58.10%	14.02%	64.67%
		THS2.2 (100.4)	9	38.11%	22.82%	0.85%	11.11%	36.44%	−14.52%	90.74%

Abbreviations: DRA, dose range assessment; h, hour; LCLM, lower confidence limit of the mean; M, mean; MP, main phase; N, number of replicates; PE, post-exposure; Q1, first quartile; Q3, third quartile; Rep, repetition number; SEM, standard error of the mean; UCLM, upper confidence limit of the mean.

13.1.5 **Supplementary Table 12.** Descriptive Statistics: Cytotoxicity (%, main phase).

	Exposure		Descriptive Statistics								
PE [h]	**Rep**	**Dose**	**N**	**M**	**SEM**	**Q1**	**Median**	**Q3**	**LCLM**	**UCLM**	**Skew**
4:00 MP	1	3R4F (Air)	9	0.85%	0.16%	0.54%	1.00%	1.23%	0.48%	1.21%	−0.74
		3R4F (49.4)	9	0.40%	0.17%	−0.09%	0.17%	0.77%	0.00%	0.79%	0.27
		3R4F (84.6)	9	0.37%	0.17%	−0.00%	0.33%	0.54%	−0.01%	0.75%	0.76
		THS2.2 (Air)	9	0.87%	0.20%	0.56%	0.90%	1.05%	0.41%	1.33%	0.92
		THS2.2 (14.4)	9	0.86%	0.19%	0.41%	1.01%	1.13%	0.43%	1.30%	0.06
		THS2.2 (54.6)	9	1.01%	0.32%	0.59%	0.84%	1.03%	0.28%	1.74%	1.53
		THS2.2 (100.4)	9	0.56%	0.14%	0.37%	0.64%	0.81%	0.23%	0.89%	−0.78
	2	3R4F (Air)	9	0.39%	0.08%	0.17%	0.40%	0.49%	0.20%	0.58%	0.20
		3R4F (49.4)	9	0.17%	0.15%	−0.07%	0.02%	0.58%	−0.17%	0.52%	0.19
		3R4F (84.6)	9	0.45%	0.14%	0.24%	0.72%	0.74%	0.14%	0.77%	−0.81
		THS2.2 (Air)	9	0.36%	0.12%	0.12%	0.22%	0.54%	0.08%	0.63%	1.47
		THS2.2 (14.4)	9	0.36%	0.15%	0.11%	0.25%	0.69%	0.02%	0.70%	0.87
		THS2.2 (54.6)	9	0.32%	0.13%	0.13%	0.31%	0.35%	0.03%	0.61%	0.74
		THS2.2 (100.4)	9	0.23%	0.07%	0.14%	0.25%	0.32%	0.07%	0.38%	−0.17
	3	3R4F (Air)	9	−0.19%	0.07%	−0.42%	−0.20%	−0.03%	−0.36%	−0.02%	0.06
		3R4F (49.4)	9	−0.18%	0.09%	−0.31%	−0.17%	−0.07%	−0.38%	0.01%	−0.16
		3R4F (84.6)	9	0.64%	0.45%	−0.21%	0.05%	1.57%	−0.40%	1.67%	1.05
		THS2.2 (Air)	9	−0.28%	0.08%	−0.47%	−0.29%	−0.09%	−0.47%	−0.09%	0.02
		THS2.2 (14.4)	9	−0.35%	0.09%	−0.54%	−0.25%	−0.15%	−0.57%	−0.14%	−0.51
		THS2.2 (54.6)	9	−0.22%	0.10%	−0.43%	−0.14%	−0.01%	−0.45%	0.01%	−0.20
		THS2.2 (100.4)	9	−0.25%	0.11%	−0.50%	−0.25%	−0.06%	−0.50%	−0.00%	0.63
	123	3R4F (Air)	9	1.05%	0.29%	0.51%	1.25%	1.49%	0.37%	1.73%	−0.27
		3R4F (49.4)	9	0.39%	0.38%	−0.28%	0.03%	1.42%	−0.48%	1.26%	0.10
		3R4F (84.6)	9	1.47%	0.56%	0.66%	2.07%	2.14%	0.19%	2.75%	−0.30
		THS2.2 (Air)	9	0.94%	0.38%	0.06%	0.83%	1.15%	0.07%	1.81%	1.12
		THS2.2 (14.4)	9	0.87%	0.40%	0.21%	1.11%	1.73%	−0.05%	1.79%	−0.05
		THS2.2 (54.6)	9	1.11%	0.49%	0.69%	0.95%	1.09%	−0.03%	2.25%	0.75
		THS2.2 (100.4)	9	0.54%	0.29%	−0.06%	0.69%	1.04%	−0.14%	1.21%	−0.42

Table Continues

		3R4F (Air)	9	0.74%	0.18%	0.28%	0.83%	0.90%	0.32%	1.16%	0.50
		3R4F (49.4)	9	0.43%	0.08%	0.32%	0.39%	0.56%	0.25%	0.62%	0.28
		3R4F (84.6)	9	0.40%	0.14%	0.11%	0.47%	0.72%	0.07%	0.73%	−0.42
	1	THS2.2 (Air)	9	0.81%	0.12%	0.70%	0.81%	1.08%	0.55%	1.08%	−0.64
		THS2.2 (14.4)	9	0.79%	0.21%	0.32%	0.79%	0.81%	0.31%	1.27%	1.88
		THS2.2 (54.6)	9	0.58%	0.15%	0.27%	0.67%	0.80%	0.23%	0.93%	0.38
		THS2.2 (100.4)	9	0.39%	0.12%	0.27%	0.52%	0.64%	0.12%	0.67%	−0.90
		3R4F (Air)	9	0.34%	0.12%	0.03%	0.23%	0.55%	0.08%	0.61%	1.21
		3R4F (49.4)	9	0.32%	0.12%	0.07%	0.28%	0.52%	0.05%	0.59%	0.96
		3R4F (84.6)	9	0.44%	0.12%	0.13%	0.47%	0.66%	0.17%	0.70%	0.23
	2	THS2.2 (Air)	9	0.28%	0.07%	0.17%	0.21%	0.39%	0.12%	0.45%	1.06
		THS2.2 (14.4)	9	0.39%	0.10%	0.14%	0.38%	0.72%	0.15%	0.63%	0.34
		THS2.2 (54.6)	9	0.34%	0.09%	0.16%	0.33%	0.44%	0.12%	0.55%	0.63
		THS2.2 (100.4)	9	0.23%	0.08%	0.11%	0.24%	0.34%	0.04%	0.43%	0.49
24:00		3R4F (Air)	9	0.55%	0.10%	0.39%	0.48%	0.68%	0.32%	0.79%	0.87
		3R4F (49.4)	9	8.35%	2.05%	2.79%	6.77%	12.27%	3.62%	13.07%	0.66
		3R4F (84.6)	9	29.20%	2.20%	27.95%	32.48%	32.89%	24.13%	34.26%	−1.98
	3	THS2.2 (Air)	9	0.52%	0.15%	0.27%	0.44%	0.57%	0.16%	0.88%	2.00
		THS2.2 (14.4)	9	0.48%	0.11%	0.28%	0.39%	0.60%	0.24%	0.73%	0.98
		THS2.2 (54.6)	9	0.54%	0.19%	0.12%	0.36%	0.68%	0.10%	0.98%	1.72
		THS2.2 (100.4)	9	0.59%	0.17%	0.16%	0.70%	0.92%	0.20%	0.98%	0.24
		3R4F (Air)	9	1.63%	0.39%	0.88%	1.52%	2.24%	0.73%	2.53%	0.86
		3R4F (49.4)	9	9.10%	2.07%	4.15%	7.06%	13.18%	4.33%	13.87%	0.72
		3R4F (84.6)	9	30.03%	2.04%	28.37%	32.69%	33.23%	25.32%	34.74%	−1.96
	123	THS2.2 (Air)	9	1.62%	0.25%	1.39%	1.67%	1.96%	1.05%	2.19%	−0.24
		THS2.2 (14.4)	9	1.66%	0.30%	1.05%	1.25%	2.59%	0.96%	2.36%	0.35
		THS2.2 (54.6)	9	1.46%	0.33%	1.14%	1.25%	1.90%	0.71%	2.22%	0.81
		THS2.2 (100.4)	9	1.21%	0.27%	0.58%	1.21%	1.48%	0.59%	1.84%	0.45

End of Table

Abbreviations: 123, cumulative data from three repetitions; h, hour; LCLM, lower confidence limit of the mean; M, mean; N, number of replicates; PE, post-exposure; Q1, first quartile; Q3, third quartile; Rep, repetition number; SEM, standard error of the mean; UCLM, upper confidence limit of the mean.

13.1.6 Descriptive Statistics: Concentration of Proinflammatory Mediators in the Basolateral Media

13.1.6.1 **Supplementary Table 13**. Descriptive Statistics: CSF3 Protein in the Basolateral Media.

Exposure				Descriptive Statistics								
E [h]	PE [h]	Rep	Dose	N	M	SEM	Q1	Median	Q3	LCLM	UCLM	Skew
0:00	0:00	1	Untr	1	25.36	.	25.36	25.36	25.36	.	.	.
			PBS	2	39.72	23.06	16.66	39.72	62.79	−253.33	332.78	.
0:28	24:00	1	3R4F (Air)	9	40.26	5.78	24.84	37.09	51.55	26.93	53.58	0.93
			3R4F (49.4)	9	43.52	4.34	35.80	41.17	51.37	33.51	53.53	−0.40
			3R4F (84.6)	9	42.65	4.97	41.55	44.07	55.20	31.19	54.11	−0.71
			THS2.2 (Air)	9	38.37	9.39	12.91	44.34	66.86	16.73	60.01	0.00
			THS2.2 (14.4)	9	37.10	8.46	8.39	43.24	57.70	17.59	56.61	−0.24
			THS2.2 (54.6)	9	32.15	6.63	10.12	36.66	40.69	16.87	47.44	−0.06
			THS2.2 (100.4)	9	35.84	7.09	13.62	40.64	52.70	19.49	52.19	−0.59
		2	3R4F (Air)	9	17.10	3.76	10.37	13.82	25.58	8.43	25.76	0.30
			3R4F (49.4)	9	29.68	7.83	13.78	16.29	54.46	11.62	47.73	0.55
			3R4F (84.6)	9	32.82	6.79	16.44	32.10	51.61	17.16	48.49	0.26
			THS2.2 (Air)	9	21.72	4.39	10.05	21.49	34.75	11.59	31.85	−0.06
			THS2.2 (14.4)	9	20.06	2.31	13.55	21.93	22.94	14.72	25.39	0.59
			THS2.2 (54.6)	9	15.94	3.11	9.14	17.89	22.34	8.78	23.11	0.05
			THS2.2 (100.4)	9	24.22	2.99	19.23	20.79	28.81	17.32	31.12	0.60
		3	3R4F (Air)	9	25.48	6.35	17.90	25.60	30.48	10.83	40.12	1.11
			3R4F (49.4)	9	81.63	8.53	65.81	71.77	98.19	61.95	101.30	0.89
			3R4F (84.6)	9	89.27	14.20	63.31	95.35	101.20	56.53	122.02	1.28
			THS2.2 (Air)	9	34.83	6.78	19.37	34.31	53.08	19.19	50.47	−0.02
			THS2.2 (14.4)	9	35.75	6.41	24.45	33.88	45.83	20.97	50.52	0.08
			THS2.2 (54.6)	9	42.70	5.85	30.66	52.30	53.81	29.21	56.19	−0.19
			THS2.2 (100.4)	9	47.07	7.25	27.39	39.89	55.61	30.35	63.79	0.65
		123	3R4F (Air)	9	82.83	9.74	59.82	74.49	107.44	60.38	105.28	0.42
			3R4F (49.4)	9	154.83	17.43	107.39	150.75	190.11	114.63	195.02	0.40
			3R4F (84.6)	9	164.74	22.43	109.36	173.66	211.06	113.02	216.47	0.15
			THS2.2 (Air)	9	94.92	18.29	41.38	73.76	139.30	52.74	137.10	0.15
			THS2.2 (14.4)	9	92.91	15.47	48.11	103.04	129.91	57.24	128.57	−0.54
			THS2.2 (54.6)	9	90.80	14.10	58.67	91.97	114.29	58.28	123.31	−0.18
			THS2.2 (100.4)	9	107.13	12.74	90.37	126.89	137.43	77.74	136.52	−0.80
24:00	0:00	1	TNFα+ILß	3	837.09	534.69	275.78	329.47	1,906.02	−1,463.50	3,137.68	1.73

Abbreviations: 123, cumulative data from three repetitions; CSF3, colony-stimulating factor 3; E, exposure; h, hours; IL, interleukin; LCLM, lower confidence limit of the mean; M, mean; N, number of replicates; PBS, phosphate-buffered saline; PE, post-exposure; Q1, first quartile; Q3, third quartile; Rep, repetition number; SEM, standard error of the mean; TNFα, tumor necrosis factor alpha; UCLM, upper confidence limit of the mean; Untr, untreated. Nicotine concentrations in 3R4F cigarette smoke or THS2.2 aerosols are indicated for each group (mg/L).

13.1.6.2 **Supplementary Table 14**. Descriptive Statistics: CSF2 Protein in the Basolateral Media.

Exposure				Descriptive Statistics								
E [h]	PE [h]	Rep	Dose	N	M	SEM	Q1	Median	Q3	LCLM	UCLM	Skew
0:00	0:00	1	Untr	1	16.75	.	16.75	16.75	16.75	.	.	.
			PBS	2	16.26	8.69	7.56	16.26	24.95	−94.21	126.72	.
0:28	24:00	1	3R4F (Air)	9	18.78	2.34	13.91	15.71	23.59	13.37	24.18	0.40
			3R4F (49.4)	9	16.39	1.54	12.61	17.70	19.81	12.84	19.93	−0.31
			3R4F (84.6)	9	19.11	2.81	12.47	15.66	21.41	12.63	25.58	1.05
			THS2.2 (Air)	9	17.36	2.63	9.86	18.76	22.06	11.29	23.42	0.60
			THS2.2 (14.4)	9	15.27	1.50	10.71	17.25	18.82	11.80	18.74	−0.60
			THS2.2 (54.6)	9	14.36	1.58	12.19	13.67	17.25	10.70	18.01	−0.08
			THS2.2 (100.4)	9	15.97	2.08	12.55	13.00	20.55	11.18	20.76	0.80
		2	3R4F (Air)	9	6.64	0.83	3.75	6.74	8.96	4.72	8.56	−0.10
			3R4F (49.4)	9	16.18	3.42	3.75	16.98	22.12	8.30	24.06	−0.20
			3R4F (84.6)	9	23.52	5.18	13.84	19.63	29.25	11.58	35.46	0.88
			THS2.2 (Air)	9	9.58	1.49	5.99	11.49	13.35	6.15	13.01	−0.23
			THS2.2 (14.4)	9	9.76	1.35	7.92	10.87	11.95	6.66	12.86	−0.39
			THS2.2 (54.6)	9	10.85	1.34	9.26	11.82	13.15	7.76	13.95	−0.50
			THS2.2 (100.4)	9	12.86	1.73	11.33	12.74	14.27	8.86	16.85	−0.08
		3	3R4F (Air)	9	8.14	1.12	7.12	7.81	9.33	5.55	10.73	0.44
			3R4F (49.4)	9	112.86	16.33	81.45	100.41	165.67	75.21	150.52	0.32
			3R4F (84.6)	9	100.95	21.48	41.87	101.26	111.88	51.42	150.47	1.00
			THS2.2 (Air)	9	11.63	1.97	8.17	13.49	14.60	7.09	16.16	−0.09
			THS2.2 (14.4)	9	13.23	1.81	9.21	13.65	18.23	9.06	17.39	−0.57
			THS2.2 (54.6)	9	16.06	1.79	13.40	16.49	20.81	11.93	20.19	−0.54
			THS2.2 (100.4)	9	19.75	2.18	16.17	22.93	23.56	14.73	24.76	−0.86
		123	3R4F (Air)	9	33.56	3.12	25.72	34.23	41.16	26.37	40.75	0.20
			3R4F (49.4)	9	145.43	19.97	100.94	116.76	209.72	99.37	191.49	0.45
			3R4F (84.6)	9	143.57	27.50	68.23	140.58	176.55	80.15	206.99	1.24
			THS2.2 (Air)	9	38.56	5.40	27.08	41.73	51.41	26.11	51.02	−0.06
			THS2.2 (14.4)	9	38.25	4.41	24.89	45.58	46.44	28.09	48.42	−0.66
			THS2.2 (54.6)	9	41.27	4.06	38.17	43.13	46.89	31.90	50.64	−0.63
			THS2.2 (100.4)	9	48.57	5.20	46.13	48.04	52.14	36.57	60.57	−0.29
24:00	0:00	1	TNFα+ILß	3	48.05	5.71	41.49	43.25	59.42	23.50	72.61	1.67

Abbreviations: 123, cumulative data from three repetitions; CSF2, colony-stimulating factor 2; E, exposure; h, hours; IL, interleukin; LCLM, lower confidence limit of the mean; M, mean; N, number of replicates; PBS, phosphate-buffered saline; PE, post-exposure; Q1, first quartile; Q3, third quartile; Rep, repetition number; SEM, standard error of the mean; TNFα, tumor necrosis factor alpha; UCLM, upper confidence limit of the mean; Untr, untreated. Nicotine concentrations in 3R4F cigarette smoke or THS2.2 aerosols are indicated for each group (mg/L).

13.1.6.3 **Supplementary Table 15**. Descriptive Statistics: CXCL1 Protein in the Basolateral Media.

		Exposure		Descriptive Statistics								
E [h]	PE [h]	Rep	Dose	N	M	SEM	Q1	Median	Q3	LCLM	UCLM	Skew
0:00	0:00	1	Untr	1	160.58	.	160.58	160.58	160.58	.	.	.
			PBS	2	244.28	131.92	112.35	244.28	376.20	−1,431.98	1920.54	.
0:28	24:00	1	3R4F (Air)	9	225.85	14.42	207.79	211.79	237.89	192.59	259.11	1.11
			3R4F (49.4)	9	186.08	10.60	163.68	189.48	201.81	161.65	210.52	−0.30
			3R4F (84.6)	9	179.56	13.78	156.90	185.55	187.97	147.79	211.33	1.57
			THS2.2 (Air)	9	198.48	29.33	113.71	230.51	244.75	130.84	266.11	0.34
			THS2.2 (14.4)	9	167.42	23.09	90.88	185.91	217.76	114.17	220.68	−0.55
			THS2.2 (54.6)	9	149.42	18.16	83.16	175.27	187.83	107.54	191.31	−0.81
			THS2.2 (100.4)	9	152.47	19.46	84.41	169.84	174.99	107.59	197.35	−0.18
		2	3R4F (Air)	9	122.11	16.73	69.06	140.47	152.46	83.53	160.69	−0.43
			3R4F (49.4)	9	101.26	15.40	44.62	122.07	141.50	65.74	136.77	−0.61
			3R4F (84.6)	9	97.26	14.38	43.60	110.39	126.77	64.09	130.42	−0.53
			THS2.2 (Air)	9	150.50	14.08	127.67	141.33	157.82	118.03	182.96	1.32
			THS2.2 (14.4)	9	136.94	12.93	118.30	138.64	149.70	107.13	166.76	0.32
			THS2.2 (54.6)	9	112.01	8.23	82.89	117.84	127.30	93.04	130.98	−0.37
			THS2.2 (100.4)	9	118.91	9.16	105.02	124.67	139.76	97.78	140.03	−0.15
		3	3R4F (Air)	9	132.05	8.19	117.92	130.01	146.83	113.16	150.93	−0.13
			3R4F (49.4)	9	270.80	20.15	236.98	262.63	329.11	224.33	317.27	−0.07
			3R4F (84.6)	9	322.18	49.62	148.62	366.14	438.14	207.76	436.61	−0.43
			THS2.2 (Air)	9	168.45	16.02	126.72	164.06	188.05	131.52	205.38	0.47
			THS2.2 (14.4)	9	152.51	12.74	128.14	144.97	194.79	123.12	181.89	0.02
			THS2.2 (54.6)	9	144.41	11.66	110.38	149.06	154.53	117.53	171.30	0.72
			THS2.2 (100.4)	9	170.94	14.50	131.88	177.26	210.50	137.51	204.37	0.15
		123	3R4F (Air)	9	480.00	36.18	389.02	496.18	559.29	396.57	563.44	−0.01
			3R4F (49.4)	9	558.14	39.28	462.61	564.29	685.14	467.57	648.72	−0.24
			3R4F (84.6)	9	599.00	71.89	368.16	653.68	736.71	433.21	764.78	−0.28
			THS2.2 (Air)	9	517.42	55.36	366.64	545.77	577.83	389.75	645.09	0.63
			THS2.2 (14.4)	9	456.88	46.14	337.32	475.35	553.95	350.48	563.27	−0.48
			THS2.2 (54.6)	9	405.84	36.54	272.00	445.60	469.65	321.59	490.10	−0.55
			THS2.2 (100.4)	9	442.32	39.95	336.94	473.95	534.00	350.19	534.44	−0.23
24:00	0:00	1	TNFα+ILß	3	1,175.60	85.60	1,057.87	1,126.82	1,342.12	807.28	1,543.93	1.32

Abbreviations: 123, cumulative data from three repetitions; CXCL, chemokine (C-X-C motif) ligand; E, exposure; h, hours; IL, interleukin; LCLM, lower confidence limit of the mean; M, mean; N, number of replicates; PBS, phosphate-buffered saline; PE, post-exposure; Q1, first quartile; Q3, third quartile; Rep, repetition number; SEM, standard error of the mean; TNFα, tumor necrosis factor alpha; UCLM, upper confidence limit of the mean; Untr, untreated. Nicotine concentrations in 3R4F cigarette smoke or THS2.2 aerosols are indicated for each group (mg/L).

13.1.6.4 **Supplementary Table 16**. Descriptive Statistics: IL1A Protein in the Basolateral Media.

		Exposure		Descriptive Statistics								
E [h]	PE [h]	Rep	Dose	N	M	SEM	Q1	Median	Q3	LCLM	UCLM	Skew
0:00	0:00	1	Untr	1	17.52	.	17.52	17.52	17.52	.	.	.
			PBS	2	34.45	16.72	17.73	34.45	51.16	−177.94	246.83	.
0:28	24:00	1	3R4F (Air)	9	35.10	2.39	30.04	36.67	42.44	29.60	40.60	−0.56
			3R4F (49.4)	9	39.92	3.52	34.33	39.50	46.71	31.80	48.03	0.00
			3R4F (84.6)	9	55.41	3.58	47.58	58.14	58.66	47.16	63.66	0.36
			THS2.2 (Air)	9	43.05	9.27	21.75	36.84	43.21	21.68	64.42	1.71
			THS2.2 (14.4)	9	36.09	7.49	24.15	27.24	37.91	18.83	53.35	2.36
			THS2.2 (54.6)	9	26.56	2.47	19.32	27.49	32.06	20.87	32.26	−0.12
			THS2.2 (100.4)	9	27.31	2.73	20.23	27.09	31.64	21.01	33.62	−0.13
		2	3R4F (Air)	9	18.80	3.61	10.75	17.08	23.45	10.46	27.14	0.59
			3R4F (49.4)	9	35.43	5.32	24.06	36.74	45.74	23.16	47.70	0.43
			3R4F (84.6)	9	51.33	9.21	18.38	58.35	72.00	30.09	72.57	−0.28
			THS2.2 (Air)	9	24.08	3.31	18.20	20.49	25.83	16.45	31.71	1.77
			THS2.2 (14.4)	9	29.64	5.36	21.28	22.42	34.48	17.27	42.01	2.12
			THS2.2 (54.6)	9	22.95	1.70	20.13	22.79	24.06	19.03	26.87	1.11
			THS2.2 (100.4)	9	28.93	3.47	21.74	26.54	36.06	20.93	36.93	0.32
		3	3R4F (Air)	9	24.61	2.66	20.64	21.49	22.18	18.48	30.74	1.60
			3R4F (49.4)	9	307.76	58.74	179.69	258.09	339.61	172.32	443.21	1.11
			3R4F (84.6)	9	528.25	114.13	122.65	682.87	699.07	265.06	791.44	−0.41
			THS2.2 (Air)	9	31.54	5.46	17.55	30.11	37.98	18.94	44.13	0.35
			THS2.2 (14.4)	9	38.54	9.34	27.39	32.41	36.56	17.00	60.08	2.61
			THS2.2 (54.6)	9	33.76	4.58	22.43	36.98	39.02	23.21	44.32	0.64
			THS2.2 (100.4)	9	40.23	5.75	26.80	37.53	57.06	26.97	53.49	0.22
		123	3R4F (Air)	9	78.51	6.19	66.47	72.91	86.27	64.23	92.78	1.03
			3R4F (49.4)	9	383.11	53.59	299.07	311.54	428.71	259.53	506.70	1.09
			3R4F (84.6)	9	634.99	123.47	184.38	823.40	824.74	350.28	919.71	−0.46
			THS2.2 (Air)	9	98.67	16.95	69.34	85.02	101.68	59.57	137.76	1.44
			THS2.2 (14.4)	9	104.27	13.68	73.68	82.89	143.07	72.74	135.81	0.99
			THS2.2 (54.6)	9	83.28	6.32	71.45	87.75	93.35	68.71	97.85	−0.33
			THS2.2 (100.4)	9	96.48	9.27	82.28	90.71	101.71	75.10	117.85	0.22
24:00	0:00	1	TNFα+ILß	3	42.38	7.22	27.98	48.65	50.51	11.32	73.45	−1.69

Abbreviations: 123, cumulative data from three repetitions; E, exposure; h, hours; IL, interleukin; LCLM, lower confidence limit of the mean; M, mean; N, number of replicates; PBS, phosphate-buffered saline; PE, post-exposure; Q1, first quartile; Q3, third quartile; Rep, repetition number; SEM, standard error of the mean; TNFα, tumor necrosis factor alpha; UCLM, upper confidence limit of the mean; Untr, untreated. Nicotine concentrations in 3R4F cigarette smoke or THS2.2 aerosols are indicated for each group (mg/L).

13.1.6.5 **Supplementary Table 17**. Descriptive Statistics: IL1B Protein in the Basolateral Media.

		Exposure		Descriptive Statistics								
E [h]	PE [h]	Rep	Dose	N	M	SEM	Q1	Median	Q3	LCLM	UCLM	Skew
0:00	0:00	1	Untr	1	1.84	.	1.84	1.84	1.84	.	.	.
			PBS	2	1.78	1.38	0.40	1.78	3.15	−15.72	19.27	.
0:28	24:00	1	3R4F (Air)	9	2.12	0.78	0.67	1.35	2.02	0.33	3.92	2.14
			3R4F (49.4)	9	2.69	0.52	1.51	2.74	4.22	1.49	3.89	−0.20
			3R4F (84.6)	9	2.11	0.46	1.12	1.79	3.24	1.05	3.18	0.62
			THS2.2 (Air)	9	1.00	0.21	0.40	0.96	1.20	0.51	1.48	1.04
			THS2.2 (14.4)	9	0.70	0.18	0.40	0.40	0.72	0.29	1.10	2.46
			THS2.2 (54.6)	9	1.04	0.23	0.40	1.10	1.29	0.51	1.57	0.55
			THS2.2 (100.4)	9	1.48	0.25	1.12	1.66	1.75	0.90	2.05	−0.21
		2	3R4F (Air)	9	1.80	0.48	0.40	1.85	2.65	0.69	2.90	0.59
			3R4F (49.4)	9	2.64	0.82	0.40	2.22	4.81	0.74	4.53	0.62
			3R4F (84.6)	9	2.31	0.54	0.40	2.57	3.36	1.05	3.56	−0.11
			THS2.2 (Air)	9	1.41	0.28	0.73	1.39	2.02	0.77	2.04	0.53
			THS2.2 (14.4)	9	1.92	0.36	1.43	1.99	2.62	1.08	2.75	−0.13
			THS2.2 (54.6)	9	1.10	0.25	0.40	1.01	1.46	0.54	1.67	0.70
			THS2.2 (100.4)	9	1.05	0.19	0.40	0.96	1.37	0.60	1.49	0.26
		3	3R4F (Air)	9	1.77	0.30	1.17	1.45	2.13	1.07	2.46	1.43
			3R4F (49.4)	9	1.69	0.26	1.04	2.06	2.20	1.08	2.29	−0.10
			3R4F (84.6)	9	2.43	0.51	1.62	2.36	3.62	1.25	3.62	0.29
			THS2.2 (Air)	9	1.48	0.41	0.40	0.63	2.40	0.54	2.42	0.54
			THS2.2 (14.4)	9	1.96	0.42	0.88	2.23	3.02	0.99	2.94	−0.11
			THS2.2 (54.6)	9	1.55	0.46	0.40	1.01	1.99	0.48	2.62	0.91
			THS2.2 (100.4)	9	1.09	0.27	0.40	0.70	1.71	0.46	1.72	0.72
		123	3R4F (Air)	9	5.69	0.86	4.21	4.76	6.19	3.70	7.67	0.68
			3R4F (49.4)	9	7.01	1.33	2.92	7.40	9.94	3.95	10.08	0.28
			3R4F (84.6)	9	6.85	1.00	4.58	6.07	9.66	4.54	9.17	0.35
			THS2.2 (Air)	9	3.88	0.59	2.42	3.82	4.41	2.51	5.25	0.50
			THS2.2 (14.4)	9	4.58	0.55	3.34	3.86	5.92	3.30	5.85	0.14
			THS2.2 (54.6)	9	3.69	0.75	2.09	2.52	4.49	1.95	5.42	0.90
			THS2.2 (100.4)	9	3.61	0.38	2.83	4.16	4.39	2.73	4.49	−0.79
24:00	0:00	1	TNFα+ILß	3	32,972.84	5,412.42	22,477.80	35,923.95	40,516.77	9,685.07	56,260.61	−1.28

Abbreviations: 123, cumulative data from three repetitions; E, exposure; h, hours; IL, interleukin; LCLM, lower confidence limit of the mean; M, mean; N, number of replicates; PBS, phosphate-buffered saline; PE, post-exposure; Q1, first quartile; Q3, third quartile; Rep, repetition number; SEM, standard error of the mean; TNFα, tumor necrosis factor alpha; UCLM, upper confidence limit of the mean; Untr, untreated. Nicotine concentrations in 3R4F cigarette smoke or THS2.2 aerosols are indicated for each group (mg/L).

13.1.6.6 **Supplementary Table 18**. Descriptive Statistics: IL6 Protein in the Basolateral Media.

		Exposure		Descriptive Statistics								
E [h]	PE [h]	Rep	Dose	N	M	SEM	Q1	Median	Q3	LCLM	UCLM	Skew
0:00	0:00	1	Untr	1	3.41	.	3.41	3.41	3.41	.	.	.
			PBS	2	6.28	4.19	2.09	6.28	10.48	−47.02	59.58	.
0:28	24:00	1	3R4F (Air)	9	6.45	0.67	4.55	6.64	7.37	4.90	8.00	0.50
			3R4F (49.4)	9	3.78	0.72	2.38	3.67	4.04	2.12	5.45	1.20
			3R4F (84.6)	9	3.81	1.02	1.57	3.07	4.21	1.47	6.16	1.34
			THS2.2 (Air)	9	4.37	0.91	2.60	3.24	6.78	2.28	6.46	1.00
			THS2.2 (14.4)	9	5.27	0.94	4.53	5.37	7.00	3.09	7.44	−0.56
			THS2.2 (54.6)	9	4.22	0.60	3.71	3.95	4.87	2.84	5.59	−0.26
			THS2.2 (100.4)	9	4.06	0.68	2.20	4.45	5.51	2.49	5.64	0.13
		2	3R4F (Air)	9	2.11	0.33	1.46	2.26	2.63	1.34	2.87	−0.01
			3R4F (49.4)	9	1.11	0.28	0.45	0.71	1.34	0.47	1.75	1.15
			3R4F (84.6)	9	0.98	0.53	0.45	0.45	0.45	−0.24	2.20	3.00
			THS2.2 (Air)	9	3.06	0.76	1.56	2.68	3.18	1.32	4.81	1.98
			THS2.2 (14.4)	9	2.68	0.46	1.79	2.54	2.97	1.62	3.74	0.71
			THS2.2 (54.6)	9	1.99	0.15	1.70	1.95	2.07	1.65	2.34	0.59
			THS2.2 (100.4)	9	1.58	0.28	1.09	1.66	1.87	0.94	2.22	1.15
		3	3R4F (Air)	9	3.82	0.59	3.61	4.04	4.54	2.47	5.17	−0.14
			3R4F (49.4)	9	2.05	0.16	1.83	1.85	1.91	1.68	2.43	1.61
			3R4F (84.6)	9	1.94	0.41	0.80	2.23	2.58	0.99	2.88	0.32
			THS2.2 (Air)	9	4.72	1.10	3.14	3.69	6.18	2.18	7.25	1.06
			THS2.2 (14.4)	9	3.33	0.53	2.08	2.98	4.35	2.12	4.55	0.33
			THS2.2 (54.6)	9	3.29	0.65	2.39	2.61	4.73	1.79	4.80	0.33
			THS2.2 (100.4)	9	3.40	0.67	1.83	2.17	5.23	1.85	4.94	0.34
		123	3R4F (Air)	9	12.38	1.26	9.63	12.64	15.32	9.48	15.28	−0.19
			3R4F (49.4)	9	6.94	0.95	4.56	6.33	8.71	4.74	9.14	1.31
			3R4F (84.6)	9	6.73	1.68	4.32	4.84	5.11	2.85	10.61	2.49
			THS2.2 (Air)	9	12.15	2.58	8.58	9.33	13.87	6.19	18.11	1.59
			THS2.2 (14.4)	9	11.28	1.64	9.13	9.89	12.69	7.50	15.06	0.72
			THS2.2 (54.6)	9	9.51	1.14	7.43	9.19	11.63	6.88	12.14	0.38
			THS2.2 (100.4)	9	9.04	1.17	6.08	7.71	10.87	6.35	11.73	0.87
24:00	0:00	1	TNFα+ILß	3	23.15	0.93	21.62	23.01	24.82	19.16	27.14	0.38

Abbreviations: 123, cumulative data from three repetitions; E, exposure; h, hours; IL, interleukin; LCLM, lower confidence limit of the mean; M, mean; N, number of replicates; PBS, phosphate-buffered saline; PE, post-exposure; Q1, first quartile; Q3, third quartile; Rep, repetition number; SEM, standard error of the mean; TNFα, tumor necrosis factor alpha; UCLM, upper confidence limit of the mean; Untr, untreated. Nicotine concentrations in 3R4F cigarette smoke or THS2.2 aerosols are indicated for each group (mg/L).

13.1.6.7 **Supplementary Table 19**. Descriptive Statistics: CXCL8 Protein in the Basolateral Media.

Exposure				Descriptive Statistics								
E [h]	PE [h]	Rep	Dose	N	M	SEM	Q1	Median	Q3	LCLM	UCLM	Skew
0:00	0:00	1	Untr	1	123.04	.	123.04	123.04	123.04	.	.	.
			PBS	2	176.24	96.84	79.40	176.24	273.07	−1,054.22	1,406.69	.
0:28	24:00	1	3R4F (Air)	9	153.74	11.40	131.62	157.44	167.18	127.46	180.02	0.54
			3R4F (49.4)	9	142.77	9.42	125.39	149.24	168.31	121.06	164.49	−0.56
			3R4F (84.6)	9	147.35	11.92	124.82	142.76	170.08	119.87	174.83	0.47
			THS2.2 (Air)	9	147.47	24.56	80.13	160.89	196.48	90.83	204.11	0.39
			THS2.2 (14.4)	9	118.22	18.09	61.16	125.58	143.16	76.51	159.93	0.16
			THS2.2 (54.6)	9	109.63	15.05	64.33	116.80	137.52	74.94	144.33	0.05
			THS2.2 (100.4)	9	119.58	18.89	71.24	104.50	151.81	76.01	163.15	0.69
		2	3R4F (Air)	9	77.48	11.20	41.93	91.61	96.15	51.65	103.31	−0.53
			3R4F (49.4)	9	90.63	14.57	38.52	104.54	131.68	57.03	124.23	−0.48
			3R4F (84.6)	9	92.01	13.49	49.23	96.12	122.33	60.90	123.12	−0.31
			THS2.2 (Air)	9	97.73	9.42	76.38	99.15	116.17	76.00	119.45	−0.21
			THS2.2 (14.4)	9	98.61	10.08	85.18	91.15	104.97	75.36	121.87	1.12
			THS2.2 (54.6)	9	84.93	5.30	73.03	86.04	96.44	72.72	97.14	−0.06
			THS2.2 (100.4)	9	97.17	6.90	87.53	101.19	104.04	81.25	113.09	0.03
		3	3R4F (Air)	9	92.71	8.84	74.22	90.14	102.93	72.32	113.09	0.27
			3R4F (49.4)	9	377.96	32.20	298.43	377.24	463.85	303.71	452.22	−0.18
			3R4F (84.6)	9	380.38	61.11	164.02	446.05	491.93	239.46	521.31	−0.47
			THS2.2 (Air)	9	125.77	16.34	83.87	125.31	147.61	88.07	163.46	0.65
			THS2.2 (14.4)	9	119.99	16.66	96.29	103.76	131.39	81.58	158.40	1.67
			THS2.2 (54.6)	9	118.14	10.16	97.35	123.63	134.11	94.70	141.57	0.47
			THS2.2 (100.4)	9	150.29	11.72	125.07	150.50	173.32	123.27	177.31	−0.29
		123	3R4F (Air)	9	323.93	28.00	277.61	327.55	367.16	259.37	388.50	−0.39
			3R4F (49.4)	9	611.36	48.32	508.95	611.89	742.49	499.94	722.79	−0.31
			3R4F (84.6)	9	619.74	79.77	373.94	731.14	764.44	435.80	803.69	−0.32
			THS2.2 (Air)	9	370.96	43.88	244.30	401.86	477.30	269.78	472.14	−0.10
			THS2.2 (14.4)	9	336.82	38.91	242.63	346.22	419.61	247.10	426.54	0.23
			THS2.2 (54.6)	9	312.70	27.42	230.26	338.51	356.98	249.46	375.94	−0.38
			THS2.2 (100.4)	9	367.04	32.67	313.05	377.87	403.50	291.69	442.39	0.24
24:00	0:00	1	TNFα+ILß	3	940.72	30.40	889.93	937.15	995.07	809.91	1071.53	0.30

Abbreviations: 123, cumulative data from three repetitions; CXCL, chemokine (C-X-C motif) ligand; E, exposure; h, hours; IL, interleukin; LCLM, lower confidence limit of the mean; M, mean; N, number of replicates; PBS, phosphate-buffered saline; PE, post-exposure; Q1, first quartile; Q3, third quartile; Rep, repetition number; SEM, standard error of the mean; TNFα, tumor necrosis factor alpha; UCLM, upper confidence limit of the mean; Untr, untreated. Nicotine concentrations in 3R4F cigarette smoke or THS2.2 aerosols are indicated for each group (mg/L).

13.1.6.8 **Supplementary Table 20**. Descriptive Statistics: CXCL10 Protein in the Basolateral Media.

Exposure				Descriptive Statistics								
E [h]	PE [h]	Rep	Dose	N	M	SEM	Q1	Median	Q3	LCLM	UCLM	Skew
0:00	0:00	1	Untr	1	27.02	.	27.02	27.02	27.02	.	.	.
			PBS	2	30.57	15.96	14.61	30.57	46.52	−172.17	233.30	.
0:28	24:00	1	3R4F (Air)	9	34.63	3.10	30.49	32.57	39.13	27.48	41.78	−0.27
			3R4F (49.4)	9	39.65	4.09	29.03	42.20	45.69	30.21	49.09	−0.38
			3R4F (84.6)	9	42.16	6.20	29.15	40.07	56.74	27.86	56.45	−0.32
			THS2.2 (Air)	9	39.31	7.69	11.16	43.50	55.30	21.58	57.05	−0.43
			THS2.2 (14.4)	9	34.75	6.31	17.32	40.32	48.13	20.20	49.30	0.00
			THS2.2 (54.6)	9	32.98	6.67	11.06	37.07	50.77	17.60	48.36	−0.16
			THS2.2 (100.4)	9	33.28	7.47	8.87	49.66	50.65	16.06	50.51	−0.37
		2	3R4F (Air)	9	20.47	3.15	13.04	20.83	27.95	13.20	27.75	−0.49
			3R4F (49.4)	9	23.20	5.34	8.45	14.93	39.63	10.89	35.52	0.32
			3R4F (84.6)	9	21.42	6.36	6.58	20.67	23.98	6.76	36.08	1.66
			THS2.2 (Air)	9	29.10	5.81	13.08	34.65	43.83	15.69	42.50	−0.61
			THS2.2 (14.4)	9	27.38	6.24	10.20	30.88	41.24	12.98	41.77	−0.04
			THS2.2 (54.6)	9	22.86	5.38	4.30	28.80	35.51	10.44	35.28	−0.20
			THS2.2 (100.4)	9	28.46	7.20	4.30	36.70	45.38	11.85	45.07	−0.12
		3	3R4F (Air)	9	12.76	2.10	7.00	12.03	19.76	7.93	17.60	0.19
			3R4F (49.4)	9	18.26	3.34	10.58	19.17	24.44	10.56	25.96	0.31
			3R4F (84.6)	9	24.23	6.71	4.30	23.62	28.11	8.75	39.71	0.94
			THS2.2 (Air)	9	21.14	4.44	13.29	20.28	30.09	10.90	31.39	0.14
			THS2.2 (14.4)	9	22.40	3.03	15.78	22.97	26.64	15.42	29.39	0.31
			THS2.2 (54.6)	9	19.88	4.50	6.65	24.43	30.45	9.51	30.26	−0.12
			THS2.2 (100.4)	9	23.98	5.03	6.78	32.06	35.69	12.39	35.57	−0.50
		123	3R4F (Air)	9	67.87	6.82	55.17	71.08	77.25	52.14	83.60	−0.33
			3R4F (49.4)	9	81.12	10.03	50.83	91.75	103.71	57.98	104.25	−0.32
			3R4F (84.6)	9	87.81	17.74	37.75	98.19	110.96	46.90	128.72	0.68
			THS2.2 (Air)	9	89.56	15.96	54.33	102.35	124.02	52.74	126.37	−0.64
			THS2.2 (14.4)	9	84.53	14.73	36.86	104.53	119.29	50.57	118.49	−0.23
			THS2.2 (54.6)	9	75.72	16.23	22.79	96.33	121.59	38.30	113.14	−0.24
			THS2.2 (100.4)	9	85.73	19.17	32.90	124.67	134.89	41.52	129.94	−0.31
24:00	0:00	1	TNFα+ILß	3	1,860.93	601.27	1,232.72	1,287.02	3,063.06	−726.12	4,447.98	1.73

Abbreviations: 123, cumulative data from three repetitions; CXCL, chemokine (C-X-C motif) ligand; E, exposure; h, hours; IL, interleukin; LCLM, lower confidence limit of the mean; M, mean; N, number of replicates; PBS, phosphate-buffered saline; PE, post-exposure; Q1, first quartile; Q3, third quartile; Rep, repetition number; SEM, standard error of the mean; TNFα, tumor necrosis factor alpha; UCLM, upper confidence limit of the mean; Untr, untreated. Nicotine concentrations in 3R4F cigarette smoke or THS2.2 aerosols are indicated for each group (mg/L).

13.1.6.9 **Supplementary Table 21**. Descriptive Statistics: MMP-1 Protein in the Basolateral Media.

		Exposure		Descriptive Statistics								
E [h]	PE [h]	Rep	Dose	N	M	SEM	Q1	Median	Q3	LCLM	UCLM	Skew
0:00	0:00	1	Untr	1	10,660.55	.	10,660.55	10,660.55	10,660.55	.	.	.
			PBS	2	25,931.15	8,766.74	17,164.41	25,931.15	34,697.89	−85,460.8	137,323.2	.

Table continues

		Exposure		Descriptive Statistics								
E [h]	PE [h]	Rep	Dose	N	M	SEM	Q1	Median	Q3	LCLM	UCLM	Skew
0:28	24:00	1	3R4F (Air)	9	30,095.34	2,489.78	24,635.62	33,524.18	36,721.09	24,353.90	35,836.78	−0.63
			3R4F (49.4)	9	45,914.35	3,274.89	40,073.23	43,075.65	50,800.54	38,362.44	53,466.26	0.43
			3R4F (84.6)	9	46,339.93	3,583.70	42,186.99	44,967.06	52,081.05	38,075.90	54,603.96	−0.16
			THS2.2 (Air)	9	27,852.11	32,16.01	18,171.41	28,231.65	36,660.11	20,435.98	35,268.24	−0.02
			THS2.2 (14.4)	9	28,478.68	2,678.26	28,047.96	30,766.94	31,204.99	22,302.61	34,654.74	-0.72
			THS2.2 (54.6)	9	33,409.18	2,428.69	32,136.58	33,525.41	37,774.81	27,808.62	39,009.74	−1.34
			THS2.2 (100.4)	9	37,686.19	2,862.42	31,971.69	33,854.21	43,560.79	31,085.44	44,286.94	1.45
		2	3R4F (Air)	9	9,344.46	933.70	7,211.88	10,501.55	11,401.95	7,191.35	11,497.57	−0.39
			3R4F (49.4)	9	19,028.33	3,187.86	12,762.65	14,534.24	29,289.15	11,677.11	26,379.55	0.86
			3R4F (84.6)	9	19,628.45	2,886.51	12,244.30	18,466.39	27,548.30	12,972.14	26,284.76	0.12
			THS2.2 (Air)	9	12,115.21	1,164.49	9,350.24	12,357.62	15,774.66	9,429.90	14,800.52	−0.03
			THS2.2 (14.4)	9	14,586.83	1,898.61	11,085.74	13,654.47	15,417.40	10,208.64	18,965.03	1.60
			THS2.2 (54.6)	9	15,375.08	897.34	14,484.74	16,271.68	17,047.99	13,305.80	17,444.37	−0.74
			THS2.2 (100.4)	9	17,759.22	1,263.22	14,504.89	18,686.76	18,889.47	14,846.23	20,672.20	0.43
		3	3R4F (Air)	9	6,202.14	575.65	4,982.46	6,411.74	7,053.05	4,874.70	7,529.59	0.11
			3R4F (49.4)	9	50,304.42	9,144.68	38,138.04	39,184.70	53,708.25	29,216.75	71,392.09	1.43
			3R4F (84.6)	9	61,285.00	11,410.26	26,107.10	76,469.18	86,635.01	34,972.90	87,597.10	−0.41
			THS2.2 (Air)	9	8,562.51	1,446.16	5,313.17	8,079.56	9,222.90	5,227.65	11,897.37	1.68
			THS2.2 (14.4)	9	11,085.68	1,238.44	7,813.30	9,335.87	15,383.72	8,229.83	13,941.52	0.31
			THS2.2 (54.6)	9	15,024.11	1,967.69	10,053.16	14,170.56	16,762.29	10,486.62	19,561.61	1.33
			THS2.2 (100.4)	9	20,919.06	2,739.06	14,113.38	17,633.43	26,158.20	14,602.77	27,235.35	0.89
		123	3R4F (Air)	9	45,641.94	3,703.26	37,566.02	45,905.19	53,666.14	37,102.21	54,181.68	−0.42

Table continues

Exposure				Descriptive Statistics								
E [h]	PE [h]	Rep	Dose	N	M	SEM	Q1	Median	Q3	LCLM	UCLM	Skew
			3R4F (49.4)	9	115,247.1	9,527.62	95,379.02	113,725.4	129,784.4	93,276.38	137,217.8	0.70
			3R4F (84.6)	9	127,253.4	13,483.16	78,630.07	135,708.3	149,241.7	96,161.15	158,345.6	−0.24
			THS2.2 (Air)	9	48,529.83	5,380.97	32,107.19	46,269.55	61,016.92	36,121.30	60,938.37	0.22
			THS2.2 (14.4)	9	54,151.19	5,244.49	49,784.62	52,569.93	61,750.37	42,057.37	66,245.00	−0.04
			THS2.2 (54.6)	9	63,808.38	4,302.90	57,911.76	65,315.18	73,933.59	53,885.87	73,730.88	−1.00
			THS2.2 (100.4)	9	76,364.46	4,867.14	65,696.17	74,712.34	83,226.38	65,140.81	87,588.12	0.74
24:00	0:00	1	TNFα+ILß	3	25,401.39	6,277.58	13,675.64	27,377.87	35,150.66	−1,608.86	52,411.64	−0.79

End of the Table

Abbreviations: 123, cumulative data from three repetitions; E, exposure; h, hours; IL, interleukin; LCLM, lower confidence limit of the mean; M, mean; MMP-1, matrix metalloproteinase 1; N, number of replicates; PBS, phosphate-buffered saline; PE, post-exposure; Q1, first quartile; Q3, third quartile; Rep, repetition number; SEM, standard error of the mean; TNFα, tumor necrosis factor alpha; UCLM, upper confidence limit of the mean; Untr, untreated. Nicotine concentrations in 3R4F cigarette smoke or THS2.2 aerosols are indicated for each group (mg/L).

13.1.6.10 **Supplementary Table 22**. Descriptive Statistics: TNFα Protein in the Basolateral Media.

Exposure				Descriptive Statistics								
E [h]	PE [h]	Rep	Dose	N	M	SEM	Q1	Median	Q3	LCLM	UCLM	Skew
0:00	0:00	1	Untr	1	2.38	.	2.38	2.38	2.38	.	.	.
			PBS	2	3.45	2.50	0.95	3.45	5.94	−28.29	35.18	.
0:28	24:00	1	3R4F (Air)	9	2.58	0.24	2.50	2.54	3.19	2.02	3.14	−0.82
			3R4F (49.4)	9	2.18	0.40	1.53	1.79	2.24	1.25	3.10	1.99
			3R4F (84.6)	9	2.59	0.71	1.30	1.98	3.66	0.96	4.22	1.08
			THS2.2 (Air)	9	2.35	0.39	1.33	2.05	3.40	1.45	3.26	0.30
			THS2.2 (14.4)	9	1.84	0.25	1.15	2.05	2.27	1.27	2.42	−0.50
			THS2.2 (54.6)	9	1.85	0.28	1.08	1.89	2.59	1.20	2.50	0.40
			THS2.2 (100.4)	9	1.97	0.31	1.07	2.06	2.62	1.26	2.68	−0.06
		2	3R4F (Air)	9	1.37	0.25	1.00	1.15	1.67	0.79	1.94	1.54
			3R4F (49.4)	9	1.37	0.35	0.58	1.18	1.53	0.56	2.17	1.79
			3R4F (84.6)	9	1.04	0.39	0.35	0.55	0.87	0.15	1.94	1.93
			THS2.2 (Air)	9	1.78	0.34	0.89	1.88	2.43	0.99	2.58	0.01
			THS2.2 (14.4)	9	1.54	0.41	0.85	1.23	1.81	0.59	2.49	1.19
			THS2.2 (54.6)	9	1.22	0.23	0.60	1.26	1.82	0.69	1.75	0.26
			THS2.2 (100.4)	9	1.51	0.21	1.07	1.57	1.92	1.02	2.00	−0.34
		3	3R4F (Air)	9	1.77	0.43	0.98	1.48	1.71	0.77	2.76	2.37
			3R4F (49.4)	9	11.56	2.67	5.15	10.25	16.47	5.41	17.72	0.52
			3R4F (84.6)	9	7.24	1.70	2.83	6.47	9.61	3.32	11.17	0.82
			THS2.2 (Air)	9	2.15	0.45	1.04	1.87	3.11	1.10	3.20	0.44
			THS2.2 (14.4)	9	1.90	0.37	1.14	1.49	2.76	1.05	2.76	0.26
			THS2.2 (54.6)	9	1.84	0.27	1.24	1.74	2.33	1.22	2.45	0.40
			THS2.2 (100.4)	9	2.05	0.38	1.39	1.77	2.98	1.17	2.94	0.15
		123	3R4F (Air)	9	5.72	0.72	4.50	5.26	5.62	4.05	7.38	2.52
			3R4F (49.4)	9	15.11	3.26	7.43	13.06	21.22	7.59	22.62	0.84
			3R4F (84.6)	9	10.87	2.34	6.14	7.95	16.84	5.47	16.27	0.85
			THS2.2 (Air)	9	6.29	0.82	5.05	6.01	7.55	4.39	8.19	0.04
			THS2.2 (14.4)	9	5.29	0.71	3.06	4.97	7.17	3.66	6.92	0.06
			THS2.2 (54.6)	9	4.91	0.49	3.91	4.78	5.21	3.78	6.03	1.20
			THS2.2 (100.4)	9	5.53	0.70	4.24	4.54	7.99	3.91	7.14	0.38
24:00	0:00	1	TNFα+ILß	3	21,270.66	6,582.69	8,125.86	27,205.85	28,480.28	−7,052.37	49,593.69	−1.71

Abbreviations: 123, cumulative data from three repetitions; E, exposure; h, hours; IL, interleukin; LCLM, lower confidence limit of the mean; M, mean; N, number of replicates; PBS, phosphate-buffered saline; PE, post-exposure; Q1, first quartile; Q3, third quartile; Rep, repetition number; SEM, standard error of the mean; TNFα, tumor necrosis factor alpha; UCLM, upper confidence limit of the mean; Untr, untreated. Nicotine concentrations in 3R4F cigarette smoke or THS2.2 aerosols are indicated for each group (mg/L).

Supplementary Table 23. Descriptive Statistics: VEGFA Protein in the Basolateral Media.

Exposure				Descriptive Statistics								
E [h]	PE [h]	Rep	Dose	N	M	SEM	Q1	Median	Q3	LCLM	UCLM	Skew
0:00	0:00	1	Untr	1	932.49	.	932.49	932.49	932.49	.	.	.
			PBS	2	855.68	37.15	818.53	855.68	892.84	383.62	1,327.74	.
0:28	24:00	1	3R4F (Air)	9	626.09	49.86	528.71	562.49	732.87	511.11	741.08	0.97
			3R4F (49.4)	9	551.11	32.25	487.11	561.36	582.26	476.76	625.47	0.60
			3R4F (84.6)	9	645.36	24.79	623.04	646.23	693.30	588.19	702.53	−0.52
			THS2.2 (Air)	9	814.23	118.61	430.45	893.45	1,132.01	540.71	1,087.75	−0.08
			THS2.2 (14.4)	9	824.25	104.88	506.00	832.57	1,072.32	582.41	1,066.10	0.12
			THS2.2 (54.6)	9	816.22	114.65	529.16	669.78	1,108.34	551.84	1,080.59	0.87
			THS2.2 (100.4)	9	910.79	116.42	586.87	864.08	1,148.45	642.33	1,179.25	0.12
		2	3R4F (Air)	9	404.72	37.85	281.79	416.31	506.73	317.43	492.01	−0.40
			3R4F (49.4)	9	442.92	49.78	282.10	486.99	549.94	328.13	557.71	−0.46
			3R4F (84.6)	9	619.97	67.99	395.02	723.58	756.71	463.17	776.76	−0.82
			THS2.2 (Air)	9	801.98	45.80	737.98	779.36	898.25	696.36	907.60	0.10
			THS2.2 (14.4)	9	929.77	70.84	802.19	932.76	1,023.92	766.42	1,093.12	0.43
			THS2.2 (54.6)	9	873.34	68.17	760.67	859.00	1,105.65	716.15	1,030.53	0.13
			THS2.2 (100.4)	9	1,052.91	62.94	948.89	1,010.95	1,212.87	907.77	1,198.06	−0.26
		3	3R4F (Air)	9	396.64	19.04	356.19	417.98	432.05	352.73	440.55	−0.78
			3R4F (49.4)	9	286.96	23.21	228.69	325.04	328.41	233.45	340.48	−0.41
			3R4F (84.6)	9	205.57	31.03	146.47	220.55	278.80	134.02	277.11	−0.11
			THS2.2 (Air)	9	638.05	50.08	584.11	623.44	693.88	522.55	753.54	0.05
			THS2.2 (14.4)	9	613.56	30.66	584.44	600.47	663.83	542.87	684.26	0.51
			THS2.2 (54.6)	9	516.83	46.55	444.55	538.06	620.95	409.48	624.18	−0.68
			THS2.2 (100.4)	9	542.14	32.30	508.81	520.11	592.97	467.64	616.63	−0.07
		123	3R4F (Air)	9	1,427.45	87.53	1,239.42	1,271.07	1,717.18	1,225.61	1,629.29	0.58
			3R4F (49.4)	9	1,281.00	85.31	1,103.73	1,226.35	1,458.32	1,084.28	1,477.71	−0.38
			3R4F (84.6)	9	1,470.89	68.18	1,336.99	1,538.75	1,595.80	1,313.68	1,628.11	−0.68
			THS2.2 (Air)	9	2,254.26	142.26	1,887.24	2,149.12	2,673.38	1,926.22	2,582.30	0.19
			THS2.2 (14.4)	9	2,367.59	130.67	2,126.89	2,254.17	2,606.81	2,066.27	2,668.91	0.53
			THS2.2 (54.6)	9	2,206.39	148.44	1,974.00	2,216.42	2,531.20	1,864.09	2,548.70	−0.15
			THS2.2 (100.4)	9	2,505.84	135.86	2,158.43	2,367.58	2,796.84	2,192.54	2,819.14	0.78
24:00	0:00	1	TNFα+ILß	3	2,275.72	775.44	1,305.65	1,712.83	3,808.69	−1,060.74	5,612.18	1.55

Abbreviations: 123, cumulative data from three repetitions; E, exposure; h, hours; IL, interleukin; LCLM, lower confidence limit of the mean; M, mean; N, number of replicates; PBS, phosphate-buffered saline; PE, post-exposure; Q1, first quartile; Q3, third quartile; Rep, repetition number; SEM, standard error of the mean; TNFα, tumor necrosis factor alpha; UCLM, upper confidence limit of the mean; Untr, untreated; VEGFA, vascular epithelial growth factor A. Nicotine concentrations in 3R4F cigarette smoke or THS2.2 aerosols are indicated for each group (mg/L).

13.1.6.11 **Supplementary Table 24**. Descriptive Statistics: CCL2 Protein in the Basolateral Media.

Exposure				Descriptive Statistics								
E [h]	PE [h]	Rep	Dose	N	M	SEM	Q1	Median	Q3	LCLM	UCLM	Skew
0:00	0:00	1	Untr	1	0.95	.	0.95	0.95	0.95	.	.	.
			PBS	2	2.37	1.42	0.95	2.37	3.79	−15.67	20.41	.
0:28	24:00	1	3R4F (Air)	9	3.88	0.71	2.31	3.43	4.71	2.26	5.51	0.92
			3R4F (49.4)	9	1.84	0.56	0.95	0.95	2.41	0.55	3.14	2.26
			3R4F (84.6)	9	3.35	0.65	2.43	3.19	3.50	1.86	4.85	1.38
			THS2.2 (Air)	9	4.35	0.79	2.32	4.54	6.80	2.53	6.18	−0.08
			THS2.2 (14.4)	9	3.60	0.59	2.06	4.29	4.64	2.24	4.96	−0.17
			THS2.2 (54.6)	9	2.26	0.62	0.95	1.50	2.87	0.83	3.68	1.66
			THS2.2 (100.4)	9	2.67	0.57	0.95	2.66	3.73	1.36	3.99	0.74
		2	3R4F (Air)	9	2.16	0.79	0.95	0.95	2.26	0.33	3.99	2.37
			3R4F (49.4)	9	2.14	0.57	0.95	1.45	2.75	0.84	3.45	1.82
			3R4F (84.6)	9	2.97	0.90	0.95	1.93	3.28	0.90	5.03	1.88
			THS2.2 (Air)	9	3.12	0.93	0.95	1.50	4.65	0.98	5.25	1.16
			THS2.2 (14.4)	9	2.75	1.06	0.95	0.95	2.68	0.31	5.20	1.96
			THS2.2 (54.6)	9	2.39	1.17	0.95	0.95	0.95	−0.30	5.08	2.73
			THS2.2 (100.4)	9	1.33	0.32	0.95	0.95	0.95	0.60	2.06	2.83
		3	3R4F (Air)	9	4.72	1.40	0.95	4.66	6.80	1.49	7.96	0.70
			3R4F (49.4)	9	4.97	1.89	0.95	3.09	5.02	0.62	9.32	2.19
			3R4F (84.6)	9	5.37	1.05	3.41	5.63	7.44	2.94	7.79	−0.27
			THS2.2 (Air)	9	3.05	0.70	1.46	2.58	4.55	1.44	4.66	0.71
			THS2.2 (14.4)	9	3.40	0.51	2.41	3.86	4.73	2.22	4.57	−0.30
			THS2.2 (54.6)	9	2.48	0.64	0.95	2.01	3.47	1.02	3.95	1.06
			THS2.2 (100.4)	9	3.51	0.73	1.78	3.82	4.89	1.83	5.18	0.17
		123	3R4F (Air)	9	10.77	2.36	6.01	10.79	14.18	5.33	16.20	1.28
			3R4F (49.4)	9	8.96	2.01	4.99	7.99	10.27	4.33	13.59	1.69
			3R4F (84.6)	9	11.69	1.55	9.04	12.82	15.39	8.12	15.25	−0.47
			THS2.2 (Air)	9	10.52	1.75	7.25	10.04	13.40	6.50	14.55	0.40
			THS2.2 (14.4)	9	9.75	1.66	6.19	9.70	10.32	5.93	13.57	0.85
			THS2.2 (54.6)	9	7.13	1.50	4.05	5.70	8.96	3.68	10.58	1.58
			THS2.2 (100.4)	9	7.51	0.95	6.13	6.71	8.64	5.32	9.69	0.29
24:00	0:00	1	TNFα+ILß	3	253.97	56.14	161.84	244.47	355.62	12.43	495.52	0.44

Abbreviations: 123, cumulative data from three repetitions; CCL, chemokine (C-C motif) ligand; E, exposure; h, hours; IL, interleukin; LCLM, lower confidence limit of the mean; M, mean; N, number of replicates; PBS, phosphate-buffered saline; PE, post-exposure; Q1, first quartile; Q3, third quartile; Rep, repetition number; SEM, standard error of the mean; TNFα, tumor necrosis factor alpha; UCLM, upper confidence limit of the mean; Untr, untreated. Nicotine concentrations in 3R4F cigarette smoke or THS2.2 aerosols are indicated for each group (mg/L).

13.1.6.12 **Supplementary Table 25**. Descriptive Statistics: CCL5 Protein in the Basolateral Media.

Exposure				Descriptive Statistics								
E[h]	PE[h]	Rep	Dose	N	M	SEM	Q1	Median	Q3	LCLM	UCLM	Skew
0:00	0:00	1	Untr	1	23.95	.	23.95	23.95	23.95	.	.	.
			PBS	2	42.28	20.82	21.47	42.28	63.10	-222.20	306.77	.
0:28	24:00	1	3R4F (Air)	9	37.29	3.57	31.60	32.75	45.92	29.04	45.53	0.80
			3R4F (49.4)	9	31.16	3.25	26.94	30.50	32.17	23.66	38.66	−0.12
			3R4F (84.6)	9	26.41	4.91	17.78	24.69	32.56	15.09	37.73	0.69
			THS2.2 (Air)	9	34.69	4.36	23.40	33.36	37.30	24.64	44.75	0.82
			THS2.2 (14.4)	9	29.74	2.59	23.77	32.65	33.62	23.76	35.71	−0.50
			THS2.2 (54.6)	9	20.92	2.77	15.85	20.69	28.90	14.53	27.31	−0.40
			THS2.2 (100.4)	9	26.73	2.80	19.68	26.62	32.99	20.28	33.19	0.29
		2	3R4F (Air)	9	33.16	5.62	20.14	29.11	44.91	20.20	46.12	0.59
			3R4F (49.4)	9	14.15	3.46	5.47	14.25	16.73	6.17	22.13	0.36
			3R4F (84.6)	9	11.04	3.57	3.53	6.65	13.87	2.79	19.28	1.32
			THS2.2 (Air)	9	41.95	3.27	36.67	39.57	49.33	34.41	49.49	0.05
			THS2.2 (14.4)	9	27.83	1.56	24.09	26.73	32.00	24.23	31.44	0.07
			THS2.2 (54.6)	9	21.21	1.32	18.81	21.02	22.36	18.17	24.25	0.62
			THS2.2 (100.4)	9	23.79	2.03	21.29	22.65	29.49	19.10	28.48	0.03
		3	3R4F (Air)	9	33.18	2.50	27.35	31.38	35.68	27.41	38.94	0.73
			3R4F (49.4)	9	18.13	2.66	12.34	14.98	26.41	12.01	24.25	0.55
			3R4F (84.6)	9	16.51	3.72	8.81	12.05	22.55	7.92	25.09	1.04
			THS2.2 (Air)	9	39.65	2.88	37.02	38.10	41.48	33.02	46.28	0.37
			THS2.2 (14.4)	9	31.44	3.44	24.78	28.51	41.13	23.50	39.38	0.16
			THS2.2 (54.6)	9	20.21	2.42	18.58	19.93	20.72	14.63	25.80	−0.32
			THS2.2 (100.4)	9	26.46	2.82	18.88	28.72	32.28	19.96	32.97	−0.20
		123	3R4F (Air)	9	103.63	10.52	79.15	98.96	108.00	79.36	127.90	0.91
			3R4F (49.4)	9	63.44	8.89	41.37	61.22	74.92	42.94	83.94	0.48
			3R4F (84.6)	9	53.95	11.23	29.40	40.27	77.90	28.06	79.84	1.00
			THS2.2 (Air)	9	116.29	8.64	95.36	114.13	127.18	96.37	136.21	0.59
			THS2.2 (14.4)	9	89.01	5.69	75.89	89.75	93.43	75.88	102.14	0.37
			THS2.2 (54.6)	9	62.34	5.29	51.58	62.86	73.77	50.13	74.55	−0.25
			THS2.2 (100.4)	9	76.99	6.15	65.00	70.29	91.78	62.81	91.17	0.45
24:00	0:00	1	TNFα+ILß	3	749.90	241.61	286.34	863.54	1,099.82	−289.65	1,789.46	−1.13

Abbreviations: 123, cumulative data from three repetitions; CCL, chemokine (C-C motif) ligand; E, exposure; h, hours; IL, interleukin; LCLM, lower confidence limit of the mean; M, mean; N, number of replicates; PBS, phosphate-buffered saline; PE, post-exposure; Q1, first quartile; Q3, third quartile; Rep, repetition number; SEM, standard error of the mean; TNFα, tumor necrosis factor alpha; UCLM, upper confidence limit of the mean; Untr, untreated. Nicotine concentrations in 3R4F cigarette smoke or THS2.2 aerosols are indicated for each group (mg/L).

Supplementary Table 26. Descriptive Statistics: MMP-9 Protein in the Basolateral Media.

		Exposure		Descriptive Statistics								
E [h]	PE [h]	Rep	Dose	N	M	SEM	Q1	Median	Q3	LCLM	UCLM	Skew
0:00	0:00	1	Untr	1	15,659.61	.	15,659.61	15,659.61	15,659.61	.	.	.
			PBS	2	11,340.36	1,241.90	10,098.47	11,340.36	12,582.26	-4,439.44	27,120.17	.

Table continues

		Exposure		Descriptive Statistics								
E [h]	PE [h]	Rep	Dose	N	M	SEM	Q1	Median	Q3	LCLM	UCLM	Skew
0:28	24:00	1	3R4F (Air)	9	15,580.43	1,697.76	10,677.72	16,927.94	18,200.57	11,665.39	19,495.48	−0.32
			3R4F (49.4)	9	13,029.52	975.48	10,223.19	12,984.83	15,055.68	10,780.07	15,278.98	0.16
			3R4F (84.6)	9	13,061.10	1,083.88	10,205.87	14,142.56	15,508.10	10,561.67	15,560.54	−0.07
			THS2.2 (Air)	9	15,608.77	1,476.75	13,403.20	16,269.87	18,098.08	12,203.36	19,014.17	−0.33
			THS2.2 (14.4)	9	64,833.75	51,445.98	10,690.66	14,976.00	16,310.17	−53,800.9	183,468.4	3.00
			THS2.2 (54.6)	9	13,340.86	1,422.90	10,690.08	12,560.28	16,775.97	10,059.64	16,622.07	−0.09
			THS2.2 (100.4)	9	14,758.03	1,296.67	12,519.99	15,155.22	17,880.47	11,767.89	17,748.16	−0.56
		2	3R4F (Air)	9	9,452.00	943.52	7,212.18	8,956.82	10,944.61	7,276.25	11,627.76	0.55
			3R4F (49.4)	9	6,146.75	705.19	5,846.68	6,177.09	6,624.53	4,520.57	7,772.92	−0.06
			3R4F (84.6)	9	4,574.30	491.61	3,377.31	4,078.37	5,747.29	3,440.65	5,707.96	0.83
			THS2.2 (Air)	9	11,660.67	869.54	10,939.96	12,584.29	13,737.94	9,655.50	13,665.84	−1.03
			THS2.2 (14.4)	9	10,637.68	908.19	8,900.65	11,537.50	11,860.75	8,543.39	12,731.98	0.38
			THS2.2 (54.6)	9	9,748.42	1,007.74	7,497.59	10,678.17	10,979.80	7,424.56	12,072.28	0.77
			THS2.2 (100.4)	9	10,155.03	808.17	8,213.25	9,867.46	11,693.61	8,291.38	12,018.68	−0.20
		3	3R4F (Air)	9	5,647.51	240.83	5,225.02	5,411.32	6,283.62	5,092.14	6,202.87	−0.16
			3R4F (49.4)	9	2,718.05	299.15	1,934.91	2,634.82	3,356.59	2,028.22	3,407.88	0.44
			3R4F (84.6)	9	2,636.83	283.40	2,251.08	2,367.91	2,764.56	1,983.31	3,290.35	1.33
			THS2.2 (Air)	9	8,125.07	1,155.89	6,498.75	6,931.77	10,472.12	5,459.58	10,790.57	0.43
			THS2.2 (14.4)	9	7,775.50	661.16	6,492.24	6,852.17	9,216.19	6,250.86	9,300.15	0.92
			THS2.2 (54.6)	9	6,356.88	755.09	4,787.93	5,931.96	6,980.98	4,615.64	8,098.11	1.67
			THS2.2 (100.4)	9	6,248.48	662.29	4,875.95	6,654.80	7,494.84	4,721.23	7,775.73	−0.23
		123	3R4F (Air)	9	30,679.94	2,091.74	26,986.06	28,281.92	35,599.75	25,856.38	35,503.50	0.01
			3R4F (49.4)	9	21,894.32	1,722.13	18,951.66	21,466.34	25,225.94	17,923.08	25,865.55	0.53

Table continues

		Exposure		Descriptive Statistics								
E [h]	PE [h]	Rep	Dose	N	M	SEM	Q1	Median	Q3	LCLM	UCLM	Skew
			3R4F (84.6)	9	20,272.23	1,157.74	18,986.21	20,255.43	22,814.70	17,602.48	22,941.99	−0.46
			THS2.2 (Air)	9	35,394.51	2,874.38	30,350.94	37,508.42	42,332.74	28,766.17	42,022.84	−0.91
			THS2.2 (14.4)	9	83,246.94	52,273.55	26,576.32	34,646.45	37,451.80	−37,296.1	203,790.0	2.99
			THS2.2 (54.6)	9	29,446.16	2,937.54	21,717.90	30,170.46	32,672.44	22,672.17	36,220.14	0.58
			THS2.2 (100.4)	9	31,161.54	2,531.93	26,968.79	31,947.29	35,404.52	25,322.89	37,000.19	−0.68
24:00	0:00	1	TNFα+ILß	3	39,614.86	16,420.87	19,702.47	26,953.42	72,188.70	−31,038.5	110,268.2	1.61

End of the Table

Abbreviations: 123, cumulative data from three repetitions; E, exposure; h, hours; IL, interleukin; LCLM, lower confidence limit of the mean; M, mean; MMP-9, Matrix metalloproteinase 9; N, number of replicates; PBS, phosphate-buffered saline; PE, post-exposure; Q1, first quartile; Q3, third quartile; Rep, repetition number; SEM, standard error of the mean; TNFα, tumor necrosis factor alpha; UCLM, upper confidence limit of the mean; Untr, untreated. Nicotine concentrations in 3R4F cigarette smoke or THS2.2 aerosols are indicated for each group (mg/L).

13.1.7 **Supplementary Table 27**. Canonical pathways affected by differentially expressed miRNA-mRNA pairs.

Canonical Pathway	*p*-value (3R4F)	# Molecules (3R4F)	*p*-value (THS2.2)	# Molecules (THS2.2)	Total # molecules in IPA database
Actin Cytoskeleton Signaling	1.82E-06	10	1.70E-04	6	221
AMPK Signaling	3.86E-06	9	7.00E-05	6	188
Protein Kinase A Signaling	5.60E-06	12	2.57E-03	6	372
IL-8 Signaling	4.28E-05	8	6.12E-03	4	196
TR/RXR Activation	4.33E-05	6	4.86E-04	4	98
Integrin Signaling	7.21E-05	8	1.32E-04	6	211
Glucocorticoid Receptor Signaling	9.54E-05	9	2.09E-02	4	282
G Protein-Coupled Receptor Signaling	3.43E-04	8	1.70E-02	4	265
Regulation of eIF4 and p70S6K Signaling	4.63E-04	6	2.46E-04	5	151
IGF-1 Signaling	6.18E-04	5	7.05E-03	3	105
UVB-Induced MAPK Signaling	8.52E-04	4	1.82E-03	3	65
HGF Signaling	8.97E-04	5	8.59E-04	4	114
NF-κB Signaling	9.46E-04	6	1.36E-01	2	173
Rac Signaling	9.70E-04	5	9.26E-03	3	116
EIF2 Signaling	1.19E-03	6	5.65E-04	5	181
Antiproliferative Role of Somatostatin Receptor 2	1.25E-03	4	2.36E-01	1	72
Protein Ubiquitination Pathway	1.29E-03	7	6.70E-02	3	251
RAR Activation	1.41E-03	6	5.19E-03	4	187
CD40 Signaling	1.60E-03	4	2.50E-01	1	77
mTOR Signaling	1.66E-03	6	7.56E-04	5	193
IL-3 Signaling	2.11E-03	4	3.66E-03	3	83
cAMP-mediated signaling	2.78E-03	6	1.89E-01	2	214
FGF Signaling	2.84E-03	4	4.59E-03	3	90
Melanocyte Development and Pigmentation Signaling	3.45E-03	4	5.34E-03	3	95
Cell Cycle: G_2/M DNA Damage Checkpoint Regulation	3.99E-03	3	8.03E-04	3	49
SAPK/JNK Signaling	4.00E-03	4	5.99E-03	3	99
VEGF Signaling	4.15E-03	4	5.35E-02	2	100
CXCR4 Signaling	4.40E-03	5	2.33E-02	3	164
RAN Signaling	4.76E-03	2	5.80E-02	1	16
Signaling by Rho Family GTPases	5.27E-03	6	6.00E-01	1	244
p53 Signaling	6.00E-03	4	8.21E-03	3	111
p38 MAPK Signaling	6.19E-03	4	4.00E+01	4	112
Glutamate Removal from Folates	6.52E-03	1	3.72E-03	1	1
ATM Signaling	6.72E-03	3	2.04E-02	2	59
Xenobiotic Metabolism Signaling	7.26E-03	6	2.86E-03	5	261
ERK5 Signaling	7.37E-03	3	2.17E-02	2	61
NRF2-mediated Oxidative Stress Response	7.76E-03	5	5.29E-03	4	188
ILK Signaling	8.46E-03	5	5.69E-03	4	192
p70S6K Signaling	1.04E-02	4	1.26E-02	3	130

Table continues

Myc-Mediated Apoptosis Signaling	1.07E-02	3	2.80E-02	2	70
STAT3 Pathway	1.20E-02	3	2.54E-03	3	73
Insulin Receptor Signaling	1.21E-02	4	1.42E-02	3	136
Superpathway of Inositol Phosphate Compounds	1.31E-02	5	1.89E-01	2	214
Epithelial Adherens Junction Signaling	1.36E-02	4	9.70E-02	2	141
VDR/RXR Activation	1.39E-02	3	3.34E-02	2	77
JAK/Stat Signaling	1.70E-02	3	3.83E-02	2	83
Role of JAK2 in Hormone-like Cytokine Signaling	1.84E-02	2	1.13E-01	1	32
VEGF Family Ligand-Receptor Interactions	1.86E-02	3	4.08E-02	2	86
1,25-Dihydroxyvitamin D3 Biosynthesis	1.94E-02	1	1.11E-02	1	3
Gαq Signaling	1.99E-02	4	1.17E-01	2	158
PDGF Signaling	2.10E-02	3	4.43E-02	2	90
Salvage Pathways of Pyrimidine Ribonucleotides	2.16E-02	3	2.89E-01	1	91
Cell Cycle Regulation by BTG Family Proteins	2.18E-02	2	1.23E-01	1	35
Tec Kinase Signaling	2.20E-02	4	1.23E-01	2	163
Ceramide Signaling	2.23E-02	3	4.61E-02	2	92
Tight Junction Signaling	2.24E-02	4	2.33E-02	3	164
autophagy	2.30E-02	2	7.93E-03	2	36
Role of NFAT in Regulation of the Immune Response	2.56E-02	4	4.73E-01	1	171
RhoGDI Signaling	2.61E-02	4	4.75E-01	1	172
UVA-Induced MAPK Signaling	2.83E-02	3	5.45E-02	2	101
UVC-Induced MAPK Signaling	3.06E-02	2	1.45E-01	1	41
Regulation of the Epithelial-Mesenchymal Transition Pathway	3.18E-02	4	1.49E-01	2	183
Gαs Signaling	3.20E-02	3	3.27E-01	1	106
IL-9 Signaling	3.47E-02	2	1.55E-01	1	45
Gαi Signaling	4.11E-02	3	3.55E-01	1	117
RhoA Signaling	4.19E-02	3	7.16E-02	2	118
Unfolded protein response	4.68E-02	2	1.67E-02	2	53
Aryl Hydrocarbon Receptor Signaling	5.62E-02	3	1.34E-02	3	133
Oleate Biosynthesis II (Animals)	5.72E-02	1	3.30E-02	1	9
Cell Cycle: G_1/S Checkpoint Regulation	6.36E-02	2	2.30E-02	2	63
Mitotic Roles of Polo-Like Kinase	6.36E-02	2	2.30E-02	2	63
BMP signaling pathway	8.40E-02	2	3.11E-02	2	74
Cyclins and Cell Cycle Regulation	8.99E-02	2	3.34E-02	2	77
Calcium Signaling	9.58E-02	3	2.44E-02	3	167

End of Table

The differentially expressed genes targeted by miRNAs between 3R4F cigarette smoke and THS2.2 aerosol exposure were used as input for the Ingenuity Pathway Analysis (IPA). Here, we highlighted the most significant enriched pathways. Columns identify the pathway name, its associated *p*-value, the number of dysregulated genes, and the number of genes in the pathway. *p*-value indicates the probability that the association between the genes in our dataset and a canonical pathway can be explained by chance alone.

13.2 Supplementary Figures

13.2.1 **Supplementary Figure 1.** Heatmap of the gene-set analysis (GSA) results for the network-related gene-set collection.

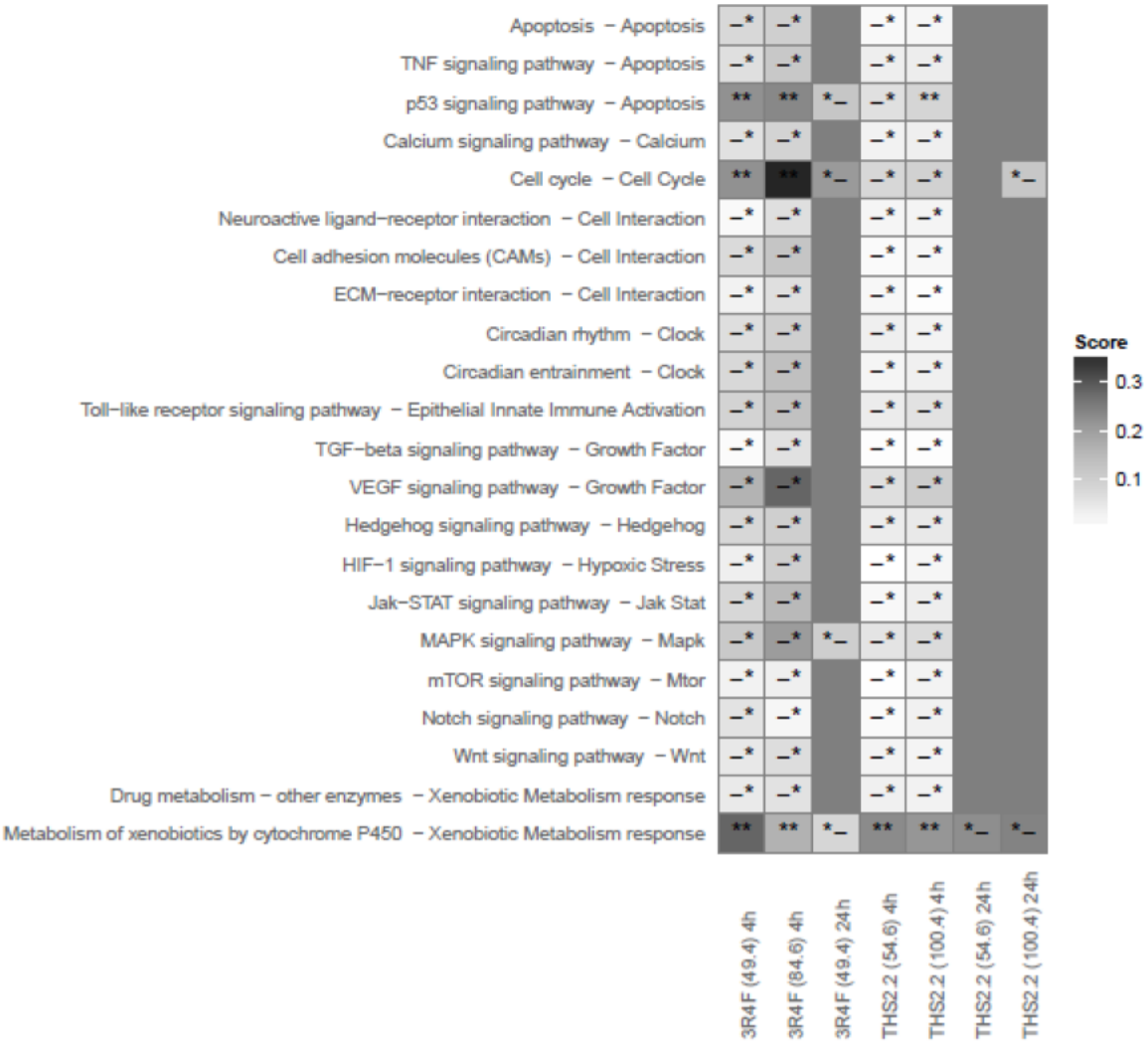

Gene-set enrichment was assessed using over-representation analysis and gene-set analysis. Three types of significance (*) are marked in each cell for each annotation: The first character indicates the adjusted Fisher *p*-value, the second character indicates the GSA Q2 test, and the third character indicates the over-representation analysis test. Non-significant statistics are indicated with the "-" symbol. The 24 h 3R4F CS condition is not represented because no samples passed the QC.

13.2.2 **Supplementary Figure 2.** Overview of the impact of 3R4F cigarette smoke or THS2.2 aerosol exposures on differential expression of genes.

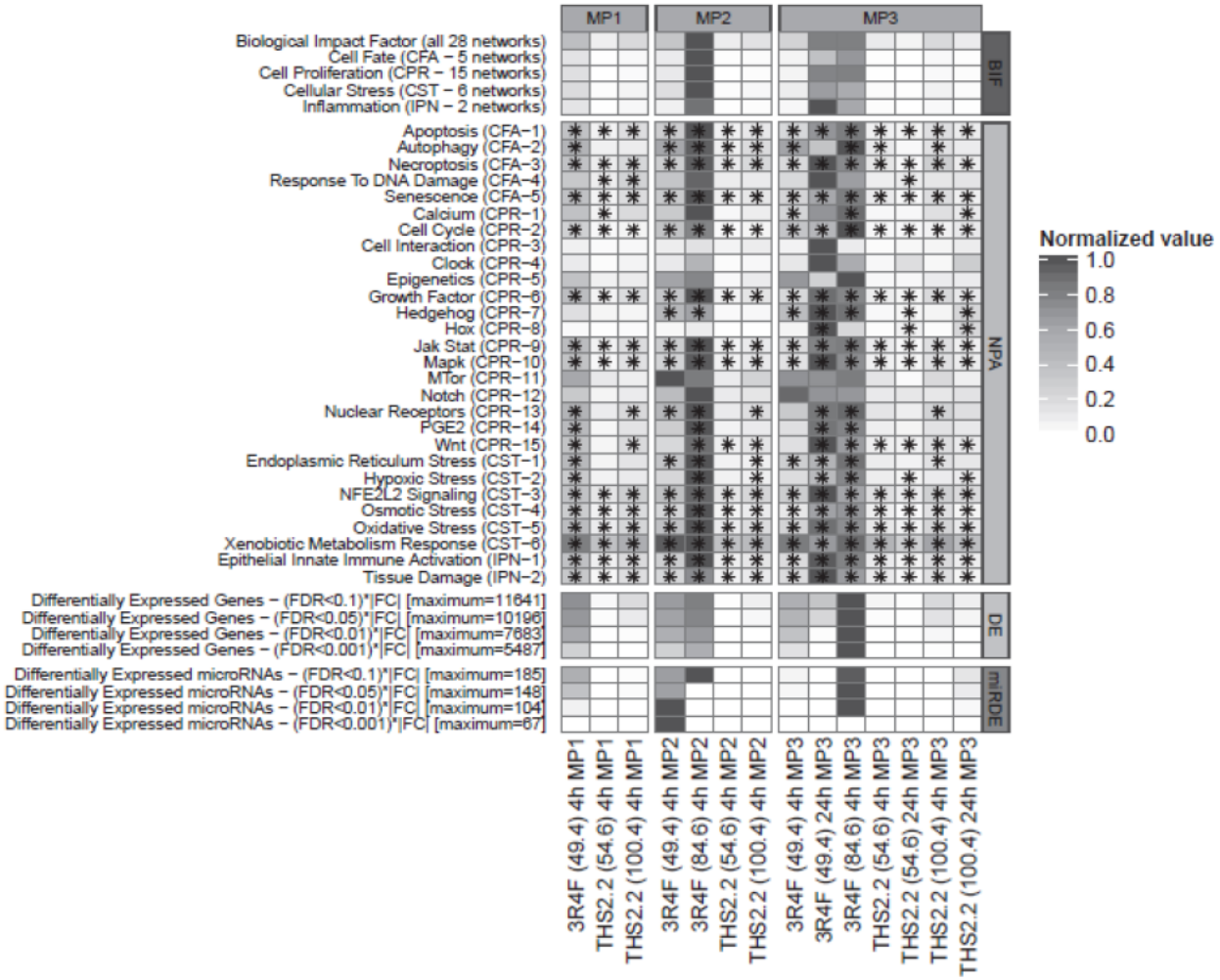

Representation as in Figure 15, but for individual experimental repetitions, also including samples for the 24-h time-point (N=3). The values are normalized to the interval [0, 1] in a row-wise manner, and the details of their calculations and meanings are given in the Statistical and Computational Methods. The uppermost panel displays the biological impact factor (BIF), which quantifies the overall impact of the exposures using the full suite of networks. The panel also includes the contribution of the four network families to the overall BIF (cell fate and angiogenesis–CFA, cell proliferation–CPR, cellular stress–CST, and pulmonary inflammation–IPN). The contributions of network families result from the aggregation of the network perturbation amplitudes (NPAs) for each single network; these are shown for each relevant network in the middle panel. * indicates statistical significance of the network perturbations, as explained in the Statistical and Computational Methods. The two lowermost panels show the number of differentially expressed genes (DEGs) and differentially expressed miRNAs (miRDE) for three distinct statistical significance thresholds, to identify possible threshold effects. The sums of the absolute value of the fold-changes of the statistically significant genes or miRNAs are displayed, to enhance the differences between the columns. Abbreviation: MP, main phase.

13.2.3 **Supplementary Figure 3.** Differential induction of oxidative stress by 3R4F CS and THS2.2 aerosol.

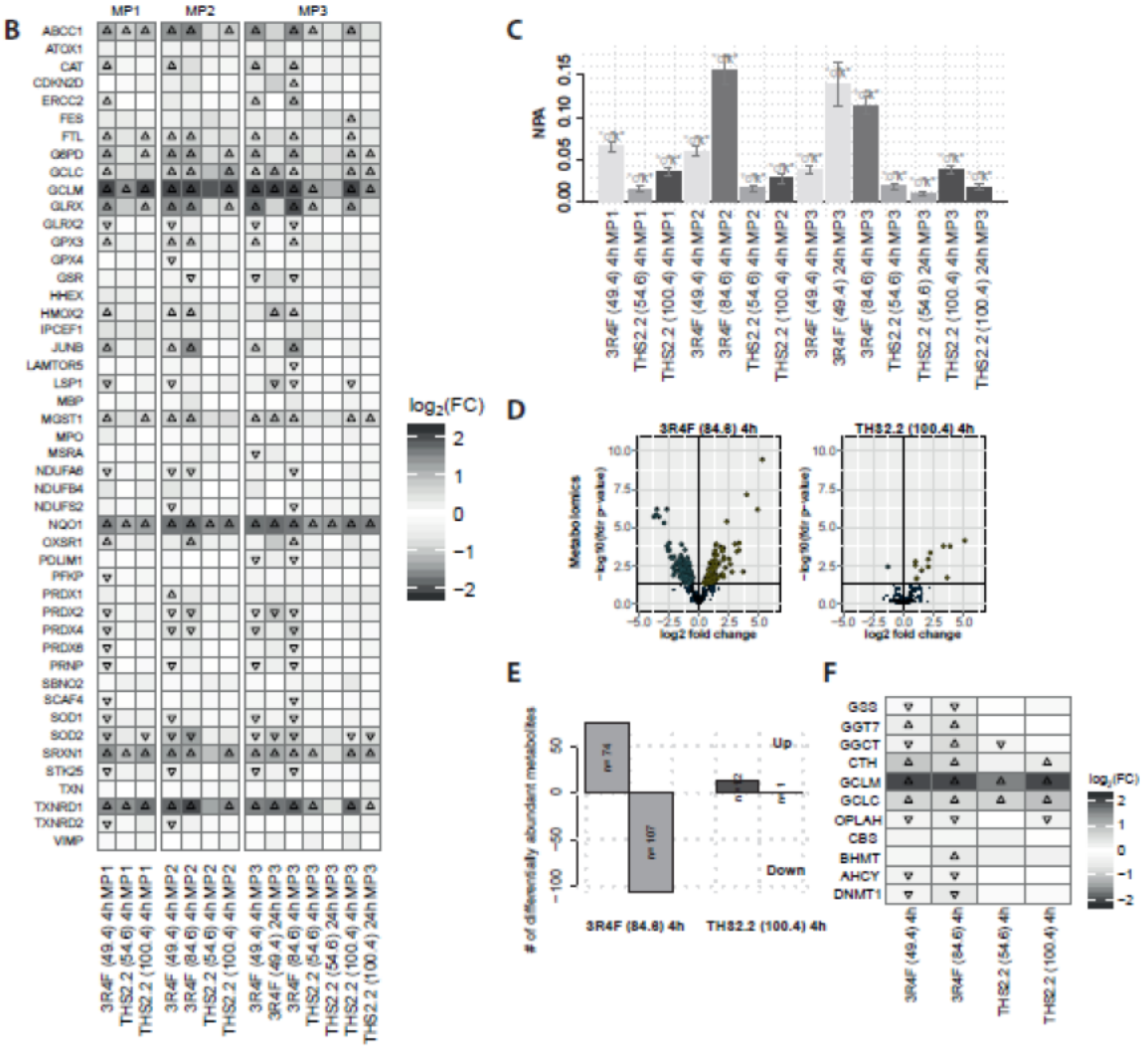

(**A**) Networks containing miRNAs and mRNA target genes assembled using the IPA® pipeline (see the Network-based integrated miRNA-mRNA assesment). The nodes were filtered for "oxidative stress". Relationships are based on the IPA Knowledge database, and molecular shapes correspond to specific molecular functions. A detailed legend for the molecular shape is found on the IPA website (http://ingenuity.force.com/ipa/articles/Feature_Description/Legend). These graphs have been drawn using the Path Designer graphical tool of the IPA software. On the right side is shown the list of Canonical Pathways (IPA) to which genes belong. + symbol close to a gene/miRNA indicates upregulation, where nothing is reported, gene/miRNA where downregulated. (**B**) Induction of the oxidative stress response program – 4 h and 24 h after exposure: Differential expression heatmap for genes of the reactive oxygen species pathway (HALLMARK_REACTIVE_OXIGEN_SPECIES_PATHWAY, M5938) (Liberzon 2015). As in Figure 17, but for experimental repetition #3, which also included samples for the 24-h time-point (N=3). (**C**) Quantitative evaluation of exposure effects on the oxidative stress network – 4 h and 24 h after exposure. As in Figure 17B, but for experimental repetition #3, which also included samples for the 24-h time-point (N=3). (**D**) Volcano plots showing differential abundant metabolites, 4 h after exposure to the high 3R4F cigarette smoke (84.6) or the high THS2.2 aerosol (100.4) concentration compared with the respective air-exposed groups (N=5). (**E**) Number of differentially abundant metabolites (FDR-adjusted *p*-value: <0.05). (**F**) Gene expression heatmap for the extended GSH metabolism pathway.

13.2.4 **Supplementary Figure 4.** Xenobiotic metabolism in 3R4F cigarette smoke- and THS2.2-exposed gingival cultures.

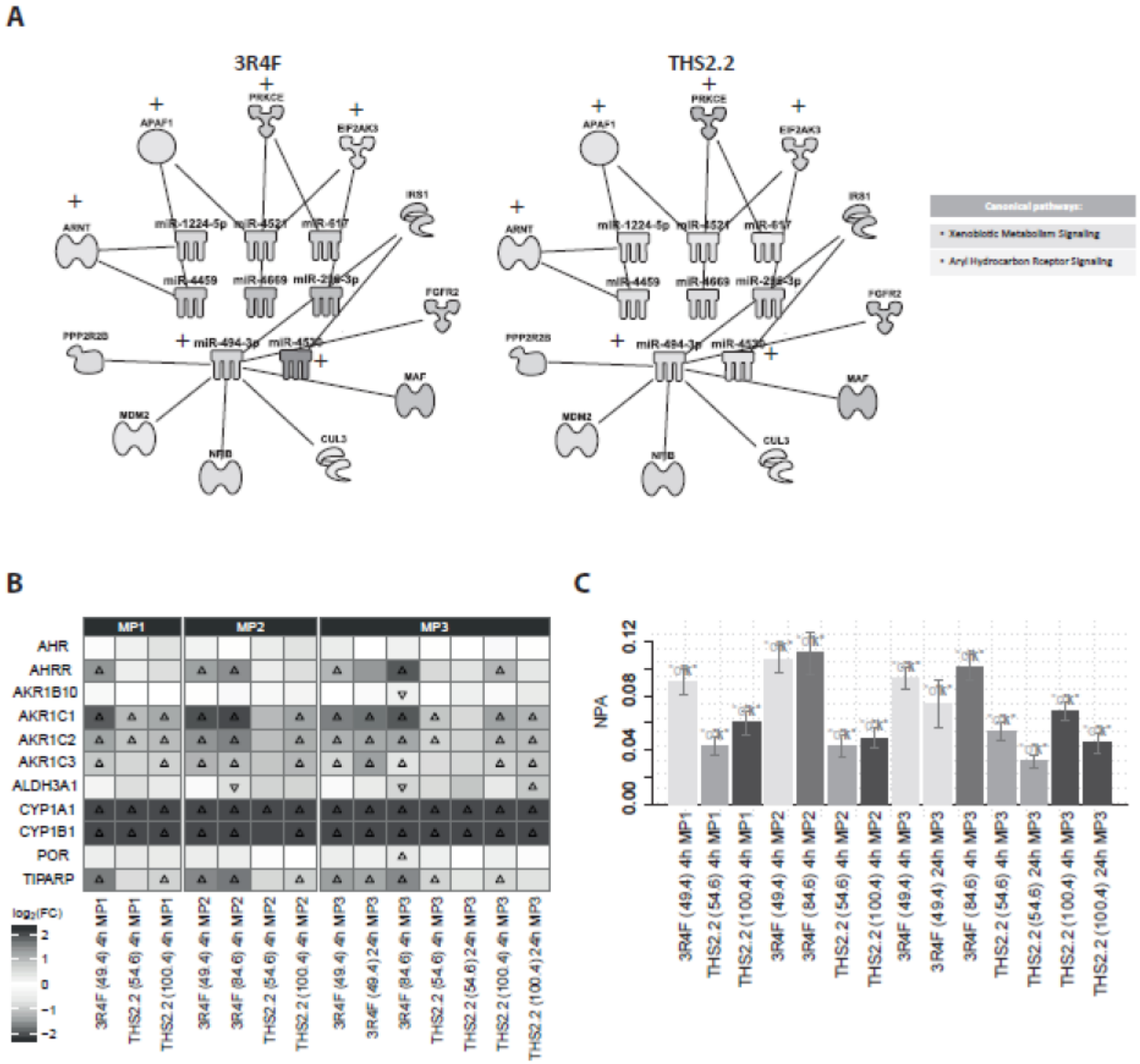

(**A**) Networks containing miRNAs and mRNA target genes involved in the xenobiotic response and assembled using the IPA® pipeline (see the Network-based integrated miRNA-mRNA assesment) (see legend above) (**B**) Induction of the xenobiotic metabolism response program – 4 h and 24 h after exposure: Heatmap shows differential expression for genes representative of xenobiotic metabolism. As in Figure 5A, but for individual experimental repetitions, also including samples for the 24-h time-point (N=3). (**C**) Quantitative evaluation of exposure effects on the "Xenobiotic Metabolism Response" network – 4 h and 24 h after exposure. As in Figure 17, but for individual experimental repetitions, also including samples for the 24-h time-point (N=3). Abbreviation: MP, main phase.

13.2.5 **Supplementary Figure 5.** Individual plots of proinflammatory mediators secreted in basolateral media.

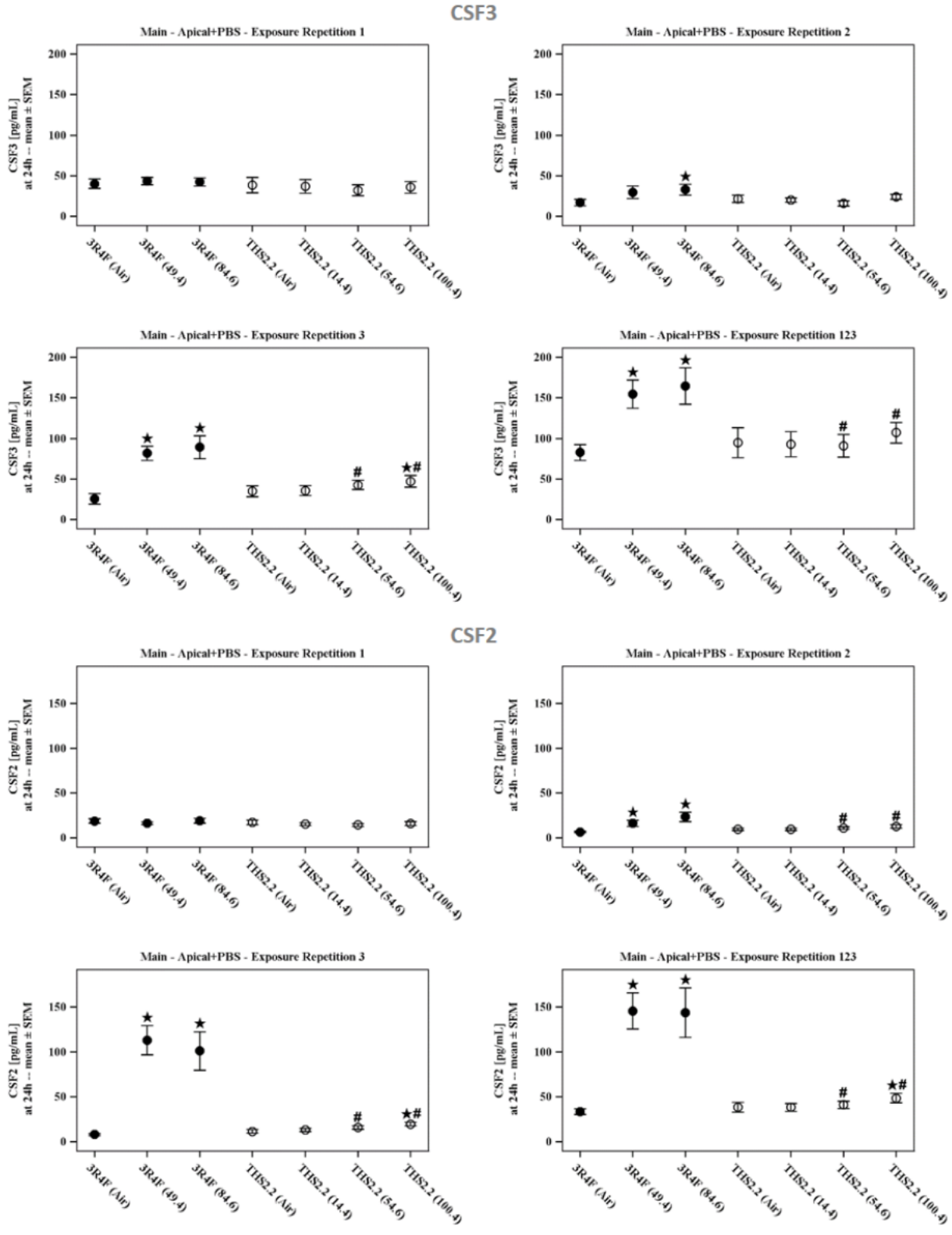

Figure continues

CXCL1/GRO1

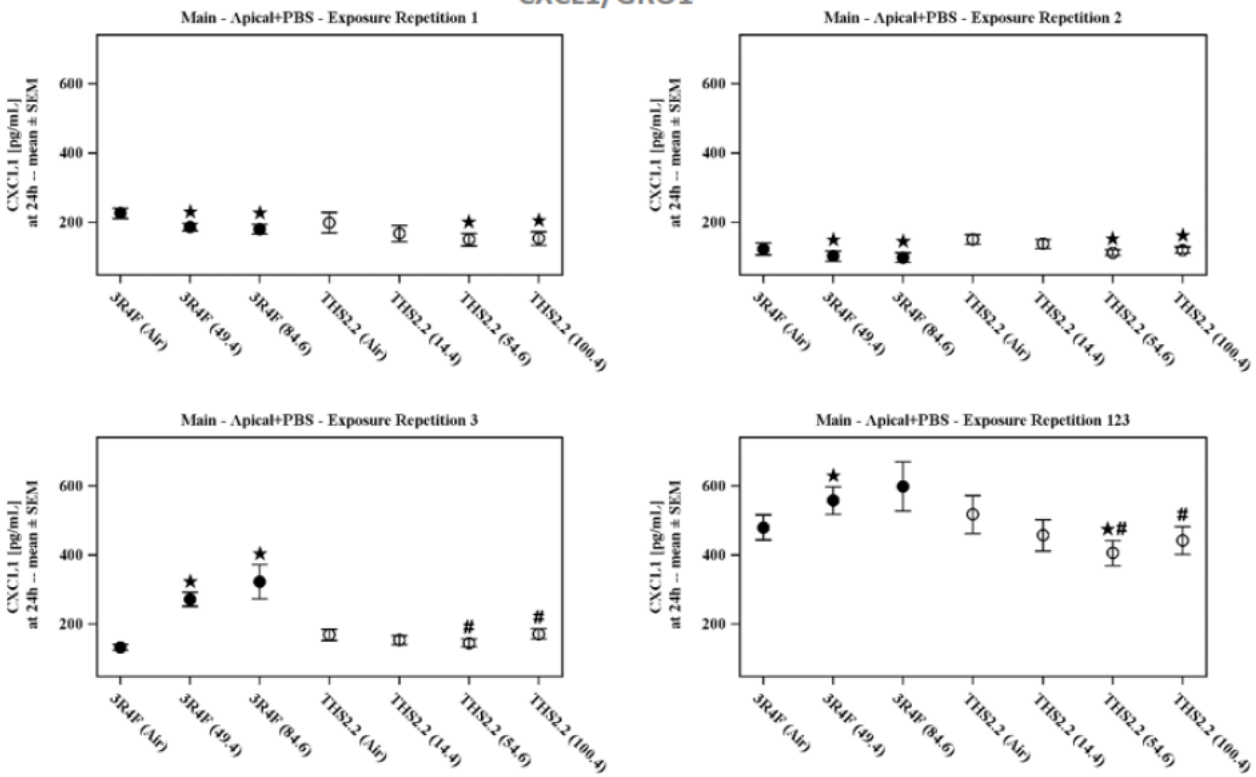

IL1A

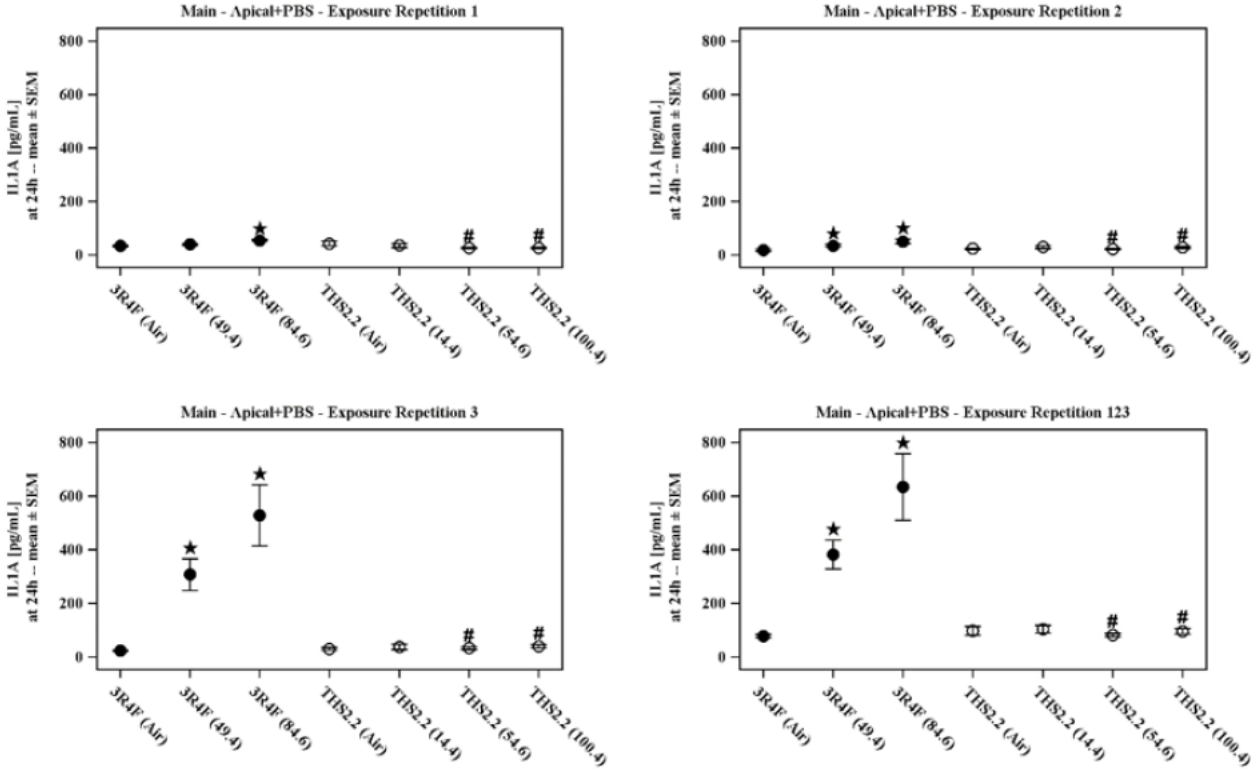

Figure continues

IL1B

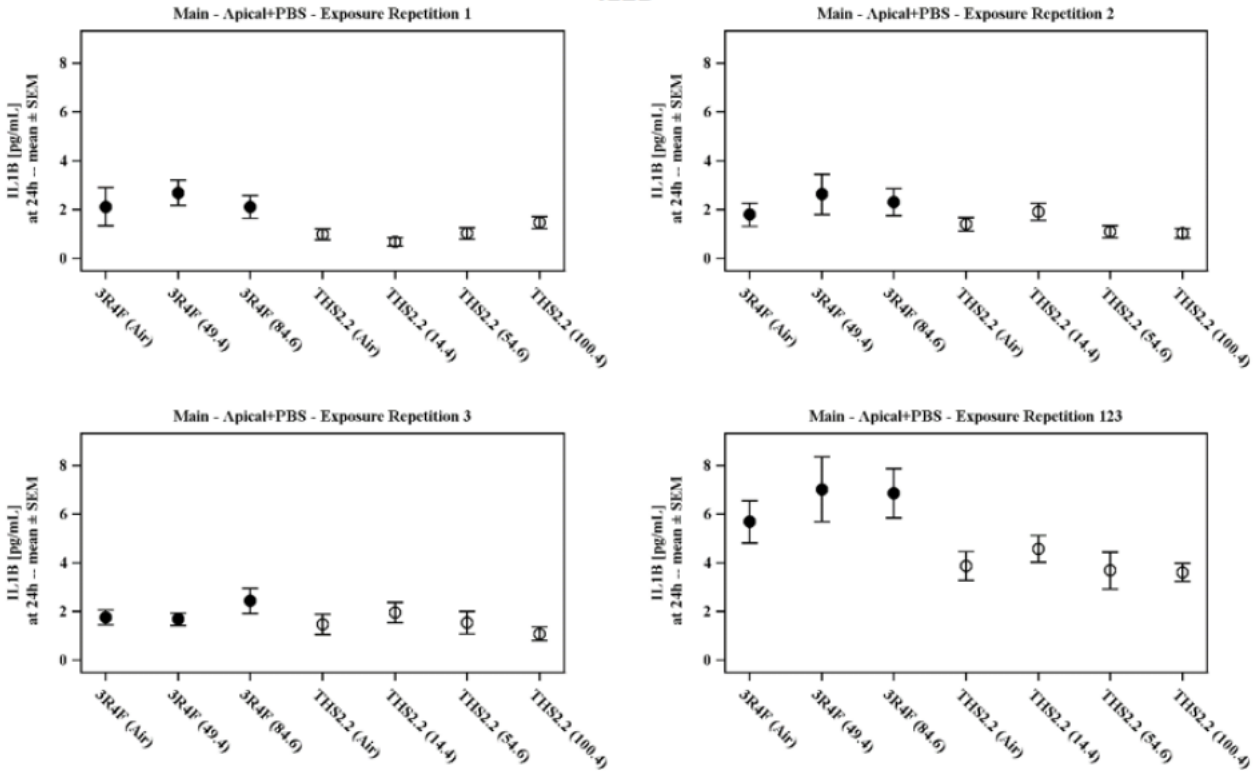

IL6

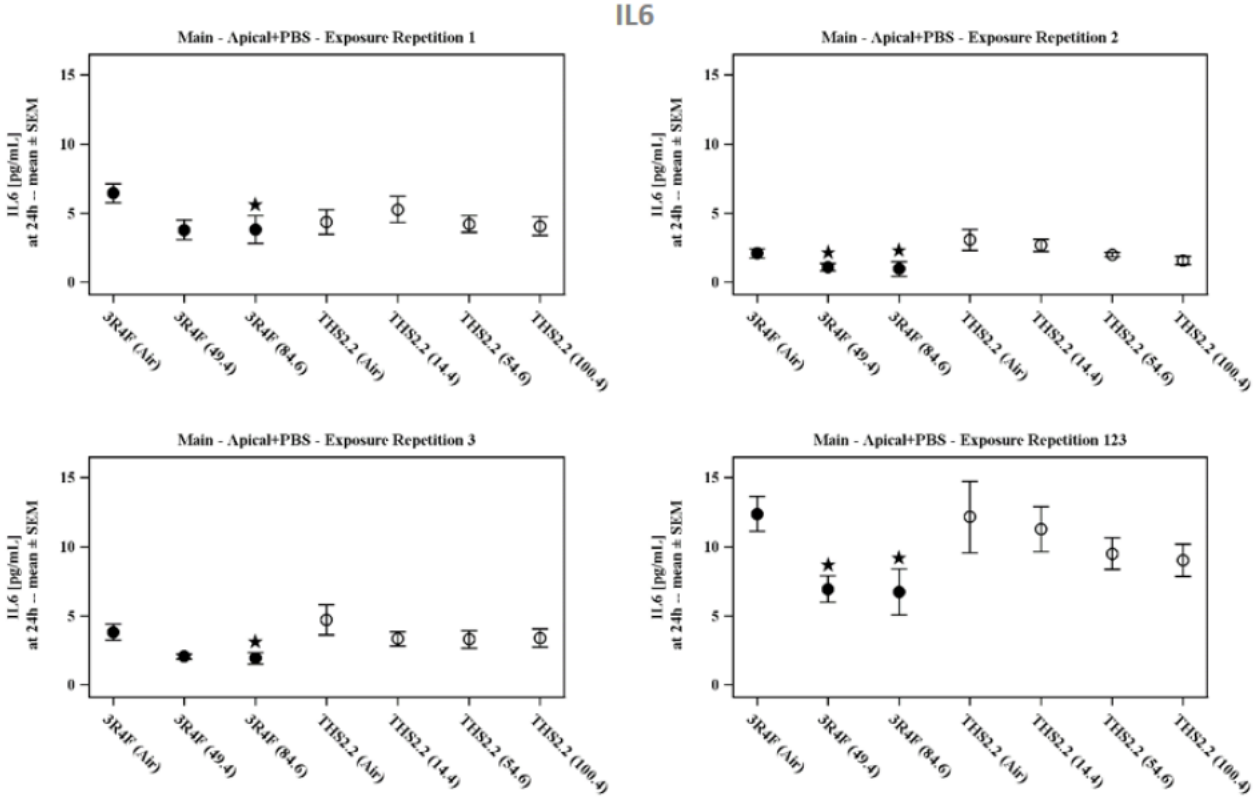

Figure continues

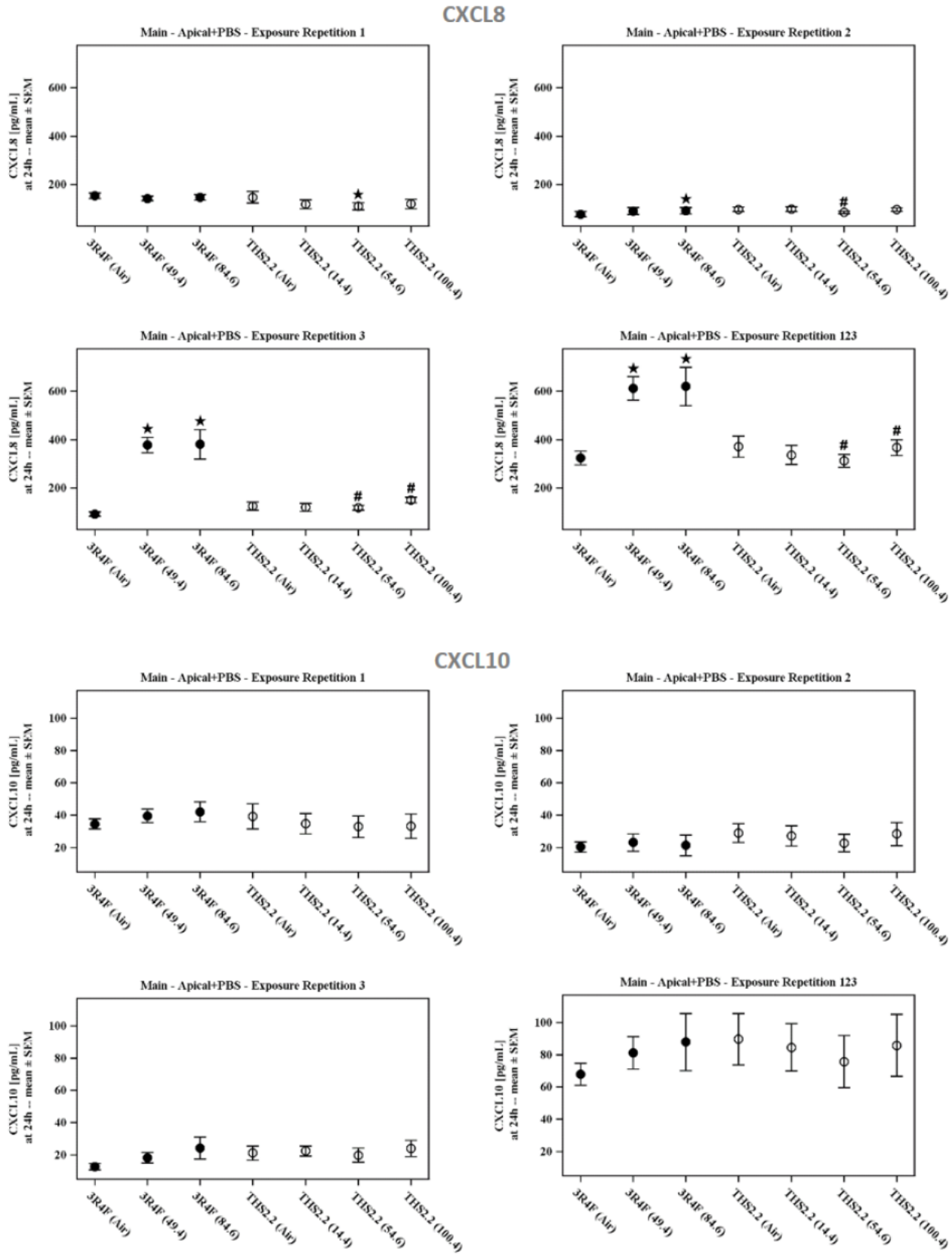

Figure continues

CCL2

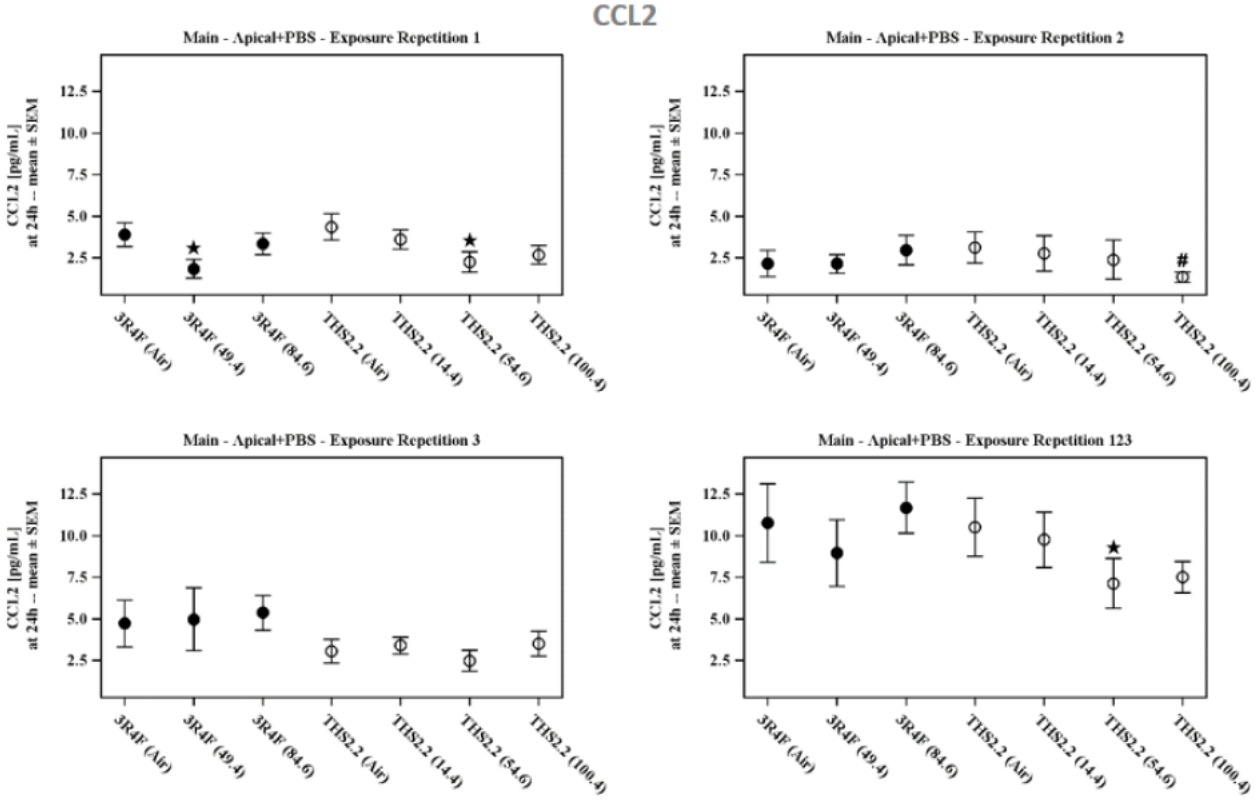

MMP-1

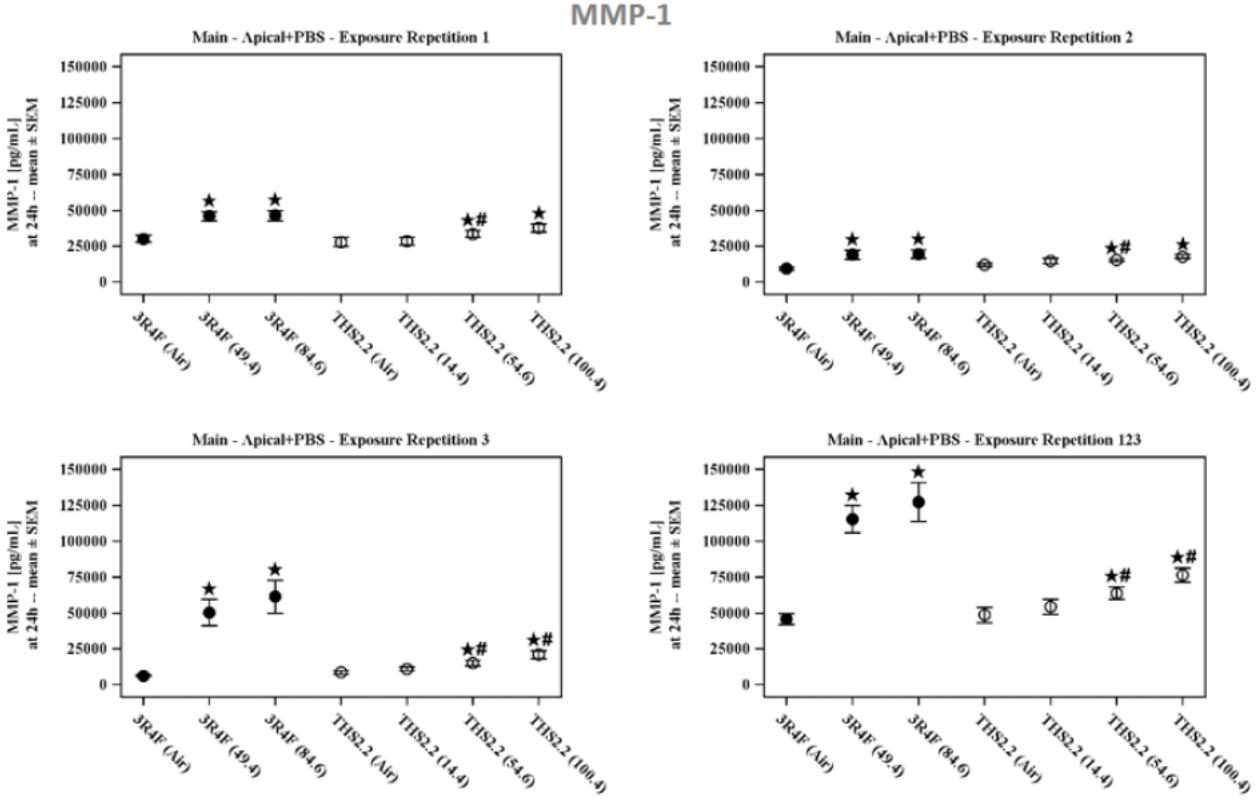

Figure continues

MMP-9

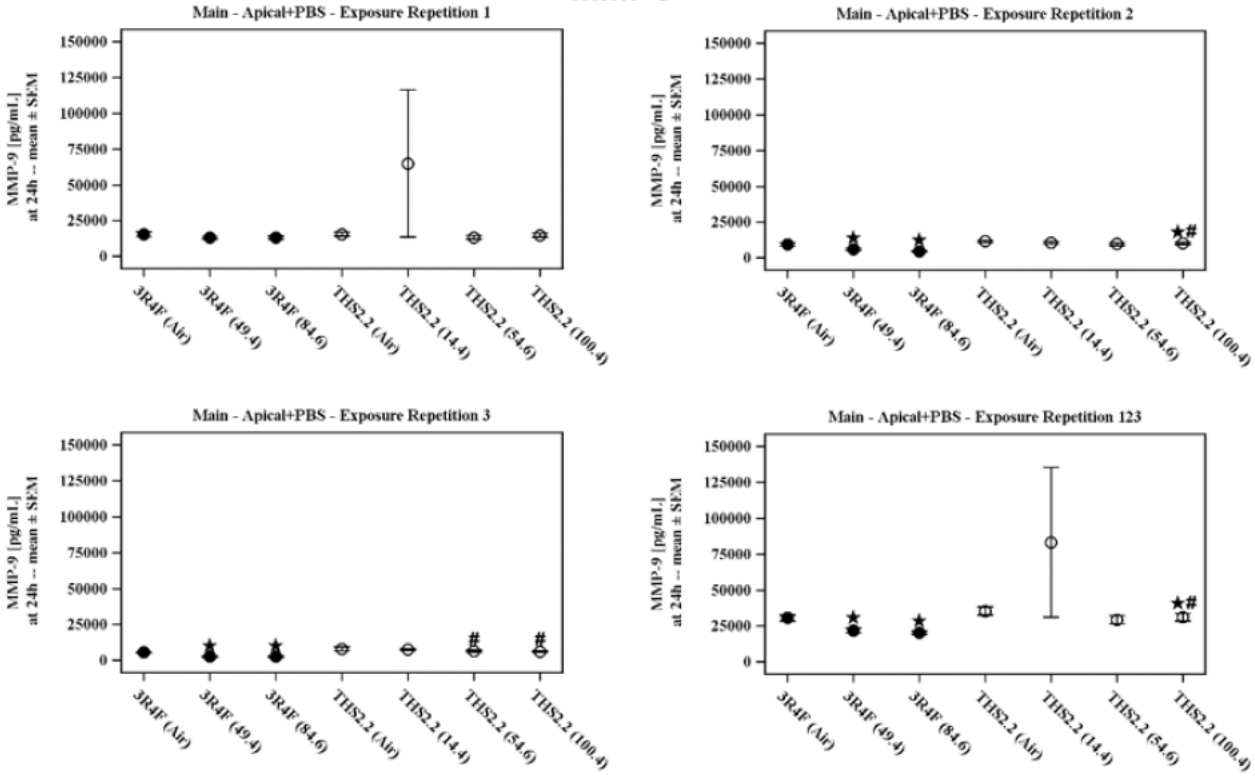

CCL5

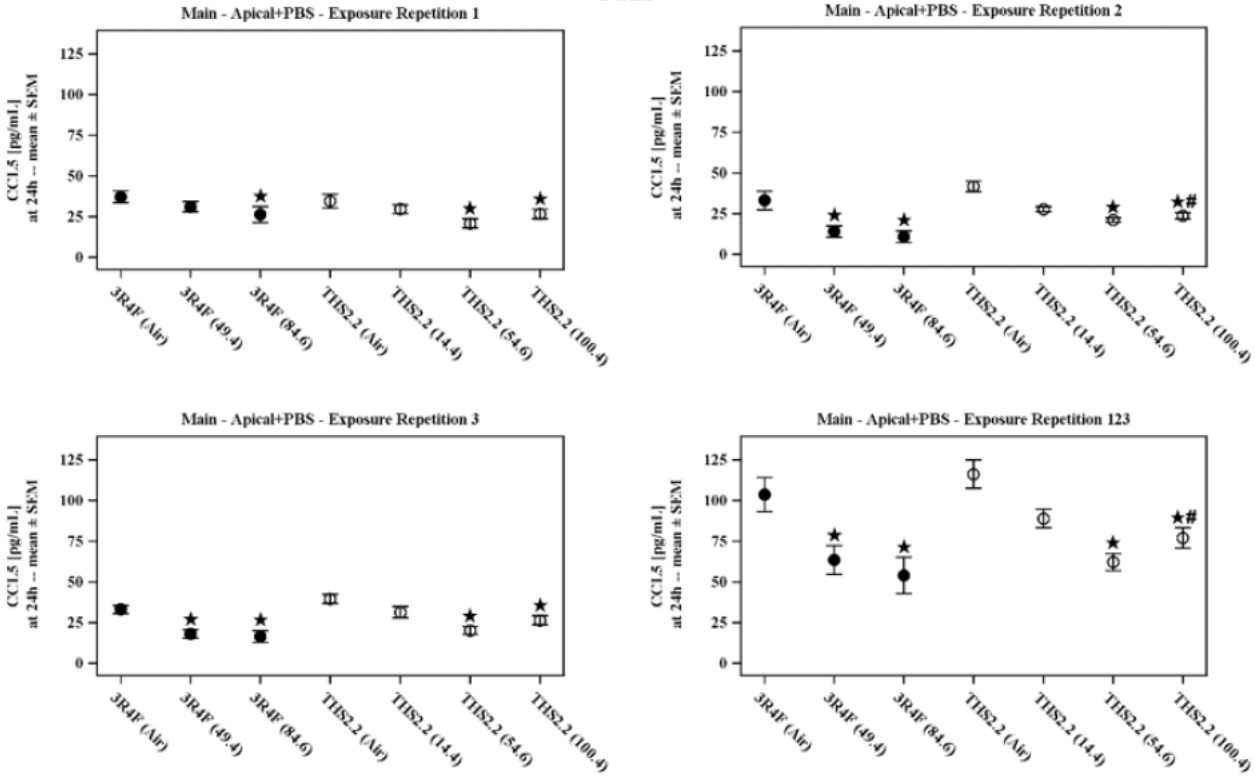

Figure continues

TNFα

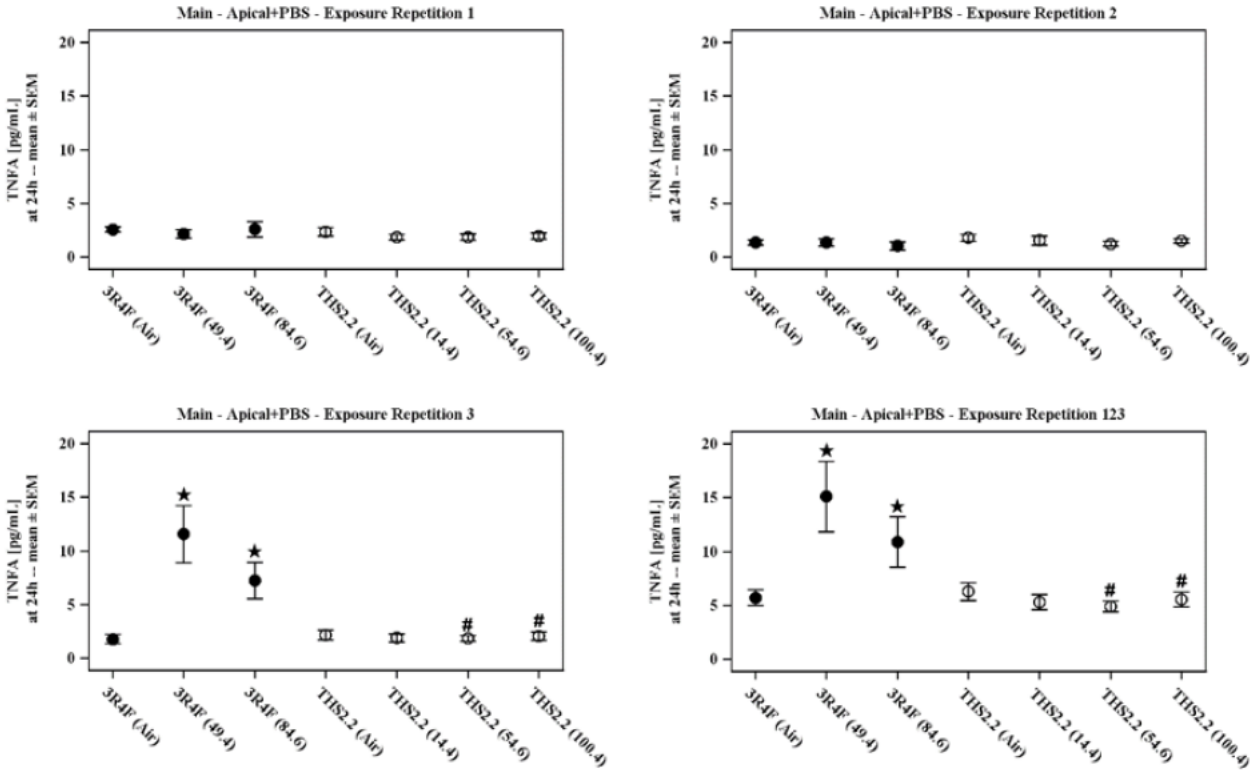

VEGFA

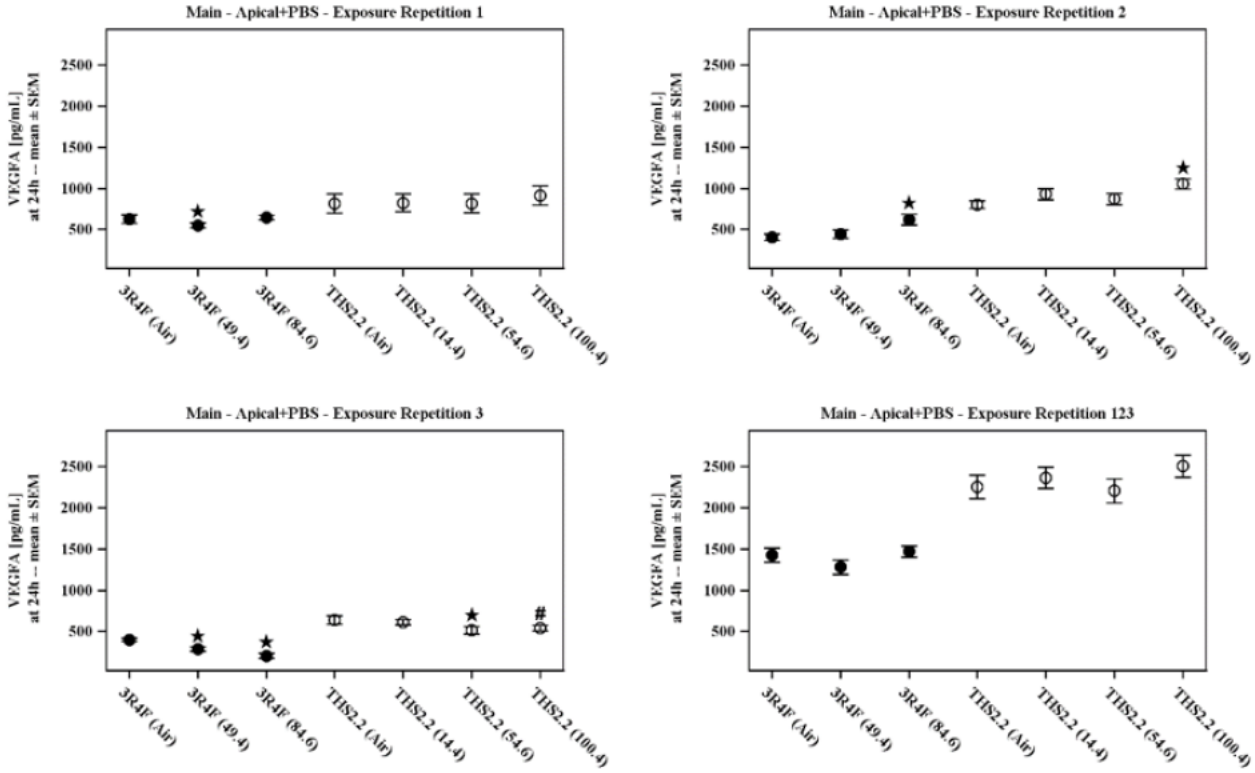

End of the Figure

The mean concentration of the indicated mediator and SEM (N=9, from three experimental repetitions with three exposure runs/repetition) are shown. ★ indicates a significant difference compared with the corresponding air controls ($p<0.05$). # indicates a significant difference compared with 3R4F at the comparable concentration ($p<0.05$). Abbreviations: CSF, colony-stimulating factor; CXCL, chemokine (C-X-C motif) ligand; h, hour; IL, interleukin; MMP, matrix metalloproteinase; SEM, standard error of the mean; TNFα, tumor necrosis factor alpha, VEGFA, vascular endothelial growth factor alpha. Nicotine concentrations in 3R4F cigarette smoke or THS2.2 aerosols are indicated for each group (mg/L).

13.2.6 **Supplementary Figure 6.** Profile of inflammation in 3R4F cigarette smoke- and THS2.2 aerosol-exposed gingival cultures.

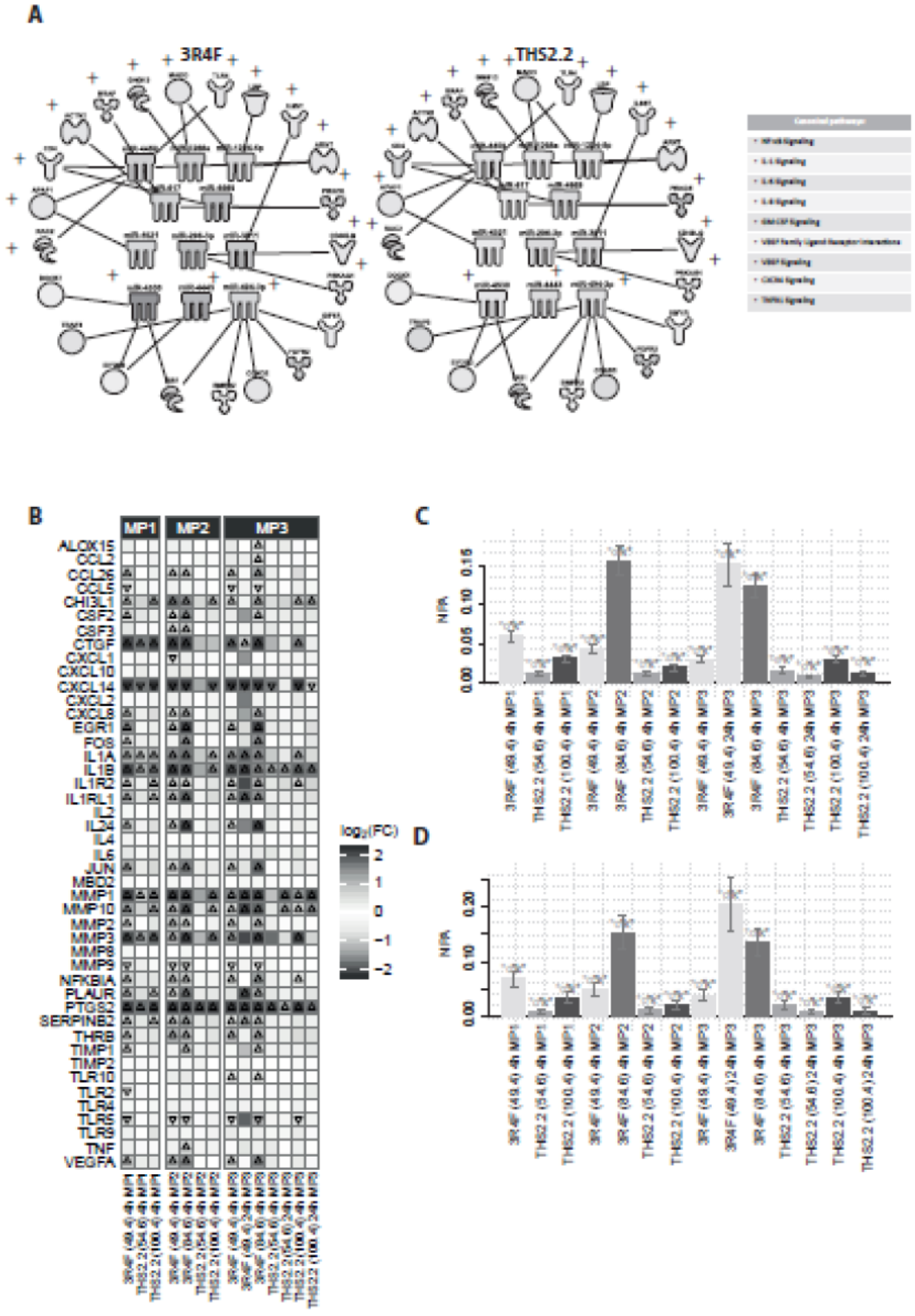

(**A**) Networks containing miRNAs and mRNA target genes involved in the inflammation response and assembled using the IPA® pipeline (see legend of Supplementary Figure 3A). (**B**) Induction of inflammatory gene expression response – 4 h and 24 h after exposure: Heatmap shows differential expression for genes representative of inflammation. As in Figure 20A, but for individual experimental repetitions, also including samples for the 24-h time-point (N=3). (**C**) Quantitative evaluation of exposure effects on the "Epithelial Innate Immune Activation" network – 4 h and 24 h after exposure. As in Figure 20B, but for individual experimental repetitions, also including samples for the 24-h time-point (N=3). (**D**) As in Supplementary Figure 6C, but for the "Tissue Damage" network. Abbreviation: MP, main phase.

14. References

Ackermann M, Strimmer K. A general modular framework for gene set enrichment analysis. BMC bioinformatics. 2009;10(1):1.

Agrawal A, Shindell E, Jordan F, Baeva L, Pfefer J, Godar DE. UV radiation increases carcinogenic risks for oral tissues compared to skin. Photochem Photobiol. 2013;89(5):1193-8. PubMed PMID: 23855371.

Alharbi IA, Rouabhia M. Repeated exposure to whole cigarette smoke promotes primary human gingival epithelial cell growth and modulates keratin expression. J Periodontal Res. 2016. PubMed PMID: 26740170.

Amara IE, Anwar-Mohamed A, El-Kadi AO. Mercury modulates the CYP1A1 at transcriptional and posttranslational levels in human hepatoma HepG2 cells. Toxicology letters. 2010;199(3):225-33. Epub 2010/09/15. PubMed PMID: 20837117.

Ames BN, Cathcart R, Schwiers E, Hochstein P. Uric acid provides an antioxidant defense in humans against oxidant- and radical-caused aging and cancer: a hypothesis. Proc Natl Acad Sci U S A. 1981;78(11):6858-62. Epub 1981/11/01. PubMed PMID: 6947260; PubMed Central PMCID: PMCPMC349151.

Andreescu CF, Mihai LL, Raescu M, Tuculina MJ, Cumpata CN, Ghergic DL. Age influence on periodontal tissues: a histological study. Rom J Morphol Embryol. 2013;54(3 Suppl):811-5. PubMed PMID: 24322032.

Anwar-Mohamed A, Klotz LO, El-Kadi AO. Inhibition of heme oxygenase-1 partially reverses the arsenite-mediated decrease of CYP1A1, CYP1A2, CYP3A23, and CYP3A2 catalytic activity in isolated rat hepatocytes. Drug metabolism and disposition: the biological fate of chemicals. 2012;40(3):504-14. Epub 2011/12/14. PubMed PMID: 22159698.

Babu SP, Ramesh V, Samidorai A, Charles NS. Cytochrome P450 2C9 gene polymorphism in phenytoin induced gingival enlargement: A case report. J Pharm Bioallied Sci. 2013;5(3):237-9. PubMed PMID: 24082701; PubMed Central PMCID: PMCPMC3778594.

Battino M, Ferreiro MS, Gallardo I, Newman HN, Bullon P. The antioxidant capacity of saliva. J Clin Periodontol. 2002;29(3):189-94. PubMed PMID: 11940135.

Baxter A, Thain S, Banerjee A, Haswell L, Parmar A, Phillips G, et al. Targeted omics analyses, and metabolic enzyme activity assays demonstrate maintenance of key mucociliary characteristics in long term cultures of reconstituted human airway epithelia. Toxicology in vitro : an international journal published in association with BIBRA. 2015;29(5):864-75. PubMed PMID: 25863282.

Beatty PW, Reed DJ. Involvement of the cystathionine pathway in the biosynthesis of glutathione by isolated rat hepatocytes. Arch Biochem Biophys. 1980;204(1):80-7. PubMed PMID: 7425648.

Benjamini Y, Hochberg Y. Controlling the false discovery rate: a practical and powerful approach to multiple testing. Journal of the royal statistical society Series B (Methodological). 1995:289-300.

Bolstad BM, Irizarry RA, Åstrand M, Speed TP. A comparison of normalization methods for high density oligonucleotide array data based on variance and bias. Bioinformatics. 2003;19(2):185-93.

Bostrom L, Linder LE, Bergstrom J. Clinical expression of TNF-alpha in smoking-associated periodontal disease. J Clin Periodontol. 1998;25(10):767-73. PubMed PMID: 9797047.

Bostrom L, Linder LE, Bergstrom J. Smoking and crevicular fluid levels of IL-6 and TNF-alpha in periodontal disease. J Clin Periodontol. 1999;26(6):352-7. PubMed PMID: 10382574.

Candi E, Schmidt R, Melino G. The cornified envelope: a model of cell death in the skin. Nature reviews Molecular cell biology. 2005;6(4):328-40. PubMed PMID: 15803139.

Carvalho BS, Irizarry RA. A framework for oligonucleotide microarray preprocessing. Bioinformatics. 2010;26(19):2363-7.

Conard GJ, Osborn JC, Pekary AD, Scholle RH. Relationship of drug metabolism and inflammation to the gingival response of rats treated with diphenylhydantoin. J Dent Res. 1975;54 Spec No B:B68-74. PubMed PMID: 1055746.

Coppe JP, Boysen M, Sun CH, Wong BJ, Kang MK, Park NH, et al. A role for fibroblasts in mediating the effects of tobacco-induced epithelial cell growth and invasion. Mol Cancer Res. 2008;6(7):1085-98. PubMed PMID: 18644973; PubMed Central PMCID: PMCPMC2768668.

D'Alessandro A, Hansen KC, Silliman CC, Moore EE, Kelher M, Banerjee A. Metabolomics of AS-5 RBC supernatants following routine storage. Vox Sang. 2015;108(2):131-40. PubMed PMID: 25200932; PubMed Central PMCID: PMCPMC4393710.

Davis MA, Eldridge S, Louden C. Chapter 10 - Biomarkers: Discovery, Qualification and Application. In: Wallig WMHGRA, editor. Haschek and Rousseaux's Handbook of Toxicologic Pathology (Third Edition). Boston: Academic Press; 2013. p. 317-52.

De Nardin E. The role of inflammatory and immunological mediators in periodontitis and cardiovascular disease. Ann Periodontol. 2001;6(1):30-40. PubMed PMID: 11887469.

Di Benedetto A, Gigante I, Colucci S, Grano M. Periodontal disease: linking the primary inflammation to bone loss. Clin Dev Immunol. 2013;2013:503754. PubMed PMID: 23762091; PubMed Central PMCID: PMCPMC3676984.

Donetti E, Gualerzi A, Bedoni M, Volpari T, Sciarabba M, Tartaglia G, et al. Desmoglein 3 and keratin 10 expressions are reduced by chronic exposure to cigarette smoke in human keratinised oral mucosa explants. Arch Oral Biol. 2010;55(10):815-23. PubMed PMID: 20667405.

Furuse M, Hata M, Furuse K, Yoshida Y, Haratake A, Sugitani Y, et al. Claudin-based tight junctions are crucial for the mammalian epidermal barrier: a lesson from claudin-1-deficient mice. J Cell Biol. 2002;156(6):1099-111. PubMed PMID: 11889141; PubMed Central PMCID: PMC2173463.

Gemmell E, Carter CL, Seymour GJ. Chemokines in human periodontal disease tissues. Clinical and experimental immunology. 2001;125(1):134-41. PubMed PMID: 11472436; PubMed Central PMCID: PMC1906105.

Genco RJ. Current view of risk factors for periodontal diseases. J Periodontol. 1996;67(10 Suppl):1041-9. PubMed PMID: 8910821.

Gentleman RC, Carey VJ, Bates DM, Bolstad B, Dettling M, Dudoit S, et al. Bioconductor: open software development for computational biology and bioinformatics. Genome Biol. 2004;5(10):R80. PubMed PMID: 15461798; PubMed Central PMCID: PMCPMC545600.

Giannopoulou C, Cappuyns I, Mombelli A. Effect of smoking on gingival crevicular fluid cytokine profile during experimental gingivitis. J Clin Periodontol. 2003a;30(11):996-1002. PubMed PMID: 14761123.

Giannopoulou C, Kamma JJ, Mombelli A. Effect of inflammation, smoking and stress on gingival crevicular fluid cytokine level. J Clin Periodontol. 2003b;30(2):145-53. PubMed PMID: 12622857.

Goldkorn T, Filosto S, Chung S. Lung injury and lung cancer caused by cigarette smoke-induced oxidative stress: Molecular mechanisms and therapeutic opportunities involving the ceramide-generating machinery and epidermal growth factor receptor. Antioxidants & redox signaling. 2014;21(15):2149-74. Epub 2014/04/02. PubMed PMID: 24684526; PubMed Central PMCID: PMCPMC4215561.

Guentsch A, Preshaw PM, Bremer-Streck S, Klinger G, Glockmann E, Sigusch BW. Lipid peroxidation and antioxidant activity in saliva of periodontitis patients: effect of smoking and periodontal treatment. Clin Oral Investig. 2008;12(4):345-52. PubMed PMID: 18509684.

Hai R, Chu A, Li H, Umamoto S, Rider P, Liu F. Infection of human cytomegalovirus in cultured human gingival tissue. Virology journal. 2006;3:84. PubMed PMID: 17022821; PubMed Central PMCID: PMC1617094.

Hasegawa M, Nelson HH, Peters E, Ringstrom E, Posner M, Kelsey KT. Patterns of gene promoter methylation in squamous cell cancer of the head and neck. Oncogene. 2002;21(27):4231-6. PubMed PMID: 12082610.

Henriksson P, Hamberg M, Diczfalusy U. Formation of 15-HETE as a major hydroxyeicosatetraenoic acid in the atherosclerotic vessel wall. Biochim Biophys Acta. 1985;834(2):272-4. PubMed PMID: 3995065.

Henry J, Toulza E, Hsu CY, Pellerin L, Balica S, Mazereeuw-Hautier J, et al. Update on the epidermal differentiation complex. Frontiers in bioscience. 2012;17:1517-32. PubMed PMID: 22201818.

Huang HY, Chen SZ, Zhang WT, Wang SS, Liu Y, Li X, et al. Induction of EMT-like response by BMP4 via up-regulation of lysyl oxidase is required for adipocyte lineage commitment. Stem Cell Res. 2013;10(3):278-87. PubMed PMID: 23395997.

Huber W, Von Heydebreck A, Sültmann H, Poustka A, Vingron M. Variance stabilization applied to microarray data calibration and to the quantification of differential expression. Bioinformatics. 2002;18(suppl 1):S96-S104.

Huh D, Hamilton GA, Ingber DE. From 3D cell culture to organs-on-chips. Trends in cell biology. 2011;21(12):745-54. PubMed PMID: 22033488; PubMed Central PMCID: PMC4386065.

Hultin-Rosenberg L, Forshed J, Branca RM, Lehtio J, Johansson HJ. Defining, comparing, and improving iTRAQ quantification in mass spectrometry proteomics data. Molecular & cellular proteomics : MCP. 2013;12(7):2021-31. Epub 2013/03/09. PubMed PMID: 23471484; PubMed Central PMCID: PMCPMC3708183.

Inoue M. Glutathionists in the battlefield of gamma-glutamyl cycle. Arch Biochem Biophys. 2016;595:61-3. PubMed PMID: 27095217.

Irizarry RA, Bolstad BM, Collin F, Cope LM, Hobbs B, Speed TP. Summaries of Affymetrix GeneChip probe level data. Nucleic acids research. 2003;31(4):e15-e.

Iskandar AR, Martin F, Talikka M, Schlage WK, Kostadinova R, Mathis C, et al. Systems approaches evaluating the perturbation of xenobiotic metabolism in response to cigarette smoke exposure in nasal and bronchial tissues. Biomed Res Int. 2013;2013:512086. PubMed PMID: 24224167; PubMed Central PMCID: PMCPMC3808713.

James JA, Sayers NM, Drucker DB, Hull PS. Effects of tobacco products on the attachment and growth of periodontal ligament fibroblasts. J Periodontol. 1999;70(5):518-25. PubMed PMID: 10368056.

Kanehisa M, Goto S, Sato Y, Kawashima M, Furumichi M, Tanabe M. Data, information, knowledge and principle: back to metabolism in KEGG. Nucleic Acids Res. 2014;42(Database issue):D199-205. PubMed PMID: 24214961; PubMed Central PMCID: PMCPMC3965122.

Kauffmann A, Gentleman R, Huber W. arrayQualityMetrics—a bioconductor package for quality assessment of microarray data. Bioinformatics. 2009;25(3):415-6.

Kentucky Tobacco Research & Development Center. Kentucky Tobacco Research & Development Center. 3R4F Preliminary Analysis. Available at: //ctrp.uky.edu/resources/pdf/webdocs/3R4F%20Preliminary%20Analysis.pdf.

Kho HS. Understanding of xerostomia and strategies for the development of artificial saliva. The Chinese journal of dental research : the official journal of the Scientific Section of the Chinese Stomatological Association. 2014;17(2):75-83. PubMed PMID: 25531014.

Kim SG, Chae CH, Cho BO, Kim HN, Kim HJ, Kim IS, et al. Apoptosis of oral epithelial cells in oral lichen planus caused by upregulation of BMP-4. J Oral Pathol Med. 2006;35(1):37-45. PubMed PMID: 16393252.

Kirkham PA, Barnes PJ. Oxidative stress in COPD. Chest. 2013;144(1):266-73. PubMed PMID: 23880677.

Korashy HM, El-Kadi AO. Transcriptional and posttranslational mechanisms modulating the expression of the cytochrome P450 1A1 gene by lead in HepG2 cells: a role of heme oxygenase. Toxicology. 2012;291(1-3):113-21. Epub 2011/11/29. PubMed PMID: 22120038.

Koster MI, Roop DR. Mechanisms regulating epithelial stratification. Annual review of cell and developmental biology. 2007;23:93-113. PubMed PMID: 17489688.

Kundumani-Sridharan V, Dyukova E, Hansen DE, Rao GN. 12/15-Lipoxygenase Mediates High-fat Diet-induced Endothelial Tight Junction Disruption and Monocyte Transmigration A NEW ROLE FOR 15 (S)-HYDROXYEICOSATETRAENOIC ACID IN ENDOTHELIAL CELL DYSFUNCTION. Journal of Biological Chemistry. 2013;288(22):15830-42.

Liberzon A, Birger C, Thorvaldsdóttir H, Ghandi M, Mesirov JP, Tamayo P. The molecular signatures database hallmark gene set collection. Cell systems. 2015;1(6):417-25.

Mahanonda R, Sa-Ard-Iam N, Eksomtramate M, Rerkyen P, Phairat B, Schaecher KE, et al. Cigarette smoke extract modulates human beta-defensin-2 and interleukin-8 expression in human gingival epithelial cells. J Periodontal Res. 2009;44(4):557-64. PubMed PMID: 19438974.

Malpass GE, Arimilli S, Prasad GL, Howlett AC. Complete artificial saliva alters expression of proinflammatory cytokines in human dermal fibroblasts. Toxicol Sci. 2013;134(1):18-25. PubMed PMID: 23629517; PubMed Central PMCID: PMCPMC3693133.

Martin F, Sewer A, Talikka M, Xiang Y, Hoeng J, Peitsch MC. Quantification of biological network perturbations for mechanistic insight and diagnostics using two-layer causal models. BMC Bioinformatics. 2014;15:238. PubMed PMID: 25015298; PubMed Central PMCID: PMCPMC4227138.

Mitchell D, Paniker L, Godar D. Nucleotide excision repair is reduced in oral epithelial tissues compared with skin. Photochem Photobiol. 2012;88(4):1027-32. PubMed PMID: 22519509; PubMed Central PMCID: PMCPMC3437763.

Moharamzadeh K, Franklin KL, Brook IM, van Noort R. Biologic assessment of antiseptic mouthwashes using a three-dimensional human oral mucosal model. J Periodontol. 2009;80(5):769-75. PubMed PMID: 19405830.

Monnouchi S, Maeda H, Yuda A, Serita S, Wada N, Tomokiyo A, et al. Benzo[a]pyrene/aryl hydrocarbon receptor signaling inhibits osteoblastic differentiation and collagen synthesis of human periodontal ligament cells. J Periodontal Res. 2016. PubMed PMID: 26738610.

Morita K, Miyachi Y, Furuse M. Tight junctions in epidermis: from barrier to keratinization. Eur J Dermatol. 2011;21(1):12-7. PubMed PMID: 21300606.

Mosharov E, Cranford MR, Banerjee R. The quantitatively important relationship between homocysteine metabolism and glutathione synthesis by the transsulfuration pathway and its regulation by redox changes. Biochemistry. 2000;39(42):13005-11.

Nam D, Kim S-Y. Gene-set approach for expression pattern analysis. Briefings in bioinformatics. 2008;9(3):189-97.

Nichols JE, Niles JA, Vega SP, Argueta LB, Eastaway A, Cortiella J. Modeling the lung: Design and development of tissue engineered macro- and micro-physiologic lung models for research use. Experimental biology and medicine. 2014;239(9):1135-69. PubMed PMID: 24962174.

Oda D, Dale BA, Bourekis G. Human oral epithelial cell culture. II. Keratin expression in fetal and adult gingival cells. In vitro cellular & developmental biology : journal of the Tissue Culture Association. 1990;26(6):596-603. PubMed PMID: 1694168.

Ojima M, Hanioka T. Destructive effects of smoking on molecular and genetic factors of periodontal disease. Tob Induc Dis. 2010;8:4. PubMed PMID: 20170537; PubMed Central PMCID: PMCPMC2836317.

Ozcaka O, Bicakci N, Pussinen P, Sorsa T, Kose T, Buduneli N. Smoking and matrix metalloproteinases, neutrophil elastase and myeloperoxidase in chronic periodontitis. Oral Dis. 2011;17(1):68-76. PubMed PMID: 20646231.

Popat RV, Bhavsar NV, Popat PR. Gingival crevicular fluid levels of Matrix Metalloproteinase-1 (MMP-1) and Tissue Inhibitor of Metalloproteinase-1 (TIMP-1) in periodontal health and disease. Singapore Dent J. 2014;35:59-64. PubMed PMID: 25496587.

Powell WS, Rokach J. Biosynthesis, biological effects, and receptors of hydroxyeicosatetraenoic acids (HETEs) and oxoeicosatetraenoic acids (oxo-ETEs) derived from arachidonic acid. Biochimica et biophysica acta. 2015;1851(4):340-55. Epub 2014/12/03. PubMed PMID: 25449650.

Preetha A, Banerjee R. Comparison of Artificial Saliva Substitutes. Trends Biomater Artif Organs. 2005;18 (2).

Romanelli R, Mancini S, Laschinger C, Overall CM, Sodek J, McCulloch CA. Activation of neutrophil collagenase in periodontitis. Infect Immun. 1999;67(5):2319-26. PubMed PMID: 10225890; PubMed Central PMCID: PMCPMC115973.

Rubini C, Artese L, Zizzi A, Fioroni M, Ascani G, Goteri G, et al. Immunohistochemical expression of vascular endothelial growth factor (VEGF) in different types of odontogenic cysts. Clinical oral investigations. 2011;15(5):757-61. PubMed PMID: 20563616.

Sales G, Calura E, Cavalieri D, Romualdi C. g raphite-a Bioconductor package to convert pathway topology to gene network. BMC bioinformatics. 2012;13(1):1.

Sapna G, Gokul S, Bagri-Manjrekar K. Matrix metalloproteinases and periodontal diseases. Oral Dis. 2014;20(6):538-50. PubMed PMID: 23849049.

Scheller J, Chalaris A, Schmidt-Arras D, Rose-John S. The pro- and anti-inflammatory properties of the cytokine interleukin-6. Biochimica et biophysica acta. 2011;1813(5):878-88. PubMed PMID: 21296109.

Schlage WK, Iskandar AR, Kostadinova R, Xiang Y, Sewer A, Majeed S, et al. In vitro systems toxicology approach to investigate the effects of repeated cigarette smoke exposure on human buccal and gingival organotypic epithelial tissue cultures. Toxicol Mech Methods. 2014;24(7):470-87. PubMed PMID: 25046638; PubMed Central PMCID: PMCPMC4219813.

Serhan CN, Jain A, Marleau S, Clish C, Kantarci A, Behbehani B, et al. Reduced inflammation and tissue damage in transgenic rabbits overexpressing 15-lipoxygenase and endogenous anti-inflammatory lipid mediators. J Immunol. 2003;171(12):6856-65. PubMed PMID: 14662892.

Shetty S, Gokul S. Keratinization and its disorders. Oman Med J. 2012;27(5):348-57.

Shirani S, Kargahi N, Razavi SM, Homayoni S. Epithelial dysplasia in oral cavity. Iranian journal of medical sciences. 2014;39(5):406-17. PubMed PMID: 25242838; PubMed Central PMCID: PMC4164887.

Smyth GK. Linear models and empirical Bayes methods for assessing differential expression in microarray experiments. Statistical applications in genetics and molecular biology. 2004;3(1):Article 3.

Sugiyama A, Uehara A, Iki K, Matsushita K, Nakamura R, Ogawa T, et al. Activation of human gingival epithelial cells by cell-surface components of black-pigmented bacteria: augmentation of production of interleukin-8, granulocyte colony-stimulating factor and granulocyte-macrophage colony-stimulating factor and expression of intercellular adhesion molecule 1. J Med Microbiol. 2002;51(1):27-33. PubMed PMID: 11800468.

Toulza E, Mattiuzzo NR, Galliano MF, Jonca N, Dossat C, Jacob D, et al. Large-scale identification of human genes implicated in epidermal barrier function. Genome biology. 2007;8(6):R107. PubMed PMID: 17562024; PubMed Central PMCID: PMC2394760.

Tucci P, Porta G, Agostini M, Dinsdale D, Iavicoli I, Cain K, et al. Metabolic effects of TiO2 nanoparticles, a common component of sunscreens and cosmetics, on human keratinocytes. Cell death & disease. 2013;4(3):e549.

Väremo L, Nielsen J, Nookaew I. Enriching the gene set analysis of genome-wide data by incorporating directionality of gene expression and combining statistical hypotheses and methods. Nucleic acids research. 2013:gkt111.

Villar CC, Lima AFMd. Smoking influences on the thickness of marginal gingival epithelium. Pesquisa Odontológica Brasileira. 2003;17(1):41-5.

Vondracek M, Xi Z, Larsson P, Baker V, Mace K, Pfeifer A, et al. Cytochrome P450 expression and related metabolism in human buccal mucosa. Carcinogenesis. 2001;22(3):481-8. Epub 2001/03/10. PubMed PMID: 11238190.

Yang J, Deol G, Myangar N. Retention of o-cymen-5-ol and zinc on reconstructed human gingival tissue from a toothpaste formulation. International dental journal. 2011;61 Suppl 3:41-5. PubMed PMID: 21762154.

Ye P, Chapple CC, Kumar RK, Hunter N. Expression patterns of E-cadherin, involucrin, and connexin gap junction proteins in the lining epithelia of inflamed gingiva. J Pathol. 2000;192(1):58-66. PubMed PMID: 10951401.

Zanetti F, Sewer A, Mathis C, Iskandar AR, Kostadinova R, Schlage WK, et al. Systems toxicology assessment of the biological impact of a candidate Modified Risk Tobacco Product on human organotypic oral epithelial cultures. Chem Res Toxicol. 2016. PubMed PMID: 27404394.

Zhou K, Muroyama A, Underwood J, Leylek R, Ray S, Soderling SH, et al. Actin-related protein2/3 complex regulates tight junctions and terminal differentiation to promote epidermal barrier formation. Proc Natl Acad Sci U S A. 2013;110(40):E3820-9. PubMed PMID: 24043783; PubMed Central PMCID: PMC3791730.

14.1 List of Standard Operating Procedures (SOPs) and Work Instructions (WKIs)

The procedures and instructions followed to perform the study are listed below.

PMI_RD_WKI_001094: Sample preparation for Carbonyl measurements

PMI_RD_WKI_001145: Generation of aerosol with a negative pressure smoking machine

PMI_RD_WKI_001155: Generation of Aerosol with SM 2000 P1

PMI_RD_WKI_001273: User guide for FlexMAP3D instrument

PMI_RD_WKI_001450: Luminex workflow in Clarity LIMS

PMI_RD_WKI_001228: Computational Practices for Omics (mRNA and miRNA) Analyses

PMI_RD_WKI_001064: Placing MatTek tissues in culture and maintenance

PMI_RD_WKI_001066: EXtrelut trapping for Nicotine measurement

PMI_RD_WKI_000409: Perform Analysis: Determination of Nicotine in diluted aerosol

PMI_RD_WKI_001048: Adenylate kinase assay for 3D cultures

PMI_RD_WKI_001049: CYP assay for 3D cultures

PMI_RD_FOR_000846: Treatment and substrate preparation for CYP1A1/1B1 activity assay

PMI_RD_SOP_000361: Luminex

PMI_RD_WKI_001032: Calibration and Maintenance of LMX200

PMI_RD_WKI_001274: Procedure for Luminex assay (FM3D)

PMI_RD_FOR_000803: Luminex Assay Working Sheet

PMI_RD_FOR_000849: Treatment with controls for MAP analysis

PMI_RD_WKI_001242: Histology Fixation procedure

PMI_RD_WKI_001243: Tissue Processing using LEICA ASP300S

PMI_RD_WKI_001260: Tissue Paraffin Embedding

PMI_RD_WKI_001262: Sectioning Paraffin Blocks using Microtome

PMI_RD_WKI_001266: Haematoxylin & Eosin with or without Alcian Blue Staining Procedure for Formalin- Fixed Paraffin Embedded and Frozen Tissues Sections

PMI_RD_WKI_001309: Immunohistochemistry Procedure on Leica Bond-Max Autostainer

PMI_RD_WKI_001314: Slides scanning with Nanozoomer

PMI_RD_WKI_001117: Isolation of total RNA including microRNAs from Tissue and Organotypic tissue inserts using miRNeasy mini kit protocol

PMI_RD_WKI_000978: Quality controls following RNA extractions

PMI_RD_WKI_001109 : Affymetrix IVT PLUS Protocol

PMI_RD_WKI_001125: Quality controls assessment of the Affymetrix IVT and Nugen amplification products using the Fragment Analyzer

PMI_RD_WKI_001126: Affymetrix-3'array-Cartridge-Hybridization (IVT_PLUS, NugenWB, PicoV2)

PMI_RD_WKI_001123: miRNA labeling using the FlashTag Biotin HSR kits

PMI_RD_WKI_001498: Xcalibur user guide for proteomics analysis

PMI_RD_WKI_001458: LCMS Non-Targeted Xcalibur and Data Analysis workflow in OMICS LIMS

PMI_RD_SOP_000346: Computational Processing for mRNA and miRNA Affymetrix Data

PMI_RD_WKI_001228: Computational Practices for Omics (mRNA and miRNA) Analyses

PMI_RD_SOP_000347: Gene Expression Profiling

PMI_RD_SOP_000354: SOP RNA Extractions

PMI_RD_WKI_001334: qRTPCR SA Bioscience.

PMI_RD_FOR_000999: Form qRT-PCR Qiagen / SA Bioscience.

PMI_RD_WKI_001358: Normalization Macro prior to Nugen WB, IVT or FlashTag protocol

PMI_RD_FOR_001072: Nugen, IVT, FlashTag calculation and tracking sheet

14.2 Philip Morris International (PMI) Internal Documents

1798_Organotypic_Gingival_SP. PMI Internal Document. Testing of repeated exposure of 3r4f cigarette smoke and ths2.2 aerosol on PBS-submersed gingival organotypic tissue cultures. Study Plan Number S179800.
https://disco.app.pmi/disco/drl/objectId/0901d4ec80563678

PMI Internal Document. Unpublished data. Certificate of THS2.2 Batch B-23862.
\\rd-bsrdata.app.pmi\BSR_Data\Cellular Systems Biology\Batch_Certificates_CellSB_activities\P1_Certificate_No_098_StickBatchNo_B-23862_Manufactured_Oct_2015.pdf

PMI Internal Document. Device Information of THS2.2 Code No. B-178731.
\\rd-bsrdata.app.pmi\BSR_Data\Cellular Systems Biology\Batch_Certificates_CellSB_activities\P1_Device_Information_B-18731_Release_Date_Feb_2015.pdf

PMI Internal Document. Unpublished data. Certificate of Epigingival CoA_PBS_pilot.

\\rd-bsrdata.app.pmi\BSR_Data\Cellular Systems Biology\S179800_P1_Repeated_Human_Gingival\PBS_Pilot_CW6_2016\Certificate fo Analysis\pilot_Certificate of analysis_EpiGingival_05.FEB.2016.pdf

PMI Internal Document. Unpublished data. Certificate of buccal EpiOral CoA_DRA. \\rd-bsrdata.app.pmi\BSR_Data\Cellular Systems Biology\S179800_P1_Repeated_Human_Gingival\DRA_CW8_2016\Certificate of analysis\DRA_Certificate of analysis_EpiGingival - 179800 19.FEB.2016.pdf

PMI Internal Document. Unpublished data. Certificate of buccal EpiOral CoA_Experiment 1. \\rd-bsrdata.app.pmi\BSR_Data\Cellular Systems Biology\S179800_P1_Repeated_Human_Gingival\MP1_CW10_2016\Certificate of Analysis\MP1_Certificate of analysis_ - 179800 Gingival_CW10_2016.pdf

PMI Internal Document. Unpublished data. Certificate of buccal EpiOral CoA_Metabolomics. \\rd-bsrdata.app.pmi\BSR_Data\Cellular Systems Biology\S179800_P1_Repeated_Human_Gingival\Metabolomics_CW12_2016\Certificate of Analysis\Certificate of analysis_GI_18.03.2016.pdf

PMI Internal Document. Unpublished data. Certificate of buccal EpiOral CoA_Experiment 2. \\rd-bsrdata.app.pmi\BSR_Data\Cellular Systems Biology\S179800_P1_Repeated_Human_Gingival\MP2_CW16_2016\Certificate of Analysis\MP2_Certificate of analysis_GI.pdf

PMI Internal Document. Unpublished data. Certificate of buccal EpiOral CoA_Experiment 3. \\rd-bsrdata.app.pmi\BSR_Data\Cellular Systems Biology\S179800_P1_Repeated_Human_Gingival\MP3_CW22_2016\Certificate of Analysis\Certificate of analysis_S179800_MP3.pdf

PMI Internal Document. Unpublished data. S179800 Histology Report. \\rd-bsrdata.app.pmi\BSR_Data\Cellular Systems Biology\Collaborations(b) (4) _Histo_Assessment_Gingival_S179800_2016\Report_gingival\Final \Gingival study signed 07 Sept 2016.doc

--- End of Document ---